Department of Chemical Engineering

Faculty of Science and Engineering

Process Efficiency Optimisation of Cascade LNG Process

Nazreen Begum Najibullah Khan

This thesis is presented for the Degree of
Doctor of Philosophy
of
Curtin University

July 2018

Declaration

To the best of my knowledge and belief this thesis contains no material previously published by any other person except where due acknowledgement has been made.

This thesis contains no material which has been accepted for the award of any other degree or diploma in any university.

Your signature : 

Date : 16 July 2018

Copyright

I acknowledged that I have obtained the approval from the copyright owners to use any of my published work such as journal and conference papers for this thesis where the ownership is held by Elsevier and CSIRO Publishing. The permission to utilise the published material by the author has been stated in the copyright link below:

Elsevier: https://www.elsevier.com/about/our-business/policies/copyright/personal-use

CSIRO Publishing: http://www.publish.csiro.au/journals/copyright

Your signature : 

Date : 16 July 2018

Author's Biography

Nazreen Begum Najibullah Khan completed her Bachelor of Chemical Engineering (Hons) from Universiti Teknologi Mara, Shah Alam (Malaysia) in 2007. She has worked for Shell Global Solutions Malaysia from 2007-2010 as a Process Engineer in the LNG and Gas department. She also worked as a contract-lecturer at Universiti Teknologi Mara, Terengganu for 5 months (June-Oct 2012). In September 2013, she commenced her PhD research in natural gas processing at Curtin University. She received a scholarship from the Ministry Higher of Education Malaysia and Universiti Malaysia Pahang, Malaysia to pursue her postgraduate study.

Journal publications (published):

1. Najibullah Khan, N.B., A. Barifcani, M. Tade, and V. Pareek, *A case study: Application of energy and exergy analysis for enhancing the process efficiency of a three stage propane pre-cooling cycle of the cascade LNG process.* Journal of Natural Gas Science and Engineering, 2016. **29**: p. 125-133. **DOI** (http://dx.doi.org/10.1016/j.jngse.2015.12.034)

2. Najibullah Khan, N.B., A. Barifcani, M. Tade, and V. Pareek, *Exergy analysis of an ethylene refrigeration cycle integrated with a NGL recovery process for a large LNG train.* The APPEA Journal, 2016. **56**(2): p. 606-606. **DOI** (https://doi.org/10.1071/AJ15112)

Manuscripts in preparation

1. Najibullah Khan, N.B., A. Barifcani, M. Tade, and V. Pareek, *Effect of deethaniser (De-C2) column pressure on the process efficiency of an integrated LNG/NGL Plant,* to be submitted to another journal.
2. Najibullah Khan, N.B., A. Barifcani, M. Tade, and V. Pareek, *A review of LNG processes that are suitable for a single large-scale LNG train,* to be submitted to another journal.

Conferences:

Oral presentation:

1. N.B. Najibullah Khan, A. Barifcani, M. Tade, V. Pareek, Energy optimization of cascade refrigeration systems for Liquefied Natural Gas (LNG) plant, in: *Chemeca 2014: Processing excellence; Powering our future*, 2014, pp. 260.

Poster presentation:

1. N.B. Najibullah Khan, A. Barifcani, M. Tade, V. Pareek, Exergy analysis of an ethylene refrigeration cycle integrated with an NGL recovery process for a large LNG train, in: *APPEA 2016 56th Conference and Exhibition*, mediadynamics, Brisbane, Australia, 2016, pp. 1-5.

Dedication

I would like to dedicate my thesis to my dear late father and uncle. My mother for her continuous prayers and help

To my husband and my daughter for their greatest help, advice, support and patience

To my siblings, family and friends for their prayers and encouragement

Table of Contents

Acknowledgements

بسم الله الرحمن الرحيم

In the name of Allah, the Entirely Merciful, the Especially Merciful.

"My Lord enable me to be grateful for Your favour which You have bestowed upon me and upon my parents and to do righteousness of which You approve. And admit me by Your mercy into [the ranks of] Your righteous servants." (Holy Quran – 27:19)

First and foremost, all the praises and thanks are due to Allah the Lord of the Worlds who has always blessed me in all the affairs. Without His help and mercy, there is nothing that I could accomplish.

I would like to thank my supervisor Professor Vishnu Pareek for his immense support, advice, patience and for providing me with some helpful tips in writing my thesis. The continuous support that he has given to me during my PhD study despite his tight schedule is highly appreciated.

I would also like to thank my co-supervisor, Professor Ahmed Barifcani for his continuous support, effort, advice, guidance and patience especially in helping me to understand and analyse the technical area of my research. He is also very supportive and always motivated me to continuously write journal papers. I am also grateful to him because he gave me the opportunity to be involved in the final year research projects where I learn more by helping and teaching others. I further would like to thank my associate supervisor - Professor Moses Tade for his time, ideas, comments and support during my study.

I would like to thank the administrative staff of the Chemical Engineering department especially to Tammy Atkins and Lemlem Selomon for helping me in settling my workstation, arranging for conferences and other official issues throughout my study. I further like to thank Mr Harisinh Parmar for assisting me in doing the turn-it-in checking for all my articles. Also, a big thank you to the community of Curtin University.

I also wish to thank the government of Malaysia and Universiti Malaysia Pahang (UMP) for giving me the opportunity to pursue my postgraduate study in Australia. Also, to Dr Ruzinah Isha (UMP), thank you for giving me the opportunity and assisting me in finding the placement and answering to my countless queries. I would like to thank Mr Noor Irwan Shah from Malaysia Hall Perth for allowing me to stay there during my last stage of thesis correction and submission.

Not to forget, I would like to thank my colleagues; Nicholas for his advice in modelling and simulation using Aspen HYSYS, Biao Sun for assisting me in installing the TeamViewer, Ahmed Al-Yaseri for guiding me with writing journal articles and Khalifa al Harooni in helping me with thesis formatting. Also, a big thank you to Varun Ghodkay, Mayeedul Islam, Yousuf, Firas, Muhammad, Samar, Sami and Rakpong.

Further, I would like to thank my friends Salmah Abdul Aziz, Maziah, Masniza, Mas, Ain, Ustadha Norizah, Zura Nashrudin and Nor Azura who have assisted me in many ways especially in helping me by taking care of my daughter.

Finally, I would like to thank my family members (mum (Shabana), siblings (Saira, Yasmeen, Inayat, Fauziah and Abbas), uncle (Zakiullah Khan), mother-in-law (Tuan Yam), husband (Khairu Shah) and daughter (Humaira Khan) for their continuous prayers, encouragement, moral support and for countless helps. I also feel grateful to Allah for giving me such an understanding, patience and wonderful daughter; who accompany my long hours in the office throughout my PhD study. She always asked me the millionaire question “Umi, how many chapters have you written?” I am truly indebted to all of them.

Abstract

A cascade LNG process consists of three refrigeration cycles namely propane, ethylene and methane cycles. This process is suitable for producing large LNG capacity per train and has a proven track record. To convert natural gas to liquid requires an extensive amount of energy. Optimisation of LNG plants is the key to minimise this huge energy demand and to improve plant efficiency. The optimisation can be done in two ways which are through operational and from design perspectives. Very limited studies are available that optimise large LNG train as well as that focus on optimisation of integrated LNG/NGL process. Hence, to close these gaps, more research is required to investigate the possible areas of optimisation for large LNG train and integrated LNG/NGL process.

This thesis discussed three main studies that were carried out to optimise the integrated LNG/NGL train for 5 MTPA production plant. Firstly, a cascade LNG process was modelled using Aspen HYSYS v. 7.2 based on Peng Robinson equation of state. The model was then used to identify the possible areas that can improve the process further. Two main energy contributors were identified which are propane and ethylene refrigeration cycles. These cycles consume a large amount of energy because propane and ethylene refrigerants are used to cool not only natural gas but also the methane refrigerant. The process efficiency of the presented studies was calculated and evaluated using first and second law of thermodynamics (energy and exergy analyses).

The optimisation of the cascade process was carried out in three consecutive steps. In Chapter 4, the propane pre-cooling cycle is optimised by varying the evaporator pressure, temperature and cooling load of the intermediate stages. Six case studies were investigated with different evaporator operating conditions. The effect of varying these process parameters on the process performance and efficiency were analysed. It was found that by reducing the cooling loads at the intermediate stages of propane evaporator, the power consumption of propane refrigeration cycle was reduced by 13.5% (from 149.48 MW to 129.36 MW), propane refrigerant flow rate lower by 8.6% (from 84,276.78 kgmole/h to 77,024.28 kgmole/h) and the coefficient of performance and exergy efficiency improved by 15.51% and 18.75% respectively. The cascade process is then further optimised using the optimal evaporator operating condition obtained from Chapter 4.

In Chapter 5, two different integrated LNG/NGL configurations were examined. In the first configuration, the deethaniser (De-C2) column is operated as a partial condenser while in the second configuration, the deethaniser (De-C2) column is operated as a total condenser. These integrated designs were analysed and assessed based on several criteria such as meeting the desired LNG capacity and its required HHV specification, consuming less amount of energy and possessing the highest process efficiency. It was found that configuration 2 consumed less energy, met the LNG capacity and its HHV requirement and possessed the highest efficiency compared to configuration 1.

In Chapter 6, the optimal configuration 2 was further optimised by manipulating the De-C2 column pressure. Five different inlet pressures were chosen based on the information available from the literature review. The effect of varying the De-C2 column pressure on the process parameters such as compressors power, heat exchangers duty and UA, refrigerants flow rate and LNG production and its HHV were analysed and discussed. The selection criteria of the optimal De-C2 column pressure are meeting the desired LNG capacity and its HHV specification, gives minimum energy consumption and gives highest process efficiency. It was found that De-C2 column pressure of 2000 kPa meets all these requirements.

From these three studies that were investigated, the reduction with respect to the total amount of power, SP, exergy loss and refrigerant flow rate achieved are 21.6%, 20.6%, 32.6% and 18.8% respectively. Whereas, the percentage increase in the total amount of COP and exergy efficiency obtained was 17.1% and 29.6% respectively. This showed a significant improvement in the process efficiency of the integrated cascade liquefaction process for 5 MTPA production plant which not only reduced the operating cost but also the capital cost i.e. lower compressor power.

In this thesis, no economic evaluation was done to assess these optimisation approaches that were applied. Future work is required to include engineering economics in the exergy analysis to obtain the operating, capital, and maintenance costs. Besides, the simulation model needs to be embedded with more actual plant data so that it can replicate the actual LNG plant.

List of Figures

List of Tables

Nomenclature

Chemical formulas

$C_{137}H_{97}O_9NS$	Bituminous coal
C2	ethane
C3	propane
C4	butane
C_4-C_{15}	Gasoline
C5+	pentane and heavier hydrocarbon
CH_4	Methane
CO	Carbon monoxide
CO_2	Carbon dioxide
H_2O	Water
H_2S	Hydrogen sulphide
Hg	Mercury
N_2	Nitrogen
NO_2	Nitrogen dioxide
O_2	Oxygen
R-SH	Mercaptans
SO_2	Sulphur dioxide

Unit of measurements

µg	microgram
b	bar
BTU	British Thermal Unit
kg	kilogram

kJ	kilojoule
kWh	kilowatt-hour
ℓ	litre
lb	pound
Nm^3	Normal cubic meter
^oC	Celsius
ppmv	part per million volumes

Symbols in chemical equations

g	gas phase
ℓ	liquid phase

Standard abbreviations

AGRU	acid gas removal unit
APCI	Air Products & Chemical Inc.
CNG	Compressed natural gas
DHU	dehydration unit
EIA	Energy Information Agency
GE	General Electric
GHG	greenhouse gas
HHV	higher heating value
HX	heat exchanger
JT	Joule Thomson
LNG	Liquefied natural gas
LPG	Liquefied petroleum gas
MCHE	main cryogenic heat exchanger

MR	mixed refrigerant
MRU	mercury removal unit
MTPA	million tonnes per annum
NGL	natural gas liquids
NRU	nitrogen removal unit
U.S.	United States

Process simulations abbreviations

AC	air cooler
CV	control valve
De-C1	Demethaniser
De-C2	Deethaniser
HXC3-1	propane evaporator HP stage
HXC3-2	propane evaporator MP stage
HXC3-3	propane evaporator LP stage
K – HP C3	propane compressor HP stage
K – MP C3	propane compressor MP stage
K – LP C3	propane compressor LP stage
MIX	mixer
TEE	splitter
V – HP C3	propane vessel HP stage
V – MP C3	propane vessel MP stage
V – LP C3	propane vessel LP stage

Chapter 1 Introduction

1.1 LNG – future energy fuel

The global energy demand is drastically increasing and it is forecasted to grow by an average of 1.2% per year [1]. According to BP [2], world energy consumption has increased by 1.7% from the year 2006 to 2016. Fossil fuels have contributed to about 85% [3] of the current global energy consumption. Meanwhile, about 33.5 billion tonnes of CO_2 emissions produced worldwide in the year 2015 in relation to fossil fuel used [2].In addition, global carbon dioxide (CO_2) emissions are expected to increase by 30% from 2005 to 2030 [1]. Hence, to fulfil the increasing energy demand and to reduce CO_2 emissions, it is necessary to initiate the search for alternative fuels. Natural gas is one of the alternative future fuels that has been globally recognised [2-6]. It has an immense potential to meet these requirements and to substitute the existing energy sources (i.e. coal and oil). Natural gas mainly consists of paraffinic hydrocarbons gases such as methane, ethane, propane, butane, other heavier components and some impurities such as CO_2, hydrogen sulphide (H_2S), nitrogen (N_2), water (H_2O) and mercury (Hg).

Natural gas can be used in various forms such as compressed natural gas (CNG), liquefied natural gas (LNG) or mixed it with hydrogen [3]. The usage of natural gas covers various sectors such as power generation [4, 7-12], transportation such as heavy-duty trucking industry, rail and marine application, port facility vehicles [4, 13-16], for homes such as cooking and heating instead of using liquefied petroleum gas (LPG). It is also the preferred feedstock for chemical, fertiliser and petrochemical industries [17].

Due to its wide range of applications, natural gas production is expected to increase by 50% by 2030 [18]. Adding to this, according to the Energy Information Agency's (EIA), 2016 [19] natural gas will overtake coal by 2030 and will be the primary global future fuel. Figure 1.1 illustrates the electricity dependence forecast for coal, natural gas and renewables to 2040 for the United States (U.S.) energy market [19].

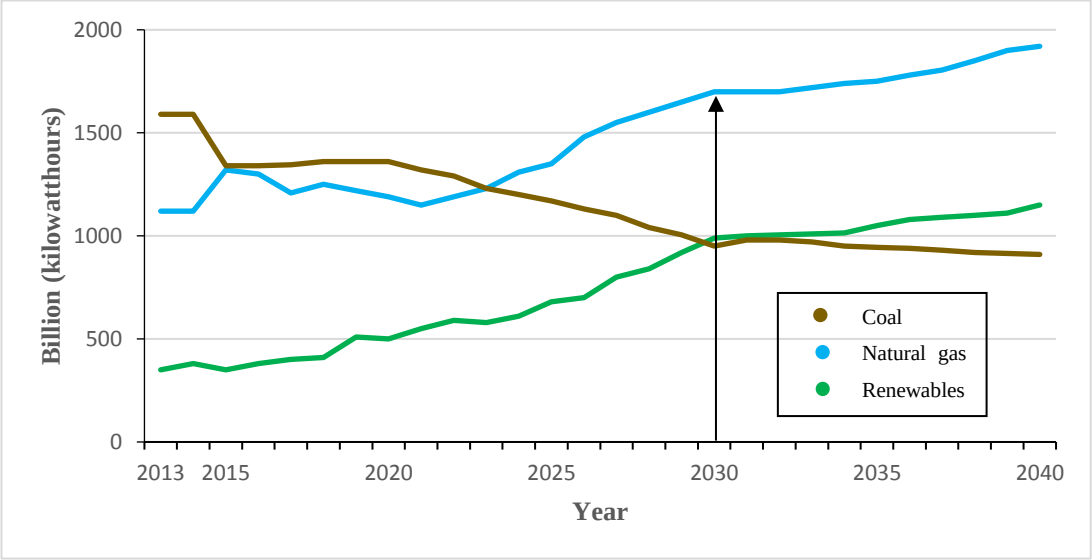

Figure 1.1: Net electricity forecast for coal, natural gas and renewables to 2040 for the United States (U.S.) energy market; adapted from [19].

Natural gas is converted to LNG by processing and cooling it down to -161°C at atmospheric pressure using various refrigeration technologies. Upon liquefying it, LNG contains about 85-98% methane, hence, it becomes synonym to methane. The ability to convert natural gas to liquid not only reduces its volume by a factor of 600 but also creates an opportunity for it to be shipped to consumers worldwide as it is not feasible to transport natural gas via pipelines for long distances. Besides, due to a geographical mismatch between the gas reserves and customer demand, transferring natural gas in LNG form is the preferred method as it is safer and more economical.

LNG has several unique characteristics that make it the preferred choice of fuel compared to coal and oil. It is clear, odourless, non-corrosive and non-toxic. Further, it has a low density of about 0.4-0.5 kg/ℓ compared to water (1.0 kg/ℓ) depending on the temperature, composition and pressure [3]. Hence, if LNG is spilled on the water, it will float on the surface and evaporate quickly, leaving no residue. Thus, no environmental clean-up is required if any spill occurs on the land or water.

In addition, LNG plays a significant role in reducing the overall greenhouse gas (GHG) emissions [16, 20-24]. As LNG synonym to methane (CH_4), it has the lowest number of carbon atoms compared to coal (bituminous – $C_{137}H_{97}O_9NS$) and oil (gasoline – C_4-C_{12}). The combustion of one molecule of CH_4 in air produces one molecule of CO_2, two molecules of H_2O and 890 kJ/moles of heat [25] as expressed below:

$$CH_4\,(g) + 2O_2\,(g) \rightarrow CO_2\,(g) + 2H_2O\,(\ell) + 890\ \text{kJ/moles} \quad (1.1)$$

Table 1.1 shows the amount of hazardous air pollutants emitted from the combustion of coal, oil and natural gas [26]. Based on equation (1.1) and Table 1.1, it shows that LNG is a clean burning fuel as it produces fewer amounts of hazardous gases compared to coal and oil.

Table 1.1: The amount of air pollutants (lb) produced per billion BTU of energy [26].

Pollutant	**Coal[a]**	**Oil[b]**	**Natural gas[c]**
Carbon dioxide (CO_2)	208, 000	164, 000	117, 000
Carbon monoxide (CO)	208	33	40
Nitrogen dioxide (NO_2)	457	448	92
Sulphur dioxide (SO_2)	2, 591	1,122	0.6

Note:

[a]*Bituminous coal burned in a spreader stoker.*

[b]*Fuel oil burned in an oil-fired utility boiler.*

[c]*Natural gas burned in uncontrolled residential gas burners.*

Meanwhile, as reported by Wood [27], global LNG production is expected to rise to approximately 450 million tonnes per annum (MTPA) by 2020. Africa, North and Latin America, Oman, Yemen, Qatar, Egypt, Australia, Indonesia and Papua New Guinea are the future LNG providers based on approved projects and in planning. In addition, the future LNG demand is expected to be from China, Japan, India, Indonesia, Thailand, Vietnam and Europe [27].

An LNG project consists of a series of steps which is known as the LNG supply chain as shown in Figure 1.2 [28]. The first step is the exploration and production of gas. This is followed by transferring natural gas via pipeline to the LNG plant which comprises of gas treating and liquefaction facilities and then shipped in a special tanker. Next, the natural gas is regasified at the receiving terminal and finally distributed to the customer or supplied to the power plants.

On the other hand, the development of an LNG plant requires a large financial investment. As shown in Figure 1.3 [26], the liquefaction section contributed the highest investment cost i.e. 41% covering the construction of an LNG plant. This is due to special and proprietary equipment required for the liquefaction section such as compressors, gas turbines and heat exchangers which are extremely expensive.

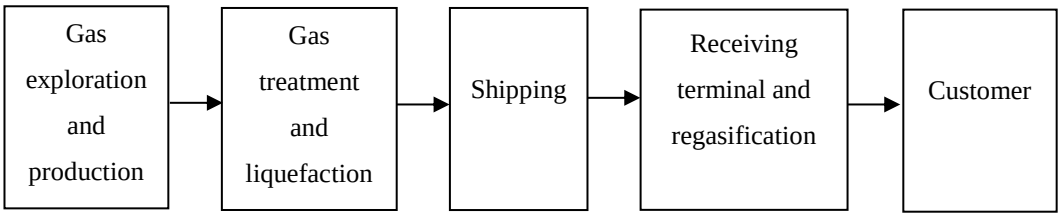

Figure 1.2: LNG supply chain [28].

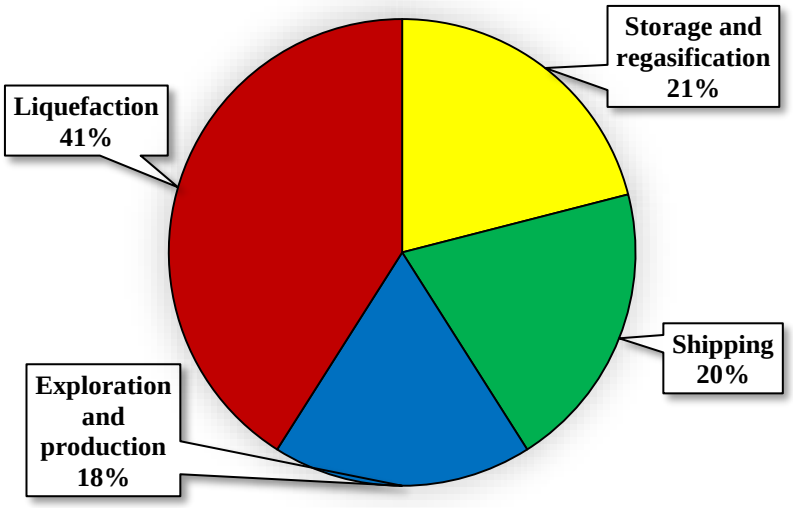

Figure 1.3: Cost allocation for an LNG plant [26].

1.2 Overview of LNG plant processes

A typical base load LNG plant mainly includes three sections namely pre-treatment, liquefaction and storage facilities. The process block diagram of an LNG process is shown in Figure 1.4. As shown in Figure 1.4, natural gas received by the processing plant is first separated in a slug catcher to remove the liquids. The liquids are then fractionated in the condensate stabiliser column whereas the off-gas from the slug catcher and overhead of stabiliser column are routed to the pre-treatment facilities. Pre-treatment facilities consist of acid gas removal unit (AGRU), dehydration unit (DHU) and mercury removal unit (MRU).

As described in section 1.1, natural gas contains various impurities such as CO_2, H_2S, mercaptans (R-SH), H_2O and Hg which need to be removed prior to the liquefaction. In the AGRU unit, the CO_2, H_2S and R-SH are removed using the solvent absorption process. These components concentration should not exceed the following limits; 50 ppmv for CO_2, 4 ppmv for H_2S and 30 ppmv for total sulphur (S) content [29] to meet the LNG product specification. CO_2 is removed to prevent it from freezing out in the downstream equipment which is operated at cryogenic temperatures. Following the removal of acidic gases, the next step is the removal of water in DHU to 0.1 ppmv to prevent it from freezing and hydrate formation in the liquefaction section. The last step in the pre-treatment is to remove Hg in the MRU to below 0.01 μg/Nm^3 [29] to protect the aluminium main cryogenic heat exchangers (MCHE) from corrosion. Leaving the pre-treatment facilities, natural gas is known as sweet gas or treated gas.

This treated natural gas then enters the liquefaction section whereby it will be cooled down to -161^oC at atmospheric pressure using a refrigeration system. The liquefaction section includes a fractionation unit and a refrigeration cycle. Natural gas is separated from the heavy hydrocarbons using the fractionation columns and is liquefied at (-155 ^oC to -161^oC) depending on the liquefaction technology used. Liquefaction of natural gas is based on the principle of refrigeration system whereby a refrigerant absorbs the heat from the natural gas stream in successive expansion and compression stages and rejecting it to a higher temperature using air coolers or cooling water. **This process consumes a significant amount of energy due to the usage of complicated refrigeration systems [26]. Details of the refrigeration system will be discussed in chapter 2.** After the liquefaction process, a nitrogen removal unit (NRU) may be required if the nitrogen (N_2) content in the LNG is above 1 mole % [30]. Finally, the LNG can be stored in specifically designed storage tanks at atmospheric pressure and -161^oC.

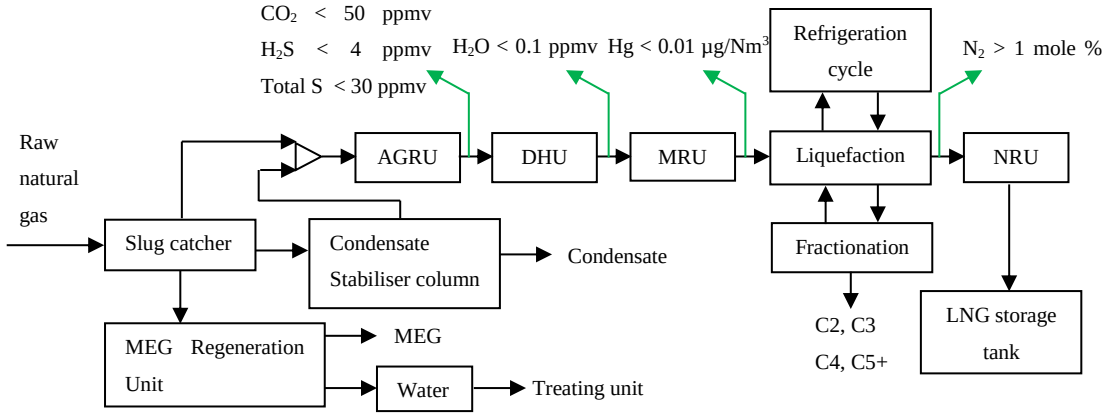

Figure 1.4: Process block diagram of LNG process for a base load LNG plant.

1.3 What is LNG process optimisation?

The optimisation can be defined as a process to obtain an optimal design using various methods. There are two areas of optimising an LNG plant i.e. from design and operational perspectives. From the design context, the LNG plant can be optimised either by adding or replacing a process component such as compressor/driver that has higher efficiency [31], integrating LNG and natural gas liquids (NGL) processes [32-34] in a single train and using expanders instead of Joule Thomson (JT) valves [35]. However, this method requires detailed economic evaluation to determine the offset between the total installed cost and profitability. Alternatively, from the operational side, the LNG plant can be optimised by analysing and improving the performance of the existing process component. For example, the expansion valves and heat exchangers (HX) [31] performances can be improved by making the necessary adjustments to their operating conditions. Some of the operating parameters such as mixed refrigerant (MR) composition (for LNG processes that use MR), their pressure levels and mass flow rates have been analysed in the previous studies. Optimisation of LNG plants is a complex and time- consuming process; hence employing optimisation techniques is essential to obtain an optimal design of the plant. Figure 1.5 represents an overview of LNG plant optimisation areas.

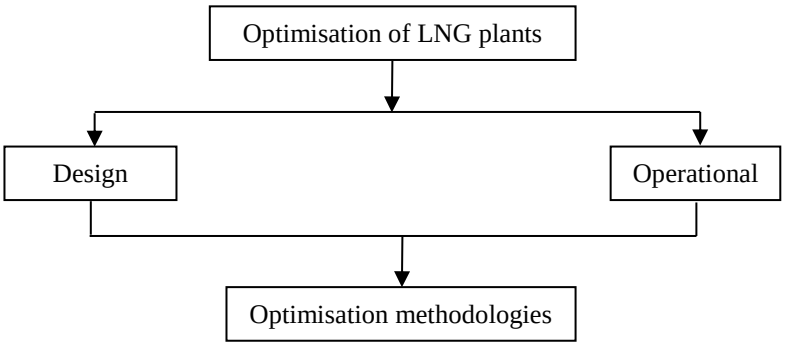

Figure 1.5: LNG plant optimisation areas.

Besides, since the operation of the first LNG plant in 1964 at Arzew, Algeria which utilised the cascade liquefaction process, significant and steady progress have been made in optimisation of LNG processes. The optimisation includes both offshore and onshore plants and covers various research areas. These include modelling, simulation and optimisation of LNG processes as well as efficiency improvement of the major equipment such as compressors, gas turbines and heat exchangers. In addition, a substantial number of publications available on this research area in the past 50 years (1967-2017) i.e. about 3,729[1] based on the Curtin University catalogue database. Hence, this indicates the importance of continuously studying and exploring in these research areas.

1.4 Why do LNG plants need to be optimised?

As shown in Figure 1.3 and explained in section 1.2, liquefaction section contributes the highest investment cost (41%) [36] and is an energy-intensive process as it utilises complex refrigeration systems [26]. According to Alfadala et al. [37] a base load LNG plant consumes about 5.5-6 kWh of energy per kgmole of LNG produced. Therefore, it is crucial to optimise the LNG plants to minimise the cost and energy consumption which will improve the overall plant efficiency.

On the other hand, unplanned operational disturbances may occur during day-to-day operation due to fluctuations in the feed gas composition and its flow rates and operating temperature and pressure as they differ between wells [38]. This will affect the LNG production and its higher heating value (HHV) specification, hence necessary adjustments need to be made through operational optimisation to meet these requirements.

[1] The keywords used is "Optimisation of LNG process". This include text resources – 2,409, articles – 760, dissertation – 262, newspaper articles – 226, conference proceedings – 41, books – 25, other – 5 and review – 1.

Another essential point to mention is that the feed flow rates of the oil and gas reservoir will deplete over time as illustrated in Figure 1.6 [38]. During the early years of gas production, the plant capacity is high, however, when the gas reserves start depleting over the years, the wells pressure decreases which result in a decrease of the gas flow rates. Consequently, this causes large temperature approach between natural gas and the refrigerants. This inefficiency can be adjusted through operation optimisation [38]. Therefore, continuous LNG plant optimisation is essential as it will impact plant performance and efficiency. Various solutions have been suggested to optimise the natural gas liquefaction process efficiency which will be discussed in the next section.

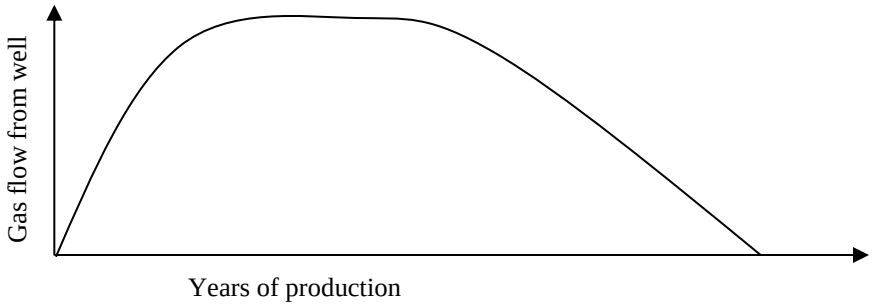

Figure 1.6: The life cycle of an oil and gas well [38].

1.5 Progress in LNG plant optimisation

In the last decade, tremendous improvements have been made in the LNG industry. Substantial advancement has been observed in the LNG technologies and major equipment design of liquefaction processes such as gas turbines, compressors and heat exchangers. Compressor and gas turbine manufacturers such as General Electric (GE), Siemens and Rolls-Royce have built larger and more efficient drivers which are suitable for single large LNG trains [30]. This development is parallel with the improvement made by the LNG technology providers such as Air Products & Chemicals Inc. (APCI), ConocoPhillips and Shell. They have developed innovative designs for the liquefaction processes that are suitable for single large LNG trains based upon the original design concepts. Single large LNG trains capacities are considered in the range of 3 to 8 MTPA. Figure 1.7 shows the progression of a single LNG train size since the 1960s. In addition, in the past 10 years, new single large LNG trains have come on-stream as shown in Table 1.2 [30, 39].

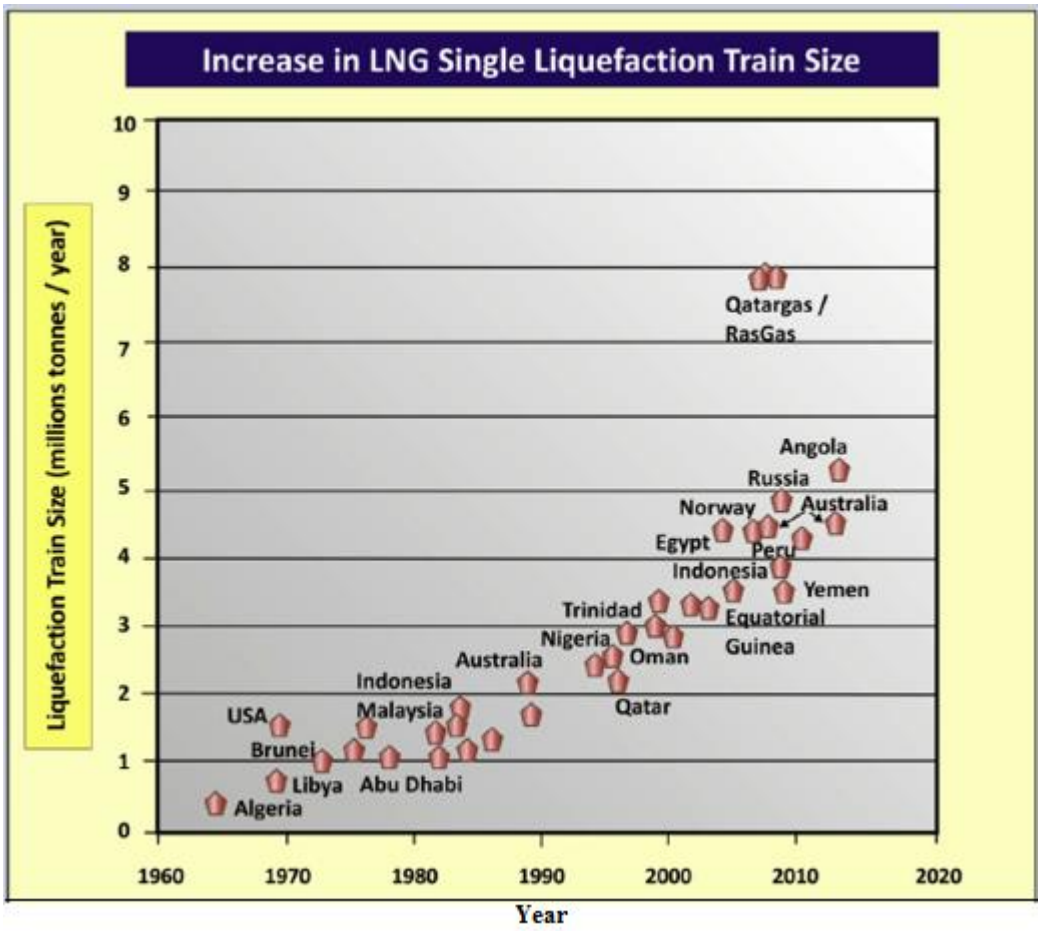

Figure 1.7: Progress in LNG plant optimisation [27].

Table 1.2: Recent single LNG trains [30, 39].

Year	Countries	Nameplate Capacity (MTPA)
2008	Australia (North West Shelf Train 5)	4.4
2009	Russia (Sakhalin)	4.8
	Indonesia (Tangguh LNG T1)	3.8
	Yemen	3.4
2010	Peru (Peru LNG T1)	4.4
	Indonesia (Tangguh LNG T2)	3.8
	Qatar (RasGas III T2, Qatargas III)	7.8; 7.8
2011	Qatar (Qatargas IV)	7.8
2012	Australia (Pluto)	4.3
2013	Algeria (Skikda – GL1K Rebuild)	4.5
2014	Papua New Guinea (LNG T1, T2)	3.45;3.45
	Angola (Angola LNG T1)	5.2
2015	Australia (Queensland Curtis LNG T1, T2)	4.25;4.25
	Indonesia (Donggi Senoro LNG)	2
2016	Australia (GLNG T1, T2)	3.9; 3.9
	Australia (Australia Pacific LNG T1)	4.5
	United States (Sabine Pass LNG T1, T2)	4.5
	Australia (Gorgon LNG T1, T2)	5.2; 5.2
2017	Australia (Australia Pacific LNG T2, Gorgon LNG T3)	4.5; 5.2
	Malaysia (MLNG T9)	3.6
	US (Sabine Pass LNG T3, T4)	4.5; 4.5
2018	Australia (Wheatstone LNG T1)	4.45
	Russia (Yamal LNG T1)	5.5

Figure 1.7 and Table 1.2 show that future LNG trains will be built as single large LNG trains. Single large LNG trains not only help to reduce the production cost but also improve project economics [26, 30, 40-43]. However, these benefits can only be achieved when the plant applies proven LNG technology and equipment, availability of large gas reservoirs, has a robust design, high plant reliability and availability is maintained, the process is simple and easy to operate and is provided with sufficient spare equipment in the case of sudden trip or shutdown. Meanwhile, very few studies are available that discuss ways to improve single large LNG train efficiencies [42, 44-46].

On the other hand, future LNG plants can be improved by integrating a single large LNG train with the NGL plant. In the past, LNG liquefaction trains were designed as a stand-alone unit [40] with no NGL plant. By installing the NGL facilities, the need for a scrub column which typically is used in the liquefaction plant to remove aromatics and heavy hydrocarbons can be eliminated [30]. Further, employing an integrated design reduced the total equipment count. For example, by utilizing common processing equipment such as refrigeration system (propane refrigeration cycle) [33, 34] will decrease the capital and operating cost of the plant. Also, the energy requirements for separation, condensation and cooling of the NGL products can be shared from the liquefaction section [40]. With this heat integration, the overall plant process efficiency can be improved [32, 47]. Besides, having an integrated design makes LNG plants more robust. For instance, the LNG capacity can be adjusted especially when fluctuations occur in the LNG market. In addition, the plant will be able to handle a wide range of feed gas compositions which helps in meeting the LNG HHV specification. Till today, no study is available that discusses the improvement of the integrated LNG/NGL design for single large train and its effect on the LNG HHV specification.

Another important subject area of focus is the usage of suitable methods to optimise the LNG plants. As discussed in section 1.3, the optimisation of LNG plants is a complex and time- consuming process which requires appropriate methods. Numerical and thermodynamics-based approaches are two common techniques which are mostly being applied to optimise the LNG plants. Some examples of numerical methods are linear (mixed integer) and nonlinear programming, deterministic and nondeterministic and stochastic approach [26]. However, there are some weaknesses discovered using these approaches. For instance, deterministic approach excludes the uncertainties changes involved in the process design and applying incomplete mathematical models within the process flow sheet program [30, 48], thus, it is not considered as the preferred method for most actual engineering problems [30]. Disregarding these aspects may cause infeasible design or inferior performance of the process. On the other hand, a nondeterministic approach (genetic algorithm and tabu search) requires long execution time which sometimes prevents it to reach the global optimum [49]. Additionally, the optimisation results obtained using numerical based methods causes ambiguity because it is not embedded with any process knowledge, hence gives no understanding of the process.

Meanwhile, the energy and exergy analyses are the methods that apply thermodynamics concepts. These methods are derived from the first and second law of thermodynamics. They have been widely used in numerous studies to evaluate the liquefaction process thermodynamics efficiency, assist in obtaining an optimal design and operation and improve the entire plant performance [50-56]. Hence, using the correct methods will not only optimise the LNG plant efficiency but also helps to understand the insight of a process. Table 1.3 shows the summary of the work done by the previous researchers using numerical and thermodynamic optimisation methods.

Table 1.3: Numerical and thermodynamic optimisation methods done by previous researchers.

Optimisation methods	Publication
Thermodynamics	Mehrpooya, Jarrahian [50], Kanoglu [51], Najibullah Khan, Barifcani [52], Najibullah Khan, Barifcani [53], Remeljej and Hoadley [54], Vatani, Mehrpooya [55], Cipolato, Lirani [56]
Numerical	Lee, Smith [57], Nogal, Kim [58], Wang, Zhang [49], Cammarata, Fichera [59], Aspelund, Gundersen [60]

In this research work, the thermodynamics approach i.e. energy and exergy analyses are used to overcome the limitations of the numerical optimisation methods. Knowing the thermodynamics properties (enthalpy and entropy) of each process stream is crucial as it provides a better understanding of the changes occurring within the process.

1.6 Scope and objectives of this study

This thesis focuses on ways to optimise the process efficiency of a single large LNG train that employed Cascade LNG process. The optimisation was carried out from operational and design perspectives for a 5 MTPA production plant using energy and exergy analyses methods. The study covers modelling of cascade LNG process, optimisation of the pre-cooling cycle, process efficiency analysis of two different integrated LNG/NGL configurations and optimisation through the deethaniser (De-C2) column pressure. The detailed objectives are as below:

1. Develop a cascade LNG process simulation model using Aspen HYSYS (v.7.2, 2010). The pre-treatment unit is not modelled as the main emphasis is on the liquefaction section.
2. Optimise a three-stage propane pre-cooling cycle by varying the cooling load at the intermediate stages of propane evaporators and investigate its effect on the process parameters and efficiency.
3. Analyse the process efficiency of two different integrated LNG/NGL configurations that meet the prescribed LNG specification. The integrated LNG/NGL process model applies the optimal operating conditions for propane pre-cooling cycle based on the findings obtained from objective number 2.
4. Examine the effect of deethaniser (De-C2) column pressure on the process parameters and efficiency of the integrated LNG/NGL process. The integrated LNG/NGL process model uses the configurations that give the highest process efficiency and meet the specified LNG specification based on the findings obtained from objective number 3.

1.7 Contributions of this thesis

Upon addressing the above objectives, the following are some important contributions made from the research work conducted through multiple simulations and thermodynamics analyses of cascade LNG process. These contributions are:

1. A new optimised design has been developed for cascade LNG process that includes integration with the NGL section specifically for large-scale LNG train; 5 MTPA production plant.
2. Introduced a new method that can improve the propane pre-cooling cycle efficiency by varying the cooling load across various compression stages. An optimised set of operating conditions for the propane evaporator has been obtained.
3. Based on the optimised operating conditions of the pre-cooling cycle, the integrated LNG/NGL cascade simulation is further improved by comparing two distinct integrated designs. An optimised integrated design has been obtained that not only improves the process efficiency but also meets the prescribed LNG HHV. A significant reduction in power consumption has been observed.
4. An important operating parameter has been discovered that plays a vital role in determining the LNG production and it prescribes HHV, that is the De-C2 column pressure. Based on the results obtained in Chapter 6 of this thesis, the LNG capacity and its HHV specification hinge on the De-C2 column pressure.
5. The usage of energy and exergy analyses in this research work provides a clear understanding of the process. This is through identifying the inefficiency occurrences in the equipment, hence assist in optimising the process by making the necessary changes to the operating parameters.

1.8 Thesis outline

This thesis discusses the presented work in the following chapters.

Chapter 1

In this chapter, an introduction about LNG has been given that covers its role as a future energy provider. This chapter also includes the following topics; overview of LNG plant processes, the importance of optimisation, issues and suggestions to improve the LNG plants, scope, objectives and contributions of this thesis. At the end of this chapter, a brief thesis outline is presented that summarised the overall research work.

Chapter 2

This chapter is the literature review of the research study. Firstly, this chapter discusses various LNG processes that are suitable for large-scale single LNG train followed by the reason for selecting cascade over the other refrigeration processes. Next, this chapter describes the fundamentals involved in the liquefaction of natural gas processes such as the thermodynamic laws, heat exchange terminologies and refrigeration systems. This chapter further discusses the energy and exergy methodologies used to complete the research study. Lastly, this chapter describes the optimisation areas such as the pre-cooling cycle, integrated LNG/NGL section and NGL process and identifies the study gaps in each of these areas.

Chapter 3

This chapter discusses the simulation basis and modelling assumptions applied in all the simulation work. It also explains the simulation constraints needed for each research work. This chapter also provides the base case process simulation flow scheme of Aspen HYSYS, the stream properties and composition. The base case simulation model is used to optimise the cascade LNG process. Besides, a brief description is given on the optimisation framework and verification of the simulation model.

Chapter 4

In Chapter 4, a three-stage propane pre-cooling cycle process efficiency is optimised. It used the base case simulation modelled that was presented in Chapter 3. The process efficiency optimisation framework of the pre-cooling cycle is also explained. The effect of varying the process parameters such as cooling load (duty), pressure and temperature of propane evaporator on the process performance and efficiency will be analysed and discussed.

Chapter 5

In this chapter, the simulation model of the integrated cascade process is further optimised by modifying the process configuration. These models use the optimal operating conditions for pre-cooling cycle based on results obtained in Chapter 4. Two different configurations of the integrated LNG/NGL cascade process are studied. The effect of changing the process configurations on the process parameters, efficiency and LNG HHV specification is analysed and evaluated.

Chapter 6

This chapter analyses the effect of varying the De-C2 column pressure on the process performance and overall efficiency. The simulation model uses the optimal integrated design based on the results obtained from Chapter 5.

Chapter 7

This chapter concludes the overall findings based on the results presented from Chapters 4 to 6. The percentage increase in overall process efficiency because of optimisation are discussed. Further, recommendations for future studies have been proposed based on the new knowledge gaps found. The overall thesis process map is shown in Figure 1.8.

The content of this thesis is presented in a hybrid format. ***Chapters 2, 3, 4 and 5*** *contents are referred to journal articles that have been published in the Journal of Natural Gas Science and Engineering and The APPEA journal. The presentation of the content is partially adjusted to be consistent with the research flow and thesis style.*

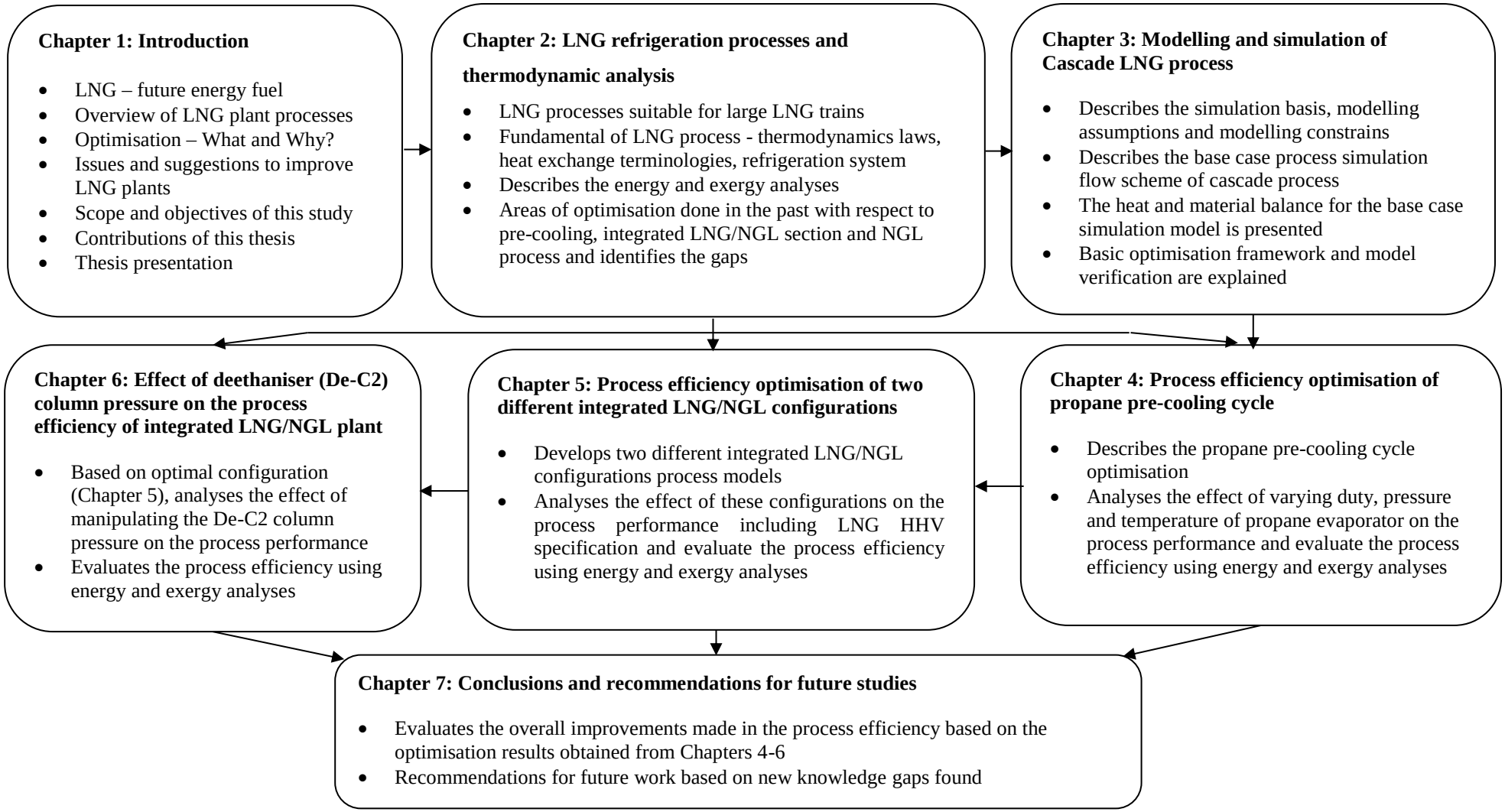

Figure 1.8: Thesis map

Chapter 2 LNG refrigeration processes and thermodynamic analysis

2.1 Introduction

In this chapter, the literature review is sub-divided into three main topics which are the LNG processes for a single large-scale LNG train, refrigeration systems and methods to evaluate the process efficiency using energy and exergy analyses and LNG processes optimisation.

2.2 LNG processes for a single large-scale LNG train

As discussed in Chapter 1 (section 1.5), the current trend of LNG plants focuses on building a single large-scale LNG train (3 to 8 MTPA) which provide economic benefits. The type of LNG process determines the size of the LNG train. With the recent technological advancement in the LNG technologies, existing liquefaction processes are upgraded and new liquefaction processes are invented that are suitable for large-scale LNG trains. The following are the liquefaction processes that are suitable for a single large LNG train; propane pre-cooled mixed refrigerant (C3MR) and AP-X^{TM} by APCI, dual mixed refrigerant (DMR) by Shell-APCI, parallel mixed refrigerant (PMR) by Shell, Liquefin^{TM} process by IFP/Axens, mixed fluid cascade (MFC) by Linde-Statoil and Phillips optimised cascade (POC) LNG process by ConocoPhillips. These processes will be discussed in the next section.

2.2.1 Propane pre-cooled mixed refrigerant (C3MR) process

The C3MR process licensed by APCI was first applied in Brunei LNG plant in the year 1972 and about 75% of the existing baseload LNG plants use this process [30]. As shown in Figure 2.1, this process consists of pre-cooling and liquefaction cycles. Pre-cooling of natural gas is achieved using pure propane while liquefaction of natural gas is attained using mixed refrigerant (MR) which comprises of nitrogen (N_2), methane (CH_4), ethane (C_2H_6), propane (C_3H_8) and butane (i/n-C_4H_{10}). In the pre-cooling cycle, pure liquid propane (green stream) cools natural gas and MR streams (blue stream) to about -35^{o}C to -40^{o}C [30, 61] in three or four pressure stages. The pre-cooling of these streams is done in kettle type heat exchangers (see Figure 2.2 [62]). The cooling of natural gas and MR causes the liquid propane to evaporate. This vaporised propane is then compressed to 15 – 25 bara [61] and condensed against ambient air or cooling water and recycled to the propane kettles.

Meanwhile, the partially condensed MR exit the propane cycle and is then separated into vapour and liquid streams in the high pressure (HP) separator. These MR streams are used to liquefy and sub-cool the natural gas to about -150^{o}C to -162^{o}C [41, 63] in the main cryogenic heat exchanger (MCHE). The liquid and vapour MR streams enter the MCHE tubes from the bottom. The MCHE consists of two sections called the cold bundle (CB) and warm bundle (WB).

The liquid MR stream exits the WB or middle bundle and is flashed across the JT valve on the shell side of MCHE. It then flows downward and evaporates providing cooling to the WB. Whereas, the vapour stream MR goes through the top of MCHE (CB) whereby it is liquefied and sub-cooled. It is then flashed across the JT valve into the shell side of MCHE. It flows downward and evaporates providing cooling to natural gas in CB and mixed with liquid MR sharing the cooling duty for the lower bundles. The overall vaporised MR exit the shell side of the MCHE and is compressed to about 45-48 bara [61]. It is then cooled by air or cooling water and then partially condensed by propane refrigerant prior to entering back in the MCHE. This process has been applied in the existing LNG plants with the capacities range from 1 to 4 MTPA per train without any major modification on the existing configuration. For a train capacity reaching 5 MTPA, split MR configuration is applied [40, 64] because the propane compressor reaches its maximum flow capacity [65].

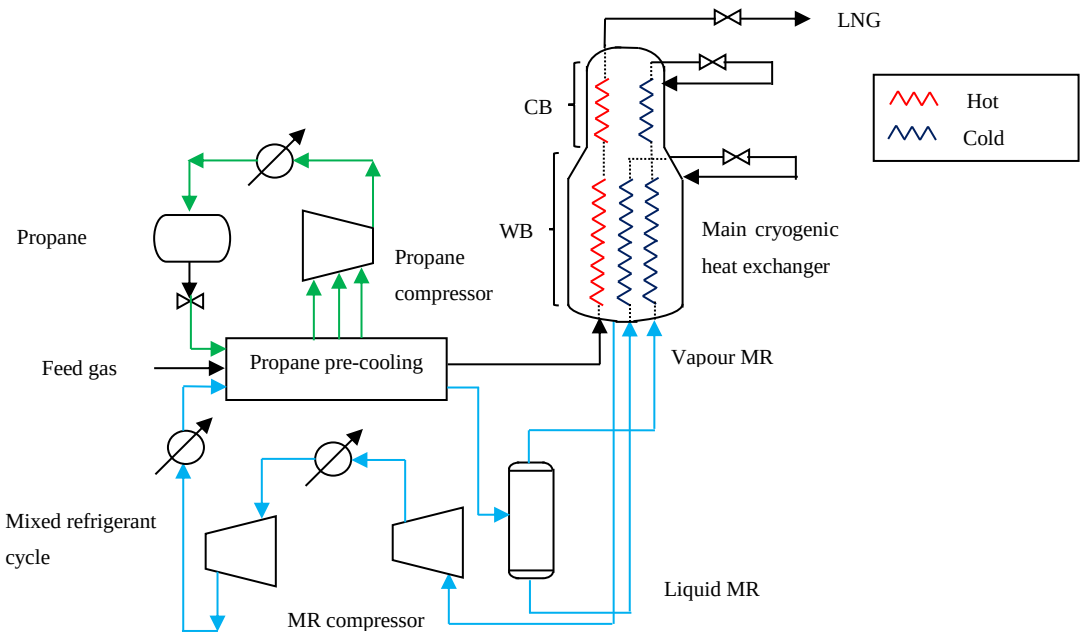

Figure 2.1: APCI Propane pre-cooled mixed refrigerant (C3MR) process; adapted from [26].

Figure 2.2: Propane kettle exchangers in LNG plants [62].

2.2.2 Split MR process

The APCI split MR or known as split C3MR process was developed to overcome the power imbalance between the propane and MR cycles [66] in the C3MR process. The process configuration for this process is the same as the C3MR process. The only difference is the arrangement of the gas turbines (GT) in the propane and MR cycles. As shown in Figure 2.3 this process utilises two GE Frame 7EA GT; the first GT drives the high-pressure MR (HP MR) and propane compressor together on the same shaft while the second GT drives the low and medium pressure MR (LP MR and MP MR) compressors only [67]. The propane compressor used here is of a single casing [40]. Besides, a helper motor below 20 MW is also installed in both cycles [40]. The available power from all the GTs and helper motors are fully utilised [30, 40, 67]. The HP MR consumes about 30% of the load from the GT. By having this process configuration, some of the MR load is transferred to the propane cycle and the power distribution between the two GTs [66] are equalised. This process has been applied in Rasgas train 3,4,5, Qatar [68]. The Rasgas train 3 capacity achieved is 4.7 MTPA [66]. Above 5 MTPA capacity, the propane compressor casing is increased into two but driven on the same shaft [40].

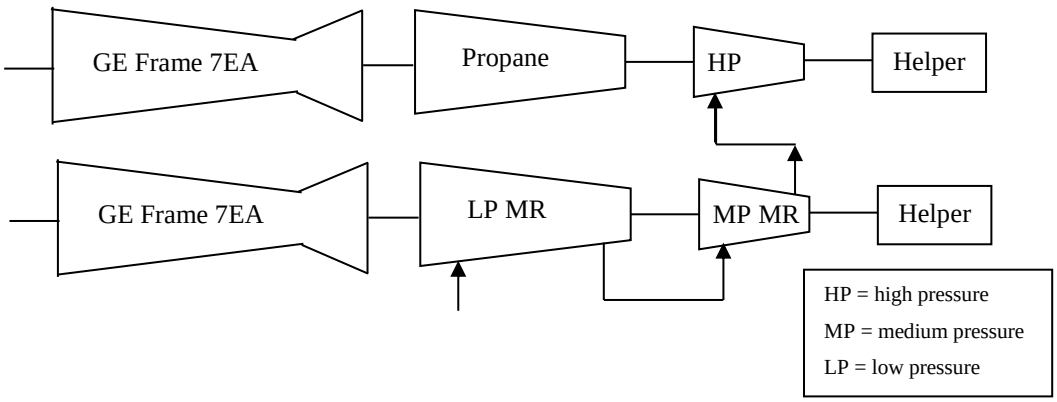

Figure 2.3: APCI Split MR (Split C3MR) process [64].

2.2.3 AP-X^{TM} process

The APCI-AP-X^{TM} process shown in Figure 2.4 [26] is derived from the C3MR process. This process consists of pre-cooling, liquefying and sub-cooling cycles. The process configuration of the pre-cooling and liquefying is similar to the C3MR process; however, two propane compressor casings are utilised. The natural gas feed stream is pre-cooled using pure liquid propane (green stream) and it is liquefied to about -120^{o}C using MR (blue stream) [26]. The only difference is the sub-cooling of natural gas is achieved using nitrogen refrigerant (purple stream).

The cold low-pressure N_2 gas from N_2-expander enters the MCHE from the top and sub-cools the natural gas. It is then pass through the plate fin heat exchanger (PFHE) followed by compression to high pressure. Next, this high-pressure N_2 gas is cooled using air and re-enters the PFHE to be further cooled by the low-pressure N_2 gas. The high-pressure N_2 gas is then expanded to lower pressure in the N_2-expander for final sub-cooling of the natural gas. The MCHEs are used for MR liquefaction and nitrogen sub-cooling cycles.

The AP-X process not only reduces the refrigerant flow rate of propane and MR but also enables a significant increase in the LNG capacity (approximately 8 to 10 MTPA) for a single train [30, 40, 69]. This process is suitable for a train size of 6.5 MTPA and beyond [40]. The first AP-X process was built in Qatar in 2008 with a nameplate capacity of 7.8 MTPA per train and it utilised three frame 9 gas turbines [40, 70]. The AP-X process layout is illustrated in Figure 2.5 [69].

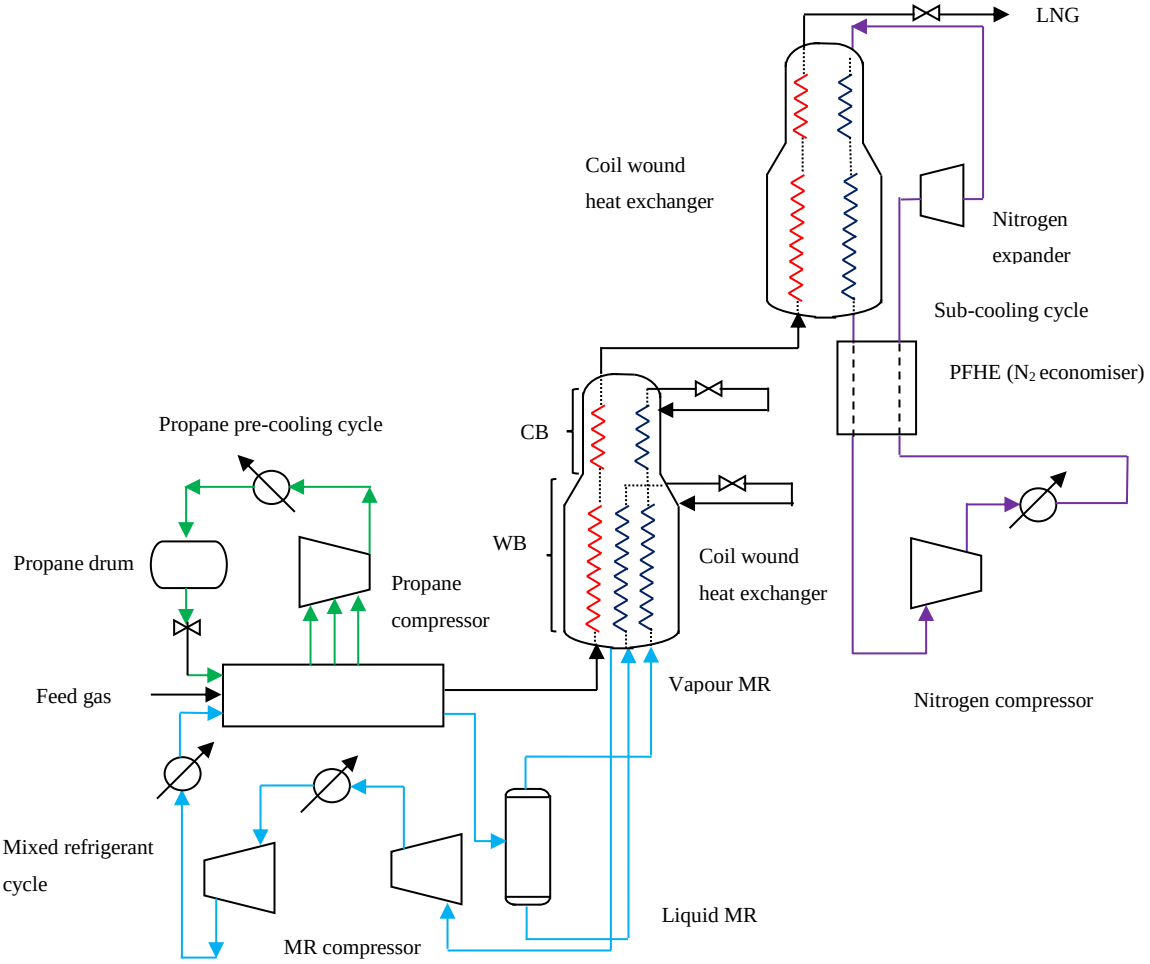

Figure 2.4: APCI-AP-X^{TM} process; adapted from [26].

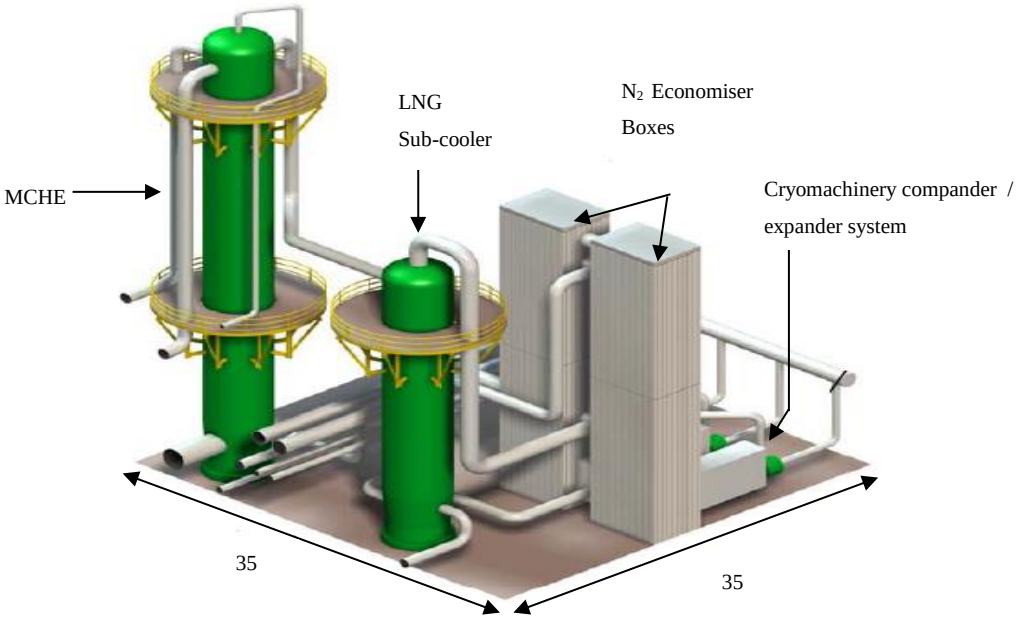

Figure 2.5: AP-X LNG process layout [69].

2.2.4 Dual mixed refrigerant (DMR) process

The licensors of DMR process are APCI and Shell. They developed this process to overcome the propane compressor size limitation [26]. The APCI-DMR version is shown in Figure 2.6 [71]. This process is a modification of the C3MR process whereby the pre-cooling cycle uses MR instead of pure propane. The pre-cooling MR can be formulated, for example using a mixture of propane and ethane [26, 30] or other components (methane, ethane, propane and butane) [71]. The MR mixture of the pre-cooling cycle is called warm MR (green stream). Both pre-cooling and liquefaction cycles use MCHEs supplied by Linde or APCI and the power requirement differs for each cycle [26].

In this process, natural gas feed is firstly pre-cooled to an approximate temperature of -50^{o}C, followed by liquefaction and sub-cooling to -153^{o}C using MR mixture of nitrogen, methane, ethane and propane [26] or called as cold MR (blue stream). The APCI-DMR process uses two compression stages for the pre-cooling cycle. The warm MR vapour leaving the MCHE-precooler is compressed in the first compressor. Next, the compressor discharge vapour is partially condensed and separated in a separator. The vapour from the separator is then further compressed in the second compressor while the liquid is pumped and mixed with the second compressor outlet. The mixed warm MR stream is then cooled prior to entering the MCHE-precooler. In the MCHE-precooler, the warm MR is flashed across a JT valve to provide cooling for the natural gas and cold MR streams.

Meanwhile, the cold MR enters the MCHE-liquefier to liquefy and sub-cool the natural gas. The process configurations can be modified and optimised to meet the project requirements [71]. The DMR process was first deployed in Sakhalin, eastern Russia for two trains each with 4.8 MTPA capacity. The trains used two MCHEs, cooled using ambient air enhanced by cold climate. Due to less number of equipment, the DMR process has also been selected for many FLNG projects [72].

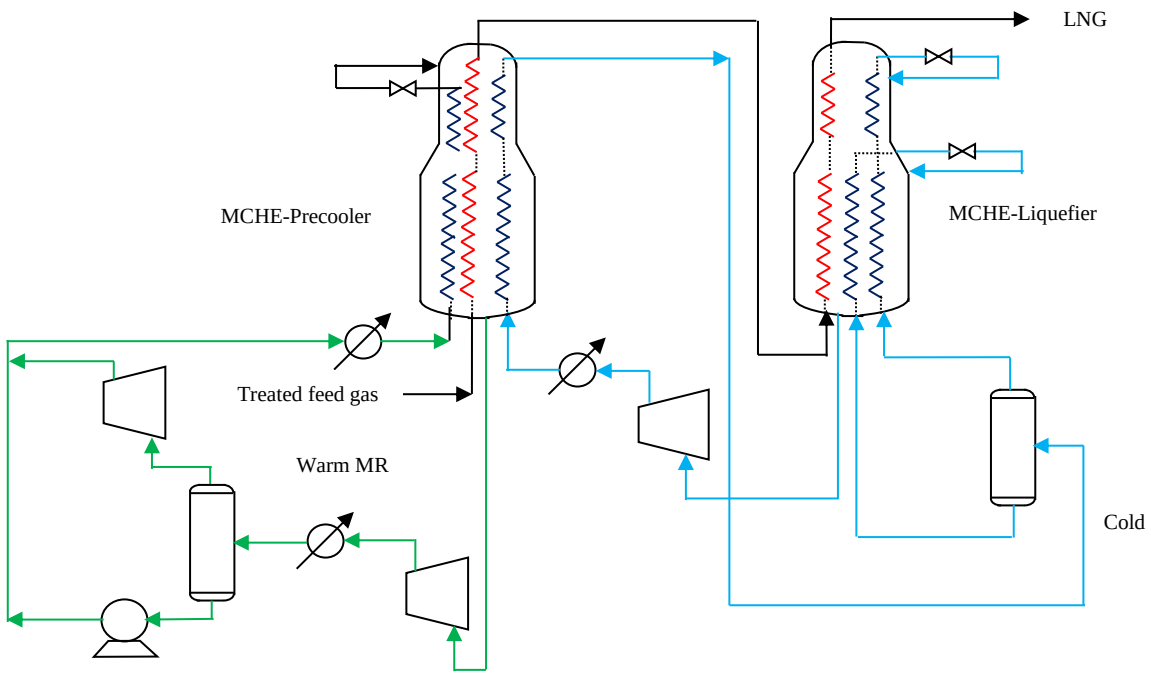

Figure 2.6: APCI- Dual mixed refrigerant (DMR) process; adapted from [71].

2.2.5 Parallel mixed refrigerant (PMR) process

Shell introduced another process called the parallel mixed refrigerant (PMR) which is an enhancement of the DMR process. As illustrated in Figure 2.7 [59], this process is similar to the DMR process as it uses two MCHEs for the cooling cycles. The PMR process can utilise either pure propane or MR as a refrigerant for the pre-cooling cycle.

As depicted in Figure 2.7, natural gas feed is first cooled in the MCHE – precooler followed by liquefaction and sub-cooled in the MCHE-liquefier. The vapour MR exiting the MCHEs is compressed and finally condensed prior to entering the MCHEs. In both cycles, electric motors are used to drive the refrigerant compressors [60] instead of the gas turbines. These compressors are set in parallel arrangement around each of the MCHE which helps to reduce the pressure drop across the system, hence enhances the process efficiency [59]. The PMR process can yield about 8 MTPA LNG capacity using existing compressors [59].

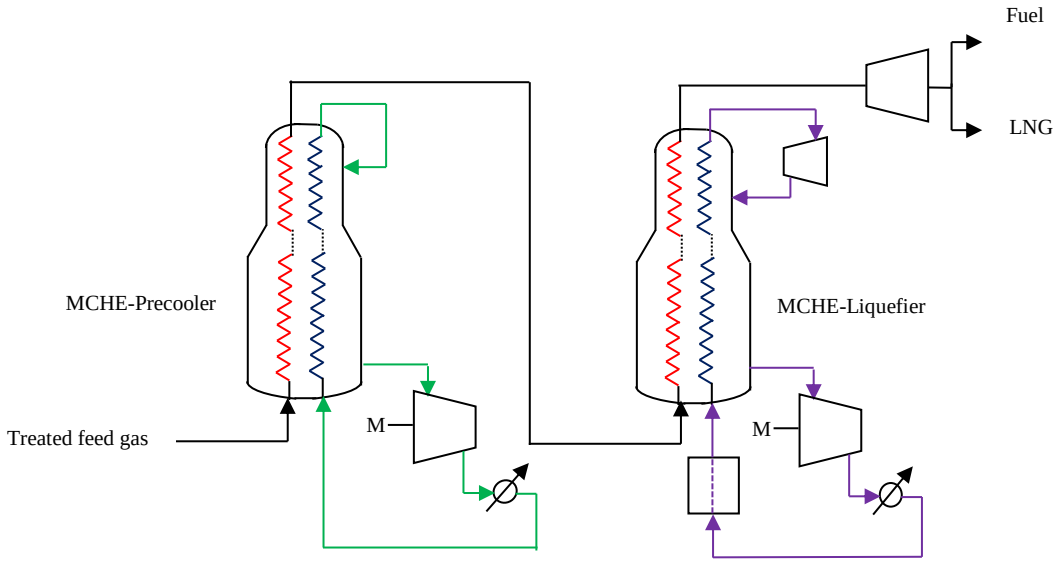

Figure 2.7: Shell - Parallel mixed refrigerant (PMR) process; adapted from [73].

2.2.6 Liquefin™ process

The Liquefin™ process was invented by IFP/Axens as shown in Figure 2.8 [74]. This process was developed to obtain a high LNG capacity using simple equipment setup with the aid of standard compressors [74, 75]. Both pre-cooling and liquefaction of natural gas are carried out using two different sets of MR compositions which are known as the heavy (green stream) and the light MR (purple stream). The heavy MR is used for the pre-cooling cycle while the light MR is used for liquefaction and the sub-cooling cycle. The MR is composed of nitrogen, methane, ethane, propane and butane [26, 61].

The overall conversion process of natural gas into liquid takes place in a bank of brazed aluminium plate-fin heat exchanger (BAPFHE). The BAPFHE is divided into two sections; pre-cooling and cryogenic section. In the pre-cooling section, the heavy MR pre-cools the natural gas feed, cools and condenses the light MR to about -50°C to -80°C [30, 76] at three different pressure levels. The pre-cooled natural gas is then separated from the NGL in a separator and re-enters the cryogenic section of the BAPFHE. Meanwhile, the condensed light MR exiting the BAPFHE is expanded and returned to the cryogenic section of BAPFHE to liquefy and sub-cool the natural gas. The light MR leaving the BAPFHE is compressed by two compression stages and cooled before re-entering the top of BAPFHE.

The pre-cooling and liquefying-sub-cooling cycles are designed such that the power-sharing is 50-50 for both cycles [77] to ensure that the same compressor driver can be used [26]. The BAPFHE can be manufactured by any independent supplier as it is non-proprietary equipment.

IFP/Axens stated that about 20% of total cost savings per tonne of LNG can be achieved compared to the C3MR process [78]. Nevertheless, the industries continue to have some doubts with regards to the commercial benefits claimed because no plant has yet been built using this technology. This process is suitable for a base load single LNG train up to 6 MTPA [61].

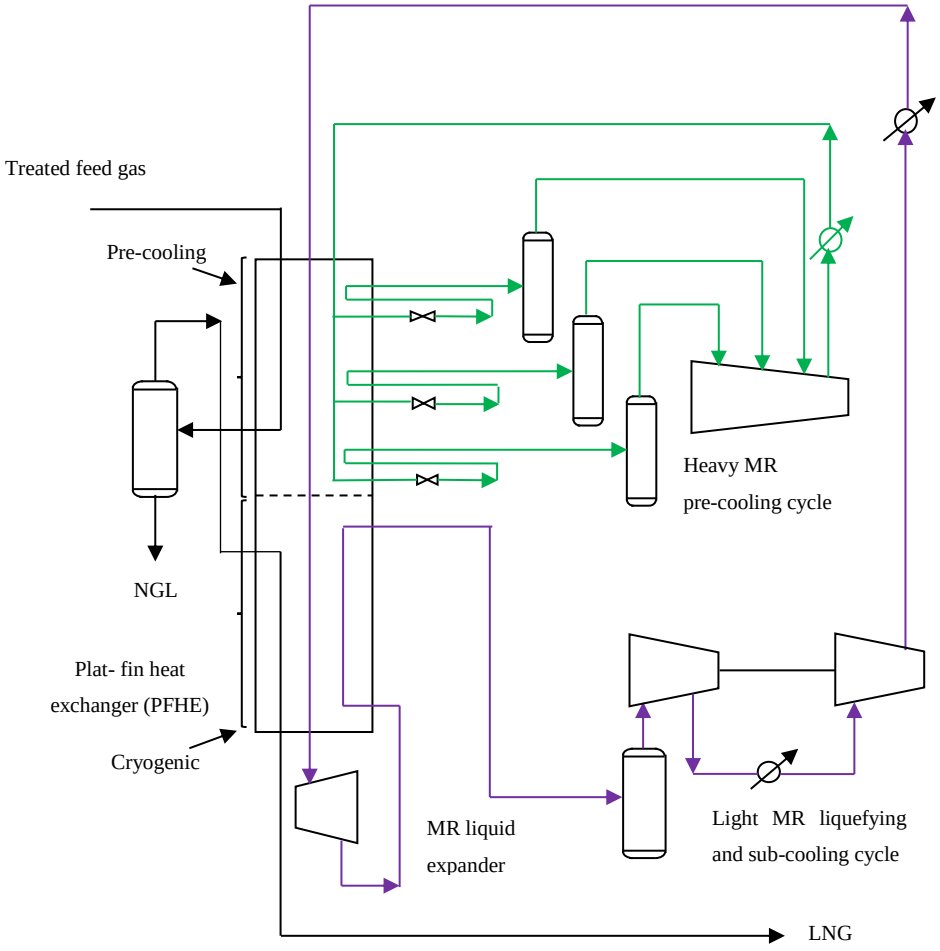

Figure 2.8: IFP/Axens - Liquefin^{TM} process; adapted from [74].

2.2.7 Mixed fluid cascade (MFC) process

The mixed fluid cascade (MFC) process was developed by Linde in collaboration with Statoil for LNG plants that are particularly located in the extreme environment. This process was selected for Snohvit LNG, Norway and installed on Melkoya Island, offshore Hammerfest (Northern North Sea) as depicted in Figure 2.9. The capacity of this single train is 4.3 MTPA [30]. This process consists of three cycles; pre-cooling, liquefaction and sub-cooling cycle. This process is solely utilising MR composed of nitrogen, methane, ethane and propane [26, 30, 61]. A different set of compositions are applied for each cycle. As shown in Figure 2.10 [79], the treated feed gas is pre-cooled, liquefied and sub-cooled using MR 1, MR 2 and MR 3 respectively in three separate cycles.

The pre-cooling cycle uses two PFHEs, whereas the liquefaction and sub-cooling cycles are employed with Spiral wound heat exchangers (SWHEs) made by Linde [80]. The SWHE can also be used for the pre-cooling cycle. Frame 6 and Frame 7 gas turbines can be used for a train size above 4 MTPA. The unique feature of this process is that the Snohvit LNG was the first and only major base load plant that used electric motors whereby three of 65 MW load-commutated inverter (LCI) drivers were installed for the purpose of start-up and variable speed control [68]. Till today, only one plant has been built using MFC process. Besides, since its start up in 2007, the plant has faced various operational issues. It has been reported that the heat exchangers were not performing well and require replacement [30].

Figure 2.9: Snohvit, LNG, Norway site construction (the year 2004) [81].

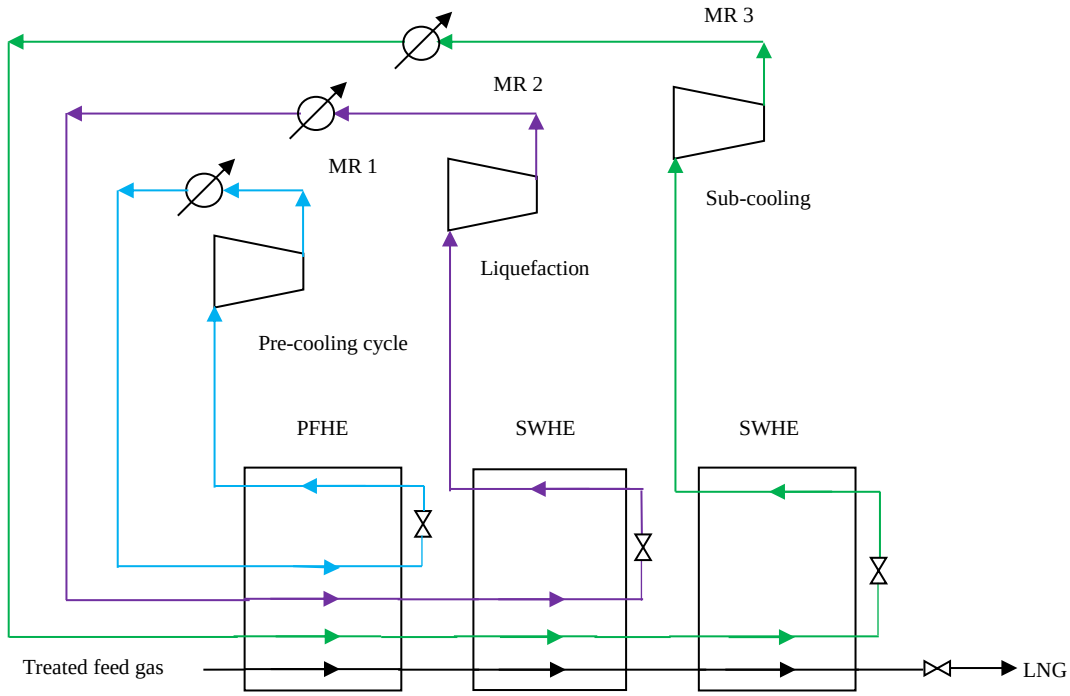

Figure 2.10: Statoil/Linde - Mixed Fluid Cascade (MFC) process; adapted from [79].

2.2.8 Phillips optimised cascade (POC) LNG process

The early version of Phillips cascade LNG process was developed in the 1960s. In 1969, this process was applied in Kenai LNG, Alaska with a single train capacity of 1.5 MTPA. The plant was built by Bechtel, United States (US) engineering company. Later, Phillips developed a new version of the cascade process called 'Phillips optimised cascade LNG process' and in 1999, it was applied in the Trinidad LNG plant [82].

As shown in Figure 2.11 [83], this process utilises three pure refrigerants namely propane, ethylene and methane for pre-cooling, liquefaction and sub-cooling cycles respectively. The pre-cooling cycle uses core-in-kettle type heat exchangers while the liquefaction and sub-cooling cycles employ a series of brazed aluminium PFHE heat exchangers arranged in vertical cold boxes [26]. In the pre-cooling cycle, the propane cools the natural gas and methane while it condenses the ethylene at approximately -30^{o}C [84]. The removal of compression heat and condensation of propane is achieved using air or cooling water. Following the pre-cooling cycle, natural gas and methane are liquefied using ethylene to about -90^{o}C [84]. Meanwhile, the heavier hydrocarbons are separated from natural gas after one or more stages of chilling by ethylene refrigerant. Finally, the condensed natural gas is sub-cooled by methane refrigerant to around -150^{o}C [84]. In the case where N_2 present in the methane refrigerant, a slip stream is drawn off to be used as fuel to avoid build-up of inerts [30]. The cooling of natural gas in each cycle occurs in two or three compression stages.

On the other hand, the POC LNG process applied 'two trains in one' configuration as depicted in Figure 2.12 [85]. As shown in Figure 2.12, each refrigeration circuit has two parallel compressors/drivers sets arrangement to serve the liquefaction exchangers. This approach improves the plant reliability and availability [26, 84-86], also assists in maintenance facility planning and provides highest turndown flexibility [84, 85, 87]. Highest turndown flexibility here is referring to continuous production even at a low rate; 0 to 100% or 60 to 80% capacity can be attained in the case where any of the refrigerant compressors is not in operation [87]. Additionally, this concept also saves time because it prevents shutting down the whole train due to repairing a machine [86]. Further, the usage of this unique design plus pure refrigerants helps to balance the power loads in each circuit [30, 82].

Though this concept increases the number of compressors/drivers per train, the overall power requirement for this process is relatively low [26]. Furthermore, according to Finn, Johnson [88], this process requires a small heat exchanger surface area per unit of capacity. This made the cascade LNG process suitable for large capacity trains as the low power demand and small heat exchanger size offsets the cost of having multiple machines [86]. This was proven in the year 2005, whereby the first single large LNG train was built in Trinidad (Train 4) with a capacity of 5.2 MTPA utilising POC LNG process [85, 87, 89]. This was considered a significant breakthrough in the liquefaction technology for the LNG industry.

Another essential point to mention is that the latest design of POC LNG process utilises aero-derivative gas turbines (Figure 2.13) which are light in weight, higher in efficiency [90] and consume less fuel gas. The overall process design has also been improved by having integrated heavies removal and nitrogen rejection units [85]. Additionally, this process has been widely applied across the world regardless of the climate conditions as shown in Table 2.1.

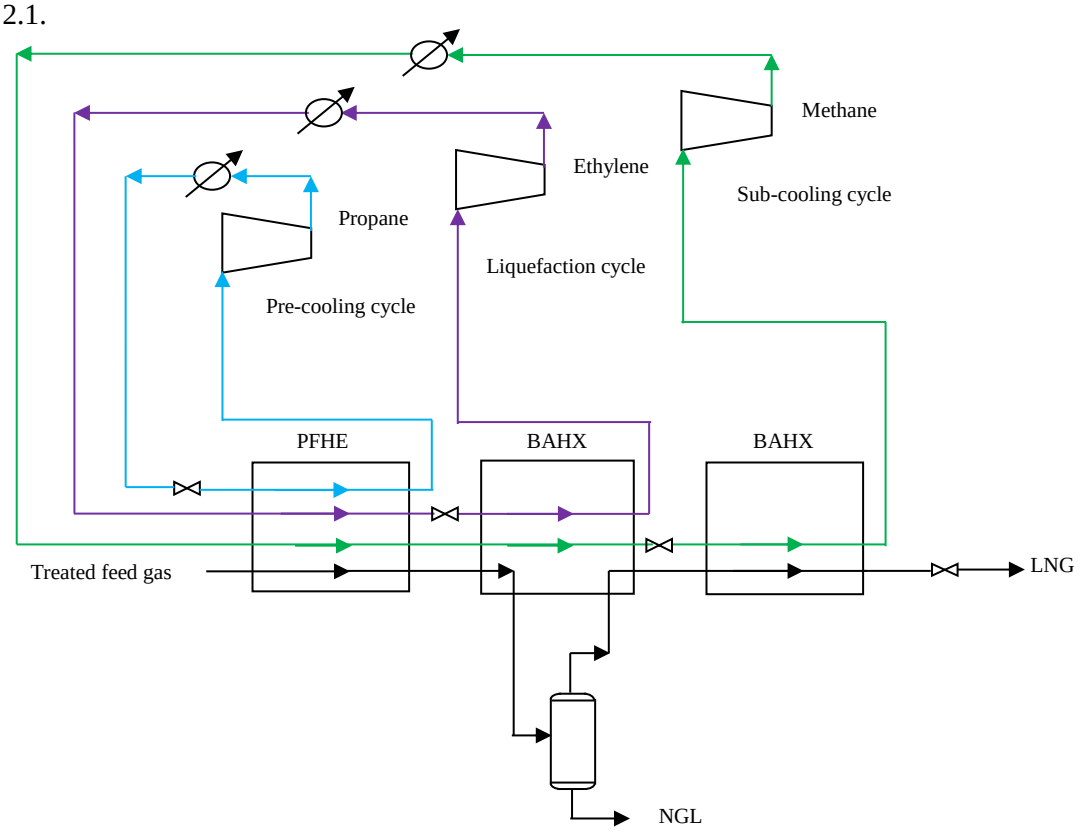

Figure 2.11: Phillips optimised cascade LNG process; adapted from [83].

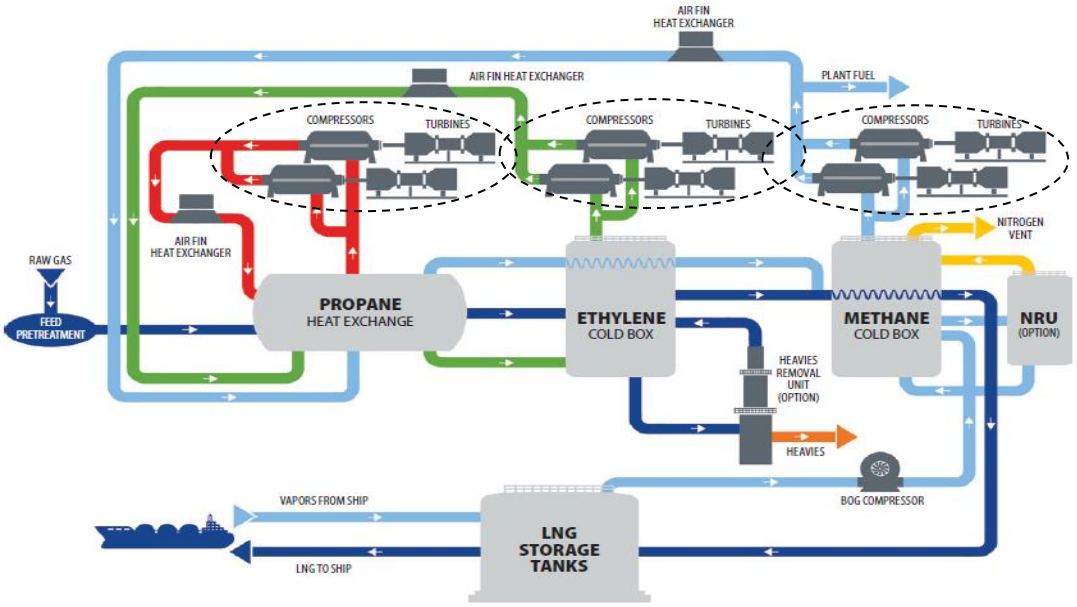

Figure 2.12: 'Two trains in one' concept of COP LNG process [78].

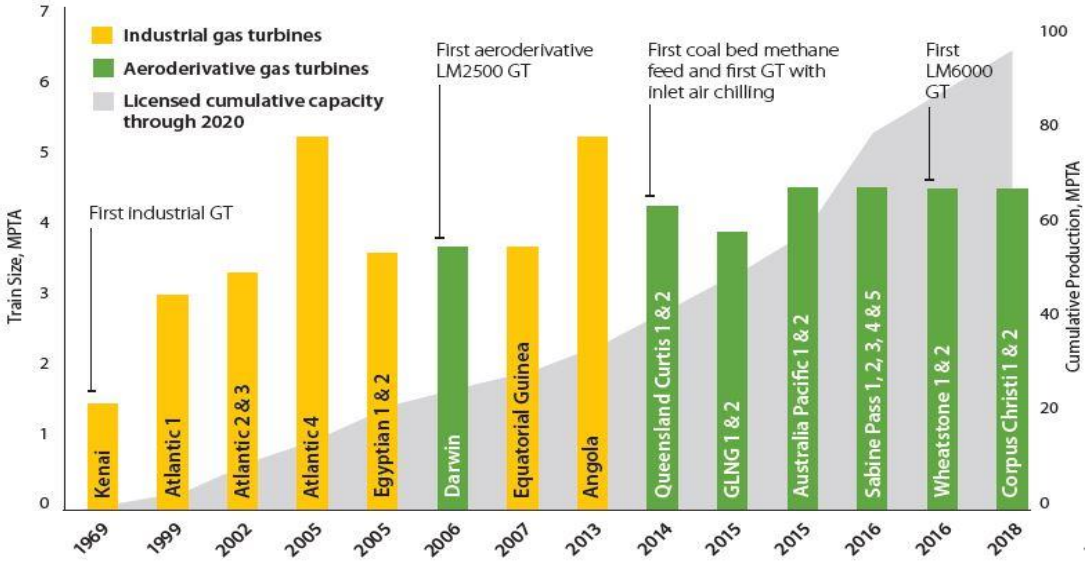

Figure 2.13: Type of gas turbine used in the past, current and future LNG plants that utilised COP cascade process [85].

Table 2.1: List of LNG plants utilising COP cascade LNG process [85].

LNG plants	Number of trains	Total trains Capacity (MTPA)	Location
Kenai LNG	1	1.5	Alaska, USA
Atlantic LNG	4	14.8	Point Fortin, Trinidad and Tobago
Egyptian LNG	2	7.2	Idku, Egypt
Darwin LNG	1	3.7	Darwin, Australia
Equatorial Guinea LNG	1	3.7	Malabo, Equatorial Guinea
Angola LNG	1	5.2	Soyo, Angola
Queensland Curtis LNG	2	8.5	Curtis Island, Queensland, Australia
Gladstone LNG (GLNG)	2	7.8	Curtis Island, Queensland, Australia
Australia Pacific LNG	2	9.0	Curtis Island, Queensland, Australia
Wheatstone LNG	2	8.9	Ashburton North, Western Australia
Sabine Pass Liquefaction	5	22.5	Cameron Parish, Louisiana, USA
Corpus Christi Liquefaction	2	9.0	San Patricio County, Texas, USA

The summary of the various LNG processes for large-scale LNG plant is given in Table 2.2. These processes are currently being applied in the LNG plants or may have been proposed for other LNG projects. In this research study, the cascade LNG process has been chosen as the preferred liquefaction technology for the production train of 5 MTPA. The detailed discussion about the selection of this process over other LNG processes is described in the next section.

Comparison	C3MR	Split MR (Split C3MR)	AP-X™	DMR	PMR	Liquefin™	MFC	POC
Nameplate capacity (MTPA)	1 – 4	4.7	7.8	4.8	8	6	4.3	5.2 (1.5 ~5.2) *existing plants
Remarks	75% of the world LNG plants utilised it [30].	Rasgas train 3,4, 5 (Qatar), Damietta plant, Egypt. *can reach up to 5 MTPA, > 5 MTPA, 2 propane compressor casings are required	suitable for train size 6.5 to 10 MTPA [40] *applied in 6 trains in Qatar	Sakhalin, Russia (only) *suitable for FLNG projects		no plant has used this process *power sharing of 50:50 for both cycles	Snohvit, Norway (only) *this process was developed for the extreme location	*can reach up to 8 MTPA [45] *applied concept of 'two trains in one'
Proven technology	Yes	Yes	Yes	Yes	No	No	Yes	Yes
Type of refrigerant used for each cooling cycle	Propane – pre-cooling MR – liquefaction and sub-cooling	Propane – pre-cooling MR – liquefaction and sub-cooling	Propane – pre-cooling MR – liquefaction N_2 – sub-cooling	MR for all cycles	MR for all cycles *Propane can be used in pre-cooling cycle	MR for all cycles	MR for all cycles	Propane – pre-cooling, Ethylene - liquefaction Methane – sub-cooling
Driver	Steam turbines and gas turbines	Gas turbines, helper motor *fully utilised power from all GTs and helper motors	Gas turbines, expander	Gas turbines	Electric motor	Gas turbines (standard compressors)	Electric motor	Gas turbines
Major equipment	Propane kettle HXs, MCHE (1), propane compressor (1), MR compressors (2)	Propane kettle HXs, MCHE (1), propane compressor (1), MR compressors (2)	Propane kettles HXs, MCHE (2), PFHE (1), expander (1), propane compressor ,2 casings (1), MR compressors (2), N_2 compressor (1)	MCHE (2), MR compressors (pre-cooler and liquefier)	MCHE (2), MR compressors (pre- cooler and liquefier), PFHE (1), expander	Brazed aluminium PFHE (1), MR compressors, liquid expander (1)	PFHE (2), SWHE (2), MR compressors (3)	Core in kettle HX, brazed aluminium HX, compressors (6)
Proprietary equipment	Yes, MCHE	Yes, MCHE	Yes, MCHE	Yes, MCHE	Yes, MCHE	No	Yes, SWHE	No

Table 2.2: Summary of LNG processes for the large-scale LNG plant

2.3 Why cascade LNG process?

The success of an LNG project is highly dependent on the type of liquefaction technology selected [26]. This is because the selected liquefaction process will determine the name plate capacity, duration of the whole LNG project planning and execution i.e. starting from the front-end engineering design (FEED) study to construction as well as the overall capital and operating costs. In this study, the cascade LNG process is chosen due to several reasons. As explained in section 2.2.8 and Table 2.2, cascade LNG process has established a strong position in the LNG industry based on its proven track record for more than four decades since the operation of its first plant; Kenai LNG, Alaska (1969). The concept of 'two trains in one' which has been applied has yields about 95% train availability and improved reliability [85]. This is proven based on Kenai, LNG plant record whereby the plant has achieved 38 years of uninterrupted cargo supply to Japanese customers [87, 91]. Other benefits obtained using this configuration have been discussed in section 2.2.8.

From an operation perspective, the use of pure components instead of MR makes this process safe, simple to operate and easy to understand [84]. In terms of safety, in the events of any flare or gas leaks occurring, the operators will take samples of the flare stream to locate the pressure safety valve (PSV) source or use infrared gas detectors to not only notify the gas leaks but also the identification of materials released [84]. The operation of this process is also flexible as each cycle is controlled separately [30], hence the power load between the cooling cycles can be adjusted by varying the pressure profile [84]. Besides, the pressure-temperature (PT) curves of the pure refrigerants can be programmed in the distributed control system (DCS) which assists the operators to act promptly in the case any refrigerants becoming off spec. Another advantage of using pure refrigerant is it can be reused after shutdown or major maintenance schedule. Whereas, the MR components (N_2, methane and ethane) can neither be stored nor reused [84] as it is usually flared during major maintenance schedules or startup as described by Brimm, Ghosh [66] for split MR process operation.

From the design context, the use of brazed aluminium heat exchangers (BAHE) or BAPFHE, standardised compressor and gas turbine type have helped to reduce the overall capital cost and duration of building a new LNG plant based on Trinidad LNG plant experience [86, 87]. This is because the exchangers can be purchased from numerous vendors at competitive prices [84] while Frame 5D gas turbine has a strong position in the market as it has been widely used in the earlier LNG plants. Meanwhile, there is no major leakage reported using this exchanger compared to MCHE. In the year 2004, Brunei LNG (BLNG), were involved in the MCHE replacement project for four trains (Train 1 to 4) due to frequent unplanned shutdown because of MCHEs leaks [92]. Besides, other LNG plants had also encountered the same incident, however, these plants are not to be disclosed in this thesis because of confidentiality reasons.

Figure 2.14: Lifting of Linde MCHE at BLNG plant [92].

Meanwhile, according to Nored [68], many new LNG projects have chosen this process because it has multiple machines, low driver power and able to utilise aeroderatives gas turbines. Based on the above discussion, hence the cascade LNG process is chosen for this research study.

2.4 Why 5 MTPA production train?

Numerous studies have been conducted that discussed the future LNG train size capacity. According to Nored [68], the current optimum LNG train size is in the range of 5 to 6 MTPA. Similarly, Spilsbury, McLauchlin [40] mentioned that the future LNG train size will be centred to 5 MTPA based on the historical LNG trend size data. In addition, Mokhatab, Mark [30] stated that the future LNG trains are likely to be in the range of 3 to 6 MTPA whereas trains size of 8 to 9 MTPA are only suitable in locations where there are very large gas reserves and huge market demand [45]. LNG train size of 8 MTPA may not be suitable for every brownfield and greenfield project because it requires continuous high plant reliability and availability, robust design, also needs to be provided with spare equipment so that the entire plant does not need to be shut down or started up in the event of equipment failure [30]. In another study, Eaton, Hernandez [45], categorized the future LNG trains size into three different capacities; 4 MTPA, 5 MTPA and 8 MTPA. Most of the LNG plants that have been built after the year 2000, the train capacity is 4 MTPA and suitable for the greenfield project that has limited gas supply. Meanwhile, the 5 MTPA train is suitable for the greenfield projects that requires lower equipment costs, have gas supply and sales availability. It is also the preferred option for LNG expansion projects, especially when copying an existing train design.

Based on these studies and data presented in Figure 1.7, Figure 2.13, Table 1.2, Table 2.1 and Table 2.2, it concludes that new liquefaction trains that have been built in the past 10 years are in the range of 3.4 to 5.2 MTPA capacities while for mega trains only 6 trains have been built. Moreover, Table 2.2 shows that only the POC LNG process has a proven track record that meets the 5 MTPA train capacity without any significant changes made in the design and meets all the criteria required to build a large LNG train. Based on this evidences and literature review, 5 MTPA is chosen for this research work.

2.5 Fundamentals principles of LNG processes

As mentioned in Chapter 1, section 1.2, liquefaction of natural gas is based on the principle of a refrigeration system whereby a refrigerant absorbs the heat from the natural gas stream in successive expansion and compression stages and rejecting it to a higher temperature using air coolers or cooling water. **This process requires a substantial amount of energy due to the usage of complicated refrigeration systems [26].** To understand better how a refrigeration system works, it is important to know and understand some basic ingredients of this system. A refrigeration system applies the fundamental laws of thermodynamics, uses various heat exchange terminologies such as latent and sensible heat to describe the internal process of the system and are based on thermodynamics expansion process. The description of these key elements will be described in the next section.

2.5.1 First and second laws of thermodynamics

The first and second law of thermodynamics is the basic principles used to understand the operation of a refrigeration system. For a process to occur, both these laws must be fulfilled [93]. The first law of thermodynamics is defined as the law of conservation of energy i.e. energy can neither be created nor destroyed and it can only change its form. In thermodynamics engineering principles, the change in energy of a system is contributed by kinetic energy (KE), internal energy (u) and potential energy (PE) [94]. Energy can be transferred to or from a system in three modes; mass, heat and work [93]. One of the important properties of this law is enthalpy (h) which has the relationship with internal energy (u), pressure (P) and specific volume (v) and can be defined as below:

$$h = u + Pv \tag{2.1}$$

where h and u are in kJ/kg, P is in kPa and v is in m^3/kg. The product of pressure times volume is kJ/kg. This property will further be used in the energy balance of a closed system. The concept of conservation of energy is depicted in Figure 2.15 [30]. As can be seen from Figure 2.15, a steady state control volume (CV) system where there is mass and energy entering and leaving the system and there is also heat and work interaction occurring between the system and the surrounding.

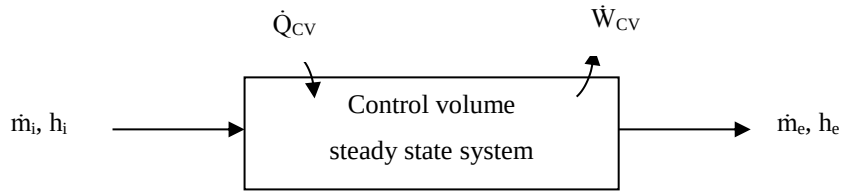

Figure 2.15: Steady-state control volume system; adapted from [30].

If the change in the kinetic, internal and potential energies are ignored, the change in the total amount of energy content of the CV between the inlet (i) and exit (e) of the system can be expressed as:

$$\sum_{i} \dot{m}_i h_i - \sum_{e} \dot{m}_e h_e + \dot{Q}_{CV} - \dot{W}_{CV} = 0 \qquad (2.2)$$

where $\dot{m}$ and h are the mass flow rate and enthalpy for the corresponding stream, $\dot{Q}_{CV}$ is the heat rate into the system and $\dot{W}_{CV}$ is the work rate leaving the system. As shown in equation (2.2), the total energy difference of the steady state CV system is zero; hence the total energy content is conserved. Equation (2.2) also represents the first law of thermodynamics.

The first law only focuses on the quantity of energy and the transformation of energy from one form to another regardless of its quality [93]. Conserving the quality of the energy (potential to produce work) [95] is important to engineers as well as degradation of energy during a process [93]. The quality of energy can be determined by performing a quantitative assessment on the system and this is done through the second law of thermodynamics. There are various statements which have been made to define the second law of thermodynamics. This is because this law is used to determine the theoretical limits for some of the engineering systems such as heat engines, refrigerators and also predicting the degree of completion of chemical reactions [93].

In this study, the second law of thermodynamics is referred to the Clausius statement which states that " it is impossible to construct a device that operates in a cycle and produces no effect other than the transfer of heat from a lower-temperature body to a higher temperature body" [93]. This statement explains the working concept of a refrigerator at home. Based on the Clausius statement, it can be said that a refrigerator will not work unless the compressor is supplied with power from an external source such as a turbine or an electric motor. The purpose of refrigeration is to maintain the refrigerated place at a low temperature (T_L) by eliminating heat (Q_L) from cooled space and rejecting this heat to an external source which is merely part of the cycle [93].

Figure 2.16 illustrates the working principle of a refrigerator as per the second law of thermodynamics. As can be seen from Figure 2.16, there is some interaction that can be observed between the system and the surroundings. Some net effect on the surroundings can be traced through the utilisation of energy in the form of work in addition to the heat transfer from the colder region to the warmer region. Hence, the refrigerator complies the Clausius statement for the second law.

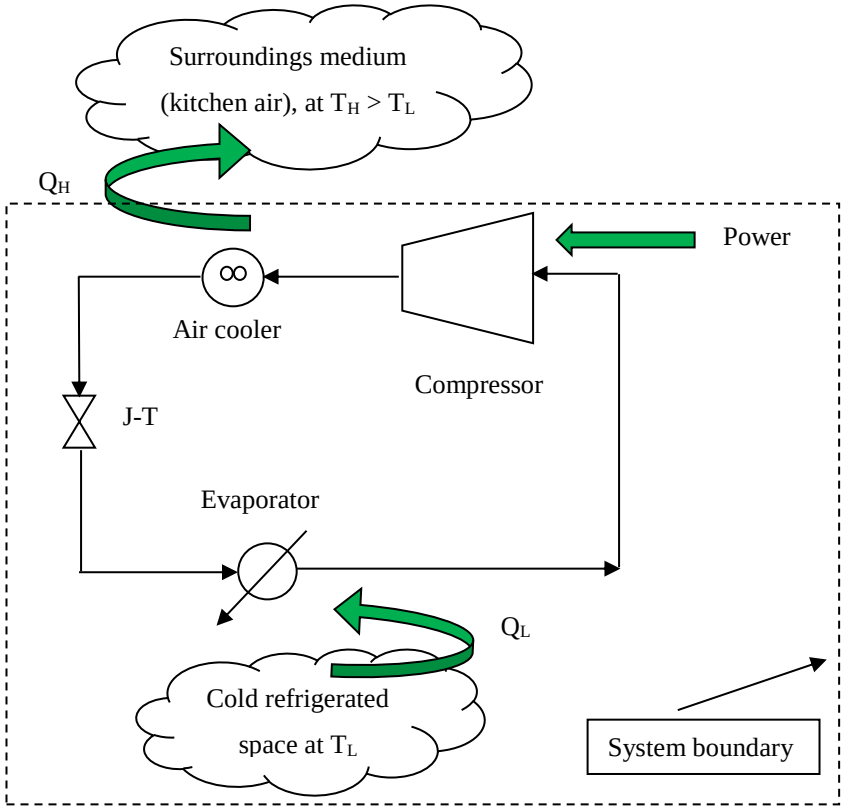

Figure 2.16: Second law of thermodynamics (Clausius statement) - Refrigerator.

Another important property that is included in applying the second law of thermodynamics is entropy. Entropy is defined as a measure of molecular arbitrariness or molecular disorder in a system and it is not conserved. The entropy of a substance is the lowest in the solid phase and highest in the gas phase [93]. This is because in the solid phase the molecules are compact and less movement occurs compared to the gas phase where the molecules move randomly and collide with each other. The presence of entropy will determine whether a process is reversible or irreversible. A process that does not generate a net entropy is called reversible. In a reversible process; both the system and surroundings can be exactly restored to their initial states while for an irreversible process this is impossible. Additionally, in a reversible process, the energy is neither degraded nor potential to do work is lost.

In an actual process, the amount of energy is always preserved as per the first law, however, the energy quality is bound to degrade due to the increase in the entropy [93]. The increase in the entropy occurs because of irreversibilities effects such as friction, unrestrained expansion of gas or liquid to a lower pressure, compression of gas to a higher pressure, mixing of the matter of different compositions or states and heat transfer through limited temperature difference [30, 93]. For example, in Figure 2.17, about 10 kJ of heat is transferred from the hot medium to the cold medium. During this process, the randomness and the entropy of the hot medium reduce while the molecular disorder and entropy of the cold medium increase. At the end of the process, the 10 kJ is still available but at lower temperature and at lower energy quality because the net entropy increased.

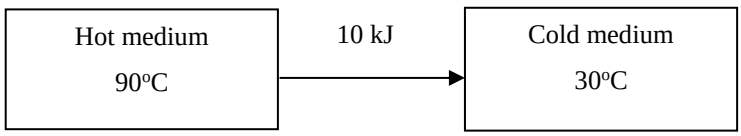

Figure 2.17: Entropy change for a heat transfer process.

As discussed above, for a process to occur, it must comply both with the first and second law of thermodynamics. The first law only discusses the change of energy from one form to another, modes of transfer (heat, work and mass) and the amount of energy of a steady state CV remains constant. Meanwhile, the second law discusses the requirement of an external power source to transfer heat from the cold to the hot medium and the potential of producing work when interacting with the surroundings. Additionally, two important thermodynamic properties were introduced which are enthalpy and entropy with respect to the first and second law. **The combined application of the first law and second law of thermodynamics will be used to evaluate the process efficiency and performance of the liquefaction process in this research work which will be further described in section 2.8 of this chapter.**

2.5.2 Heat exchange terminologies of a refrigeration system

There are various heat exchange terminologies applied in a refrigeration process such as superheat, sub-cooling and sensible and latent heats. It is important to recognize the definition of these terminologies to understand the thermodynamics and troubleshoot the refrigeration cycle. These terminologies are explained by using propane as an example in the propane refrigeration cycle.

2.5.2.1 Superheat

The term superheat is only applicable for a substance that is in a gas or vapour state. For example, liquid propane has a boiling point of -42^{o}C, at 1 atm. When propane is heated up to -32^{o}C, it is said that propane vapour contains 10^{o}C of superheat. In the propane refrigeration cycle, as shown in Figure 2.18, the propane is in vapour phase before entering the compressor. It is then compressed to a higher pressure; 20.73 bar and has a temperature of 82.6^{o}C. At this stage, the propane is in superheated condition. Desuperheater is used in the propane cycle to remove this superheat condition. The boiling temperature of a liquid depends on its pressure. By increasing the evaporator pressure, it increases the boiling point of the liquid propane. This is because there is more pressure exerted on the liquid surface to be overcome by the liquid molecules. Hence, by controlling the pressure of the liquid through the evaporator pressure, the boiling temperature can be altered. This is one of the important parameters that is used in this study to improve the propane cycle efficiency.

2.5.2.2 Sub-cooling

Sub-cooling is a term applied for a substance which is in the liquid or solid state. For example, in Figure 2.18 above, the propane is in liquid form after the condenser at a temperature of 57^{o}C and 19.93 bar. It is the further cooled to 42^{o}C at pressure 19.58 bar. It is said that the propane has been sub-cooled from 57^{o}C to 42^{o}C that is sub-cooled by 15^{o}C.

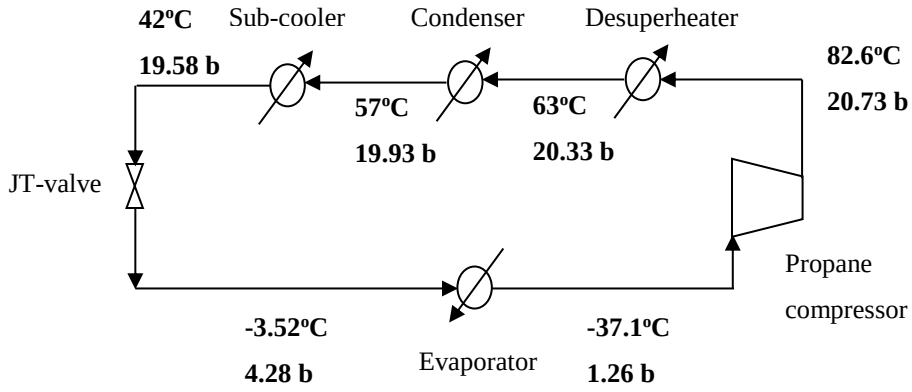

Figure 2.18: Simplified propane refrigeration cycle.

2.5.2.3 Sensible heat and latent heat

Any change in the temperature of a substance without changes in a phase is called sensible heat. This change in temperature can be measured using a thermometer. Sensible heat is used for superheat and sub-cooling as both processes involve changes in temperature. In the propane refrigeration cycle, for superheated propane, its temperature changes from -37.1ºC to 82.6ºC while for the sub-cooled propane, the temperature drops from 57ºC to 42ºC. Both these processes don't involve phase change. Meanwhile, the term 'latent heat' or in Latin the word 'latent' means hidden due to this heat cannot be measured by a thermometer as the temperature remains constant. This latent heat involves phase change of a substance from a liquid to vapour phase or vice versa and it occurs at a constant temperature. In the propane refrigeration cycle, the latent heat of vaporisation takes place in the evaporator whereby the liquid propane is boiled at constant temperature provided the evaporator pressure is maintained. The quantity of heat (energy) absorbed during vaporisation is equivalent to the amount of heat (energy) released during condensation and it is specifically called the 'latent heat of vaporisation'[93]. The amount of latent heat depends on the temperature or pressure at which the phase change takes place.

2.6 Thermodynamics expansion processes

The refrigeration system design is based on different thermodynamics expansion processes. There are three types of thermodynamics expansion processes which have been applied in the existing LNG plants namely Joule-Thomson (JT) expansion, Brayton expansion and Claude expansion. Two most commonly used expansion processes are the JT and Brayton.

2.6.1 Joule Thomson expansion process

During the early developments of LNG plants, the Joule Thomson (JT) expansion process was the first and the only method applied to cool the gas streams [96]. The JT expansion process is shown in Figure 2.19 [97]. This expansion process does not involve any work or heat transfer. This is because the JT valve is insulated which make it adiabatic i.e. no heat transfer occurs with the surroundings and no net change of internal energy to KE of mass motion is observed [96-98]. Therefore, the enthalpy of the fluid (refrigerant) remains constant, hence it is an isenthalpic expansion process. The JT expansion works by throttling a refrigerant via a flow resistor such as valve or orifice [96] whereby reverse of the fluid is impossible, thus it is an irreversible process.

The liquid refrigerant flows across the valve and expanded into two phases; liquid and vapour. This causes a reduction in the temperature and pressure of the refrigerant. The cooled refrigerant exchanges heat with natural gas (NG) feed flowing in the counter current direction. The refrigerant vaporises and is compressed to a higher pressure. Then, the high-pressure refrigerant is desuperheated using an air cooler (AC) and is condensed in the heat exchanger (HX) prior to being expanded again via the JT valve. The degree of cooling or cooling effect is highly dependent on the thermodynamics property of the refrigerant [97]. This is due to the different composition of the refrigerant as both pure and MR can be used in the JT expansion process. The JT expansion is a simple and low capital cost process [99]. A refrigerant cycle with the JT expansion configuration is known as ‘JT cycle’[97]. In this study, the cascade LNG process applies to the JT expansion process.

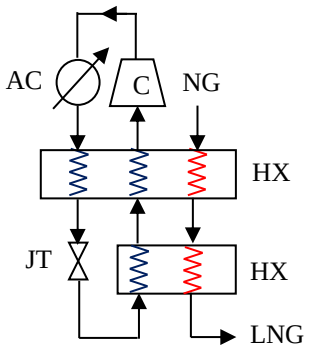

Figure 2.19: JT expansion; adapted from [97].

2.6.2 Brayton expansion process

The Brayton expansion utilises a turbo-expander or an expansion engine. As shown in Figure 2.20 [97], the Brayton expansion process provides cooling through the isentropic expansion of a gas at high pressure to lower pressure. The reduction in enthalpy of the expanded gas stream generates power. The power generated from the expander can be used to drive the compressor shaft in a refrigeration system [100]. The refrigerant must be in gas phase throughout the cycle above its saturated vapour pressure to ensure safe operation of the expander [97]. This process is a reversible process as it is operated isentropically (constant entropy), hence known as 'reverse-Brayton cycle'. This expansion process is suitable for offshore LNG plants and plants with small capacities [30, 100, 101]. The Brayton expansion process forms the root of liquefaction expander based process [26].

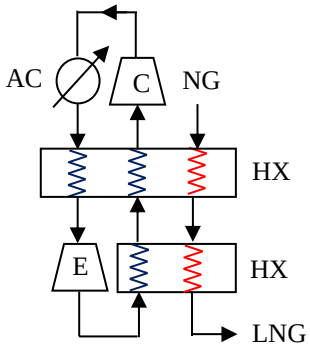

Figure 2.20: Brayton expansion process; adapted from [97].

2.6.3 Claude expansion process

As shown in Figure 2.21, the Claude expansion process is a combination of JT and Brayton cycles. The cooled high-pressure refrigerant leaving the top HX is separated into two streams. for further cooling. The first stream is expanded isentropically using an expander while the second stream is cooled in the subsequent HX and finally throttled through a JT valve to achieve the lowest temperature. This combined expansion process has been applied in the AP-X (APCI) liquefaction technology as previously shown in Figure 2.4.

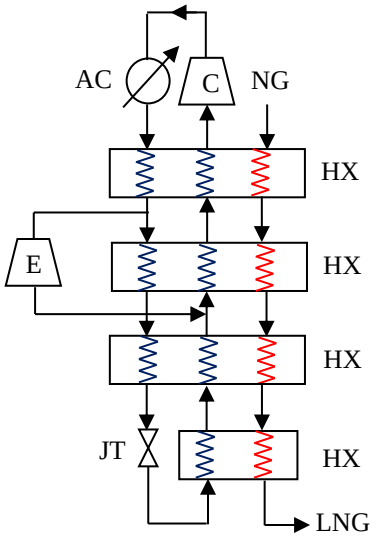

Figure 2.21: Claude expansion process; adapted from [97].

2.7 Refrigeration systems

Liquefaction of natural gas is achieved by removing the sensible and latent heat over a wide range of temperatures with the aid of single or multiple refrigerants [88], hence a complex refrigeration system is required. Two types of refrigeration systems are available namely compression refrigeration and absorption refrigeration [102]. In the LNG plants, mostly compression refrigeration systems are employed [26].

2.7.1 Types of the compression cycle

There are two types of refrigeration compression cycles viz. ideal compression and non-ideal compression cycle. Ideal here means the process is conducted isentropically i.e. no change in the entropy [102] and every equipment in the cycle is working perfectly. For example, the adiabatic efficiency of expanders and compressors are assumed 100% (i.e. isentropic process) while the heat exchangers minimum temperature difference and pressure drop across all flow components is zero [97].

2.7.1.1 Ideal compression cycle

The ideal compression cycle is shown in Figure 2.22 [102]. This single cycle consists of an evaporator, a compressor, a condenser and an expander. The working principle of this cycle is described using a pure refrigerant as the working fluid. The cycle operates as follows. At point 1, a mixture of vapour and liquid refrigerant enters the evaporator. The liquid refrigerant absorbs the heat at a constant temperature (isothermal) and pressure (isobaric) and vaporises; producing the cooling effect prior to exiting the evaporator at point 2. This heat is called 'latent heat of evaporation' as described earlier in section 2.5.2.3. Next, all the vapour refrigerant is compressed isentropically in the compressor to higher pressure from point 2 to 3. At point 3, the vapour refrigerant is at superheated state due to the compression process. Following the compressor, from point 3 to 4 the superheated vapour refrigerant is desuperheated and condensed at constant pressure in the condenser. This process causes a decrease in the enthalpy of the refrigerant and it leaves the condenser at saturated liquid state. Finally, the liquid refrigerant is expanded isentropically in the expander to lower pressure from point 4 to 1. The expansion of the liquid refrigerant produces a cooling effect for the refrigeration and the cycle continues.

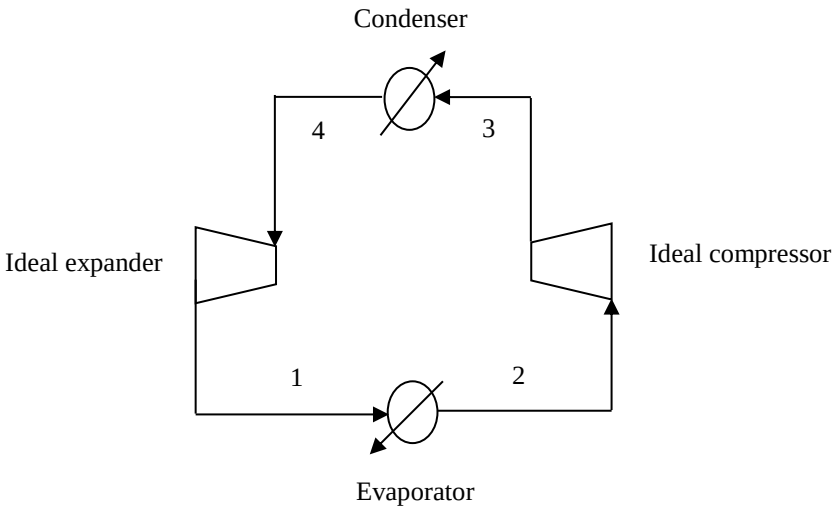

Figure 2.22: Ideal compression cycle; adapted from [102].

The relationship between temperature (T) and entropy (S) and pressure (P) and enthalpy (H) of the ideal compression cycle are illustrated in Figure 2.23 and Figure 2.24 respectively. Figure 2.23 shows the ideal compression on the temperature-entropy (T-S) diagram. The diagram is a two-phase envelope of a refrigerant; right-hand side of the curve indicates that the refrigerant is in the vapour (V) phase, inside the curve the refrigerant present in both liquid (L) and vapour (V) phases and to left-hand side of the curve, the refrigerant is in liquid (L) phase. Beginning from point 1 to 2, the refrigerant in two-phase mixture enters the evaporator where isothermal vaporisation takes place. From point 2 to 3, the vaporised refrigerant is compressed isentropically in the compressor and this stage is assumed to be ideal. The isentropic process ends at point 3. Next, the superheated refrigerant is first desuperheated (remove heat) and finally condensed isothermally in the condenser to point 4. At this stage (4), the refrigerant is in a saturated liquid state. Lastly, from point 4 to 1, the liquid refrigerant is expanded isentropically and this expansion is ideal where no entropy increase occurs.

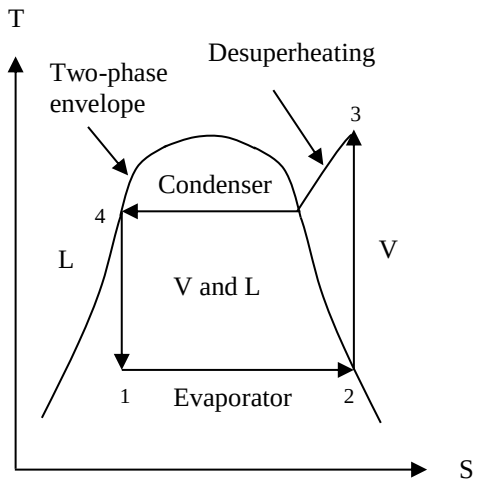

Figure 2.23: Ideal compression cycle on temperature-entropy (T-S) diagram; adapted from [102].

Meanwhile, Figure 2.24 shows the same cycle represented on pressure-enthalpy (P-H) diagram. As can be seen from Figure 2.24, the enthalpy of the refrigerant rises from point 1 to 2 in the evaporator. Then, from point 2 to 3, an increase in the pressure and enthalpy of compressor occurs. Next, from point 3 to 4, the pressure remains unchanged but a decrease in the enthalpy is observed due to desuperheating and condensation. Finally, the decrease in pressure occurs in the expander from point 4 to 1 and since the expansion is isentropic, drop in enthalpy is observed.

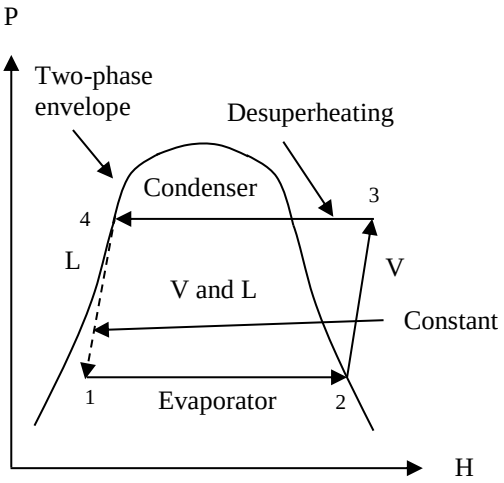

Figure 2.24: Ideal compression on pressure-enthalpy (P-H) diagram; adapted from [102].

2.7.1.2 Non-ideal compression cycle

The non-ideal compression cycle is shown in Figure 2.25 [102]. This single cycle is made up of an evaporator, a compressor, a condenser and a valve. The cycle operation is the same as the ideal-compression cycle; however, the compression of the refrigerant features non-isentropic and the expansion is done at constant enthalpy (i.e. isenthalpic) using an expansion valve instead of the ideal expander.

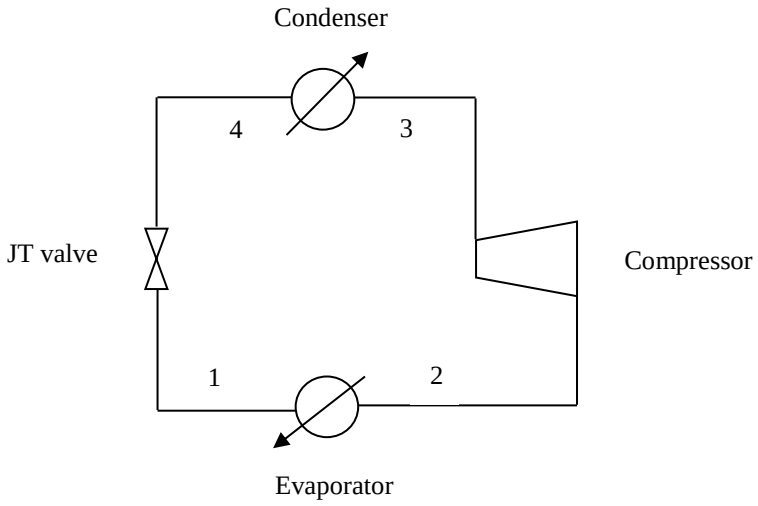

Figure 2.25: Non-ideal compression cycle; adapted from [102].

Figure 2.26 [102] represent the non-ideal compression on the temperature-entropy (T-S) diagram. The cycle operates at the same condition from point 1 to 2 and 3 to 4 as per the ideal compression. However, from point 2 to 3 and 4 to 1, the compression and expansion of the refrigerant features increase in entropy compared to the ideal compression (dotted line). The increase in the entropy makes this cycle a non-ideal compression.

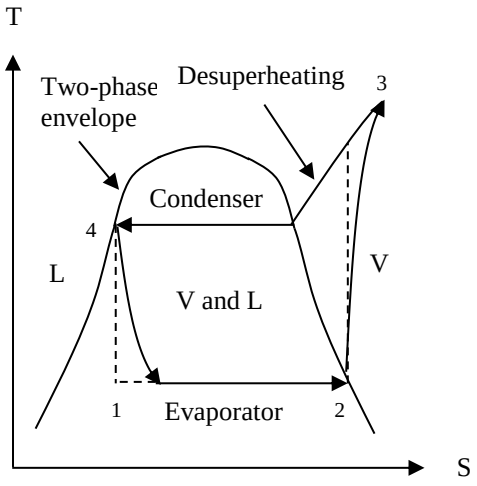

Figure 2.26: Non-ideal compression cycle on temperature-entropy (T-S) diagram; adapted from [96].

The non-ideal compression is presented on the pressure-enthalpy (P-H) diagram as per Figure 2.27 [102]. The operation of this cycle is basically the same as per the ideal compression from point 1 to 2 and 3 to 4. However, from point 2 to 3 the compression of the refrigerant causes a substantial increase in the enthalpy compared to the ideal compression (dotted line). Whilst, the expansion of the refrigerant is achieved isenthalpically from point 4 to 1 which differ from the ideal case.

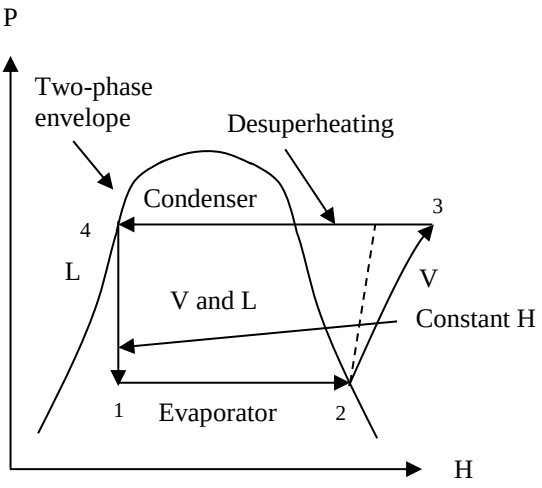

Figure 2.27: Non-ideal compression cycle on pressure-enthalpy (P-H) diagram; adapted from [102].

Based on the discussion in section 2.5, 2.6 and the operation of ideal and non-ideal compression cycles forms the fundamentals of the refrigeration cycle applied in a base load LNG plants. Most of these plants utilise complex refrigeration systems which are derived from a single refrigeration cycle. A single refrigeration cycle is not suitable to cool LNG over a wide range of temperatures. As mentioned by Khan and Lee [103], to obtain LNG, a large amount of energy is required; (about 1370 kJ/kg of LNG is required). Hence, to minimise this huge energy consumption, the refrigeration cycle configuration needs to be modified. One of the ways to change the configuration is by introducing multistage compression and expansion [102] which not only reduces the workload of a single refrigerant compressor but optimises the overall efficiency [26]**.** In this study, the cascade LNG process uses the multistage compression and expansion configuration which is based on non-ideal compression cycle principle. There are various multistage compression and expansion configurations available which will be discussed in the next section.

2.7.2 Multistage compression and expansion

Three types of multistage compression and expansion cycles are available which are as follows; multistage compression and expansion using a separator (economiser) with an inter-cooler, multistage compression and expansion with a presaturator and cascade cycle. Figure 2.28 [102] illustrate the multistage compression and expansion using a separator. The expansion process is conducted in two stages; from point 6 to 7 and from 8 to 1. A separator is utilised after the first expansion where the liquid leaving from the separator (stream 8) is further expanded (stream 1). The vaporised refrigerant (stream 2) is fed into low pressure (LP) compression stage. The discharge of the LP compressor stage (stream 3) is then cooled using an inter-cooler followed by mixing with the vapour refrigerant stream (stream 9) from the separator and then fed (stream 4) to the HP compressor stage.

The introduction of a separator between these two stages reduces the amount of refrigerant vapour flow from entering the LP compressor stage while the inter-cooler assists in reducing the inlet temperature (degree of superheat) to the HP compressor stage. The use of a separator and inter-cooler between these stages reduces the total compression power. However, the installation of an inter-cooler is not practicable for a low-temperature cycle [26]. The pressure-enthalpy (P-H) diagram of this configuration is shown in Figure 2.29 [102]. As can be seen from Figure 2.29 [102], the overall operation method is the same as per non-ideal compression cycle whereby the evaporation and condensation are occurring at isobaric (constant pressure) conditions while the expansion is isenthalpic. The only difference is the introduction of an intermediate level with a separator and inter-cooler between the two compression stages.

Another point to mention is although the degree of superheat of stream 3 is reduced due to the inter-cooler, the inlet vapour refrigerant stream to HP stage i.e. stream 4 is still in a superheated state.

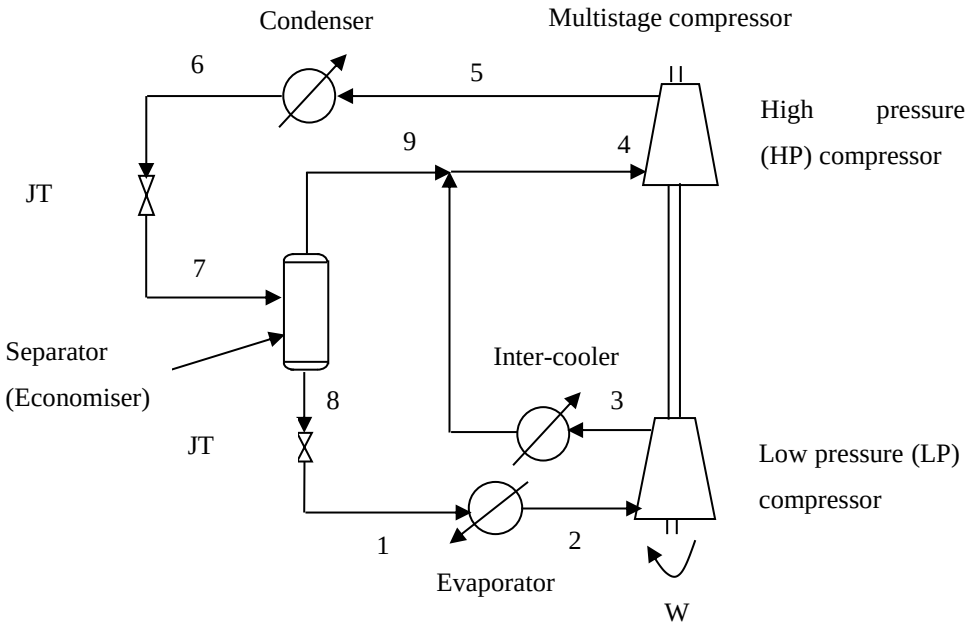

Figure 2.28: Multistage compression and expansion using a separator, adapted from [102].

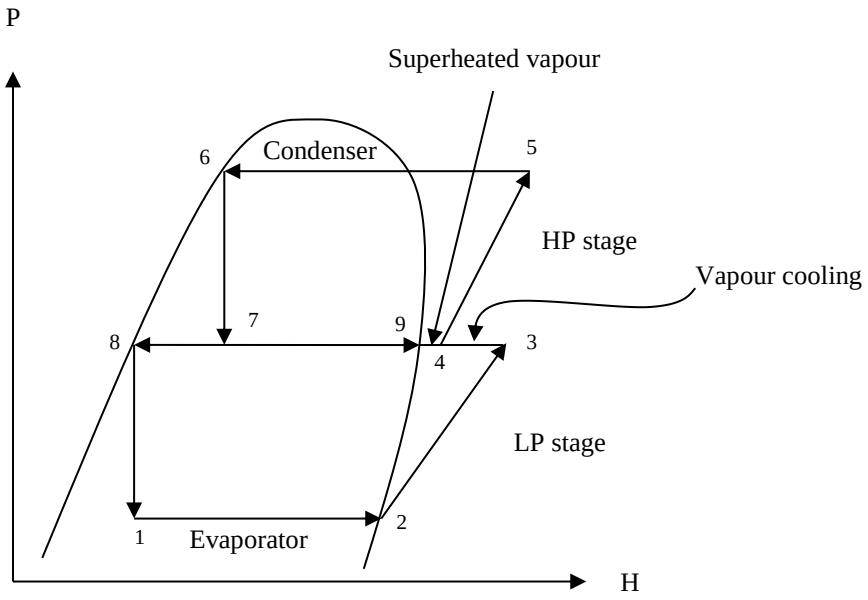

Figure 2.29: Pressure-enthalpy (P-H) diagram for multistage compression and expansion with a separator; adapted from [102].

Figure 2.30 [102] shows another scheme of multistage compression and expansion that can reduce the overall power consumption of a refrigeration cycle. The separation between the vapour and liquid is attained using a presaturator instead of a separator. The refrigerant vapour (stream 3) from LP stage is fed to the presaturator which cools it to saturated vapour state (i.e. remove the degree of superheat to zero). The presaturator reduces the inlet temperature of stream 4 to the HP stage via direct contact with the liquid refrigerant, thus reduces the compression power. Nevertheless, the presaturation process needs a large amount of vapour refrigerant flow rate [26].

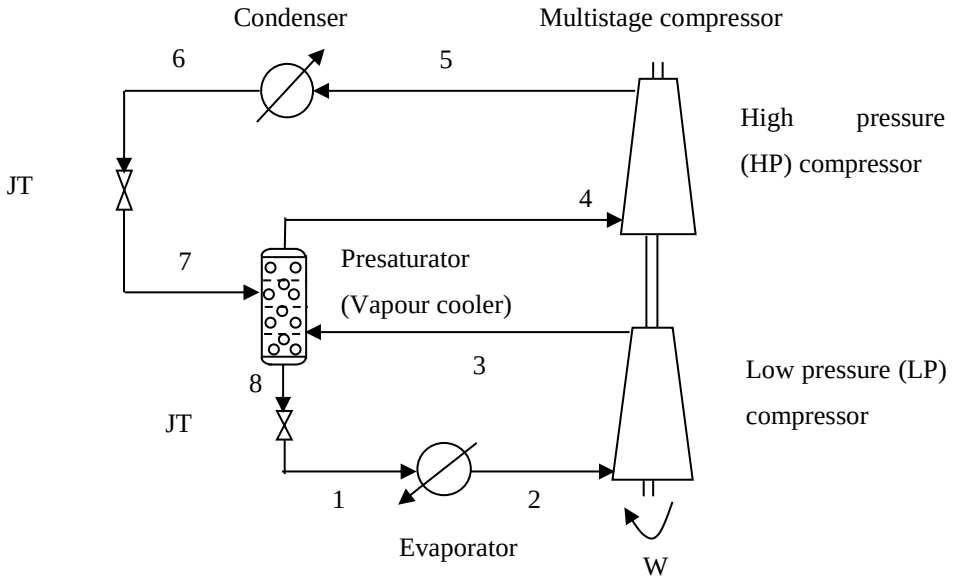

Figure 2.30: Multistage compression and expansion with a presaturator; adapted from [102].

The pressure-enthalpy (P-H) diagram of Figure 2.30 [102] is presented in Figure 2.31 [102]. As can be seen from Figure 2.31 [102], the vapour refrigerant discharge from the LP stage (stream 3) is desuperheated until it reaches the saturation vapour line. The degree of superheat at this saturation line is zero, hence the inlet temperature to the next compression stage is reduced. This minimises the compression power. Other processes such as evaporation, condensation and expansion occur as per the non-ideal compression cycle.

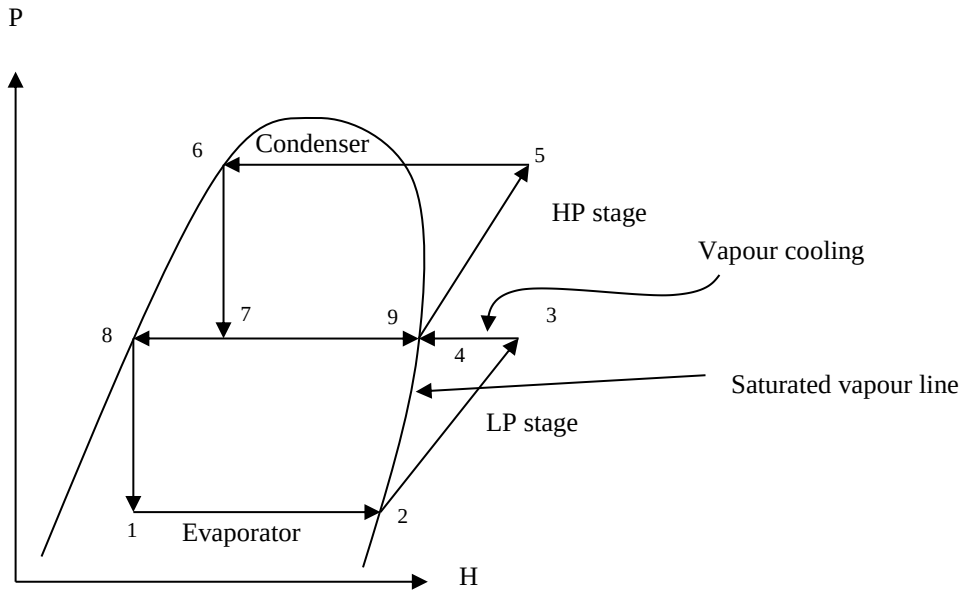

Figure 2.31: Pressure-enthalpy (P-H) diagram for multistage compression and expansion with a presaturator; adapted from [102].

The multistage compression and expansion can also be modified in another way that can reduce the refrigeration cycle energy consumption. This configuration is known as the cascade cycle; shown in Figure 2.32 [102]. It involves two or more cycles utilising different refrigerant (purple and black streams) that can be operated using the same heat exchanger (evaporator – B/cascade condenser). Each cycle has its own dedicated refrigerant compressor. The cascade cycle is shown on the pressure-enthalpy (P-H) diagram in Figure 2.33 [102]. In this figure, the phase envelopes are denoted with purple and black colours which represent refrigerant A and B respectively. As can be seen from point 1 to 2, the refrigerant A cools the process stream in the evaporator - A at constant pressure and is compressed to point 3. It then rejects its heat to another cycle from point 3 to 4 in the evaporator - B. Whereas from point 5 to 6, the refrigerant B absorbs the refrigerant A heat and is vaporised at constant pressure. Also, the refrigerant B at the same time condensed refrigerant A. Due to this dual function, evaporator B is also called a cascade condenser. Meanwhile, the vaporised refrigerant B is then compressed to higher pressure from point 6 to 7. It then rejects its heat in the condenser at constant pressure to the cooling water or air from point 7 to 8. The cascade cycle is applied for very low-temperature refrigeration processes and the usage of single refrigerant is not suitable to cool over a wide range temperature [26, 102].

Another essential fact to mention is the interface temperature between these two cycles is typically dictated by the evaporator temperature in the higher temperature cycle and it is known as the partition temperature. This parameter is a crucial degree of freedom [102]. This parameter is used in this study to optimise the propane refrigeration cycle which will be further discussed in chapter 4 of this thesis.

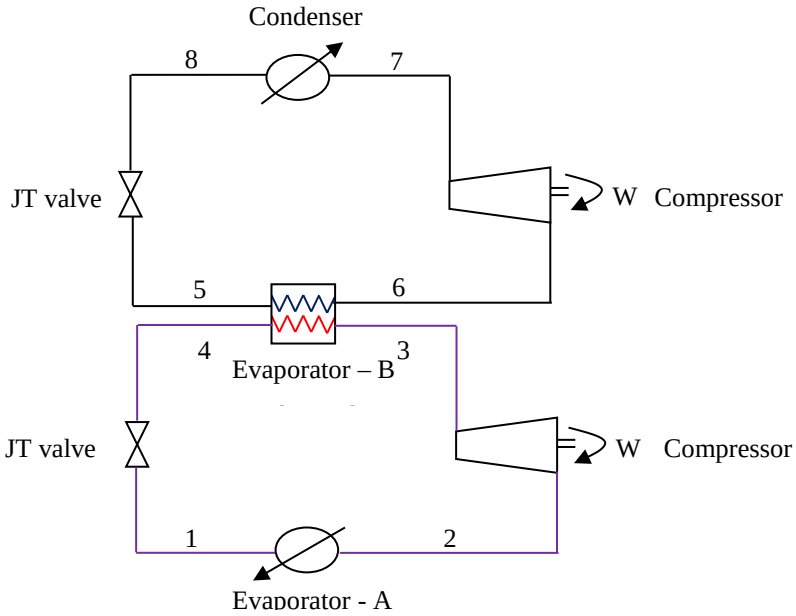

Figure 2.32: Cascade cycle, adapted from [102].

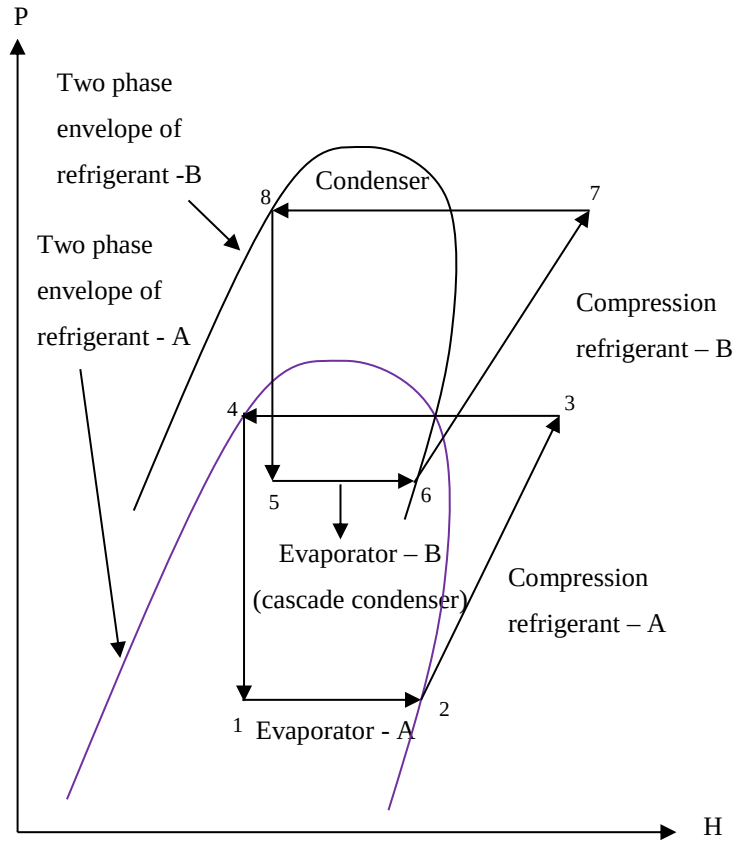

Figure 2.33: Pressure-enthalpy (P-H) diagram for the cascade cycle; adapted from [96].

Cascade cycle can also be configured as multistage compression and expansion as shown in Figure 2.34. This unique configuration is operated in a similar manner as discussed previously, however, two different refrigerants are utilised to cool the process stream over a wide range of temperatures. The refrigerant streamlines are denoted with purple and black colours which represent refrigerant A and B respectively. Both refrigerant A and B have their own dedicated compressors. As shown in Figure 2.34, merging of stream 7 with stream 13 reduces the inlet temperature to the HP stage, hence reduces the overall power consumption of the cascade cycle. The pressure-enthalpy (P-H) diagram of this configuration is illustrated in Figure 2.35. As can be seen from Figure 2.35, from point 5 to 6, evaporator B acts as a condenser to condense refrigerant A by absorbing its heat; it is then compressed to higher pressure from point 6 to 7. The discharge stream 7 is then desuperheated through merging with the overhead vapour stream 13. The degree of superheat of the merged stream i.e. stream 8 is reduced, hence reducing the inlet temperature to HP stage. This reduces the overall power consumption of the cascade cycle. **This configuration is used as a basis in this research study.**

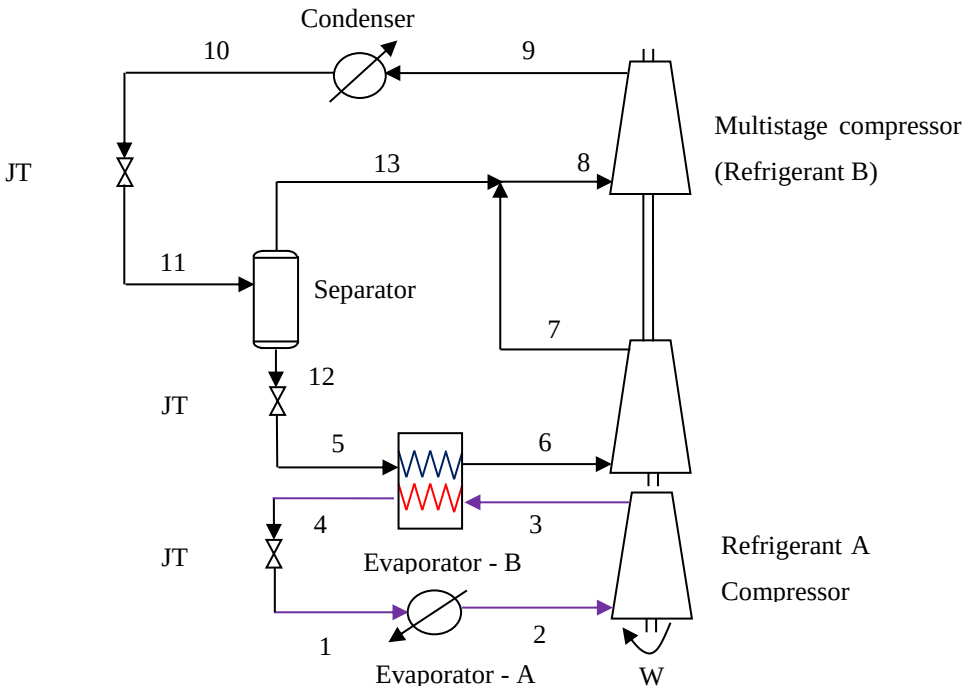

Figure 2.34: Multistage compression and expansion of the cascade cycle (own research work).

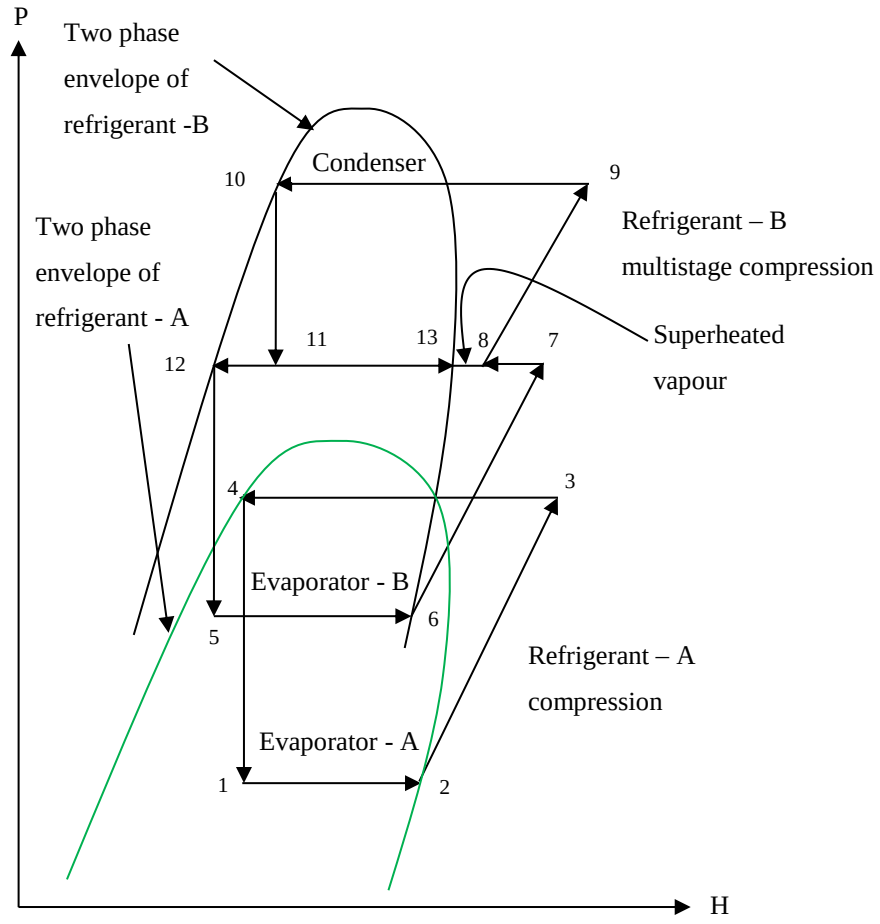

Figure 2.35: Pressure-enthalpy (P-H) diagram for multistage compression and expansion of the cascade cycle (own research work).

From the above discussion, it indicates that the refrigeration cycle can be modified and configured in many ways to reduce energy consumption. All the LNG processes that have been discussed in section 2.2 and others which are not mentioned in this thesis are developed by combining features of different refrigeration cycles. As refrigeration is the heart of the liquefaction process, optimising its design and operation parameter will improve the overall process efficiency. **In this study, the refrigeration cycle of the cascade LNG process is optimised through the design and operational parameters which will be discussed in chapter 3 onwards.**

2.7.3 Refrigeration cycle performance

The performance of the refrigeration system is analysed by measuring the coefficient of performance (COP) as illustrated in Figure 2.37 [102]. This parameter is defined as the ratio of the total heat absorbed by the refrigerant from the process stream to the amount of compressor power required by the system as expressed below:

$$COP = Q / W \tag{2.3}$$

where Q is the refrigerant duty (MW) and W is the compressor power (MW).

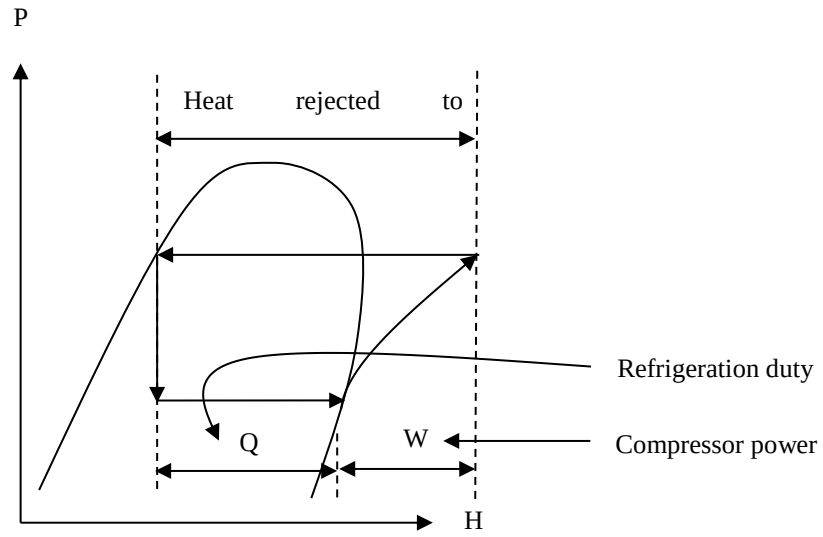

Figure 2.36: Measuring the coefficient of performance of a refrigeration cycle, adapted from [102].

The higher the value of COP, the more efficient is the refrigeration cycle. Usually, the COP value is greater than 1 [104]. In this study, COP is one of the parameters used to analyse the cascade LNG process efficiency. The COP value is also affected by the selection of the refrigerant which will be explained in the next section.

2.7.4 Selection criteria for a refrigerant

The choices of refrigerants vary according to their applications. Refrigerants that are used for refrigeration and liquefaction cycles can be grouped based on their chemical compositions as described below [30]:

a. Halocarbons - They are refrigerants based on organic compounds i.e. carbon chains that are initially attached to hydrogen and then replaced with one or more of halogens such as chlorine, bromine and fluorine.
b. Inorganic compounds such as ammonia and carbon dioxide.
c. Hydrocarbons such as ethane, ethylene, propylene, propane and others which are suitable as refrigerants and have been applied widely in the petroleum and petrochemical industries.
d. Cryogenic gases have a very low triple point and normal boiling temperatures; below -153^{o}C and they are mainly used for cryogenic applications. These refrigerants are methane, air, oxygen, nitrogen, helium and others.

For LNG plants, the selection of the right refrigerant depends on the type of LNG process; whether it utilises either pure, MR or combination of both, its cooling range because natural gas need to be liquefied from ambient temperature to -161^{o}C, availability, the effect of refrigerant on the COP, thermophysical properties such as the freezing point and latent heat of vaporisation, evaporator pressure, refrigerant phase envelope, their compliance with health, safety and environmental regulation and other general considerations [102, 105, 106]. Some of the thermophysical properties and other factors that affect the selection of refrigerants are described below:

1. Freezing point

   At a given evaporator pressure, the resultant operating temperature of a refrigerant should be well above its freezing temperature to ensure smooth operation by preventing any formation of solid refrigerant. The physical properties of some common refrigerants that are used in the refrigeration cycle is presented in Table 2.3 [102].

Table 2.3: Physical properties of some common refrigerants at atmospheric pressure [93, 102, 107, 108].

Refrigerant	Freezing point, T_f (°C)	Boiling point, T_b (°C)	Critical temperature, T_c (°C)	Critical pressure, P_c (bar)	Latent heat of vaporisation, h_{fg} (kJ/kg)
Ammonia (NH_3)	-78	-33	132.3	113	1, 370
Ethylene (C_2H_4)	-169	-104	9.2	50.4	482.5
Ethane (C_2H_6)	-183	-89	32.2	48.7	489.7
Methane (CH_4)	-182	-161	-82	46.4	510.4
Propane (C_3H_8)	-182	-42	97	42.5	426.1
Propylene (C_3H_6)	-185	-48	92.4	46.7	439.5
Nitrogen (N_2)	-210	-196	-147	33.9	198.6
Carbon dioxide (CO_2)	< -78.5	> -78.5	30.98	73.8	349.5[a]

[a] Given at -56°C.

2. Latent heat of vaporisation

   The latent heat of a refrigerant should be as high as possible because evaporation of liquid refrigerant is the only way that determines the amount of cooling and not the vapour [105]. Having a refrigerant with a high latent heat content will not only reduce the overall refrigerant flow rate across the cycle but also the power consumption [102]. Thus, the COP of the refrigeration cycle will increase.

   Another important point to mention is to ensure that the refrigerant temperature is below the critical temperature as shown in the phase diagram in Figure 2.37 [102]. This is because when the refrigerant temperature increases, the latent heat of vaporisation decreases as the critical point is reached. As can be seen from Figure 2.37 (a) to Figure 2.37 (b), as the condenser temperature reaches close to the critical temperature, a significant amount of heat is removed through desuperheating via the condenser. This causes an increase in the heat transfer area of the condenser as the average heat rejection temperature exceeded [102]. In addition, the COP of the refrigeration cycle also reduces as more power is required. Therefore, it is feasible to operate the evaporator and condenser temperatures below the critical temperature to ensure high latent heat of vaporisation.

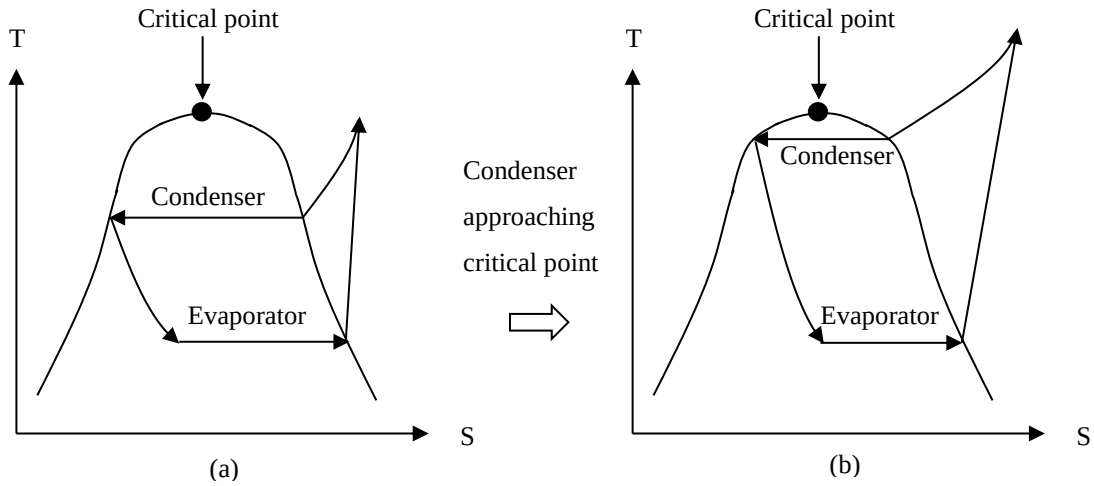

Figure 2.37: Selection of refrigerant based on a critical point, adapted from [102].

Besides, the relationship between latent heat of vaporisation and temperature can be described using the Watson equation [109] as expressed below:

$$\frac{\Delta H_{VAP2}}{\Delta H_{VAP1}} = \left(\frac{T_C - T_2}{T_C - T_1}\right)^{0.38} \tag{2.4}$$

where ΔH_{VAP1} and ΔH_{VAP2} represent the latent heat of vaporisation at temperature T_1 and T_2 correspondingly, T_1, T_2 are temperatures in K and T_C is the critical temperature in K.

Equation (2.4) is rewritten where ΔH_{VAP1} is replaced with $\Delta H_{VAP, NBP}$, T_1 is replaced T_{NBT} and T_2 is replaced with temperature, T [102]:

$$\frac{\Delta H_{VAP}}{\Delta H_{VAP,NBP}} = \left(\frac{T_C - T}{T_C - T_{NBT}}\right)^{0.38} \tag{2.5}$$

where $\Delta H_{VAP, NBP}$ is the latent heat of vaporisation at normal boiling point and T_{NBP} is the temperature at normal boiling point. The ratio of latent heat of vaporisation is denoted with λ, hence the equation becomes:

$$\lambda = \left(\frac{T_C - T}{T_C - T_{NBP}}\right)^{0.38} \tag{2.6}$$

Rearranging equation (2.5) gives:

$$T = T_C - \lambda^{2.63} (T_C - T_{NBP}) \quad (2.7)$$

From equation (2.6), given the corresponding normal boiling point and critical temperature of a refrigerant, the maximum operating temperature of refrigerant can be fixed if the minimum value of λ is stated. The conservatives value of λ is between 60 to 70% and 50% may be suitable for many other applications [102].

3. Evaporator pressure

   As shown in Figure 2.38 [102], the evaporator pressure should be above the atmospheric pressure to prevent any air ingress into the cycle that may cause safety and performance issue.

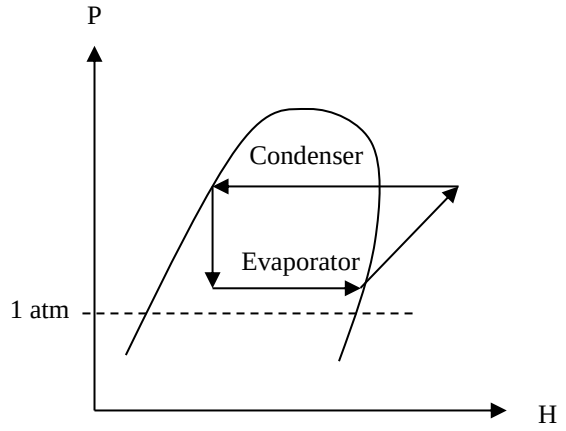

Figure 2.38: Operating pressure of an evaporator [102].

4. Refrigerant phase envelope

Another aspect that affects the selection of a refrigerant is the saturation vapour line (SVL) of the refrigerant in the phase envelope as shown in Figure 2.39 [102]. Moving from Figure 2.39 (a) to Figure 2.39 (b), the saturation line becomes steeper. This causes a reduction in the amount of desuperheating of the refrigerant with respect to condensation. Thus, the heat transfer area of the condenser also decreases as the normal heat rejection load reduces [102]. Additionally, the steep saturation line also increases the COP as less power is required [102].

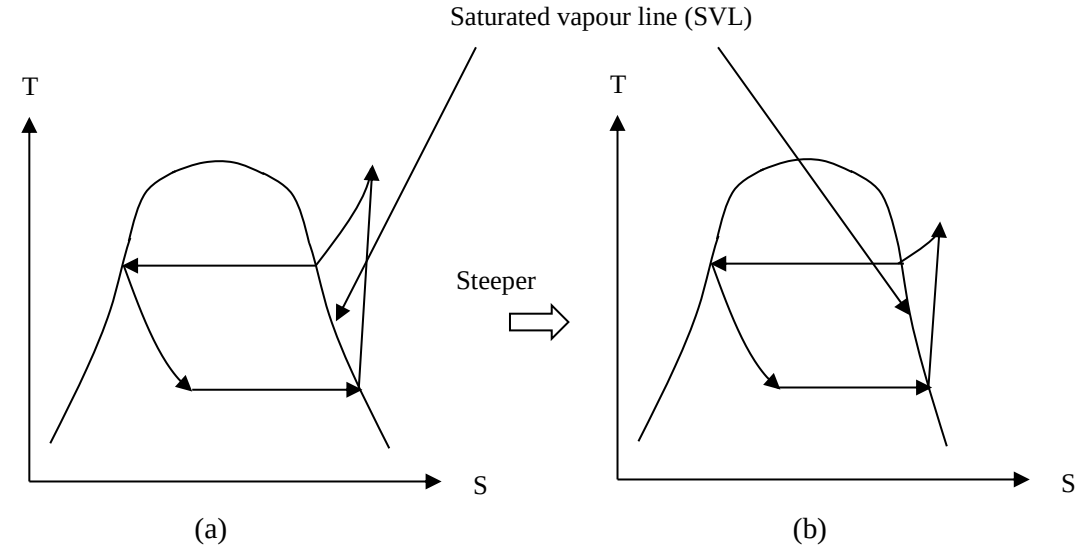

Figure 2.39: Refrigerant phase envelope-saturation vapour line (SVL), adapted from [102].

5. General considerations

Some other general considerations which is required while selecting a refrigerant are as follows; the refrigerant should be nontoxic, non-flammable, noncorrosive, free of water, have low or no impact on the ozone depletion and global warming, low viscosity and low surface tension is preferred, it has high refrigerant capacity (i.e. latent heat) and low power requirement, high oil solubility and low freezing point and has a high saturation pressure [102, 105, 110]. It is desirable if the refrigerant is readily available from the process because introducing a new refrigerant will add to the cost of the plants such as new storage requirements. Moreover, the new refrigerant needs to comply with the safety and environmental standards [102]. Meanwhile, the data related to toxicity and flammability of refrigerants can be obtained from the American Society of Heating, Refrigerating and Air-Conditioning Engineers (ASHRAE) standard 15. This standard serves the fundamental mechanical safety code for air conditioning and refrigeration equipment in the US [105].

Based on the above discussion, the selection criteria for a refrigerant is a crucial process to ensure safe operation plus its effect on the refrigeration cycle performance (COP) [106]. Moreover, the refrigerants that were selected will also be based on the desired operating temperature ranges and the cooling temperature of the process streams [26]. In this study, the cascade LNG process utilises propane-ethylene-methane (C_3H_8–C_2H_4–CH_4) refrigerants for its refrigeration cycles. The combination of these pairs was chosen because the refrigerants such as propane and methane are readily available from the plant, proven technology, fulfil the desired operating cooling range for pre-cooling, liquefaction and sub-cooling which are from ambient temperature to -40^{o}C, -40^{o}C to -100^{o}C and -100^{o}C to 153^{o}C respectively. Besides, the combination of these pairs of refrigerants for cascade cycle gives the highest COP based on the study done by Yoon, Choi [106].

2.7.5 LNG higher heating value (HHV)

In LNG custody transfer, the LNG is sold based on its higher heating value (HHV). The HHV (gross HHV) is defined as the heat released by the complete combustion in the air for a specified amount of gas measured at a specified reference pressure and temperature where the water produced is in liquid formed. LNG consists of more than 40% of HHV compared to other liquid fuels obtained from chemical conversion of natural gas [111]. Meeting the LNG HHV is one of the most critical requirements for any LNG plant as it is used for the Sale and Purchase agreements (SPA), gas interchangeability and for plant performance guarantee.

A comprehensive discussion for HHV measurements, inclusive of the correction with respect to the ideal gas values to the real gas state which uses compressibility factor (z) can be found in GPA-2172-96 standard [96], (Gas Processors Association, GPA, 1996). The HHV of the pure components is presented in Table 2.4 [96]. In this study, two distinct integrated LNG/NGL designs are proposed to meet the LNG HHV requirement set for the cascade LNG process. This will be further discussed in chapter 5.

Table 2.4: Higher heating value of pure components [96].

Components	Higher heating value (Btu/Scf)
Helium (He)	0
Nitrogen (N_2)	0
Carbon dioxide (CO_2)	0
Hydrogen sulphide (H_2S)	637.1
Methane (CH_4)	1010.0
Ethane (C_2H_6)	1769.7
Propane (C_3H_8)	2516.2
Butanes as isobutane	3252.0
Pentanes and heavier as hexane	4756.0

Note: For LNG HHV, the H_2S HHV is not included as its removal limit prior to liquefaction is 4 ppmv as mentioned previously in section 1.2.

2.8 Energy and exergy analyses

As discussed in chapter 1, section 1.5 and chapter 2, section 2.5.1, energy and exergy analyses will be used as an optimisation tool to evaluate the process efficiency of the cascade LNG process. The term thermodynamics efficiency or process efficiency will be interchangeably used in this thesis. As explained in chapter 1, section 1.5, these methods are used to overcome the limitations of the numerical optimisation methods. Identifying and analysing the thermodynamics properties such as enthalpy and entropy of each process stream is crucial as it provides a better understanding of the changes occurring within the process. Moreover, the process engineer can utilise this valuable information for improving the process from the equipment and process design point of view. In this section, the details about the energy and exergy analyses will be explained.

2.8.1 Background of energy and exergy analyses

Energy and exergy analyses are derived from the first and second law of thermodynamics. The first law of thermodynamics provides the theoretical basic analysis of energy. Its main emphasis is on the conservation of energy principle; during a reaction, the amount of energy remains constant when it changes from one form to another. The thermodynamic property that is used to calculate the quantity of energy is enthalpy. The thermodynamic efficiency and energy consumption of the overall cascade LNG process is determined through energy analysis by measuring its two quantitative parameters namely the coefficient of performance (COP) and specific power (SP). COP is the standard criterion used not only to measure the refrigeration cycle performance as explained in section 2.7.3 but also for evaluating the overall efficiency of the cryogenic process [53].

The definition of COP and its equation are described in section 2.7.3 and equation (2.3) respectively. Whereas, SP is defined as the total power required by the system per unit mass flow rate of LNG produced. SP is expressed as below:

$$SP = \frac{\Sigma W_{req}}{\dot{m}_{LNG}} \tag{2.8}$$

where ΣW_{req} is the total compressor power required (MW) and $\dot{m}_{LNG}$ is the quantity of LNG produced (tonne/h).

However, energy analysis alone is insufficient to examine and evaluate the internal thermodynamic efficiency of a process with regards to its components. This is because it only indicates the overall thermodynamic efficiency and does not give any insight information about the sources and locations of irreversibilities that occur within the process and due to unit operation. For instance, all LNG processes that have been applied in the LNG plants are based on real refrigeration cycles that give some sort of irreversibilities. These irreversibilities are originated due to several reasons such as friction, unrestrained expansion of gas or liquid to a lower pressure in the expander or throttling valve, compression of gas to a higher pressure in the compressor, mixing of matter at different compositions or states and heat transfer across finite temperature difference in the evaporator and in the condenser [30, 55, 93]. Besides, as explained in section 2.5.1, the first law solely evaluates the quantity of energy and not the quality [93]. From thermodynamic perspectives, the quality of energy here means the capacity for producing work [95]. Therefore, to analyse the quality of energy and to obtain the sources and locations of energy degradation, the second law of thermodynamic which is exergy is required.

According to Rant [112], the term exergy is derived from Greek and it is defined as ‘ex’ means out and ‘erg’ means work. Exergy (E_x) is defined as the maximum magnitude of work that can be achieved by a system when the system components are brought into a thermodynamic equilibrium state with its environment in a hypothetical reversible process [95, 113]. Though all processes are irreversible, engineers are keen to use the reversible process concept. This is because when a system approaches a reversible state, the amount of work required will be less by the work-consuming devices such as compressors, pumps and fans. Whereas more work is generated by the work-delivering device such as turbines work [93].

There are four main types of exergy that may involve in an energy conversion process namely kinetic exergy, potential exergy, chemical exergy and physical exergy. Kinetic exergy is referring to the kinetic energy where the velocity of the components relative to the surface of the earth is measured [95]. Potential exergy is like the potential energy measured based on the energy kept within the components at various levels of the surface of the earth. Whereas, chemical exergy is evaluated with respect to exergy of the components related to the departure of the chemical composition of a system from that environment [94]. While physical exergy is associated with work produced when the system components change from initial state to final state in a hypothetical reversible process with respect to the temperature, T_o and pressure, P_o of the environment. Hence, the exergy can be expressed as:

$$E_x = E_k + E_p + E_{chem} + E_{phys} \tag{2.9}$$

where E_k, E_p, E_{chem} and E_{phys} are kinetic exergy, potential exergy, chemical exergy and physical exergy respectively.

In this study, the cascade LNG process only applies to physical exergy because the liquefaction of natural gas process has more impact due to temperature and pressure based exergy while the effect of mechanical exergy such as E_k and E_p is not significant. Besides, the process also does not involve any chemical mixing, reactions and separation. Thus, E_k, E_p and E_{chem} terms are ignored from the exergy calculations [114]. Ignoring these terms, the flow of physical exergy at equilibrium state with the environment is calculated as below:

$$E_x = (H_o - H_i) - T_a (S_o - S_i) \tag{2.10}$$

where T_a is the ambient temperature in K, H_o and S_o represent the enthalpy and entropy respectively of outlet streams while H_i and S_i represent the enthalpy and entropy of the inlet streams. The unit of enthalpy is in MJ/kg while entropy is in MJ/kg K. Exergy can be delivered in three modes; exergy transfer accompanying with work, exergy transfer due to heat transfer and exergy transfer related to mass entering and leaving a system [93, 94]. Equation (2.10) is a simplified form of exergy balance for a control volume system where no exergy related to work, heat transfer and mass entering and leaving the system are considered. This equation is also considered as an adiabatic and where no work is done by the system or by the surroundings.

The exergy analysis consists of two main quantitative parameters which are the exergy loss or lost work and exergy efficiency. To identify and locate the irreversibilities that occur within a process and unit operation, the exergy loss that is contributed by each unit operation is calculated. The expressions of exergy loss rate for the unit operation such as LNG heat exchanger, compressor, valve, mixer, air cooler and pump are shown in Table 2.5 [30].

Meanwhile, the exergy efficiency is used to assess the usefulness of energy utilisation of the liquefaction system and it is determined after obtaining the total exergy loss exhibited by each unit operation. The exergy efficiency (η_{ex}) is defined as the ratio of the difference between the actual power supplied and the total exergy loss dissipated by the unit operation to the actual power supplied by the system [30] and is expressed as:

$$\eta_{ex} = 1 - \left(\frac{\Sigma \text{ exergy loss of each unit operation}}{\text{actual power supplied}}\right) \tag{2.11}$$

Table 2.5: Exergy loss expression for unit operation, adapted from [30].

Unit operation	Inlet and outlet streams	Exergy loss expressions
LNG heat exchanger	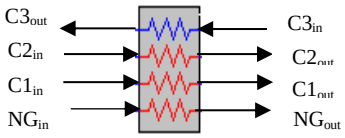	$\dot{E}x_{HX,\,loss} = \sum_i \dot{m}_{i,in}\, ex_{i,in} - \sum_i \dot{m}_{i,out}\, ex_{i,out}$
Compressor	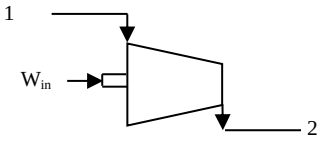	$\dot{E}x_{COMP,\,loss} = \dot{m}\,(ex_1 - ex_2) - \dot{W}_{in}$
Valves	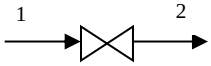	$\dot{E}x_{V,\,loss} = \dot{m}T_o\,(S_2 - S_1),\ h_1 = h_2$
Mixer	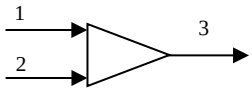	$\dot{E}x_{MIX,\,loss=}\ \dot{m}_1 ex_1 + \dot{m}_2 ex_2 - \dot{m}_3 ex_3$
Air cooler	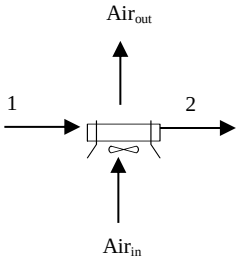	$\dot{E}x_{AC,\,loss} = (\dot{m}_1 ex_1 + \dot{m}_a ex_a)_{in} - (\dot{m}_2 ex_2 + \dot{m}_a ex_a)_{out}$
Pump	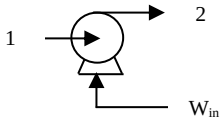	$\dot{E}x_{Pump,\,loss} = \dot{m}\,(ex_1 - ex_2) - \dot{W}_{in}$

where ‘i’ is referring to various components at inlet and outlet streams of the LNG heat exchanger, $\dot{m}$, $\dot{m}_1$, $\dot{m}_2$, and $\dot{m}_3$ are the mass flow rates of respective streams in kg/s, $\dot{m}_a$ is the mass flow rate of air in kg/s, ex is the specific exergy in MJ/kg for the corresponding stream, T_o is the environment temperature in K, S is the entropy in MJ/kg K, h is the enthalpy in MJ/kg and $\dot{W}$ is the power in MW.

2.8.2 Benefits of using energy and exergy analyses

The benefits of using energy and exergy analyses in optimising and evaluating the cascade liquefaction process have many folds. For instance, by analysing the COP and SP, it gives an idea about the maximum power required to achieve the desired LNG capacity and the overall efficiency of the process. Whereas, through the computation of exergy loss and exergy efficiency, various information can be obtained such as the location, reason and actual magnitude of energy waste [53, 94]. Moreover, it also provides valuable measures of true effectiveness and performance of an energy system from the thermodynamic context which gives the direction for potential improvements [26, 53, 94]. Besides, through the calculation of exergy loss of individual components and exergy efficiency, it gives better evaluation compared with more other calculated efficiencies such as thermal efficiency of a power plant, compressor or turbine isentropic efficiency and heat exchanger effectiveness as it is based on the first and second law of thermodynamics [94].

Once the energy and exergy analyses are computed, this information is utilised to optimise the thermodynamic efficiency of the cascade process by making the necessary adjustment to the design and operating parameters. Many studies have used this approach to optimise the LNG processes which will be discussed in the next section.

2.8.3 Application of energy and exergy analyses in LNG processes

Energy and exergy analyses have been widely used to optimise the LNG processes. Kanoglu [51] investigated the performance of multistage cascade refrigeration cycle using energy and exergy analyses by evaluating the COP, exergy destruction (exergy loss) and exergetic efficiency. Based on his analyses, it was found that to obtain the minimum power in the cascade cycle, it hinges on the properties of the inlet and outlet natural gas stream and the power increases with decreasing in the liquefaction temperature. Kanoglu also suggested that this method can be used for design, optimisation and performance evaluation of actual liquefaction LNG plants utilising cascade process [51]. This approach has also been used by Remeljej and Hoadley [54] for evaluating four different LNG processes suitable for small-scale capacity.

Meanwhile, Mehrpooya, Jarrahian [50] applied this method to analyse the behaviour of propane refrigeration cycle used in the NGL plants. It was found that the increase in the pressure drop of evaporators causes a decrease in the COP and exergy efficiency. Cipolato, Lirani [56] further optimised the multistage cascade refrigeration cycle from Kanoglu [51] using exergetic analysis by analysing the effect of pressure at six different streams. Based on the results, it indicates that the exergy loss rate was reduced by 48% compared to the base case.

Vatani, Mehrpooya [55] reviewed the performance of five existing liquefaction processes namely single mixed refrigerant (SMR) by Linde, SMR by APCI, C3MR by Linde, DMR by APCI and MFC by Statoil/Linde. Energy and exergy analyses methods were used to measure the performance of these processes. Results showed that the MFC has less energy consumption, highest COP and exergy efficiency compared to the other processes. Lastly, this technique is also commonly used to optimise and evaluate the efficiency of power plants as discussed by the following references [115-118]. Based on the above discussion, it indicated that this approach has been considered as a reliable and powerful tool for design, optimisation and performance evaluation [51] not only for LNG processes but also by other energy conversion systems.

2.9 Optimisation of LNG processes

The optimisation of the LNG plant is an important research area as previously mentioned in Chapter 1, section 1.4. Other main drivers to optimise the LNG plants are such as significant growth in LNG usage in various sectors, to minimise the GHG emission, minimise energy consumption as well as the cost with prime focus on large scale LNG plants. Optimisation of LNG plants is often measured based on improvements made in the process efficiency. An LNG plant is said to be efficient when it has high reliability and high LNG production rate, low energy consumption and low cost as well as when product quality is maintained. There is a large number of studies have been performed that discussed the optimisation of LNG processes from various aspects. In this section, the optimisation of LNG processes will be discussed in three different areas which are the pre-cooling, liquefaction integrated with NGL recovery process and standalone NGL process.

2.9.1 Pre-cooling cycle optimisation

As described in section 2.2 (Table 2.2), all the proven and newly invented LNG processes have employed pre-cooling cycles. Only single mixed refrigerant (SMR) process do not use any pre-cooling cycle because the natural gas is directly cooled to -161^{o}C using a single mixed refrigerant composition. This process is not discussed in this thesis as it is only suitable for small scale LNG plants [54, 119, 120]. The pre-cooling cycle is the first cycle in any liquefaction process which eradicates the heat from natural gas stream and other refrigerants to a temperature approximately between -30^{o}C to -55^{o}C [53] based on the type of refrigerant or based on various combination of MR the process used. This pre-cooling temperature range depends on the type of LNG technology applied. The pre-cooling cycle also provides cooling for the pre-cooler, cold box (cryogenic section) and fractionation section of an LNG plant [31].

Due to the substantial progress in the liquefaction technologies, the pre-cooling cycle can employ either pure (single) refrigerant or mixed refrigerant. According to Castillo, Majzoub Dahouk [121], 95% of the existing LNG plants have the pre-cooling cycle installed in their LNG process and 85% of them have utilised propane in their pre-cooling cycle instead of the mixed refrigerant. The pre-cooling cycle consumes more than 50% of the total power of an LNG process based on the data obtained from the following references [31, 46, 104]. Many studies have been done that discussed various ways to optimise the efficiency of the pre-cooling cycle. Castillo and Dorao [122] studied the appropriate refrigerants choice for the pre-cooling cycle by analysing the effect of methane, ethane and propane and a mixture of these components on the compressor power, refrigerant effect, refrigerants flow rates, coefficient of performance (COP) and heat exchanger duty and UA using Linde-Hampson process. It was found that propane refrigerant consumed the least amount of power, has a higher specific refrigerant effect (i.e. high capability to remove heat), low molar flow rates, high COP and required less duty and low UA compared to other refrigerants for the same process conditions which makes it the preferred refrigerant for the pre-cooling cycle.

Paradowski, Bamba [46] analysed the propane pre-cooling temperature of LP stage (-34^{o}C to -31^{o}C) and its compressor speed (3000 to 4670 rpm) for C3MR process that could debottleneck the existing LNG plant capacity to 5.5 MTPA as well as improve the process efficiency. It was found that the optimal propane pre-cooling temperature for LP stage is -31^{o}C and the required compressor speed is 3600 rpm to meet this new LNG production capacity. Ransbarger [123] compared between the three-stage and four-stage propane refrigeration cycle of cascade LNG process with the aim to optimise the refrigeration levels. Results showed that adding the fourth stage in the propane cycle will only reduce the required power by 1%, thus the economics did not justify the increased in the capital cost due to the additional stage.

Majzoub [124] studied the effect of using only pure components (ethane and propane) and mixed refrigerant (made up of ethane and propane) for various pre-cooling cycle configurations which are suitable for both cold (6ºC) and hot (25ºC) climate conditions for C3MR and MFC LNG processes. He analysed the proposed pre-cooling cycle configurations by computing the following variables such as the COP, compression power, pressure ratio, inlet volumetric flow of compressor and heat exchanger UA (product of overall heat transfer coefficient and heat exchanger area). The results showed that utilising only propane in the pre-cooling cycle gives the lowest compression power, heat exchanger UA, intermediate inlet volumetric flowrate and highest COP compared to mixed refrigerants for both climates conditions. Besides, a three-stage propane pre-cooled cycle was found to be a better option from an energy efficiency perspective compared to a two-stage mixed refrigerant (ethane and propane) cycle for both climate conditions. Majzoub also suggested a novel and efficient configuration for MFC whereby propane is used instead of mixed refrigerant for the pre-cooling cycle.

Fathalla [125] investigated the performance of a four-stage propane pre-cooling cycle for C3MR process at Segas LNG plant in Egypt during hot climate conditions. The temperatures range from 25ºC to 35ºC. He studied the effect of routing the discharge of propane compressor directly to the recycle cooler before entering the propane condenser and analysed the effect of altering the propane refrigerant composition by adding methane and ethane components. Results deduced that with the aid of the recycle cooler during the hot climate conditions, full condensation of propane was achieved after the propane condenser. Further, altering the propane refrigerant composition by adding the lighter components give the highest power consumption and air cooler duty across the propane condenser and lowest UA. The compressor power increased due to a rise in the lighter components while the air cooler duty increased because of the large condensing duty required to condense the lighter components. Hence, propane is considered as the most suitable refrigerant for the pre-cooling cycle.

Meanwhile, the design of the pre-cooling cycle has been evolved in recent decades. In this context, various studies have been presented that were related to the optimisation of the efficiency of the propane cycle with respect to its design configuration. Mortazavi, Somers [31] suggested the replacement of the conventional expansion valves in the C3MR process with expanders to improve the liquefaction efficiency. Results showed that about 2.68 MW reduction in the compressor power, 3.82 MW recovery of expansion work and 1.24% increase in the LNG production can be achieved through this modification. Further, the specific power was minimised by 7.07% by considering the deduction of the recovered power from the total required power and 3.68% without considering it.

In another study, Mortazavi, Somers [126] optimised the energy efficiency of the C3MR process by utilising the waste heat from a gas turbine powering the absorption chillers in the propane cycle. They simulated eight options for the gas turbine waste heat utilisation using Aspen Plus. Based on the simulation results, reduction of 21.32% was achieved in terms of the compressor power and fuel consumption which obtained through replacement of the evaporators at 22^{o}C and 9^{o}C. Also, condensing the propane at 14^{o}C and using the absorption chillers for inter-cooling of the mixed refrigerant cycle. Kalinowski, Hwang [127] proposed the replacement of the propane chillers with an absorption refrigeration system in the LNG recovery process. This refrigeration system utilised the waste heat from the electrical power generating gas turbines. From this modification, it was found that from the 9 MW electricity generated, 5.2 MW of waste heat was used for cooling purpose in the LNG plant and saved 1.9 MW of electricity usage. Therefore, having an energy-efficient refrigeration cycle will improve the plant operation and provide economic benefits [57].

2.9.2 Gaps in the optimisation of the pre-cooling cycle

Table 2.6 presents the summary of the optimisation studies done for the pre-cooling cycle in the open literature and highlights the process variables that were analysed. As can be seen from Table 2.6, the optimisation of propane pre-cooling cycle in the previous literature was mainly centred on its design such as varying the types of refrigerants used in this cycle i.e. pure vs. MR, a number of refrigeration stages and replacing the conventional equipment of the propane cycle with other equipment. Most of these studies have focused on optimisation of MR based liquefaction processes but not many studies are available for the cascade process. Further, very scant studies are obtainable that discuss optimisation from an operational perspective. In this research work, a three-stage propane cycle is optimised by altering the operating conditions of the propane evaporator. A three-stage propane pre-cooling cycle configuration is chosen for this research work as it was found to be the most energy efficient and economical option as described in the following references [121, 123, 124]. Detailed work will be further discussed in Chapter 4 of this thesis.

Table 2.6: Summary of pre-cooling cycle optimisation studies in the open literature.

Year	Reference	Simulation software	Optimisation studies
2013	L. Castillo and C.A. Dorao	Aspen HYSYS,	Compared using of pure propane and mixed refrigerant in the pre-cooling cycle for *Linde-Hampson* process. Analysed the compressor power, refrigerant effect and refrigerants flow rates, coefficient of performance (COP) and heat exchanger duty and UA.
2004	Paradowski, et al.	Not stated	Analysed propane pre-cooling temperature of LP stage and its compressor speed for 5.5 MTPA *C3MR* process
2007	Weldon Ransbarger	Not stated	Compared three-stage and four-stage propane refrigeration cycle for *cascade* LNG. Analysed the amount of energy saving.
2012	Majzoub	Aspen HYSYS, Peng Robinson	Compared to the use of pure components and mixed refrigerant in the pre-cooling cycle. Analysed the COP, compression power, pressure ratio, inlet volumetric flow of compressor and heat exchanger UA.
2013	Fathalla	Aspen HYSYS	Investigated the performance of a four-stage propane pre-cooling cycle for *C3MR* process at Segas LNG plant, Egypt during hot climate conditions. Studied the effect of routing the discharge of propane compressor directly to recycle cooler before entering the propane condenser and analysed the effect of altering the propane refrigerant composition.
2012	Mortazavi, et al.	Aspen Plus	Proposed replacement of expansion valves with expanders in the *C3MR* process.
2010	Mortazavi, et al.	Aspen Plus	Optimise the energy efficiency of the *C3MR* process by utilising the waste heat from the gas turbine to powered absorption chillers in the propane cycle.
2009	Kalinowski et al.	Not stated	Proposed the replacement of the propane chillers with an absorption refrigeration system in the *LNG recovery* process. This refrigeration system utilised the waste heat from the electrical power generating gas turbines.

2.9.3 Integrated LNG/NGL processing plant optimisation

In the earlier design of LNG plants, natural gas liquid (NGL) plants were built upstream of the liquefaction plants and there was no integration between these two processing plants [33]. Alternatively, as described in section 2.7.5, the LNG product is sold based on the HHV specification. Therefore, to meet this criterion, the removal of heavier hydrocarbons or the NGL unit is necessary for the LNG plant. According to Hudson, Wilkinson [32] having an NGL unit in an LNG plant not only assist in meeting the HHV specification [40] but protect the plant from having operational problems such as freezing of aromatics in the downstream equipment (i.e. liquefaction unit) and the plant operation is less affected if changes in the feed gas composition occurred. This is because the liquid recovery unit can maintain the removal efficiency over a wide range of compositions. Besides, this integrated configuration gives low specific power which means that there is more room to increase the train size for a given driver selection.

On the other hand, in a standalone LNG plant, the required refrigerant such as propane is obtained from the external cycles and separate heat exchangers, whereas in the integrated LNG plant, the required refrigerant is obtained from joint refrigeration cycles and shared devices [128]. In addition, there are other advantages of this integration such as a reduction in the capital and operating cost of the plant [34], elimination of combined emissions of carbon dioxide (CO_2) and nitrogen oxides (NOx) and improvement of the overall thermodynamic process efficiency [33, 34, 40]. In another study, NGL facilities have been introduced at LNG receiving terminals to meet stringent HHV specifications set by the local stakeholders [129].

The integrated LNG/NGL process has been considered as one of the simple and practical ways to improve the process efficiency of the plants [26, 32, 34]. For instance, when the liquefaction section is integrated with the NGL section, the energy requirement for separation, condensation and sometimes cooling of these liquid products obtain power from the liquefaction drivers [40]. As the demand of building larger and process efficient LNG plants grow rapidly [40], many of the LNG process licensers such as Air Products (APCI), ConocoPhillips (COP) and Shell have developed various integrated processes. For example, ConocoPhillips had applied this integrated concept to three of the LNG plants that resulted in about a 7% increase in the LNG production for the same required power [33]. Fluor Technologies reported that 10% of energy saving has been obtained through integration of LNG and NGL processes [130].

Various studies are available that discuss areas to optimise the integrated LNG/NGL plants. Khan, Chaniago [131] studied three different NGL configurations namely the conventional separation sequence (base case), direct sequence thermal coupling (TCDS) and dividing wall distribution column (DWC) whereby they were integrated with Korea single mixed refrigerant (KSMR) liquefaction process. The studied plant capacity was 2.5 MTPA and suitable for offshore-based LNG plants. These configurations were investigated for their energy efficiency, product recovery and purity. After the integration, the MR cycle was optimised with the aim to minimise the compression energy requirement by changing its composition and varying the pressure levels of the MR compressor. They used an in-house knowledge-based optimisation method. The results showed the proposed KSMR liquefaction process integrated with TCDS NGL configuration gain 9% reduction in the compression energy requirement and SP compared to the base case.

Mehrpooya, Hossieni [128] applied energy and exergy analyses methods to minimise the energy consumption and to obtain high ethane recovery for three novels integrated LNG/NGL processes. DMR, C3MR and MFC liquefaction processes are used to supply the required refrigeration for the process. The ethane recovery and the specific power (SP) are optimised by varying the cold recycle flow rate and its temperature in the NGL column (T-100). Recycle ratio is another important parameter that influences these results. From the analyses, all the proposed configurations can recover ethane above 90% and the specific power are between 0.35 to 0.38 kWh/kg LNG. This integration provides several benefits such as elimination of compressor, multi-stream heat exchanger and reduction in the required cold and hot utility.

Pillarella, Bronfenbrenner [42] optimised the efficiency of AP-X process by analysing the effect of reducing the temperature approach of hot and cold streams in the propane condenser. They also computed the exergy loss exhibited by the equipment in the process. It was found that reducing the temperature approach not only improved the efficiency of the main heat exchanger but also reduced the SP of the liquefaction process. This can be achieved by increasing the heat exchanger surface area. However, when the minimum SP is reached, a substantial increase in the heat exchanger area is observed, hence this indicates that there is an economic evaluation required to obtain a feasible design. Further, the exergy analysis results showed that the refrigerant compressors, air coolers and heat exchangers attained the largest exergy losses, hence affect the efficiency. Exergy results are used to make necessary adjustments on the process flow sheet and evaluate the process efficiency.

He and Ju [132] optimised a novel mixed refrigerant cycle (MRC) integrated with an NGL process for a small-scale LNG plant using a genetic algorithm (GA) and exergy analysis. They investigated the effect of MR composition and its pressure and the inlet pressures of the demethaniser (De-C1) and De-C2 columns to reduce the energy consumption of the process. However, they did not analyse the effect De-C2 column pressure on the process parameters, irreversibility and efficiency. The results showed that about 9.64% and 11.68% reduction in the energy consumption and refrigerant molar flow rate respectively can be achieved compared to the base case. Further, the inlet pressure of De-C1 does affect the energy consumption, reboiler and condenser duty, hence an optimal value of De-C1 should be chosen to minimise the energy consumption. Conversely, the inlet pressure of De-C2 gives no significant effect on energy consumption and other process variables.

With respect to cascade liquefaction optimisation, Ransbarger [133] proposed four different process configurations for an integrated LNG/NGL cascade process using propane, ethane and methane open cycles. Though the description for these processes was given, however no technical data on the process simulation were stated, hence no information on the amount of energy consumption and other parameters are available which can be used as a reference for future studies. Cipolato, Lirani [56] further optimised the multistage cascade liquefaction process based on the work done by Kanoglu [51] and Filstead [134] using exergetic optimisation approach. They simulated the process in Aspen HYSYS v. 3.2 and employed Peng Robinson equation of state to obtain the thermodynamic properties of the process. They studied the influence of pressure in six different locations in the propane, ethane and methane cycles using a full factorial experimental planning. These pressures are located after the compressor and expansion valves in for each cycle. The results showed that 48% reduction in the exergy loss can be obtained by using the new set of operational data compared with the base case.

Meanwhile, Yoon, Choi [104] compared three different cascade cycles that used different combination sets of refrigerants namely carbon dioxide-ethylene-nitrogen cycle (CO_2–C_2H_6–N_2), propane-ethylene-methane cycle (C_3H_8–C_2H_4–CH_4) and carbon dioxide-nitrogen cycle (CO_2–N_2). Results indicate that C_3H_8–C_2H_4–CH_4 cycle gives the highest COP and refrigeration capacity and lowest compressor power compared to other proposed cycles. Furthermore, among the three liquefaction cycles, the total exergy loss of C_3H_8–C_2H_4–CH_4 cycle was the lowest, followed by the liquefaction of CO_2–C_2H_6–N_2 cycle and CO_2–N_2 cycle.

Fahmy, Nabih [135] optimised the performance of Open Cycle Philips optimised cascade process for the production of 4.24 MTPA LNG capacity through replacement of J-T valves with liquid expanders. Firstly, they simulated the conventional process with J-T valves in Aspen HYSYS v. 7. Later, the J-T valves were replaced with liquid expanders at various locations in the propane, ethylene, methane cycles and upstream of heavy's removal column. It was found that by replacing the J-T valves with liquid expanders, about 5.8% power saving, 92.81% thermal efficiency and a 7% rise in the LNG production can be achieved.

2.9.4 NGL process optimisation

With respect to optimisation of NGL process, Shin, Yoon [136] focused on improving the energy consumption of NGL process by varying the type of feed gas (lean and rich) and a number of stages of De-C1 column (10 and 30-stages) using exergy analysis method. Three NGL processes were investigated namely the gas sub-cooled (GSP), recycle split vapour (RSV) and cold residue reflux (CRR). It was found that the total energy usage and exergy loss for GSP is the lowest for the majority of the case studies such as the lean feed gas (De-C1 column with 10 stages) and rich feed gas (De-C1 column with 10 and 30-stages). In contrary, GSP consumes the highest energy consumption and exergy loss for lean feed gas case study (De-C1 column with 30-stages).

Lee, Long [137] proposed a new design for the NGL recovery process consisting of De-C1 column and a top dividing wall column (TDWC). This configuration is suitable for floating LNG (FLNG) applications. TDWC is used to integrate the depropaniser (De-C3) and debutaniser (De-C4) columns to improve energy efficiency and minimise the number of columns in the NGL recovery process. The results indicate that by using TDWC, 35.09% of refrigeration costs can be saved compared to the conventional process line up used in an onshore integrated NGL recovery process. Further, the duties of propane condenser and reboiler can be minimised by 21.42% and 11.79% respectively. With TDWC diameter of 1.5 m, the energy usage can be reduced by 15.36% relative to total annual cost (TAC) compared to conventional NGL column sequence.

2.9.5 Gaps in the optimisation of the integrated LNG/NGL plants and NGL processes

Table 2.7 shows the summary of the optimisation studies conducted for integrated LNG/NGL and standalone NGL recovery plants in the open literature and highlights the process variables that were analysed. As can be seen from Table 2.7, most of the former optimisation studies available for integrated LNG/NGL and NGL processing plants have focused on the design and operation of MR based integrated liquefaction processes and applicable for either small scale or offshore LNG plants.

For instance, some of the common optimisation parameters that were studied for the integrated LNG/NGL plants are the MR composition, its pressure levels, lean vs. rich feed gas, NGL column temperature and it recycle flow rate and inlet pressures of De-C1 and De-C2 columns. As discussed earlier, for the cascade process, Ransbarger did not provide any numerical data about the amount of energy consumption required for the proposed integrated configurations. This could be due to the confidentiality issue and limitation on sharing the ConocoPhillips technical data. As mentioned above, some areas that were studied to optimise the NGL process are several types of feed gas, different sets of De-C1 column stages and proposal of new NGL recovery design for FLNG application.

On the other hand, no studies are available that discuss the optimisation areas for the integrated LNG/NGL cascade process for a large single train. For example, the effect of different integrated LNG/NGL designs on the LNG HHV specification, process parameters, the effect of De-C2 column pressure on the process performance and efficiency have not been studied. Therefore, in this research work, 5 MTPA integrated LNG/NGL cascade process is optimised to close these studies gaps.

The optimisation of the integrated cascade process is carried out in three steps. Firstly, optimisation of the propane pre-cooling cycle as explained in section 2.9.2. Based on the energy and exergy analyses results, optimal operating conditions of the pre-cooling cycle are obtained. Next, using this optimal pre-cooling operating data, the cascade process is further optimised by determining the optimal design for integrated ethylene refrigeration cycle with NGL section. Lastly, the optimal integrated LNG/NGL design is selected and again further optimised by manipulating the deethaniser (De-C2) column pressure. A detailed discussion about these optimisation areas of cascade LNG process is covered in chapter 4, 5 and 6 of this thesis.

Table 2.7: Summary of optimisation studies for integrated LNG/NGL processing plants and standalone NGL recovery plant.

Year	Reference	Simulation software and EOS	Optimisation studies
2014	Khan et al.	Aspen HYSYS, Peng Robinson and Lee Kestler	Studied three different NGL configurations integrated with *Korea single mixed refrigerant (KSMR)* liquefaction process suitable for the *offshore* based LNG plant. Optimised the MR composition and its compressor pressure levels.
2014	Mehrpooya et al.	Recommend Aspen Plus or Aspen HYSYS, Peng Robinson	Minimised the energy consumption and maximised high ethane recovery for three novels integrated LNG/NGL processes *(DMR, C3MR, MFC)* by varying the cold recycle flow rate and its temperature in the NGL column.
2005	Pillarella, et al.	Not stated	Studied the effect of minimising the temperature approach in the propane condenser towards the heat exchanger area and SP for *AP-X* process. Computed the exergy loss of the process equipment.
2014	He and Ju	Aspen HYSYS	Optimised a novel *MRC* integrated with NGL for the *small-scale* LNG plant. Analysed the effect of MR composition and its pressures and De-C1 and De-C2 columns inlet pressures.
2008	Ransbarger	Not stated	Proposed four different process configurations for an integrated LNG/NGL cascade process using propane, ethane and methane open cycle. No numerical data are available on the energy consumption required for these configurations.
2012	Cipolato, et al.	Aspen HYSYS v. 3.2, Peng Robinson	Studied the influence of pressure in six different locations in the propane, ethane and methane cycles for *cascade process*.
2014	Yoon, et al.	Aspen HYSYS, Peng Robinson and Lee–Kesler–Plocker	Compared C_3H_8–C_2H_4–CH_4, CO_2–C_2H_6–N_2 and CO_2–N_2 *cascade cycles* efficiencies and computed the exergy loss of the process equipment.
2016	Fahmy, et al.	Aspen HYSYS v. 7	Studied the effect of replacing the J-T valves with liquid expanders in the *Open Cycle Phillips optimised cascade process* for the production of 4.24 MTPA LNG.

2002	Kanoglu	Not stated	Studied the performance of multistage cascade refrigeration cycle. No information available on the process simulation results.
2006	Mehrpooya, et al.	Aspen HYSYS v.3.2, PRSV	Analysed the effect of pressure drop of evaporators in the propane refrigeration cycle used in the *NGL* plant. Computed the exergy loss of the process equipment.
2014	Vatani, et al.	Aspen HYSYS, PRSV	Reviewed the performance of *SMR (APCI)*, *SMR (Linde)*, *C3MR (Linde)*, *DMR (APCI)* and *MFC (Statoil/Linde)* processes.
2015	Shin et al.	Unisim	Optimised the *NGL* process by varying the type of feed gas and different sets of De-C1 column stages.
2012	Lee et al.	Aspen HYSYS 7.1, Lee Kestler	Proposed new design for NGL recovery for *FLNG* application that gives low energy usage.

Chapter 3 Process modelling and simulation of Cascade LNG process

3.1 Introduction

This chapter describes the basis of process modelling and simulation applied for cascade LNG process for 5 MTPA production capacity. The cascade LNG process is first modelled and simulated using the operational data obtained from the following literature [31, 46, 51, 54, 120, 122, 123, 125-127] and existing LNG plants located in the Southeast Asia region, Australia, Gulf countries, Northern Asia and Africa. These plants are not disclosed because of confidentiality issues. In this study, the cascade LNG process is simulated and optimised in three steps. Firstly, a three-stage propane pre-cooling cycle is modelled and simulated. The propane pre-cooling cycle is optimised, and the detail of this work is described in Chapter 4. After optimisation of the propane cycle, two different configurations of the ethylene refrigeration cycle integrated with the NGL section are compared to find the optimum design. Based on the optimisation results, the optimum integrated design is selected. Detail of this work is described in Chapter 5. Finally, the selected optimum integrated cascade design is further optimised by manipulating the deethaniser (De-C2) column pressure which will be discussed in Chapter 6. The modelling assumptions and simulation constraints applied in all the three optimisation areas are explained in the next section. Additionally, the simulation description, process simulation flow scheme, stream properties and composition for each stream are also presented.

3.2 Simulation basis and modelling assumptions

The cascade LNG process is modelled and simulated in a steady state mode using Aspen HYSYS (v.7.2, 2010). The pre-treatment unit was not modelled in this work as the main emphasis is on the optimisation of the pre-cooling, liquefaction and NGL section. Peng Robinson equation of state (EOS) is used to obtain the physiochemical properties of the fluid [138]. The process simulator and EOS are prevalent for simulating the LNG and NGL processes and have been confirmed in previous studies [31, 55, 60, 132, 139, 140]. The feed gas conditions [53] and modelling assumptions applied in this study are summarised in Table 3.1. For all the research works, the same simulation basis and modelling assumptions are applied.

Table 3.1: Feed gas condition and modelling assumptions.

Process parameters	Condition
NG feed condition	
Flow rate (kgmole h^{-1})	41,700
Pressure (kPa)	7500
Temperature (°C)	29
NG feed gas composition [a][53]	mole fraction
Nitrogen	0.0028
Methane	0.8974
Ethane	0.0496
Propane	0.0343
i-Butane	0.0079
n-Butane	0.0073
i-Pentane	0.0005
n-Pentane	0.0002
Mechanical efficiency	
Compressor polytropic efficiency [132]	80 %
Pump adiabatic efficiency	85 %
Pressure drops (kPa)	
LNG HX	20
AC	30
Minimum temperature approach (MITA) in HX	> 2 °C
Column hydraulics[b]	
Demethaniser (De-C1)	
Operating pressure (kPa)	3400
Number of theoretical stages	43
Deeethaniser (De-C2)	
Operating pressure (kPa) **[132]**	1800-2200
Number of theoretical stages	38
Ambient temperature (°C)	27
Air cooler exit temperature (°C)	49
Plant availability, days/year	330

[a] Feed gas composition and condition are taken after the treating section.

[b] The demethaniser and deethaniser theoretical stages are taken from a petrochemical plant located at Basrah, Bagdad, Iraq [141].

3.3 Process simulation constraints

The following are the constraints applied in modelling the integrated cascade process:

1. The inlet temperature of all the compressors should be maintained above its dew point temperature to prevent the ingress of liquid droplets. Compressor discharge temperature should be below 120^{o}C to safeguard its mechanical components [142].
2. LNG higher heating value (HHV) requirement is 39.12 – 41.92 MJ/m^{3} (1,050 – 1,125 Btu/Scf)
3. The targeted LNG plant capacity is 5 MTPA (631,313 kg/h).
4. The minimum temperature approach (MITA) in the LNG heat exchanger is to be assured above 2^{o}C to avoid temperature cross.

3.4 Cascade LNG process simulation description

The process simulation flow scheme of cascade LNG process (base case) is shown in Figure 3.1 and Figure 3.2. The treated natural gas at 29^{o}C and 75 bar enters the propane refrigeration cycle and is cooled consecutively in three heat exchangers namely HXC3-1, HXC3-2 and HXC3-3 to -25^{o}C, -30^{o}C and -40^{o}C respectively. The propane also cools methane and condenses ethylene refrigerants simultaneously along with natural gas. The vaporised propane refrigerant is then compressed in three different stages (K-100 LP C3, K-101 MP C3 and K-102 HP C3) to 18 bar. The compressed propane refrigerant is finally condensed in a series of air coolers and expanded via CV-1.

The natural gas and methane refrigerant are then cooled by ethylene refrigerant to -55^{o}C in the first heat exchanger (HXC2-1). The cooled natural gas is then expanded via CV-6 and then enters the demethaniser column (De-C1) at 34 bar. The De-C1 column is operated as a total condenser. The bottom of De-C1 column (1_NGL) is expanded via CV-7 to 20 bar before entering the deethaniser column (De-C2). The De-C2 column is operated as full reflux. The De-C2 column bottom is sent to the depropaniser column (De-C3) while the overhead of De-C2 column (10_NG) is compressed to 33.8 bar. The overhead of De-C1 column (9_NG) and De-C2 column (10_NG) are mixed together before being cooled by the second ethylene heat exchanger (HXC2-2) to -95^{o}C. Whereas methane refrigerant finally condensed after been cooled by the second ethylene heat exchanger. The vaporised ethylene refrigerant is then compressed in two stages (K-100 LP C2, K-101 MP C2) to 25 bar. The compressed ethylene is then cooled in a series of air coolers and condensed by propane refrigerant before finally reduced in pressure via CV-4.

The natural gas is further cooled by methane refrigerant to -115ºC, -140ºC and -152ºC in three heat exchangers (HXC1-1, HXC1-2 and HXC1-3) respectively. The liquefied natural gas is then expanded to 1.01 bar via CV-11 before entering the LNG tank. Meanwhile, the vaporised methane refrigerant is compressed in three compression stages (K-100 LP C1, K-101 MP C1 and K-102 HP C1) to 36.5 bar. The superheated methane refrigerant is then cooled by the propane refrigerant and condensed by ethylene refrigerant before been expanded via CV-8. The details stream properties are presented in Table 3.2 and Table 3.3 while the composition for each stream is presented in Table 3.4, Table 3.5 and Table 3.6.

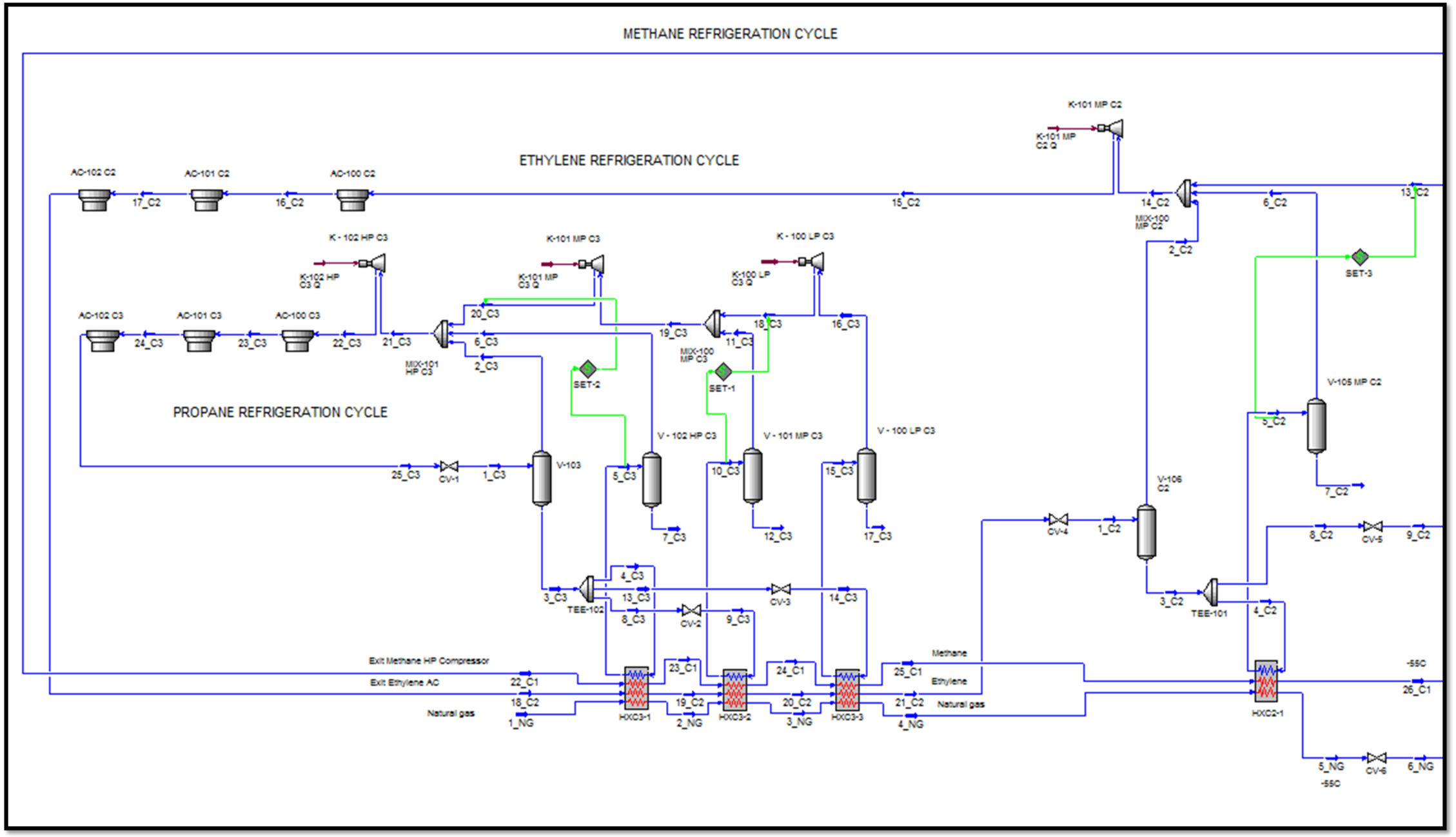

Figure 3.1: Aspen HYSYS process simulation flow scheme for the cascade LNG process (base case) – propane and partly ethylene refrigeration cycles.

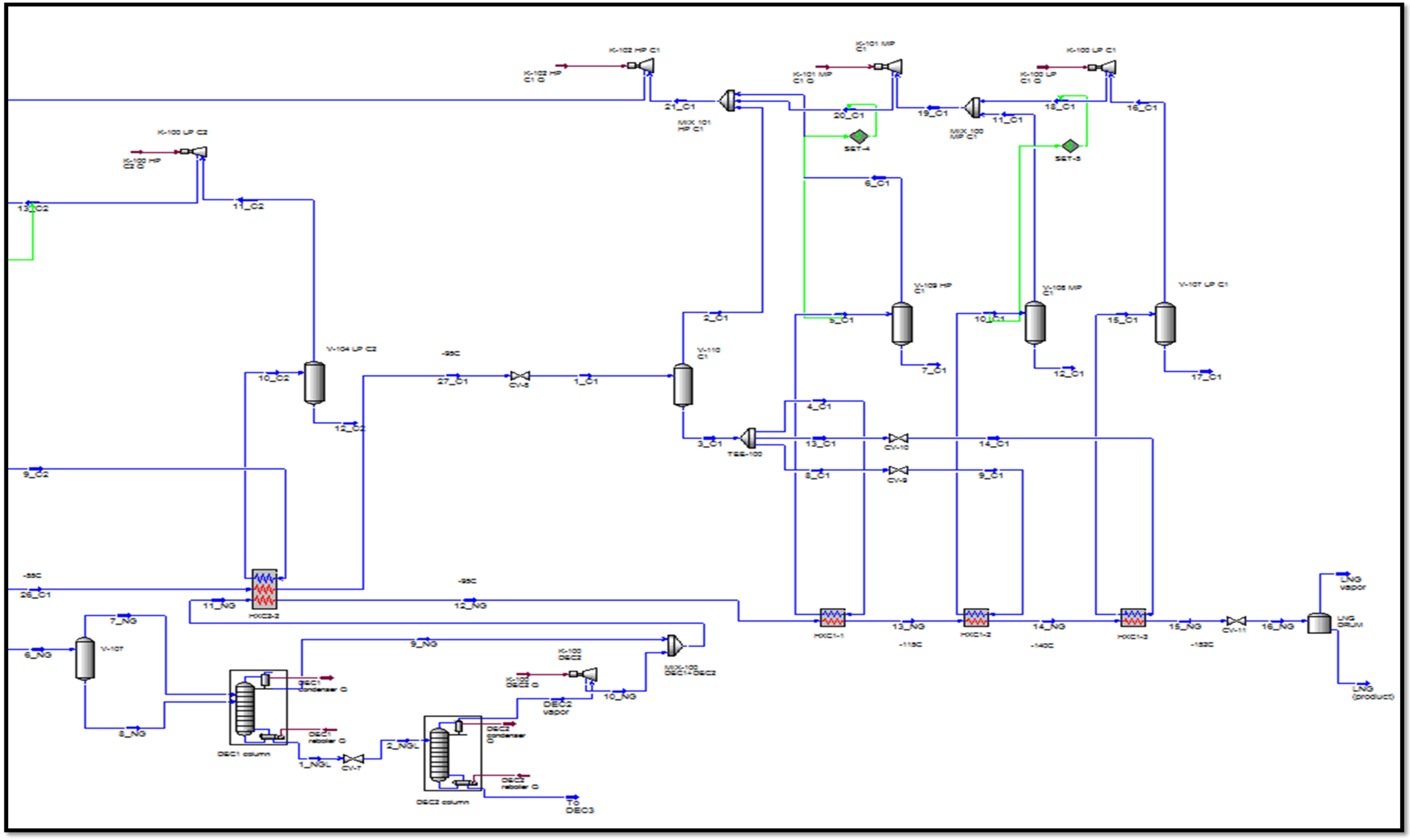

Figure 3.2: Aspen HYSYS process simulation flow scheme for the cascade LNG process (base case) – ethylene and methane refrigeration cycles.

Table 3.2: Base case stream properties (a)

Stream name	1_NG	2_NG	3_NG	4_NG	1_C3	2_C3	3_C3	4_C3	5_C3	6_C3	7_C3	8_C3	9_C3	10_C3	11_C3	12_C3
Vapour fraction	1.00	1.00	0.98	0.93	0.50	1.00	0.00	0.00	1.00	1.00	0.00	0.00	0.03	1.00	1.00	0.00
Temperature (C)	29.00	-25.00	-30.00	-40.00	-27.48	-27.48	-27.48	-27.49	-23.00	-23.00	-23.00	-27.49	-32.34	-27.00	-27.00	-27.00
Pressure (bar)	75.00	74.80	74.60	74.40	1.85	1.85	1.85	1.85	1.85	1.85	1.85	1.85	1.53	1.53	1.53	1.53
Molar flow (kgmole/h)	41700.00	41700.00	41700.00	41700.00	84276.78	42298.46	41978.33	34527.83	34527.83	34527.83	0.00	2422.14	2422.14	2422.14	2422.14	0.00
Mass flow (kg/s)	213.29	213.29	213.29	213.29	1032.32	518.12	514.20	422.94	422.94	422.94	0.00	29.67	29.67	29.67	29.67	0.00
Liquid volume flow (m3/h)	2376.40	2376.40	2376.40	2376.40	7334.74	3681.30	3653.44	3005.01	3005.01	3005.01	0.00	210.80	210.80	210.80	210.80	0.00
Heat flow (MW)	-910.97	-948.23	-953.32	-964.85	-2735.15	-1267.01	-1468.14	-1207.57	-1031.37	-1031.37	0.00	-84.71	-84.71	-72.50	-72.50	0.00
Mass entropy (kJ/kgK)	7.99	7.35	7.25	7.03	2.40	3.24	1.57	1.57	3.26	3.26	1.61	1.57	1.57	3.28	3.28	1.57
Stream name	13_C3	14_C3	15_C3	16_C3	17_C3	18_C3	19_C3	20_C3	21_C3	22_C3	23_C3	24_C3	25_C3	5_NG	6_NG	7_NG
Vapour fraction	0.00	0.08	1.00	1.00	0.00	1.00	1.00	1.00	1.00	1.00	1.00	1.00	0.00	1.00	0.62	1.00
Temperature (C)	-27.49	-42.19	-33.00	-33.00	-33.00	-16.34	-19.77	-11.98	-24.25	79.88	70.00	60.00	49.00	-55.00	-82.16	-82.16
Pressure (bar)	1.85	1.01	1.01	1.01	1.01	1.53	1.53	1.85	1.85	18.00	17.70	17.40	17.10	74.20	34.00	34.00
Molar flow (kgmole/h)	5028.36	5028.36	5028.36	5028.36	0.00	5028.36	7450.50	7450.50	84276.78	84276.78	84276.78	84276.78	84276.78	41700.00	41700.00	25970.88
Mass flow (kg/s)	61.59	61.59	61.59	61.59	0.00	61.59	91.26	91.26	1032.32	1032.32	1032.32	1032.32	1032.32	213.29	213.29	118.14
Liquid volume flow (m3/h)	437.63	437.63	437.63	437.63	0.00	437.63	648.43	648.43	7334.74	7334.74	7334.74	7334.74	7334.74	2376.40	2376.40	1404.03
Heat flow (MW)	-175.86	-175.86	-150.94	-150.94	0.00	-149.50	-222.00	-220.99	-2519.38	-2372.34	-2393.92	-2415.67	-2735.15	-989.55	-989.55	-578.54
Mass entropy (kJ/kgK)	1.57	1.57	3.32	3.32	1.52	3.34	3.32	3.33	3.26	3.35	3.30	3.24	2.28	6.51	6.64	8.17
Stream name	8_NG	9_NG	1_NGL	2_NGL	DEC2 vapor	To DEC3	10_NG	11_NG	12_NG	1_C2	2_C2	3_C2	4_C2	5_C2	6_C2	7_C2
Vapour fraction	0.00	0.00	0.00	0.29	1.00	0.00	1.00	0.29	0.00	0.22	1.00	0.00	0.00	1.00	1.00	0.00
Temperature (C)	-82.16	-92.95	49.00	27.44	5.41	72.70	41.67	-88.75	-95.00	-75.15	-75.15	-75.15	-75.15	-50.00	-50.00	-50.00
Pressure (bar)	34.00	33.80	34.00	20.00	19.80	20.00	33.80	33.80	33.60	4.20	4.20	4.20	4.20	4.20	4.20	4.20
Molar flow (kgmole/h)	15729.12	37523.73	4176.27	4176.27	2375.33	1800.93	2375.33	39899.07	39899.07	38342.11	8477.25	29864.87	8341.51	8341.51	8341.51	0.00
Mass flow (kg/s)	95.14	167.62	45.67	45.67	20.91	24.76	20.91	188.53	188.53	298.79	66.06	232.73	65.00	65.00	65.00	0.00
Liquid volume flow (m3/h)	972.37	2008.57	367.82	367.82	201.01	166.81	201.01	2209.58	2209.58	2806.81	620.57	2186.24	610.63	610.63	610.63	0.00
Heat flow (MW)	-411.01	-879.14	-126.86	-126.86	-59.27	-62.57	-58.50	-937.63	-956.35	409.09	112.84	296.25	82.75	113.38	113.38	0.00
Mass entropy (kJ/kgK)	4.74	6.78	3.24	3.27	5.11	2.24	5.13	6.79	6.25	3.52	5.24	3.04	3.04	5.41	5.41	3.36

Table 3.3: Base case stream properties (b)

Stream name	8_C2	9_C2	10_C2	11_C2	12_C2	13_C2	14_C2	15_C2	16_C2	17_C2	18_C2	19_C2	20_C2	21_C2	13_NG	14_NG
Vapour fraction	0.00	0.13	1.00	1.00	0.00	1.00	1.00	1.00	1.00	1.00	1.00	0.00	0.00	0.00	0.00	0.00
Temperature (C)	-75.15	-100.09	-80.00	-80.00	-80.00	-6.61	-30.74	99.94	80.00	68.00	49.00	-25.00	-30.00	-40.00	-115.00	-140.00
Pressure (bar)	4.20	1.27	1.27	1.27	1.27	4.20	4.20	25.00	24.70	24.40	24.10	23.90	23.70	23.50	33.40	33.20
Molar flow (kgmole/h)	21523.35	21523.35	21523.35	21523.35	0.00	21523.35	38342.11	38342.11	38342.11	38342.11	38342.11	38342.11	38342.11	38342.11	39899.07	39899.07
Mass flow (kg/s)	167.73	167.73	167.73	167.73	0.00	167.73	298.79	298.79	298.79	298.79	298.79	298.79	298.79	298.79	188.53	188.53
Liquid volume flow (m3/h)	1575.60	1575.60	1575.60	1575.60	0.00	1575.60	2806.81	2806.81	2806.81	2806.81	2806.81	2806.81	2806.81	2806.81	2209.58	2209.58
Heat flow (MW)	213.50	213.50	286.98	286.98	0.00	303.39	529.62	585.81	574.53	567.89	557.42	423.99	418.70	409.09	-973.28	-990.50
Mass entropy (kJ/kgK)	3.04	3.06	5.59	5.59	2.98	5.67	5.53	5.65	5.55	5.49	5.39	3.67	3.60	3.47	5.72	5.09
Stream name	15_NG	16_NG	LNG vapor	LNG (product)	1_C1	2_C1	3_C1	4_C1	5_C1	6_C1	7_C1	8_C1	9_C1	10_C1	11_C1	12_C1
Vapour fraction	0.00	0.07	1.00	0.00	0.30	1.00	0.00	0.00	1.00	1.00	0.00	0.00	0.22	1.00	1.00	0.00
Temperature (C)	-152.00	-161.16	-161.16	-161.16	-118.33	-118.33	-118.33	-118.33	-100.00	-100.00	-100.00	-118.33	-144.76	-130.00	-130.00	-130.00
Pressure (bar)	33.00	1.01	1.01	1.01	13.00	13.00	13.00	13.00	13.00	13.00	13.00	13.00	3.36	3.36	3.36	3.36
Molar flow (kgmole/h)	39899.07	39899.07	2849.77	37049.30	32569.42	9866.87	22702.56	8618.64	8618.64	8618.64	0.00	9562.45	9562.45	9562.45	9562.45	0.00
Mass flow (kg/s)	188.53	188.53	12.97	175.57	145.14	43.97	101.17	38.41	38.41	38.41	0.00	42.61	42.61	42.61	42.61	0.00
Liquid volume flow (m3/h)	2209.58	2209.58	151.22	2058.37	1745.22	528.71	1216.51	461.83	461.83	461.83	0.00	512.40	512.40	512.40	512.40	0.00
Heat flow (MW)	-998.11	-998.11	-62.66	-935.45	-768.19	-220.64	-547.55	-207.87	-190.94	-190.94	0.00	-230.63	-230.63	-213.42	-213.42	0.00
Mass entropy (kJ/kgK)	4.77	4.84	9.18	4.52	6.77	8.54	6.00	6.00	8.83	8.83	6.65	6.00	6.09	9.22	9.22	5.68
Stream name	13_C1	14_C1	15_C1	16_C1	17_C1	18_C1	19_C1	20_C1	21_C1	22_C1	23_C1	24_C1	25_C1	26_C1	27_C1	
Vapour fraction	0.00	0.29	1.00	1.00	0.00	1.00	1.00	1.00	1.00	1.00	1.00	1.00	1.00	1.00	0.00	
Temperature (C)	-118.33	-155.00	-145.00	-145.00	-145.00	-113.85	-124.84	-45.55	-82.98	-10.05	-25.00	-30.00	-40.00	-55.00	-95.00	
Pressure (bar)	13.00	1.69	1.69	1.69	1.69	3.36	3.36	13.00	13.00	36.50	36.30	36.10	35.90	35.70	35.50	
Molar flow (kgmole/h)	4521.47	4521.47	4521.47	4521.47	0.00	4521.47	14083.92	14083.92	32569.42	32569.42	32569.42	32569.42	32569.42	32569.42	32569.42	
Mass flow (kg/s)	20.15	20.15	20.15	20.15	0.00	20.15	62.76	62.76	145.14	145.14	145.14	145.14	145.14	145.14	145.14	
Liquid volume flow (m3/h)	242.28	242.28	242.28	242.28	0.00	242.28	754.68	754.68	1745.22	1745.22	1745.22	1745.22	1745.22	1745.22	1745.22	
Heat flow (MW)	-109.05	-109.05	-101.44	-101.44	0.00	-100.21	-313.62	-304.06	-715.64	-696.36	-701.87	-703.71	-707.49	-713.43	-768.19	
Mass entropy (kJ/kgK)	6.00	6.18	9.37	9.37	5.26	9.46	9.30	9.47	9.05	9.17	9.02	8.98	8.87	8.69	6.67	

Table 3.4: Base case stream composition (a).

Stream name	1_NG	2_NG	3_NG	4_NG	1_C3	2_C3	3_C3	4_C3	5_C3	6_C3	7_C3	8_C3	9_C3	10_C3	11_C3	12_C3
Mole Fraction																
Methane	0.8974	0.8974	0.8974	0.8974	0.0000	0.0000	0.0000	0.0000	0.0000	0.0000	0.0000	0.0000	0.0000	0.0000	0.0000	0.0000
Ethylene	0.0000	0.0000	0.0000	0.0000	0.0000	0.0000	0.0000	0.0000	0.0000	0.0000	0.0000	0.0000	0.0000	0.0000	0.0000	0.0000
Ethane	0.0496	0.0496	0.0496	0.0496	0.0000	0.0000	0.0000	0.0000	0.0000	0.0000	0.0000	0.0000	0.0000	0.0000	0.0000	0.0000
Propane	0.0343	0.0343	0.0343	0.0343	1.0000	1.0000	1.0000	1.0000	1.0000	1.0000	1.0000	1.0000	1.0000	1.0000	1.0000	1.0000
i-Butane	0.0079	0.0079	0.0079	0.0079	0.0000	0.0000	0.0000	0.0000	0.0000	0.0000	0.0000	0.0000	0.0000	0.0000	0.0000	0.0000
n-Butane	0.0073	0.0073	0.0073	0.0073	0.0000	0.0000	0.0000	0.0000	0.0000	0.0000	0.0000	0.0000	0.0000	0.0000	0.0000	0.0000
i-Pentane	0.0005	0.0005	0.0005	0.0005	0.0000	0.0000	0.0000	0.0000	0.0000	0.0000	0.0000	0.0000	0.0000	0.0000	0.0000	0.0000
n-Pentane	0.0002	0.0002	0.0002	0.0002	0.0000	0.0000	0.0000	0.0000	0.0000	0.0000	0.0000	0.0000	0.0000	0.0000	0.0000	0.0000
n-Hexane	0.0000	0.0000	0.0000	0.0000	0.0000	0.0000	0.0000	0.0000	0.0000	0.0000	0.0000	0.0000	0.0000	0.0000	0.0000	0.0000
Nitrogen	0.0028	0.0028	0.0028	0.0028	0.0000	0.0000	0.0000	0.0000	0.0000	0.0000	0.0000	0.0000	0.0000	0.0000	0.0000	0.0000
Stream name	13_C3	14_C3	15_C3	16_C3	17_C3	18_C3	19_C3	20_C3	21_C3	22_C3	23_C3	24_C3	25_C3	5_NG	6_NG	7_NG
Mole Fraction																
Methane	0.0000	0.0000	0.0000	0.0000	0.0000	0.0000	0.0000	0.0000	0.0000	0.0000	0.0000	0.0000	0.0000	0.8974	0.8974	0.9785
Ethylene	0.0000	0.0000	0.0000	0.0000	0.0000	0.0000	0.0000	0.0000	0.0000	0.0000	0.0000	0.0000	0.0000	0.0000	0.0000	0.0000
Propane	1.0000	1.0000	1.0000	1.0000	1.0000	1.0000	1.0000	1.0000	1.0000	1.0000	1.0000	1.0000	1.0000	0.0343	0.0343	0.0024
Ethane	0.0000	0.0000	0.0000	0.0000	0.0000	0.0000	0.0000	0.0000	0.0000	0.0000	0.0000	0.0000	0.0000	0.0496	0.0496	0.0148
i-Butane	0.0000	0.0000	0.0000	0.0000	0.0000	0.0000	0.0000	0.0000	0.0000	0.0000	0.0000	0.0000	0.0000	0.0079	0.0079	0.0002
n-Butane	0.0000	0.0000	0.0000	0.0000	0.0000	0.0000	0.0000	0.0000	0.0000	0.0000	0.0000	0.0000	0.0000	0.0073	0.0073	0.0001
i-Pentane	0.0000	0.0000	0.0000	0.0000	0.0000	0.0000	0.0000	0.0000	0.0000	0.0000	0.0000	0.0000	0.0000	0.0005	0.0005	0.0000
n-Pentane	0.0000	0.0000	0.0000	0.0000	0.0000	0.0000	0.0000	0.0000	0.0000	0.0000	0.0000	0.0000	0.0000	0.0002	0.0002	0.0000
n-Hexane	0.0000	0.0000	0.0000	0.0000	0.0000	0.0000	0.0000	0.0000	0.0000	0.0000	0.0000	0.0000	0.0000	0.0000	0.0000	0.0000
Nitrogen	0.0000	0.0000	0.0000	0.0000	0.0000	0.0000	0.0000	0.0000	0.0000	0.0000	0.0000	0.0000	0.0000	0.0028	0.0028	0.0040

Table 3.5: Base case stream composition (b).

Stream name	8_NG	9_NG	1_NGL	2_NGL	DEC2 vapor	To DEC3	10_NG	11_NG	12_NG	1_C2	2_C2	3_C2	4_C2	5_C2	6_C2	7_C2
Mole Fraction																
Methane	0.7634	0.9968	0.0041	0.0041	0.0072	0.0000	0.0072	0.9379	0.9379	0.0000	0.0000	0.0000	0.0000	0.0000	0.0000	0.0000
Ethylene	0.0000	0.0000	0.0000	0.0000	0.0000	0.0000	0.0000	0.0000	0.0000	1.0000	1.0000	1.0000	1.0000	1.0000	1.0000	1.0000
Ethane	0.1070	0.0001	0.4946	0.4946	0.8697	0.0000	0.8697	0.0518	0.0518	0.0000	0.0000	0.0000	0.0000	0.0000	0.0000	0.0000
Propane	0.0871	0.0000	0.3425	0.3425	0.1231	0.6319	0.1231	0.0073	0.0073	0.0000	0.0000	0.0000	0.0000	0.0000	0.0000	0.0000
i-Butane	0.0207	0.0000	0.0789	0.0789	0.0000	0.1829	0.0000	0.0000	0.0000	0.0000	0.0000	0.0000	0.0000	0.0000	0.0000	0.0000
n-Butane	0.0192	0.0000	0.0729	0.0729	0.0000	0.1690	0.0000	0.0000	0.0000	0.0000	0.0000	0.0000	0.0000	0.0000	0.0000	0.0000
i-Pentane	0.0013	0.0000	0.0050	0.0050	0.0000	0.0116	0.0000	0.0000	0.0000	0.0000	0.0000	0.0000	0.0000	0.0000	0.0000	0.0000
n-Pentane	0.0005	0.0000	0.0020	0.0020	0.0000	0.0046	0.0000	0.0000	0.0000	0.0000	0.0000	0.0000	0.0000	0.0000	0.0000	0.0000
n-Hexane	0.0000	0.0000	0.0000	0.0000	0.0000	0.0000	0.0000	0.0000	0.0000	0.0000	0.0000	0.0000	0.0000	0.0000	0.0000	0.0000
Nitrogen	0.0008	0.0031	0.0000	0.0000	0.0000	0.0000	0.0000	0.0029	0.0029	0.0000	0.0000	0.0000	0.0000	0.0000	0.0000	0.0000
Stream name	8_C2	9_C2	10_C2	11_C2	12_C2	13_C2	14_C2	15_C2	16_C2	17_C2	18_C2	19_C2	20_C2	21_C2	13_NG	14_NG
Mole Fraction																
Methane	0.0000	0.0000	0.0000	0.0000	0.0000	0.0000	0.0000	0.0000	0.0000	0.0000	0.0000	0.0000	0.0000	0.0000	0.9379	0.9379
Ethylene	1.0000	1.0000	1.0000	1.0000	1.0000	1.0000	1.0000	1.0000	1.0000	1.0000	1.0000	1.0000	1.0000	1.0000	0.0000	0.0000
Ethane	0.0000	0.0000	0.0000	0.0000	0.0000	0.0000	0.0000	0.0000	0.0000	0.0000	0.0000	0.0000	0.0000	0.0000	0.0518	0.0518
Propane	0.0000	0.0000	0.0000	0.0000	0.0000	0.0000	0.0000	0.0000	0.0000	0.0000	0.0000	0.0000	0.0000	0.0000	0.0073	0.0073
i-Butane	0.0000	0.0000	0.0000	0.0000	0.0000	0.0000	0.0000	0.0000	0.0000	0.0000	0.0000	0.0000	0.0000	0.0000	0.0000	0.0000
n-Butane	0.0000	0.0000	0.0000	0.0000	0.0000	0.0000	0.0000	0.0000	0.0000	0.0000	0.0000	0.0000	0.0000	0.0000	0.0000	0.0000
i-Pentane	0.0000	0.0000	0.0000	0.0000	0.0000	0.0000	0.0000	0.0000	0.0000	0.0000	0.0000	0.0000	0.0000	0.0000	0.0000	0.0000
n-Pentane	0.0000	0.0000	0.0000	0.0000	0.0000	0.0000	0.0000	0.0000	0.0000	0.0000	0.0000	0.0000	0.0000	0.0000	0.0000	0.0000
n-Hexane	0.0000	0.0000	0.0000	0.0000	0.0000	0.0000	0.0000	0.0000	0.0000	0.0000	0.0000	0.0000	0.0000	0.0000	0.0000	0.0000
Nitrogen	0.0000	0.0000	0.0000	0.0000	0.0000	0.0000	0.0000	0.0000	0.0000	0.0000	0.0000	0.0000	0.0000	0.0000	0.0029	0.0029

Table 3.6: Base case stream composition (c).

Stream name	15_NG	16_NG	LNG vapor	LNG (product)	1_C1	2_C1	3_C1	4_C1	5_C1	6_C1	7_C1	8_C1	9_C1	10_C1	11_C1	12_C1
Mole Fraction																
Methane	0.9379	0.9379	0.9720	0.9353	1.0000	1.0000	1.0000	1.0000	1.0000	1.0000	1.0000	1.0000	1.0000	1.0000	1.0000	1.0000
Ethylene	0.0000	0.0000	0.0000	0.0000	0.0000	0.0000	0.0000	0.0000	0.0000	0.0000	0.0000	0.0000	0.0000	0.0000	0.0000	0.0000
Ethane	0.0518	0.0518	0.0001	0.0558	0.0000	0.0000	0.0000	0.0000	0.0000	0.0000	0.0000	0.0000	0.0000	0.0000	0.0000	0.0000
Propane	0.0073	0.0073	0.0000	0.0079	0.0000	0.0000	0.0000	0.0000	0.0000	0.0000	0.0000	0.0000	0.0000	0.0000	0.0000	0.0000
i-Butane	0.0000	0.0000	0.0000	0.0000	0.0000	0.0000	0.0000	0.0000	0.0000	0.0000	0.0000	0.0000	0.0000	0.0000	0.0000	0.0000
n-Butane	0.0000	0.0000	0.0000	0.0000	0.0000	0.0000	0.0000	0.0000	0.0000	0.0000	0.0000	0.0000	0.0000	0.0000	0.0000	0.0000
i-Pentane	0.0000	0.0000	0.0000	0.0000	0.0000	0.0000	0.0000	0.0000	0.0000	0.0000	0.0000	0.0000	0.0000	0.0000	0.0000	0.0000
n-Pentane	0.0000	0.0000	0.0000	0.0000	0.0000	0.0000	0.0000	0.0000	0.0000	0.0000	0.0000	0.0000	0.0000	0.0000	0.0000	0.0000
n-Hexane	0.0000	0.0000	0.0000	0.0000	0.0000	0.0000	0.0000	0.0000	0.0000	0.0000	0.0000	0.0000	0.0000	0.0000	0.0000	0.0000
Nitrogen	0.0029	0.0029	0.0279	0.0010	0.0000	0.0000	0.0000	0.0000	0.0000	0.0000	0.0000	0.0000	0.0000	0.0000	0.0000	0.0000
Stream name	13_C1	14_C1	15_C1	16_C1	17_C1	18_C1	19_C1	20_C1	21_C1	22_C1	23_C1	24_C1	25_C1	26_C1	27_C1	
Mole Fraction																
Methane	1.0000	1.0000	1.0000	1.0000	1.0000	1.0000	1.0000	1.0000	1.0000	1.0000	1.0000	1.0000	1.0000	1.0000	1.0000	
Ethylene	0.0000	0.0000	0.0000	0.0000	0.0000	0.0000	0.0000	0.0000	0.0000	0.0000	0.0000	0.0000	0.0000	0.0000	0.0000	
Ethane	0.0000	0.0000	0.0000	0.0000	0.0000	0.0000	0.0000	0.0000	0.0000	0.0000	0.0000	0.0000	0.0000	0.0000	0.0000	
Propane	0.0000	0.0000	0.0000	0.0000	0.0000	0.0000	0.0000	0.0000	0.0000	0.0000	0.0000	0.0000	0.0000	0.0000	0.0000	
i-Butane	0.0000	0.0000	0.0000	0.0000	0.0000	0.0000	0.0000	0.0000	0.0000	0.0000	0.0000	0.0000	0.0000	0.0000	0.0000	
n-Butane	0.0000	0.0000	0.0000	0.0000	0.0000	0.0000	0.0000	0.0000	0.0000	0.0000	0.0000	0.0000	0.0000	0.0000	0.0000	
i-Pentane	0.0000	0.0000	0.0000	0.0000	0.0000	0.0000	0.0000	0.0000	0.0000	0.0000	0.0000	0.0000	0.0000	0.0000	0.0000	
n-Pentane	0.0000	0.0000	0.0000	0.0000	0.0000	0.0000	0.0000	0.0000	0.0000	0.0000	0.0000	0.0000	0.0000	0.0000	0.0000	
n-Hexane	0.0000	0.0000	0.0000	0.0000	0.0000	0.0000	0.0000	0.0000	0.0000	0.0000	0.0000	0.0000	0.0000	0.0000	0.0000	
Nitrogen	0.0000	0.0000	0.0000	0.0000	0.0000	0.0000	0.0000	0.0000	0.0000	0.0000	0.0000	0.0000	0.0000	0.0000	0.0000	

3.5 Optimisation framework of Cascade LNG process

After the Cascade LNG process is modelled and simulated in Aspen HYSYS v. 7.2, a calculation spreadsheet has been developed within this software. This spreadsheet contained detailed thermodynamics information for each refrigeration cycle such as the inlet and outlet enthalpies and entropies for all the unit operations (compressors, LNG heat exchangers, valves, mixers and air coolers), LNG heat exchanger duty, UA, temperature approach, log-mean temperature difference (LMTD) and heat balance. Also, the energy and exergy equations have been developed within the spreadsheet. These thermodynamics data and equations are used to calculate the efficiency of the cascade process. This information is then transferred to Microsoft Excel for further analysis and the optimisation results are presented in the graphical form. Based on the energy and exergy analyses results, the cascade process is further optimised. This approach is in agreement with the optimisation work done by Cipolato, Lirani [56], Kanoglu [51], Mokhatab, Mark [30] and Vatani, Mehrpooya [55].

Details of the optimisation framework for the propane pre-cooling cycle, integrated ethylene refrigeration cycle with NGL section and effect of De-C2 column are discussed in Chapter 4, Chapter 5 and Chapter 6 respectively in the thesis.

3.6 Simulation model verification

The model verification for propane pre-cooling cycle and integrated LNG/NGL processes are discussed below.

3.6.1 Model verification (propane pre-cooling cycle)

The propane pre-cooling cycle simulation model is verified by performing the heat and mass balance. The heat balance across LNG heat exchanger is expressed as:

$$Q_{process\ (NG+C1+C2)} = Q_{refrigerant\ (C3)} \tag{3.1}$$

$$(Q_{NG} + Q_{C1} + Q_{C2})_{HXC3\text{-}1/2/3} = (Q_{C3})_{HXC3\text{-}1/2/3} \tag{3.2}$$

where $Q_{NG,}$ Q_{C1}, Q_{C2} and Q_{C3} are the duty of natural gas stream, methane, ethylene and propane respectively in MW. The overall heat balance for case 1 and case 6 are detailed in Appendix A.

The overall mass balance of the process is shown in Figure 3.3 and expressed as:

$NG_{feed} = LNG_{vapour} + LNG_{product} + \text{De-C2 bottom product} + \text{ethane}$

(3.3)

where NG_{feed} is the inlet feed flow rate of the natural gas and LNG_{vapour}, $LNG_{product}$, De-C2 bottom product and ethane are the outlet streams in kgmole/h.

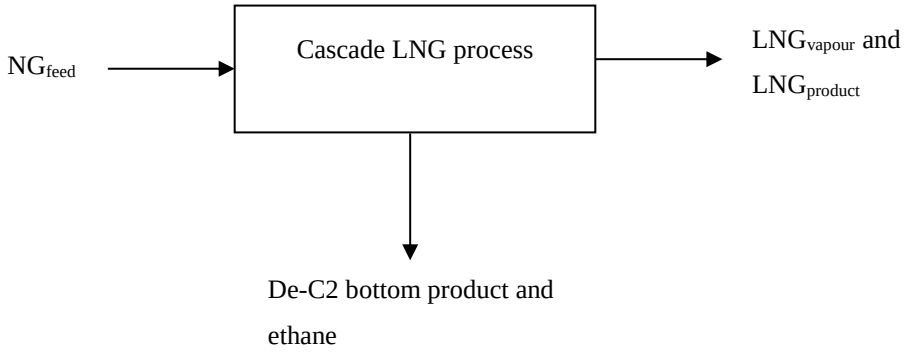

Figure 3.3: Overall mass balance of cascade LNG process.

3.6.2 Model verification for integrated LNG/NGL processes

The integrated LNG/NGL designs are verified by performing the heat and mass balance. The heat balance across LNG heat exchanger is expressed as:

$$Q_{process\ (NG+C1)} = Q_{refrigerant\ (C2)}$$

(3.4)

$$(Q_{NG} + Q_{C1})_{HX\text{-}C2\text{-}1/2} = (Q_{C2})_{HX\text{-}C2\text{-}1/2}$$

(3.5)

where $Q_{NG,}$ Q_{C1}, and Q_{C2} are the duty of natural gas, methane and ethylene streams respectively in MW and HX-C2-1/2 are the ethylene heat exchangers. The overall heat balance for configuration 1 and configuration 2 are detailed in Appendix A. The overall mass balance of the process is calculated using equation (3.3)

Chapter 4 Process efficiency optimisation of propane pre-cooling cycle

4.1 Background

In this chapter, the process efficiency of a three-stage propane pre-cooling cycle is optimised by determining the optimal operating conditions of the propane evaporator that gives maximum energy reduction and highest process efficiency. Detailed background and significance of this research area have been discussed in Chapter 2 (section 2.9.1 and 2.9.2). Six case studies were presented with different operating conditions applied to the propane evaporator at each stage. The process efficiency is evaluated by analysing the quantitative parameters of energy and exergy analyses for all the case studies that were presented. **The content of this chapter has been published in the Journal of Natural Gas Science and Engineering [53].**

4.2 Introduction

As the demand on LNG is drastically increasing and the discovery of new large gas fields is continuously taking place worldwide, the pace of change and development in LNG liquefaction technology is becoming more rapid than ever before. LNG production is estimated to hit 320 million tonnes per annum (MTPA) by 2015 and to 450 MTPA by 2020 as reported by Wood [27]. In order to meet this escalating demand, most of the existing and new LNG plants are looking for opportunities to make a further increase in their LNG capacity and building larger LNG trains which will provide economic benefits and process efficient. Since the 1970s, when the kick started for the LNG plant and until the present day, three main LNG processes have been applied in the LNG plants viz. Single mixed refrigerant (SMR), Propane precooled mixed refrigerant (C3MR) and cascade liquefaction process [26].

In the last 10 to 15 years, the innovations of LNG technologies have drastically progressed whereby new LNG processes have been introduced such as Mixed fluid cascade (MFC), Air Products (AP-X^{TM}), Dual mixed refrigerant (DMR) and Parallel mixed refrigerant (PMR) [143]. Most of the existing LNG plants have three main cooling cycles, namely the pre-cooling, liquefying and sub-cooling cycle. Earlier LNG plants that employed the SMR process did not have the pre-cooling cycle, instead, the natural gas was cooled directly to -160^{o}C using a single mixed refrigerant. The pre-cooling cycle is the first cycle in an LNG process which removes the heat from natural gas to a temperature range between -30^{o}C to -55^{o}C depending on the pre-cooling technology applied. As a result of technological advancement, the pre-cooling cycle can now be designed using either a pure refrigerant or mixed refrigerant. Castillo, Majzoub Dahouk [121] reported that 95% of the current LNG plants employ the pre-cooling cycle; 85% of which are dominated by propane refrigerant compared to the mixed refrigerant.

Thermodynamic analysis has been widely used in the LNG plants to determine the sources and locations of the main process irreversibilities that occur within the process or are due to an individual unit operation. Energy analysis or the first law of thermodynamic method only indicates the energy conservation of the overall process which is measured using two parameters i.e. COP and specific power (SP). However, to locate the irreversibility that occurs within the unit operation of the process, the exergy analysis method is applied. These methods are widely applied by other scholars to evaluate the energy conversion process efficiency. Kanoglu [51], Vatani, Mehrpooya [55], Cipolato, Lirani [56], Al-Otaibi, Dincer [144] and Mehrpooya, Jarrahian [50] applied the energy and exergy analysis methods for analysing the process efficiency of various LNG processes. In a nutshell, these methods are also widely used in some power plants as mentioned in the following references [115, 117, 118].

Converting natural gas to liquid utilizes an extensive amount of energy. According to Alfadala et al. [37], a typical base load LNG plant consumes about 5.5-6 kWh of energy per kgmole of LNG produced. An energy-efficient refrigeration system will enhance plant operation and provide economic benefits [57]. Several authors have discussed the area of enhancing the efficiency of the pre-cooling cycle. Paradowski, Bamba [46] discussed two operating parameters of the pre-cooling cycle in the C3MR process that can enhance the process efficiency plus debottleneck the existing LNG plant capacity to 5.5 MTPA. The pre-cooling temperature of the low pressure (LP) stage and the propane compressor speed were the operating parameters that were adjusted to meet the new capacity requirement.

Castillo et al. [122] studied suitable choices of refrigerants that are applicable for the pre-cooling cycle by analysing the effects of various refrigerants (i.e. N_2, CH_4, C_2H_6, C_3H_8) on the compressor power using the Linde-Hampson process. It was found that compared to other refrigerants, propane has a higher specific refrigerant effect which makes it the preferred refrigerant to be used in the pre-cooling cycle. Ransbarger [123] studied the comparison between three stages and four stages propane cycles for the cascade LNG process which resulted in a power reduction of 1%; nonetheless, the economic evaluations did not justify the increased cost associated with the additional stage.

Evolution in the design of the propane pre-cooling cycle has emerged in recent decades. In this context, various studies have been presented that were related to the enhancement of the efficiency of the propane cycle with respect to significant changes made in the process configuration. Mortazavi, Somers [31] suggested the replacement of the conventional expansion valves in the C3MR process with expanders to improve the liquefaction efficiency. In another study, Mortazavi, Somers [126] investigated the usage of waste heat from gas turbines by installing absorption chillers in the propane cycle of the C3MR process. Kalinowski, Hwang [127] proposed the replacement of the propane evaporator with an absorption refrigeration system utilizing waste heat from the electrical power generating gas turbines.

Although many studies have been conducted focusing on the efficiency enhancement of the LNG plants through modification of the process configuration [31, 51, 54, 126, 127], there is only very scant information available which focuses on the operation perspective. In this study, we would like to analyse the impact of changing the operating conditions of the propane evaporator towards the energy consumption of the process. Six case studies are proposed with different operating conditions applied to the propane evaporator. The development of these case studies is discussed in section 2.2 of the manuscript. The sensitivity of the COP, the specific power (SP), and the exergy loss and exergy efficiency are analysed for all case studies presented.

Nomenclature

E_x	exergy [MW]
$Ex_{HX,\ loss}$	exergy loss of heat exchanger [MW]
$Ex_{COMP,\ loss}$	exergy loss of compressor [MW]
$Ex_{v,\ loss}$	exergy loss of valve [MW]
$Ex_{MIX,\ loss}$	exergy loss of mixer [MW]
$Ex_{AC,\ loss}$	exergy loss of air cooler [MW]
e	specific exergy (MJ/kg)
H	enthalpy (MJ/kg)
n	mass flow rate [kg/s]
P	pressure [bar]
Q	refrigeration duty [MW]
S	entropy [MJ/kg K]
T_0	ambient temperature [K]
W	compressor power [MW]

Abbreviations

AC	air cooler
COP	coefficient of performance
EOS	equation of state
HP	high pressure
HX	heat exchanger
LNG	liquefied natural gas
LP	low pressure
MP	medium pressure
MTPA	million tonnes per annum
PR	Peng Robinson
UA	product of overall heat transfer coefficient and heat exchanger area
SP	specific power

Subscripts

f	fluid
i	inlet
o	outlet
r	ratio

Greek symbol

n_{ex}	exergy efficiency

List of symbols

C_2H_6	ethane
C_2H_4	ethylene
C_3H_8	propane
CH_4	methane
N_2	nitrogen

4.3 Description of propane pre-cooling cycle process

Treated feed gas enters the three-stage propane cycles at 29ºC and 75 bar and is cooled to -40ºC. The propane evaporator (i.e. kettle type) also cools methane and condenses ethylene. Cooling of the process stream is achieved by the evaporation of propane in the pool on the shell side with the process streams flowing inside the immersed tubes. The propane compressor (i.e. centrifugal type) with side streams recovers the evaporated propane and compresses the vapour to 18 bar. Propane is finally condensed at 49ºC using the air cooler. The condensed propane is then recycled back to the propane evaporator. Figure 4.1 shows the simplified process scheme of propane pre-cooling cycle.

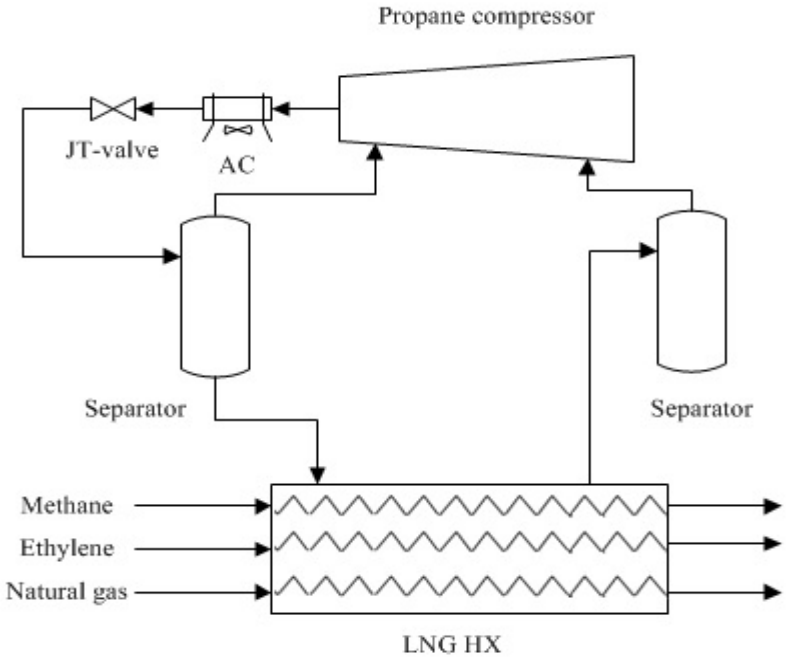

Figure 4.1: Simplified process scheme of propane pre-cooling cycle. Only one stage is shown for simplicity.

4.4 Simulation method and modelling assumptions

Aspen HYSYS which is a steady state process modelling software was employed to model the three-stage propane pre-cooling refrigeration cycles. Peng Robinson equation of state (PR-EOS) fluid package was used for modelling the property of the substances. This process simulator is well known for modelling the LNG processes and has been widely used by others [38, 60, 145, 146]. The feed gas composition and modelling assumptions are summarized in Table 4.1 and Table 4.2 respectively.

Table 4.1: Feed gas composition after sweetening.

Component[a]	Mole fraction
Nitrogen	0.0028
Methane	0.8974
Ethane	0.0496
Propane	0.0343
i-Butane	0.0079
n-Butane	0.0073
i-Pentane	0.0005
n-Pentane	0.0002
n-Hexane	0.0000
Total	1.0000

[a] Feed gas composition obtained from LNG plant located at the Southeast Asia region.

Table 4.2: Modelling assumptions.

Natural gas temperature	29^0C
Natural gas pressure	75 bar
Natural gas flow rate	41,700 kgmole/h
Compressor polytropic efficiency	80%
Pressure drop in LNG heat exchanger	0.2 bar
Pressure drop in air cool heat exchanger	0.3 bar
Minimum temperature approach in heat exchanger	> 2°C
Ambient temperature	27^0C
Air cooler exit temperature	49^0C

The following are the constraints applied in modelling the propane pre-cooling cycle:

1. Temperature approach (T_{app}) in the LNG heat exchanger should be above 2°C to prevent temperature cross.
2. The inlet temperature of the propane compressor should be above its dew point temperature to safeguard the operation of the compressor.

4.4.1 Process simulation description

In this study, six case studies as shown in Table 4.3 have been studied with different operating conditions applied at each evaporator stage to analyse the performance of the propane pre-cooling cycle. The operating conditions of the propane evaporator are changed through an expansion valve that is located upstream of each evaporator (i.e. CV-1: HP stage; CV-2: MP stage and CV-3: LP stage) as depicted in Figure 4.2. The expansion valve pressure is the key manipulated variable that is adjusted to obtain the desired cooling duty for each stage propane evaporator and to maintain the temperature approach above 2°C. The discharge pressure of LP and MP stage propane compressors is connected to the MP and HP propane evaporator stage respectively to obtain the resultant compressor power as shown in Figure 4.2 and Figure 4.3. Propane pre-cooling cycle configuration for the baseline case and case 6 are also shown in Figure 4.2 and Figure 4.3 respectively and changes made on the operating parameters are marked with dotted lines on these figures.

Table 4.3: Propane evaporator operating conditions for all case studies.

Case studies	Propane evaporator operating conditions
Case 1[a]	-25˚C, -30˚C, -40˚C
Case 2	-15˚C, -20˚C, -40˚C
Case 3	-10˚C, -15˚C, -40˚C
Case 3	-5˚C, -10˚C, -40˚C
Case 5	0˚C, -5˚C, -40˚C
Case 6	5˚C, 0˚C, -40˚C

[a] (-25ºC, -30ºC, -40ºC means process exit temperature at HP, MP and LP stage respectively)

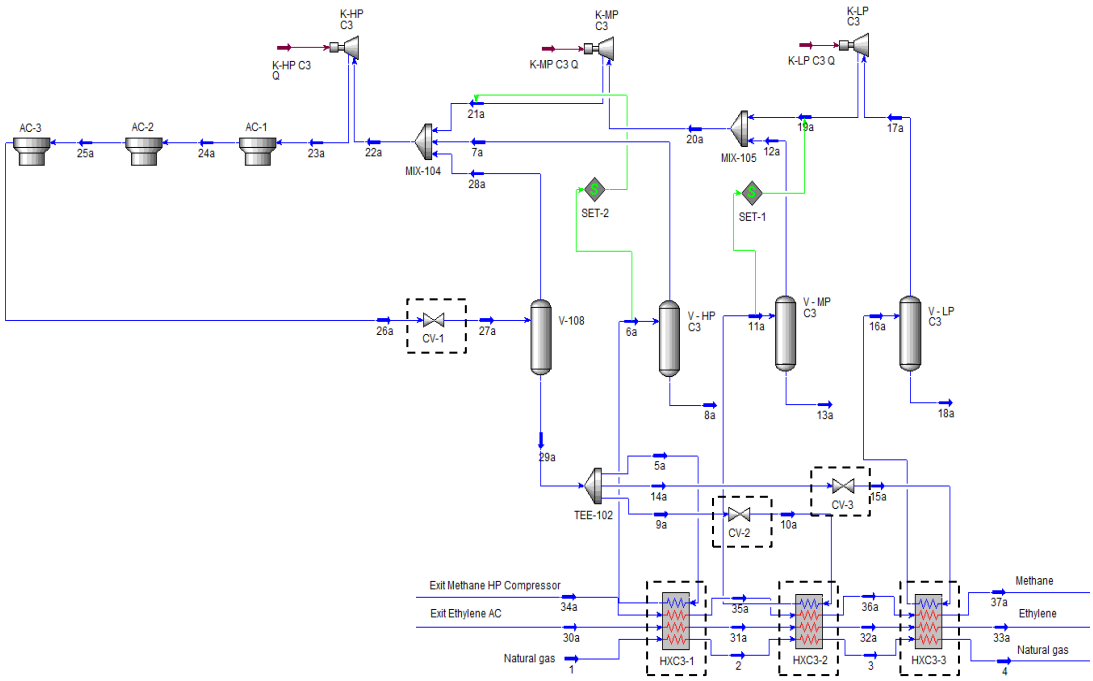

Figure 4.2: Propane pre-cooling cycle Case 1 configuration.

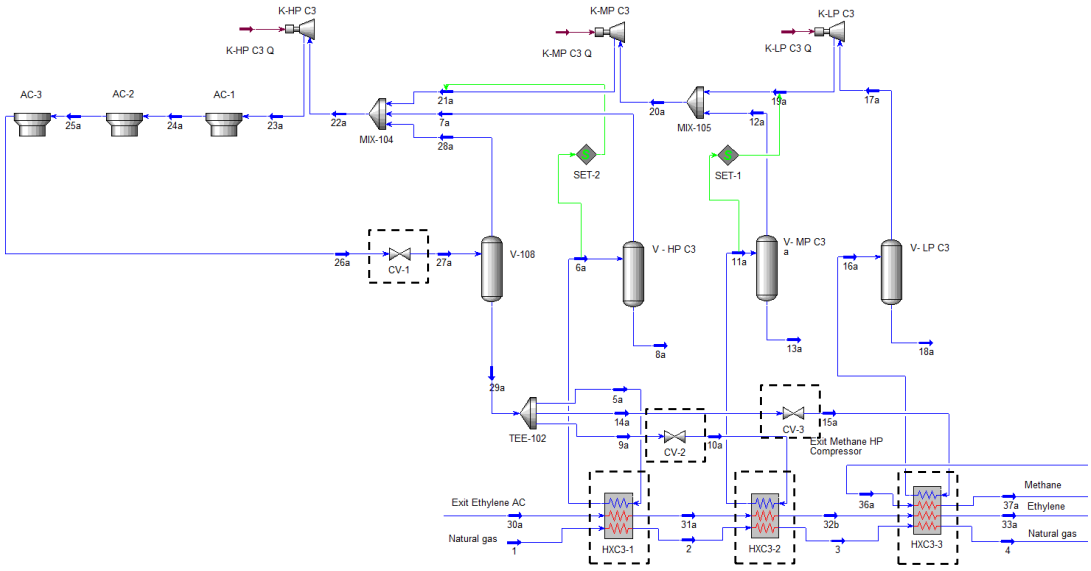

Figure 4.3: Propane pre-cooling cycle Case 6 configuration.

4.4.2 Case studies development of propane pre-cooling cycle

These six case studies were derived by analysing various operating conditions of current LNG plants located in Southeast Asia region, Australia and also based on the information available from the literature [31, 46, 51, 54, 120, 122, 123, 126, 127]. Figure 4.4 illustrates the development of the propane pre-cooling cycle case studies.

Case studies presented are defined as follows:

Case 1: Baseline case (i.e. higher cooling duty at the intermediate stages (i.e. HP and MP stage)

Case 6: (i.e. lower cooling duty at intermediate stages)

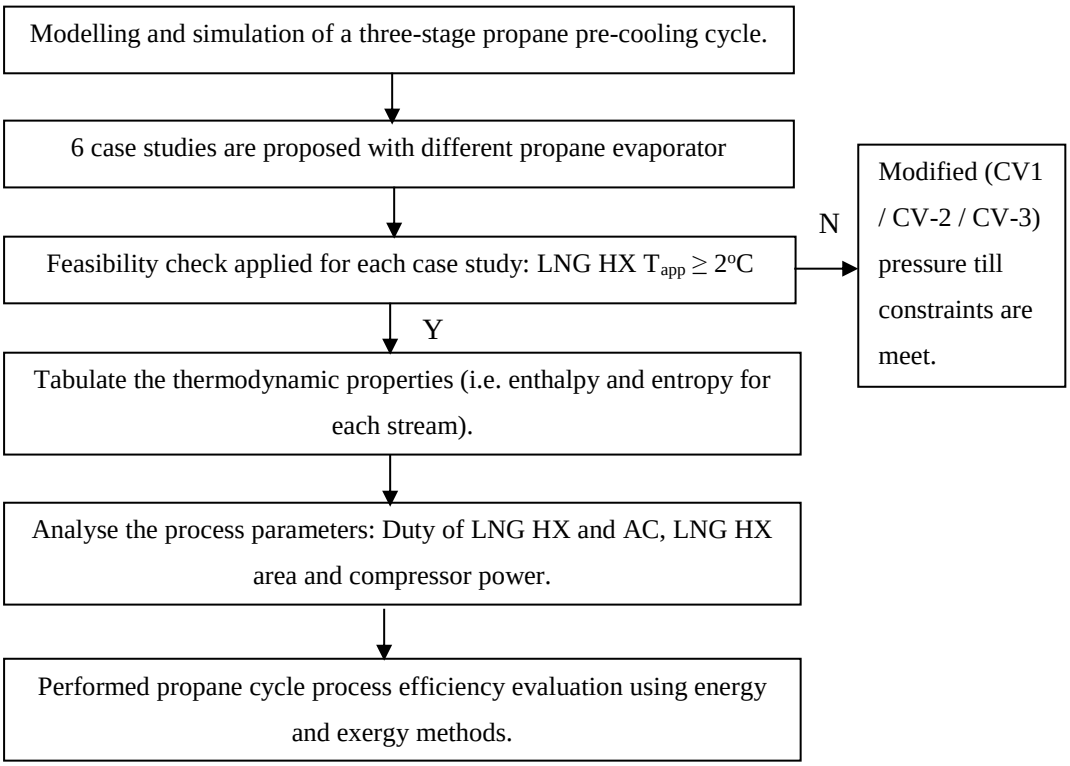

Figure 4.4: Development of the propane pre-cooling cycle case studies.

4.5 Energy analyses

Energy consumption and process efficiency of the overall process are determined through energy analysis. This method has two quantitative parameters; COP and SP. COP is a standard criterion applied in evaluating the efficiency of a cryogenic system. It is defined as the ratio of total heat removed by the refrigerant to the amount of power required by the system (Eq. (4.1)) while SP is defined as total power consumption per unit mass of LNG (Eq. (4.2)).

$$COP = Q/W \tag{4.1}$$

$$SP\ (MWh/tonne\ LNG) = \sum W_{req} / \dot{m}_{LNG} \tag{4.2}$$

where the nomenclature for the above equations are as follows: Q is refrigeration duty (MW); W is compressor power (MW), $\Sigma\ W_{req}$ is the total compressor power required (MW) and $\dot{m}_{LNG}$ is the amount of LNG produced in tonne/h.

4.6 Exergy analysis

In this study, exergy analysis is applied to locate the irreversibility that occurs within the unit operations of the propane pre-cooling cycle. This method identifies the individual unit operation that exhibits a higher amount of lost work which gives the process engineer valuable information for improving the process from the equipment and process design point of view. Exergy which is derived from the second law of thermodynamics is defined as the amount of reversible work achieved by a system when the system components are brought into a thermodynamic equilibrium state with its environment in a reversible process [95]. The exergy change of a system is a function of two main parameters which are the enthalpy and entropy. Change in exergy (ΔE_x) between the initial and the final state of a system is expressed as:

$$\Delta E_x=(H_o-H_i)- T_o(S_o-S_i) \tag{4.3}$$

where T_o is the ambient temperature, H_o and S_o represent the enthalpy and entropy of the outlet stream and H_i and S_i represent the enthalpy and entropy of the inlet stream respectively. The difference of this property will define whether the processing system requires or produces work as the systems moves from initial state to final state. If the exergy difference (ΔE_x) is greater than 0, this indicates that the processing system produces work, whereas if the exergy difference is less than 0, this indicates the processing system requires work from the outer system for the state change [147].

The exergy efficiency of the process is defined as the ratio of the difference between the total compressor power required and the total exergy loss to the total amount of power required by the system (Eq. (4.4)). The exergy efficiency is expressed as:

$$\eta_{ex}(\%) = \frac{(\Sigma W_{req} - \Sigma W_{loss})}{\Sigma W_{req}} \times 100 \quad [51] \tag{4.4}$$

where ΣW_{loss} is the total exergy loss work from each unit operation.

The expressions to determine the exergy loss for all the unit operations in this study are summarised in Table 4.4.

Table 4.4: Exergy loss calculation of various unit operations in propane cycle.

LNG heat exchanger	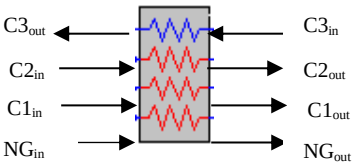	$Ex_{HX,\,loss} = \dot{m} \sum ex_i - ex_o$
Compressor	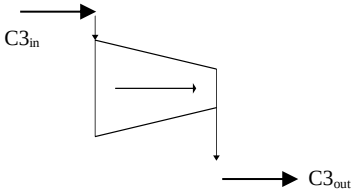	$Ex_{COMP,\,loss} = \dot{m}\,(ex_i - ex_o) - W$
Valves	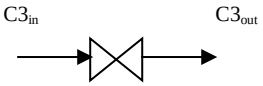	$Ex_{V,\,loss} = \dot{m}T_o\,(S_o - S_i),\ h_i = h_o$
Mixer	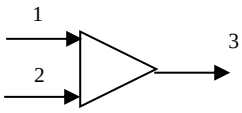	$Ex_{MIX,\,loss=}\ \dot{m}_1e_1 + \dot{m}_2e_2 - \dot{m}_3e_3$
Air cooler	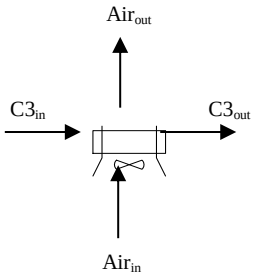	$Ex_{AC,\ loss} = (\dot{m}_f e_f + \dot{m}_a e_a)_i$ –

In the above equations, $\dot{m}$ is the mass flow rate of propane at the inlet stream (kg/s), W is the compressor power (MW), S is the entropy (MJ/kg. K), $\dot{m}_a$ is the mass flow rate of air in (kg/s) and e is the specific exergy for the respective stream in (MJ/kg).

Thermodynamic analysis comprising of the first and second law is used in this study to overcome the limitations of the deterministic optimization method i.e. a numerical approach which excludes the uncertainty changes involved in the design process, hence it is not considered as the best option for many actual engineering problems [30]. Additionally, the optimization result obtained using this method causes ambiguity because it is not embedded with any process knowledge (i.e. enthalpy and entropy) [145]. Knowing these important process parameters for each process stream provides a better understanding of the changes occurring within the process. Hence, necessary adjustment can be done on the operating parameter to improve the process performance.

4.7 Results and discussion

Operating conditions of the baseline (Case 1) and Case 6 are summarized in Table 4.5. The effect of different operating conditions at each evaporator stage on the heat exchangers, compressors and air coolers are discussed in section 4.7.1.

4.7.1 Results of different operating conditions of propane evaporator on the process parameters

A simple and practical way of minimizing the energy consumption of a process is by adjusting the operating conditions of it. Based on the case studies presented, different propane evaporator operating conditions affect the overall energy consumption of the process. As depicted in Figure 4.5, Case 6 consumes the lowest compression power and air cooler duty which are 129.36 MW and 342.60 MW respectively compared to the baseline case. This can be translated into an energy saving of 13.5% and 5.57 % for the compressor power and air cooler duty respectively. Meanwhile, as can be seen in Figure 4.6, the total propane flow rate of Case 6 is also reduced by 8.6% compared to the baseline case. Though, the overall duty of the propane evaporator remains constant, having a greater cooling duty at the intermediate stages of propane evaporator results in the increased of power consumption, air cooler duty and propane flow rate which reduces the process efficiency.

Table 4.5: Operating conditions of each stream in propane pre-cooling cycle.

	(Case 1)				Case 6			
Stream no	x	T (°C)	P(bar)	S(kJ/kg K)	x	T (°C)	P(bar)	S(kJ/kg K)
1	1	29	75	7.98	1	29	75	7.98
2	0.99	-25	74.80	7.34	1	5	74.80	7.74
3	0.98	-30	74.60	7.25	1	0	74.60	7.69
4	0.92	-40	74.40	7.02	0.92	-40	74.40	7.02
5a	0	-27.49	1.85	1.56	0	2.12	5.05	1.84
6a	1	-23	1.85	3.26	1	7	5.05	3.23
7a	1	-23	1.85	3.26	1	7	5.05	3.23
8a	0	-23	1.85	1.60	0	7	5.05	1.88
9a	0	-27.49	1.85	1.56	0	2.12	5.05	1.84
10a	0.02	-32.34	1.53	1.56	0.03	-2.96	4.32	1.84
11a	1	-27	1.53	3.27	1	2	4.32	3.23
12a	1	-27	1.53	3.27	1	2	4.32	3.23
13a	0	-27	1.53	1.57	0	2	4.32	1.84
14a	0	-27.49	1.85	1.56	0	2.12	5.05	1.84
15a	0.07	-42.19	1.01	1.57	0.24	-42.19	1.01	1.88
16a	1	-33	1.01	3.32	1	-25	1.01	3.37
17a	1	-33	1.01	3.32	1	-25	1.01	3.37
18a	0	-33	1.01	1.57	0	-25	1.01	1.59
19a	1	-16.34	1.53	3.34	1	35.95	4.32	3.43
20a	1	-19.77	1.53	3.32	1	34.91	4.32	3.43
21a	1	-11.98	1.85	3.33	1	41.83	5.05	3.43
22a	1	-24.25	1.85	3.25	1	24.18	5.05	3.33
23a	1	79.88	18	3.35	1	85.16	18	3.38
24a	1	70	17.70	3.29	1	70	17.70	3.29
25a	1	60	17.40	3.23	1	60	17.40	3.23
26a	0	49	17.10	2.28	0	49	17.10	2.28
27a	0.50	-27.48	1.85	2.40	0.35	2.12	5.05	2.32
28a	1	-27.48	1.85	3.23	1	2.12	5.05	3.20
29a	0	-27.48	1.85	1.56	0	2.12	5.05	1.84
30a	1	49	24.10	5.38	1	49	24.10	5.38
31a	0	-25	23.90	3.67	1	5	23.90	5.11
32a	0	-30	23.70	3.60	1	0	23.70	5.08
33a	0	-40	23.50	3.46	0	-40	23.50	3.46
34a[a]	1	-10.01	36.50	9.17	-	-	-	-
35a[b]	1	-25	36.30	9.02	-	-	-	-
36a	1	-30	36.10	8.97	1	-9.97	36.50	9.17
37a	1	-40	35.90	8.86	1	-40	36.30	8.86

[a,b] There is no stream data for case 6 due to the exit temperature of methane stream is -9.97°C and the cooling range for case 6 is (5˚C, 0˚C, -40˚C). Therefore, methane stream enters HXC3-3. Refer to Figure 4.3 for the configuration.

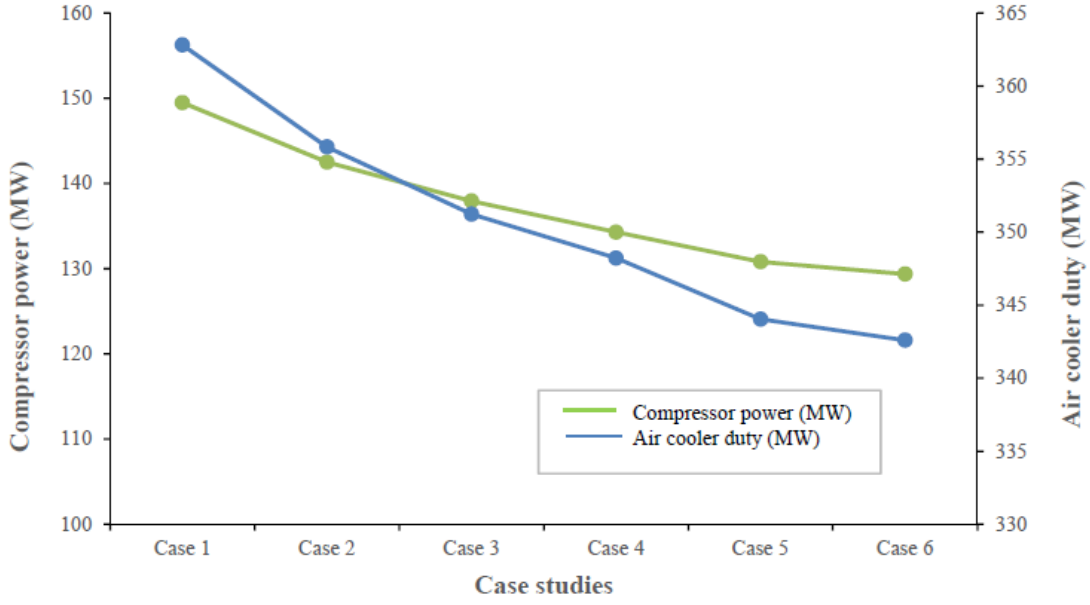

Figure 4.5: Effect of different operating conditions of propane evaporator on compressor power and air cooler duty.

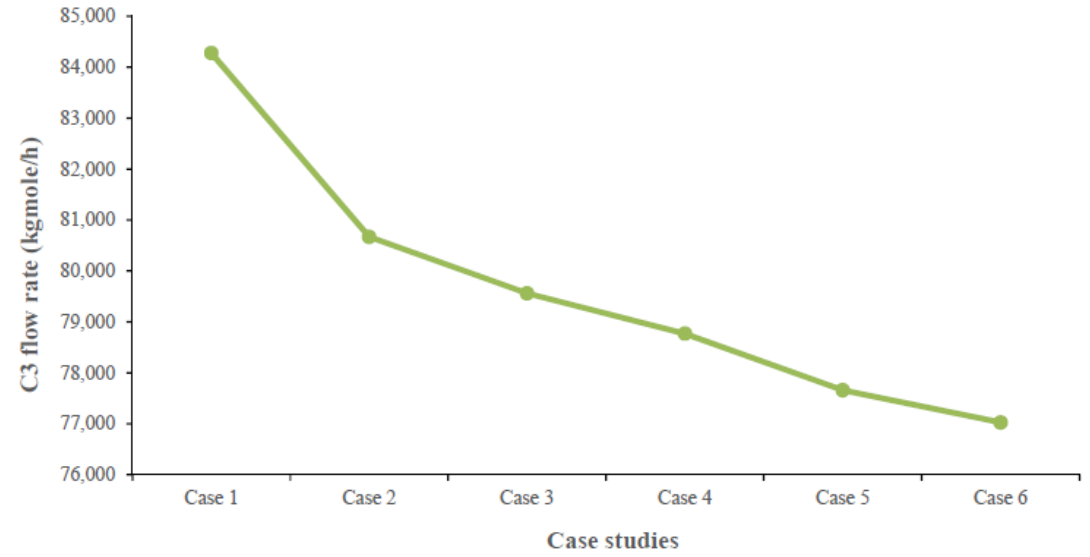

Figure 4.6: Effect of different operating conditions of propane evaporator on the propane flow rate.

Distribution of the propane evaporator duty at each stage and its total area required for all case studies are shown in Figure 4.7 and Table 4.6. As can be seen in Figure 4.7, the cooling duty is transferred from the HP stage to the LP stage of propane evaporator (i.e. Case 1 to Case 6). Duty of the propane evaporator is determined using equation (4.5). Rearranging equation ((4.5) gives equation (4.6) which is used to determine the propane evaporator area. The overall heat transfer coefficient (U) for propane refrigeration cycles was taken as an average value of 425 W/(m^2.K) [148]. Based on this U value, the propane evaporator area for each case was determined. As shown in Table 4.6, Case 6 gives the lowest propane evaporator area for the same cooling duty which is 46.89% lower compared to the baseline case (Case 1). This indicates that increasing the cooling duty at the intermediate stages of the propane evaporator results in the increasing of the total propane evaporator area.

$$Q = UA\Delta T_{LMTD} \tag{4.5}$$

whereby $A = Q/(U.\Delta T_{LMTD})$

(4.6)

where Q is the duty of heat exchanger in MW, U is the overall heat transfer coefficient in MW/m^2 ^oC, ΔT_{LMTD} is the log min temperature difference in ^oC and A is the heat exchanger area in m^2.

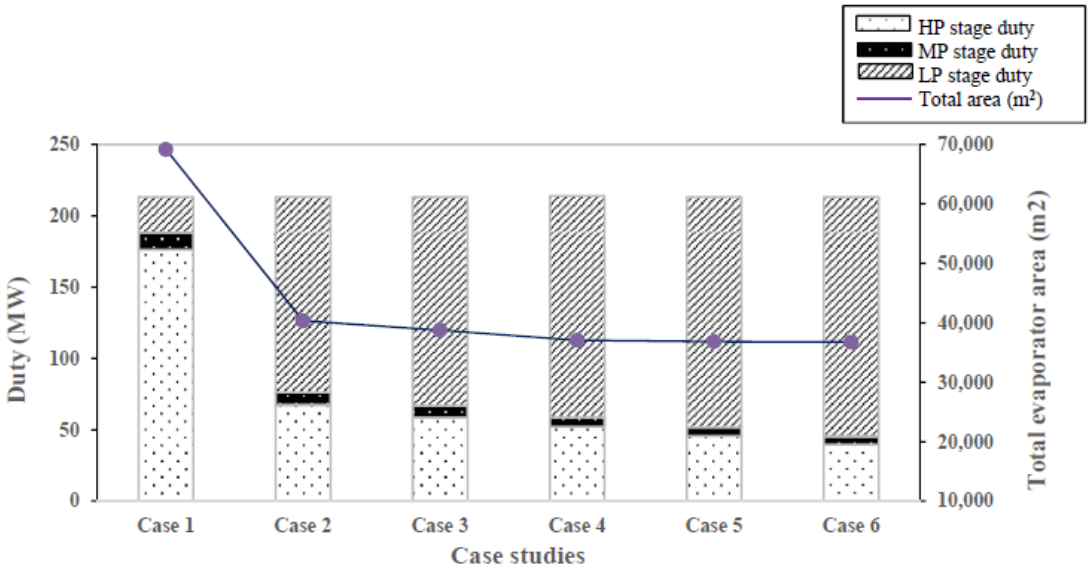

Figure 4.7: Effect of different operating conditions of propane evaporator on its duty and total area.

Table 4.6: Propane evaporator duty for each stage and its total area for all case studies.

Duty (MW)	Case 1	Case 2	Case 3	Case 4	Case 5	Case 6
HP	176.20	67.34	58.65	52.19	45.64	39.42
MP	12.21	8.72	8.36	6.33	6.13	5.98
LP	24.92	137.28	146.27	155.46	161.47	167.84
Total area (m^2)	69,183.61	40,320.54	38,753.54	37,047.88	36,826.10	36,746.38

4.7.2 Sensitivity analysis of propane pre-cooling cycle

In this study, the sensitivity of COP, SP, exergy loss and exergy efficiency of the propane pre-cooling cycle were analysed with respect to different operating conditions of the propane evaporator. Effect of different evaporator operating conditions on COP and SP are presented in Figure 4.8. The exergy loss and exergy efficiency results are shown in Table 4.7 and Figure 4.9. As can be seen in Figure 4.8, the COP of Case 6 increases by 15.51% while the SP reduces by 13.5% in comparison to the baseline case (case 1). Based on the above observation, the required shaft power can be minimized by reducing the cooling duty at the intermediate stages of the propane evaporator. Variation of the cooling duty in the propane evaporator is achieved by manipulation of the expansion valve which is located prior to each stage.

Exergy loss for each unit operation in the propane pre-cooling cycle was determined using the equations as presented in Table 4.4. As shown in Table 4.7, the valves, compressors and heat exchangers were identified as the primary contributors to the exergy loss in the propane cycle. For the baseline case (Case 1), the valves allocated the highest exergy loss, 38.52%, followed by the compressors, 30.89% and the heat exchangers, 16.63%. Valves provided the highest exergy loss in the baseline case due to the increase in entropy generation when a larger pressure drop is applied across the system. Valves provided the highest exergy loss in the baseline case due to the increase in entropy generation when a larger pressure drop is applied across the system. These findings are in line with the findings obtained by Mehrpooya, Jarrahian [50] for evaluation of pressure drop in the evaporator; whereby an increase in the pressure drop causes increases in the irreversibilities. Besides, according to Mortazavi, Somers [31], the availability of pressure exergy is destroyed during expansion process via viscous dissipation and turbulent frictional losses which otherwise could be used, this phenomenon makes the valves highly irreversible.

Compressors are the second contributor in exergy loss due to the increase in power demand when the increase in cooling duty occurred at the intermediate stages. However, for all other case studies, the exergy loss across the other components reduced marginally when a lower cooling duty was applied at the intermediate stages. The exergy efficiency of Case 1 is the lowest (33.87%) which indicates that larger irreversibilities occur within the process. Case 6 shows the highest exergy efficiency (40.22%) which indicates high potential improvement of the process. The exergy efficiency has improved by 4.6% compared to the work done by Kanoglu [51].

Based on Figure 4.9, the total exergy loss decreases by 21.78 % for Case 6 compared to the baseline case which improved the overall process efficiency. From the results, it can be deduced that change in the operating conditions of the propane evaporator results in a lower entropy generation which reduces the exergy loss and increases the exergy efficiency. Exergy loss is influenced by larger temperature or pressure difference applied across the refrigerant stream and not by the number of equipment used in the propane cycle [106].

Based on the exergy analysis, it can be concluded that both the valves and the compressors are the main contributors to exergy loss. These unit operations can be improved by replacing the existing JT valves with two-phase expanders [31] or by using a higher efficiency compressor [132]. Nevertheless, the reduction in energy consumption by installing these new components should be economically assessed to determine its feasibility. Based on the energy and exergy analyses results, the cascade process is further optimised, and the optimisation work is reported in the next chapter.

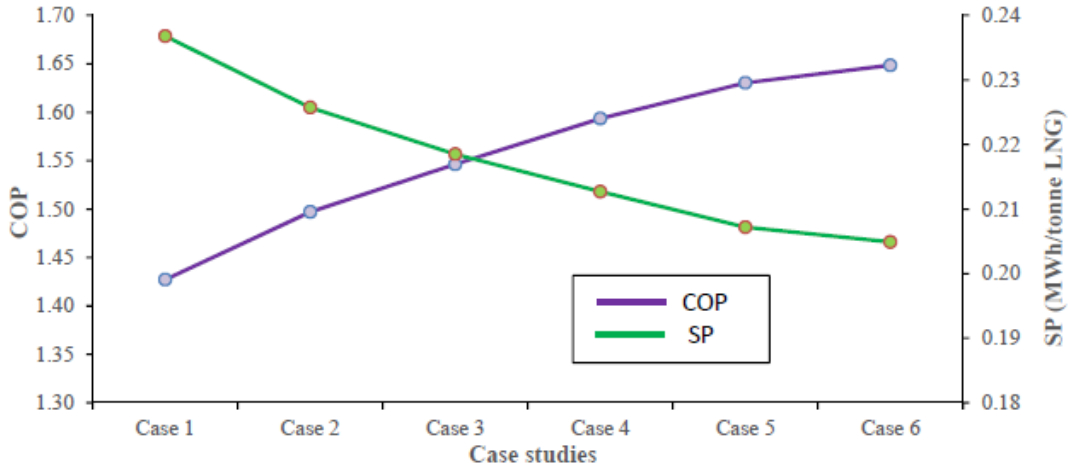

Figure 4.8: Effect of different operating conditions of propane evaporator on COP and SP.

Table 4.7: Exergy loss of each unit operation in the propane cycle and exergy efficiency (%).

Exergy loss (MW)	Case 1	Case 2	Case 3	Case 4	Case 5	Case 6
Heat exchangers	16.63	20.34	20.01	20.02	19.78	20.00
Compressors	30.89	28.55	27.45	26.56	25.73	25.35
Valves	38.52	28.62	25.66	22.90	20.69	19.37
Air coolers	12.74	12.20	13.08	11.61	11.77	11.49
Mixer	0.08	0.76	0.85	0.96	1.04	1.11
η_{ex} (%)	33.87	36.52	36.89	38.90	39.58	40.22

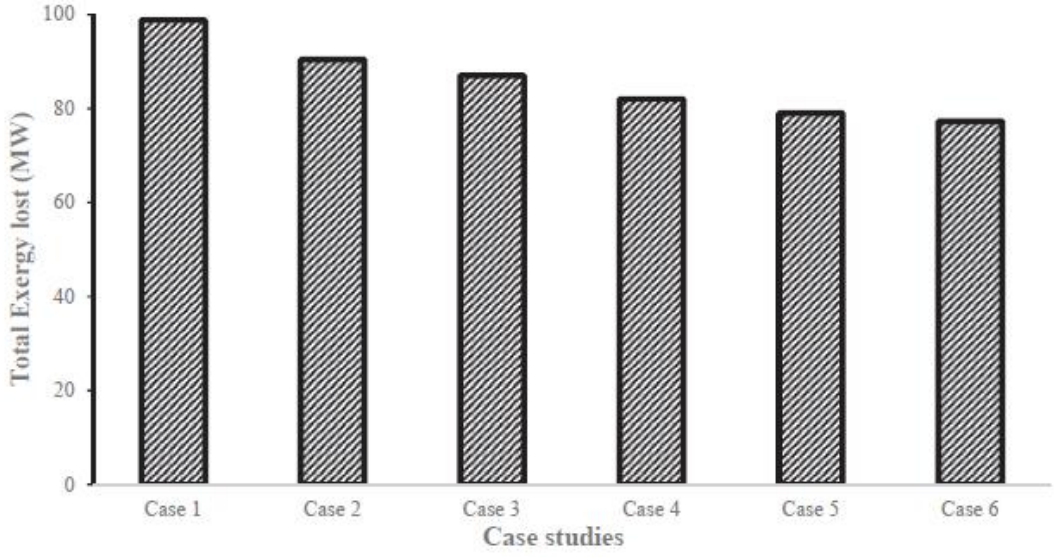

Figure 4.9: Total exergy loss for each case studies.

4.8 Conclusions

In this study, enhancement in the process efficiency of a three-stage propane pre-cooling cycle was studied using energy and exergy analysis. The results show that Case 6 achieves the highest COP (1.65), lowest SP (0.205 MWh/tonne of LNG) and highest exergy efficiency (40.22%) due to low cooling duty distribution at the intermediate stages. This show increment of 15.51% and 18.75% for COP and exergy efficiency respectively and 13.5% reduction in SP. This shows a significant increase in the overall performance of the refrigeration cycle. In addition, the total exergy loss exhibited by all the unit operation dropped by 21.8% i.e. from 98.86 MW to 77.32 MW. Energy and exergy analysis can be a useful guide in enhancing the process efficiency of the existing LNG plant and as a reference for future greenfield LNG projects. Changing the operating conditions of the propane evaporator stage can be considered as an option to minimize the energy consumption of the process which does not involve any additional cost. Besides, the evaporator pressure is also considered an important degree of freedom as it changes the cut point temperature between refrigeration levels [102] which results in changes the cooling load. Additionally, this enhancement not only reduces the propane compression power but also reduces the size of the heat exchanger as well as the refrigeration flow rate. Reducing energy consumption leads to smaller equipment sizes which generally reduce the capital and operating costs of the LNG plants.

4.9 Recommendations

In this study, no consideration is made from an economic point of view. As this process is considered as licensed processed, cost related to the proprietary equipment such as compressor and heat exchanger is treated confidentially. Thus, the detailed breakdowns on the equipment size, price, licensing fees are not available. Therefore, future work is to be considered which simultaneously provide the trade-off between the capital and operating cost of the plant with exergy analysis.

4.10 Acknowledgement

The authors wish to acknowledge the Ministry of Education (MOE) of Malaysia and University Malaysia Pahang for funding the presented study. The authors also wish to acknowledge the support provided by staff from Curtin University, Australia.

4.11 References

[1] D.A. Wood, A review and outlook for the global LNG trade, *Journal of Natural Gas Science and Engineering*, 9 (2012) 16-27.

[2] W. Lim, K. Choi, I. Moon, Current Status and Perspectives of Liquefied Natural Gas (LNG) Plant Design, *Industrial & Engineering Chemistry Research*, 52 (2013) 3065-88.

[3] L. Castillo, R. Nadales, C. González, C. Dorao, A. Viloria, Technology selection for liquefied natural gas (LNG) on base-load plants, in: *Jornadas de Investigación de la Facultad de Ingeniería (JIFI). Universidad Central de Venezuela*, 2010.

[4] L. Castillo, M. Majzoub Dahouk, S. Di Scipio, C.A. Dorao, Conceptual analysis of the precooling stage for LNG processes, *Energy Conversion and Management*, 66 (2013) 41-47.

[5] A. Vatani, M. Mehrpooya, A. Palizdar, Energy and exergy analyses of five conventional liquefied natural gas processes, *International Journal of Energy Research*, (2014) 1843-63.

[6] M. Kanoglu, Exergy analysis of multistage cascade refrigeration cycle used for natural gas liquefaction, *International Journal of Energy Research*, 26 (2002) 763-74.

[7] L. Cipolato, M.C.A. Lirani, T.V. Costa, F.M. Fábrega, J.V.H. d'Angelo, Exergetic optimization of a refrigeration cycle for natural gas liquefaction, 31 (2012) 440-44.

[8] D.A. Al-Otaibi, I. Dincer, M. Kalyon, Thermoeconomic optimization of vapour-compression refrigeration systems, *International Communications in Heat and Mass Transfer*, 31 (2004) 95-107.

[9] M. Mehrpooya, A. Jarrahian, M.R. Pishvaie, Simulation and exergy-method analysis of an industrial refrigeration cycle used in NGL recovery units, *International Journal of Energy Research*, 30 (2006) 1336-51.

[10] A. Cihan, O. Hacıhafızog˘lu, K. Kahveci, Energy–exergy analysis and modernization suggestions for a combined-cycle power plant, *International Journal of Energy Research*, 30 (2006) 115-26.

[11] I.H. Aljundi, Energy and exergy analysis of a steam power plant in Jordan, *Applied Thermal Engineering*, 29 (2009) 324-28.

[12] S.C. Kaushik, V.S. Reddy, S.K. Tyagi, Energy and exergy analyses of thermal power plants: A review, *Renewable and Sustainable Energy Reviews*, 15 (2011) 1857-72.

[13] M.M.F. Hasan, I.A. Karimi, H.E. Alfadala, Optimizing Compressor Operation in an LNG Plant, in: H. Alfadala, G.V.R. Reklaitis, M.M. El-Halwagi (eds.) *Proceedings of the 1st Annual Gas Processing Symposium*, Elsevier, Amsterdam, 2009.

[14] G. Lee, R. Smith, X. Zhu, Optimal synthesis of mixed-refrigerant systems for low-temperature processes, *Industrial & engineering chemistry research*, 41 (2002) 5016-28.

[15] H. Paradowski, M. Bamba, C.Bladanet, Propane Precooling Cycles for Increased LNG Train Capacity, in: *14th International Conference and Exhibitions on Liquefied Natural Gas* Doha, Qatar 21-24 March, 2004, pp. 1-18.

[16] L. Castillo, C.A. Dorao, On the conceptual design of pre-cooling stage of LNG plants using propane or an ethane/propane mixture, *Energy Conversion and Management*, 65 (2013) 140-46.

[17] W. Ransbarger, A fresh look at LNG process efficiency, *LNG industry*, (2007).

[18] A. Mortazavi, C. Somers, Y. Hwang, R. Radermacher, P. Rodgers, S. Al-Hashimi, Performance enhancement of propane pre-cooled mixed refrigerant LNG plant, *Applied Energy*, 93 (2012) 125-31.

[19] A. Mortazavi, C. Somers, A. Alabdulkarem, Y. Hwang, R. Radermacher, Enhancement of APCI cycle efficiency with absorption chillers, *Energy*, 35 (2010) 3877-82.

[20] P. Kalinowski, Y. Hwang, R. Radermacher, S. Al Hashimi, P. Rodgers, Application of waste heat powered absorption refrigeration system to the LNG recovery process, *International Journal of Refrigeration*, 32 (2009) 687-94.

[21] C. Remeljej, A. Hoadley, An exergy analysis of small-scale liquefied natural gas (LNG) liquefaction processes, *Energy*, 31 (2006) 2005-19.

[22] P. Hatcher, R. Khalilpour, A. Abbas, Optimisation of LNG mixed-refrigerant processes considering operation and design objectives, *Computers & Chemical Engineering*, 41 (2012) 123-33.

[23] M.S. Khan, S. Lee, G.P. Rangaiah, M. Lee, Knowledge based decision making method for the selection of mixed refrigerant systems for energy efficient LNG processes, *Applied Energy*, 111 (2013) 1018-31.

[24] A. Aspelund, T. Gundersen, J. Myklebust, M.P. Nowak, A. Tomasgard, An optimization-simulation model for a simple LNG process, *Computers & Chemical Engineering*, 34 (2010) 1606-17.

[25] W.-s. Cao, X.-s. Lu, W.-s. Lin, A.-z. Gu, Parameter comparison of two small-scale natural gas liquefaction processes in skid-mounted packages, *Applied Thermal Engineering*, 26 (2006) 898-904.

[26] D.-E. Helgestad, Modelling and optimization of the C3MR process for liquefaction of natural gas, *Process Systems Engineering*, (2009) 44.

[27] J. Szargut, International Progress in Second Law Analysis *Energy* 5(1980) 709-18.

[28] X. Xu, J. Liu, C. Jiang, L. Cao, The correlation between mixed refrigerant composition and ambient conditions in the PRICO LNG process, *Applied Energy*, 102 (2013) 1127-36.

[29] S. Mokhatab, *Handbook of liquefied natural gas*, Elsevier Science, Burlington, 2013.

[30] J.M. Campbell, *Gas conditioning and processing: volume 2, the equipment modules / by John M. Campbell*, 8th ed., John M. Campbell and Company, Norman, Oklahoma, 2004.

[31] J.-I. Yoon, K.-H. Choi, H.-S. Lee, H.-J. Kim, C.-H. Son, Assessment of the performance of a natural gas liquefaction cycle using natural refrigerants, *Heat and Mass Transfer*, 51 (2014) 95-105.

[32] T. He, Y. Ju, Design and Optimization of a Novel Mixed Refrigerant Cycle Integrated with NGL Recovery Process for Small-Scale LNG Plant, *Industrial & Engineering Chemistry Research*, 53 (2014) 5545-53.

Chapter 5 Process efficiency optimisation of two different integrated LNG/NGL configurations

5.1 Background

In this chapter, the cascade LNG process is further optimised by using the optimal operating conditions obtained for propane pre-cooling cycle from the previous chapter. As mentioned in section 2.9.5, no study has been done that discusses on the improvement of the design of integrated LNG/NGL cascade process and its effect on the LNG HHV specification for the single large train. Detailed background, the importance of having an integrated design and the study gaps have been discussed in Chapter 2 (section 2.9.3 and 2.9.5). This chapter will discuss two different configurations of the integrated LNG/NGL process. These integrated designs will be analysed and assess based on several criteria such as meeting the required LNG HHV specification, consume less energy, meet the desired LNG capacity and possess highest process efficiency. The process efficiency is evaluated by analysing the quantitative parameters of energy and exergy analyses. The content of this chapter has been published in the APPEA Journal (2016).

5.2 Introduction

The history of liquefied natural gas (LNG) plants started over five decades ago whereby the first LNG plant that was built in Kenai, Alaska used cascade LNG process. In the earlier design of LNG plants, the natural gas liquids (NGL) units were built upstream of the liquefaction unit and there was no integration between these two units [33]. As the demand of building larger and process efficient LNG plant is increasing drastically [40], many of the LNG process licensors such as Air Products (APCI), Conoco Phillips (COP) and Shell have developed various integrated processes. For example, Conoco Phillips has applied this integrated concept to three of the LNG plants which resulted in about a 7% increase in the LNG production for the same required power [33]. Fluor Technologies reported that 10% of energy saving is obtained by the integration of LNG and NGL processes [149].

In a standalone LNG plant, the required refrigerant such as propane is obtained from external cycles and separate heat exchangers while in the integrated processes, the required refrigerant is obtained from joint refrigeration cycles and shared devices [128]. Besides, there are also other advantages of this integrated processes such as reduction in the capital and operating cost of the plant, combined emissions of carbon dioxide (CO_2) and nitrogen oxides (NO_x) can be eliminated, improving the overall thermodynamic process efficiency and also assist in meeting the higher heating value (HHV) specification [33, 40]. In another study, NGL facilities have been introduced at LNG receiving terminals in order to meet stringent HHV specification set by the local stakeholders [129]. Hence, having an integrated LNG and NGL facilities will provide flexibility in meeting the HHV requirement, improve the process efficiency of the plant as well as provide economic benefits.

In this study, two different configurations of integrated LNG and NGL processes for cascade LNG process are proposed. The desired LNG capacity for this study is 5 million tonnes per annum (MTPA). The aim of this study is to evaluate which configuration meets the required HHV specification and gives minimum power consumption. The process efficiency of these configurations is evaluated using the energy and exergy methods.

5.3 Process description of the integrated LNG and NGL configurations

The separation of heavies' hydrocarbon or NGL is performed in the ethylene refrigeration cycle. This cycle is considered as the key section of the cascade LNG process whereby ethylene (C_2H_4) is used to liquefy the natural gas and condenses the methane refrigerant. The separation of natural gas from the NGL is performed using a demethaniser column (De-C1) that operates at 34 bar. The bottom product from the De-C1 column (i.e. NGL) is fed to the deethaniser column (De-C2) at 20 bar. The top product from the De-C1 column is mixed with the top product from the (De-C2) column and is further cooled to -95°C using ethylene refrigerant. The separation of methane from NGL components using ethylene refrigeration cycle determines the final HHV specification of the LNG product.

5.4 Methodology

In this study, a commercial process simulation software, ASPEN HYSYS is used to simulate the LNG and NGL processes and Peng Robinson equation of state (EOS) was used to determine the physiochemical properties of the natural gas substances. The required HHV for this process is 1050-1125 Btu/scf. The operating conditions of the process remained unchanged so that the effect of the changes made in the process configurations towards the power consumption and in meeting the HHV requirement can be analysed. The following are the modelling assumptions applied in this study; adiabatic efficiency of the pump is 85% and compressors polytropic efficiency is 80%. All compressors are assumed to be centrifugal type.

Exergy which is derived from the second law of thermodynamics is defined as the maximum theoretical work achievable by a system when the system is brought into an equilibrium state with the environment [150]. Exergy analysis is a useful method applied in evaluating the performance of the energy systems and chemical processes, optimisation and also for improving the process design [51]. Exergy analysis is performed by obtaining the exergy loss from the following equipment namely heat exchangers, compressors, valves, air coolers and mixers in the integrated LNG and NGL processes. Exergy loss for each equipment is calculated using equation (5.1) below.

$$\Delta Ex = (H - T_o S)_{state2} - (H - T_o S)_{state1} \quad (5.1)$$

In equation (5.1), ΔEx is the change of exergy loss from state 2 to state 1, H is the enthalpy (MJ/kg), T_o is the ambient temperature (K) and S is the entropy (MJ/kgK).

Process efficiency of both configurations is evaluated by determining the exergy efficiency. Exergy efficiency can be defined as equation (5.2):

$$\eta_{ex}(\%) = \frac{(\Sigma W_{req} - \Sigma W_{loss})}{\Sigma W_{req}} \times 100 \quad [51] \quad (5.2)$$

In equation ((5.2), η_{ex} is the exergy efficiency (%), ΣW_{req} is the total compressor power required (MW) and ΣW_{loss} is the total exergy loss work (MW) from each unit operation.

5.5 Modelling assumptions and simulation method and constrains

The feed gas condition and modelling assumptions applied are outlined in Table 3.1, section 3.2 of the thesis. The simulation method and simulation constrains used to develop these integrated LNG/NGL designs are explained in 0 (section 3.2 and 3.3). The required HHV for this process is 1,050–1,125 Btu/Scf. The operating conditions of the process remained unchanged to analyse the effect of modification made in the process configurations towards the power consumption, process parameters, efficiency and LNG HHV requirement.

5.5.1 Development of two different integrated LNG/NGL process configurations

The description of two different integrated LNG/NGL designs are discussed below:

Configuration 1 (C1): The De-C2 column overhead is operated as a partial condenser; the top vapour product is compressed to 33.8 bar and mixed with the top product stream of De-C1 column and the liquid ethane is recovered as a product. Figure 5.1 represents the simple embodiment of LNG and NGL integration using a compressor.

Configuration 2 (C2): The De-C2 column overhead is operated as a total condenser; liquid ethane is split into two streams. The first portion of liquid ethane is pumped to 33.8 bar and mixed with the top product stream of De-C1 column. The second portion of liquid ethane is recovered as a product. Figure 5.2 represents the simple embodiment of LNG and NGL integration using a pump.

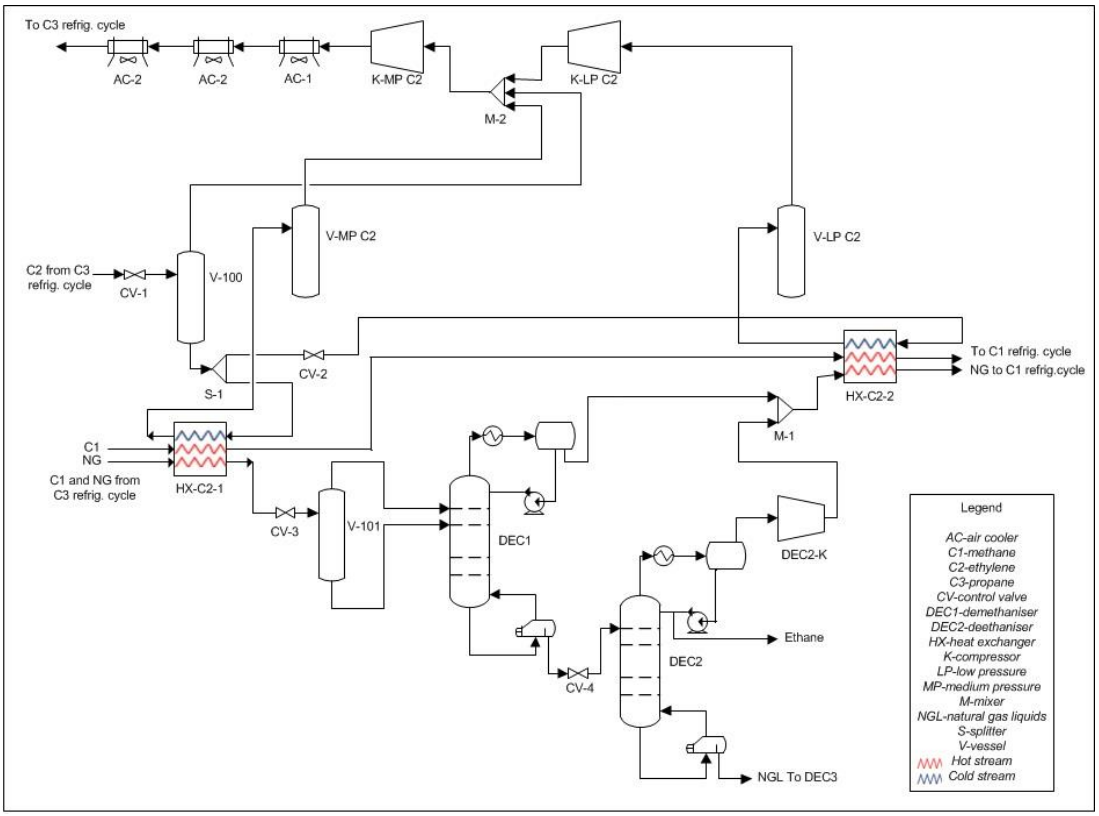

Figure 5.1: Configuration 1 (C1) - the simple embodiment of LNG and NGL integration using a compressor.

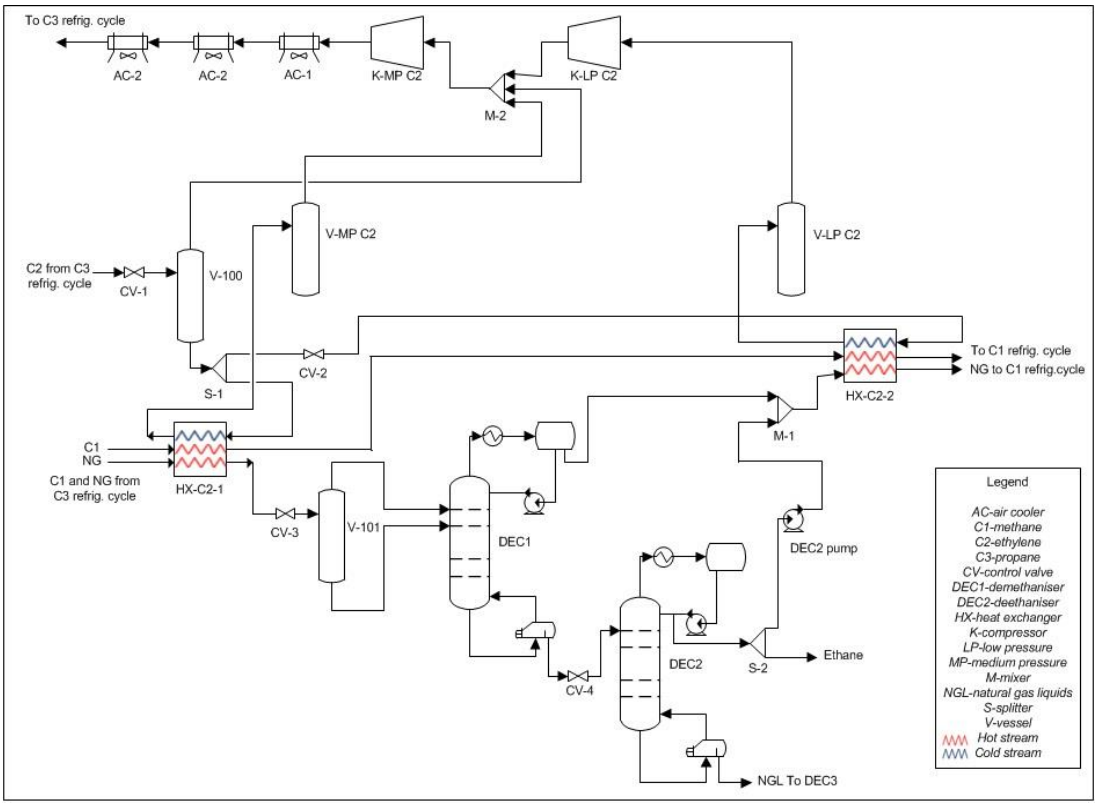

Figure 5.2: Configuration 2 (C2) - the simple embodiment of LNG and NGL integration using a pump.

5.5.2 Optimisation framework of two different integrated LNG/NGL configurations

As described above, two different integrated LNG/NGL configurations are proposed. The cascade process is optimised from the design perspective and the optimisation flowchart is shown in Figure 5.3 below.

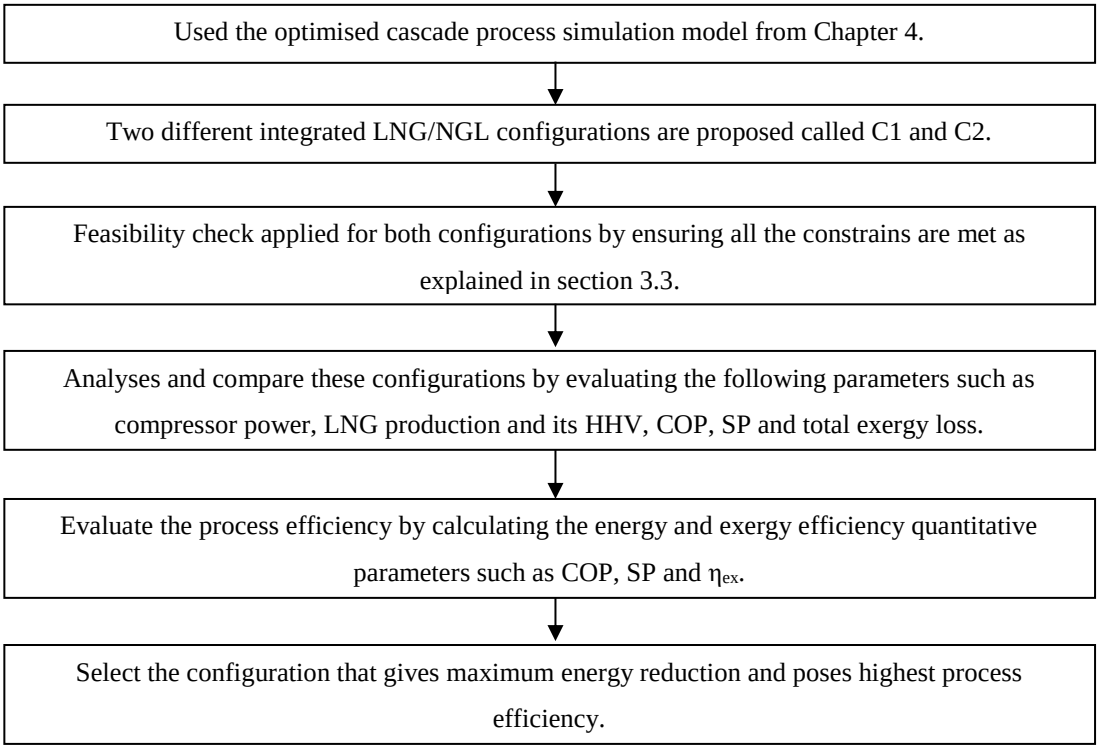

Figure 5.3: Optimisation framework of integrated LNG/NGL process.

5.6 Energy and exergy analyses of two different integrated LNG/NGL configurations

The evaluation of the process efficiency of the overall process is determined through energy and exergy analyses. A detailed explanation of these methods has been described in Chapter 2, section 2.8.1. The calculation of the quantitative parameters of energy and exergy analyses are done using the following equations (2.3), (2.8) ((2.11) and also equations presented in Table 2.5 [30].

5.7 Results and discussion

The simulation results of the proposed configurations are summarised in Table 5.1. These configurations are analysed and assessed based on several criteria such as meeting the required LNG HHV specification, consume less energy, meet the desired LNG capacity and possess highest process efficiency.

Table 5.1: Simulation results of two different configurations of integrated LNG and NGL process.

Evaluation parameters	Configuration 1	Configuration 2
Compressor power (MW)	69.04	65.71
LNG production (kg/h)	611, 806.03	626, 482.42
HHV (Btu/Scf)	1,040.30	1,050.88
COP	1.432	1.451
Specific power (kWh/kg LNG)	0.113	0.105
Total exergy loss (MW)	55.59	51.52
η_{ex} (%)	19.48	21.59

The results show that configuration 2 gives the lowest power consumption (65.71 MW) which can be translated into an energy saving of 4.82% compared to configuration 1. The LNG production capacity is also impacted by different integrated designs. The LNG capacities for Configuration 1 and 2 are 4.85 MTPA and 4.96 MTPA respectively. This indicates that configuration 2 LNG capacity is 2.39% higher compared to configuration 1 and close towards meeting the desired LNG capacity (5 MTPA). In term of LNG HHV specification, configuration 2 HHV specification is 1,050.88 which meet the specified range i.e. 1,050–1,125 Btu/Scf.

Meanwhile, the COP of performance of design 2 is 1.3% higher than design 1. This shows a significant increase in the overall performance of the refrigeration cycle. Whereas, the specific power (SP) for configuration 2 is 7.1% lower than configuration 1. The SP of configuration 2 is also much lower compared to the one reported in the literature [128] which are in the range of 0.28 to 0.5. This indicates the configuration 2 and cascade LNG process is more efficient than configuration 1 and other LNG processes. In addition, the total amount of exergy loss dissipated by the unit operation in configuration 2 is also reduced by 7.32% compared to configuration 1. Also, the exergy efficiency increases by 10.83% for configuration 2 compared to configuration 1. This shows that the irreversibilities in design 2 are minimal and the process is energy efficient.

Through exergy analysis on the energy conversion process, it acts as a guideline in the process design of an LNG plant. This information is useful for project execution as well, as it reduces the capital and operating cost of the LNG plant [88]. This implies that change in the process design of the ethylene refrigeration cycle and NGL recovery process has a great impact in meeting the required LNG HHV specification, power consumption, LNG capacity and process efficiency.

On the other hand, depending on the market conditions, the operation of the integrated LNG/NGL design can be changed. For instance, if the market demand is to maximise LNG throughput, then the HHV of LNG can be increased by sending more heavier components to the overhead column [30].

5.8 Conclusions

In this study, two different configurations of the integrated LNG/NGL cascade process are proposed and analysed. These configurations were evaluated based on meeting the required LNG HHV specification, consume less energy, meet the desired LNG capacity (5 MTPA) and possess highest process efficiency. Energy and exergy analyses methods were selected to evaluate the efficiency of the process. The simulation results demonstrate that configuration 2 meets the required HHV specification (1,050.88 Btu/Scf) and reduces the power consumption by 4.82% compared to configuration 1. The LNG capacity is increased by 2.39% compared to design 1. The specific power of design 2 is the lowest i.e. 0.105. Meanwhile, the exergy loss of configuration 2 is reduced by 7.32% which shows minimal irreversibilities while the exergy efficiency of configuration 2 increases by 10.83% compared to configuration 1. Based on these results, it can be concluded that configuration 2 gives the highest process efficiency and can be used to produce both LNG and NGL at minimum energy consumption. Having these integrated concepts gives the flexibility to the plant to switch their operation by either producing more LNG or more NGL when the market conditions changes.

5.9 Future work

In this study, the exergy analysis for demethaniser and deethaniser is excluded due to insufficient information that is enthalpy and entropy for each tray. A detailed dynamic simulation is proposed for these configurations to obtain this information. Also, there is no consideration is made from an economic perspective to evaluate the feasibility of these proposed configurations. Therefore, future work is to be considered to analyse these configurations using the exergy analysis that gives economic trade-off between the operating and capital cost of the integrated LNG and NGL plant.

5.10 Acknowledgements

The authors would like to acknowledge the support provided by the staff from Curtin University, Australia. The authors also would like to acknowledge the Ministry of Education (MOE) of Malaysia and University Malaysia Pahang for funding the presented study.

5.11 References

1. BROSTOW, A.A., AND ROBERTS, M.J. 2012—Integrated NGL recovery in the production of liquefied natural gas. US Patent No. I. Air Products and Chemicals.
2. CHO, J., VEGA, F.D.L., KOTZOT, H., AND DURR, C., 2005.— Innovative Gas Processing with various LNG sources. LNG journal (January/February), 23-27.
3. ELLIOT, D., QUALLS, W., HUANG, S., CHEN, J., LEE, R., YAO, J., AND ZHANG, Y., 2005.— Benefits of integrating NGL extraction and LNG liquefaction technology. AIChE Journal, 1943-1958.
4. FINN, A.J., JOHNSON, G.L., AND TOMLINSON, T.R., 1999.— Developments in natural gas liquefaction. Hydrocarbon Processing, 78(4), 1-18.
5. KANOGLU, M., 2002.— Exergy analysis of multistage cascade refrigeration cycle used for natural gas liquefaction. International Journal of Energy Research, 26(8), 763-774. doi: 10.1002/er.814
6. MEHRPOOYA, M., HOSSIENI, M., AND VATANI, A., 2014.— Novel LNG-Based Integrated Process Configuration Alternatives for Coproduction of LNG and NGL. Industrial & Engineering Chemistry Research, 53(45), 17705-17721. doi: 10.1021/ie502370p
7. MORAN, M.J., 2011— Fundamentals of engineering thermodynamics Hoboken, New Jersey: Wiley
8. SPILSBURY, C., MCLAUCHLIN, S., AND KENNINGTON, B., 2005.— Optimising the LNG liquefaction Process. LNG journal (January/February), 40-43.

Chapter 6 Effect of Deethaniser (De-C2) column pressure on the process efficiency of an integrated LNG/NGL cascade process

6.1 Introduction

In this chapter, the process efficiency of the integrated LNG/NGL cascade process is further optimised by using the optimal integrated design (configuration 2) from the previous chapter. The integrated LNG/NGL process is optimised by manipulating the deethaniser (De-C2) column pressure. Detailed background, the significance of this research area and the study gaps have been discussed in Chapter 2 (section 2.9.3, 2.9.4 and 2.9.5). This is a new research area as no study is available in the literature that has analysed this parameter to optimise the efficiency of an integrated LNG/NGL cascade LNG process for a large train. Thermodynamic analyses; energy and exergy were used to evaluate the process efficiency. Also, the effect of varying the (De-C2) column pressure on the process parameters such as compressors power, heat exchangers duty and UA, refrigerants flow rate, LNG production and its HHV are analysed and discussed. The optimal De-C2 column pressure should meet the desired LNG capacity and its HHV specification, gives minimum energy consumption and possess highest process efficiency.

6.2 Modelling assumptions and simulation method and constraints

The feed gas condition and modelling assumptions applied are outlined in Table 3.1, section 3.2 of the thesis. The simulation method and simulation constraint applied to optimise the integrated LNG/NGL process by varying the (De-C2) column pressure is explained in 0 (section 3.2 and 3.3). The operating conditions of other process parameters remained unchanged to analyse the sole effect of De-C2 column pressure on the process performance.

6.2.1 Process simulation description of integrated LNG/NGL cascade process

The simplified process flow scheme on the integrated LNG/NGL cascade process is shown in Figure 6.1. In Figure 6.1, the green and purple streams represent the ethylene and methane refrigerants respectively. The cooling of the natural gas and methane refrigerant were done in two compression stages using ethylene as a refrigerant. The condensed ethylene from the propane refrigeration cycle (stream 1) is expanded via (VLV-100) and flashed into the separator (V-100) into two phases. The flashed liquid (stream 4) is divided into two parts. The first part (stream 5) is used for cooling the natural gas and methane streams to -55^{o}C in the first ethylene heat exchanger (E-1401). The second part (stream 11) is expanded via (VLV-101) and used to further cool down the methane and natural gas streams. The cooled natural gas at -55^{o}C (stream 14) is expanded via (VLV-102) and flashed into the separator (V-101) into streams 16 and 17. These streams are then fed into the demethaniser column (C-1401) at 3400 kPa.

The demethaniser column (C-1401) is operated as a full condenser column. The NGL (stream 19) is expanded via (VLV-103) before entering the deethaniser column (C-1501). The deethaniser column (C-1501) is also operated as a full condenser. The overhead liquid product of the deethaniser column (C-1501), stream 21 is divided into two streams, 23 and 24. The liquid stream 23 which mainly contains ethane and some remaining methane is pumped by (P-100) to 3380 kPa and mixed with the overhead stream of the demethaniser column (C-1401), stream 18. Whereas, stream 24 is liquid ethane.

The mixed stream (stream 26) and methane refrigerant (stream 13) are further cooled to -95^{o}C in the second ethylene heat exchanger (E-1402). The natural gas (stream 28) and methane (stream 27) are routed to the methane refrigeration cycle whereby the condensed methane is used to sub-cooled the natural gas. Meanwhile, the vaporised ethylene (stream 29) is flashed into the separator (V-103) and compressed (stream 30) in the first compressor (K-100) to 420 kPa. The discharge of K-100 (stream 32), is mixed with the vaporised ethylene i.e. stream 3 and 9 from V-100 and V-102 respectively. The mixed vapour stream (stream 33) is further compressed (K-101) to 2500 kPa. The discharge of K-101 (stream 34) is cooled in a series of air coolers (AC-100, AC-101 and AC-102). The cooled ethylene (stream 37) is then condensed in the propane refrigeration cycle before it is expanded again via VLV-100 and flashed into the separator (V-100). The primary focus of this study is to optimise the process efficiency of the integrated process by manipulating the deethaniser column (C-1501) pressure via VLV-103 as marked by the yellow dotted line in Figure 6.1.

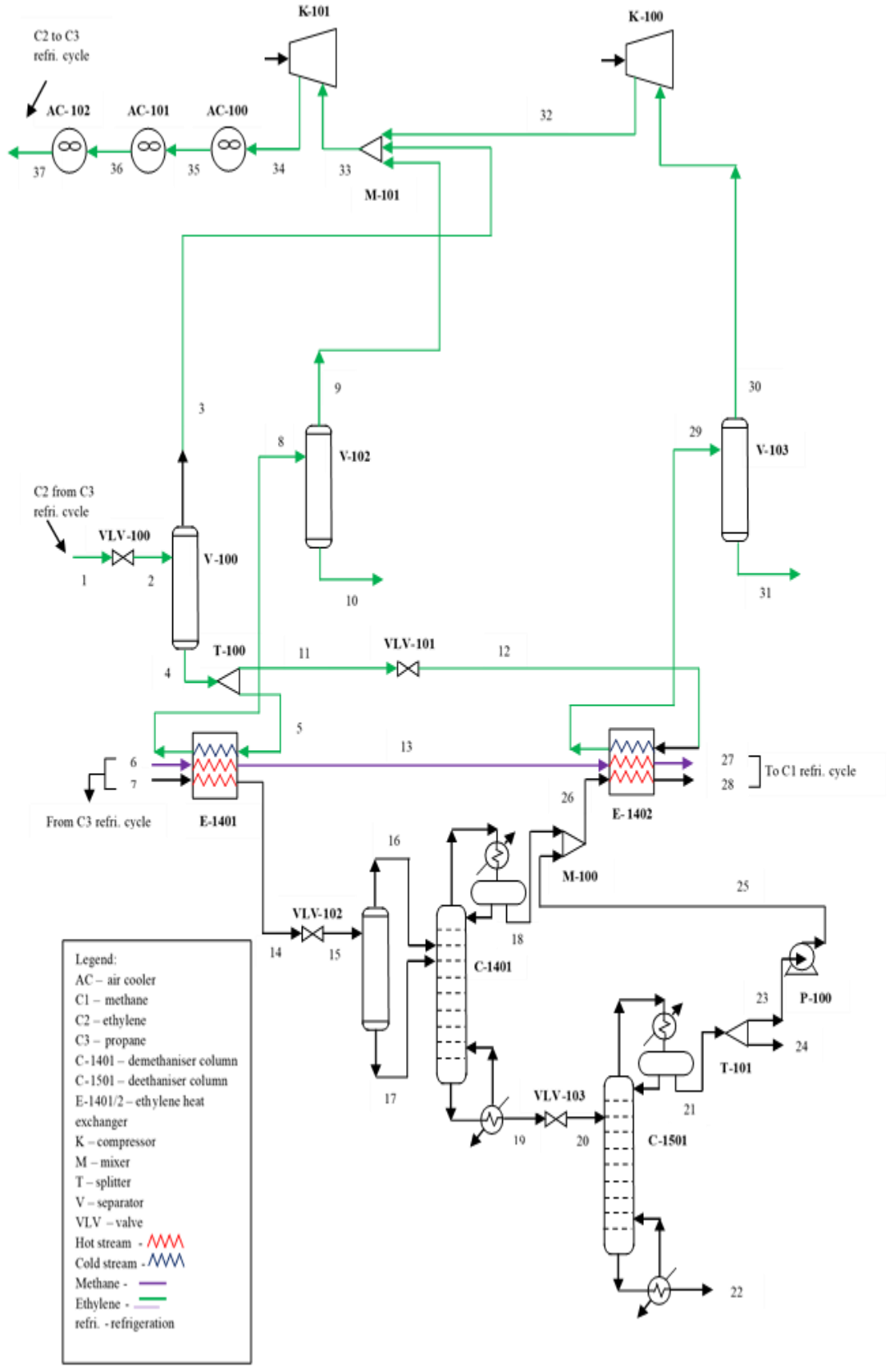

Figure 6.1: Process flow scheme of integrated LNG/NGL cascade process modelled in Aspen HYSYS.

6.2.2 Process simulation model verification

The integrated LNG/NGL process modelled verification is done in a similar manner as explained in section 3.6.2. The overall mass balance of the process is calculated using equation (3.3). The overall heat balance for the process is presented in Appendix A.

6.2.3 Optimisation framework of integrated LNG/NGL process via various deethaniser column pressure

The optimisation framework of integrated LNG/NGL cascade process through various deethaniser column pressure is shown in Figure 6.2. The typical operating pressure range of the De-C2 column is obtained based on the existing literature [132] and by referring to the operating conditions of current LNG plants located in Southeast Asia, Australia, Gulf countries, Northern Asia and Africa. These plants are not to be disclosed due to confidentiality.

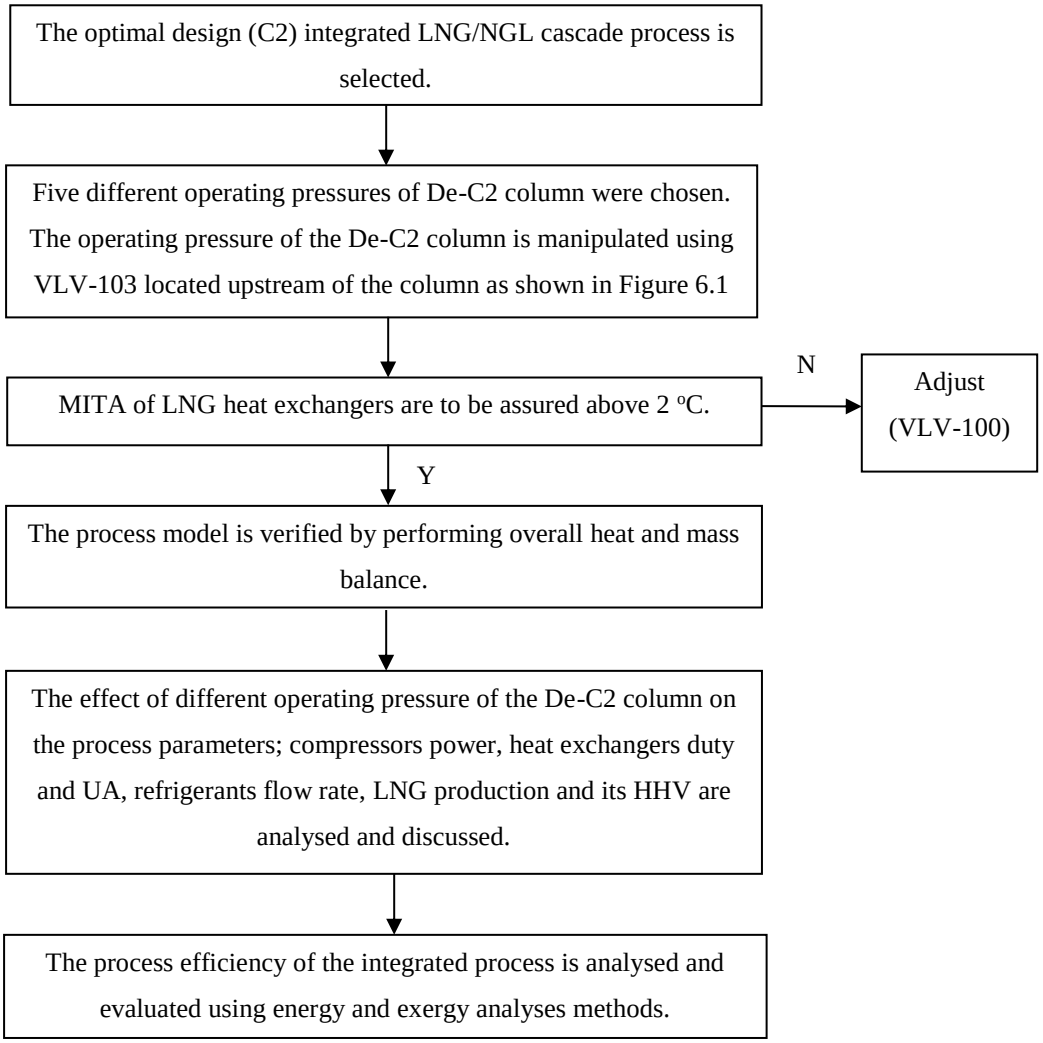

Figure 6.2: Optimisation framework of integrated LNG/NGL cascade process through various deethaniser column pressures.

6.3 Energy and exergy analyses of integrated LNG/NGL process with different deethaniser (De-C2) column pressures

The evaluation of the process efficiency of the overall process is determined through energy and exergy analyses. The detailed explanation of these methods have been described in Chapter 2, section 2.8.1. The calculation of the quantitative parameters of energy and exergy analyses are done using the following equations (2.3), (2.8), (2.11) and also equations presented in Table 2.5 [30].

6.4 Results and discussion

Section 6.4.1 to 6.4.4 discussed the effect of the deethaniser (De-C2) column pressures on the refrigerants compressors power, heat exchangers duty and UA, refrigerants flow rate, higher heating value (HHV) and LNG production.

6.4.1 Effect of De-C2 column pressures on the refrigerant's compressor power.

Effect of De-C2 column pressures on the refrigerant's compressors power is shown in Figure 6.3. As depicted in Figure 6.3, De-C2 column pressure of 2000 kPa gives the lowest power consumption for propane and ethylene compressors power which are 121.73 MW and 65.71 MW respectively compared to 1800 kPa column pressure. This can be translated into an energy saving of 1.25% and 2% for propane and ethylene compressors respectively which are indeed significant savings. Meanwhile, the change of De-C2 column pressure gives no significant effect on methane refrigerant compressor power because methane refrigerant was only used to sub-cool the natural gas stream.

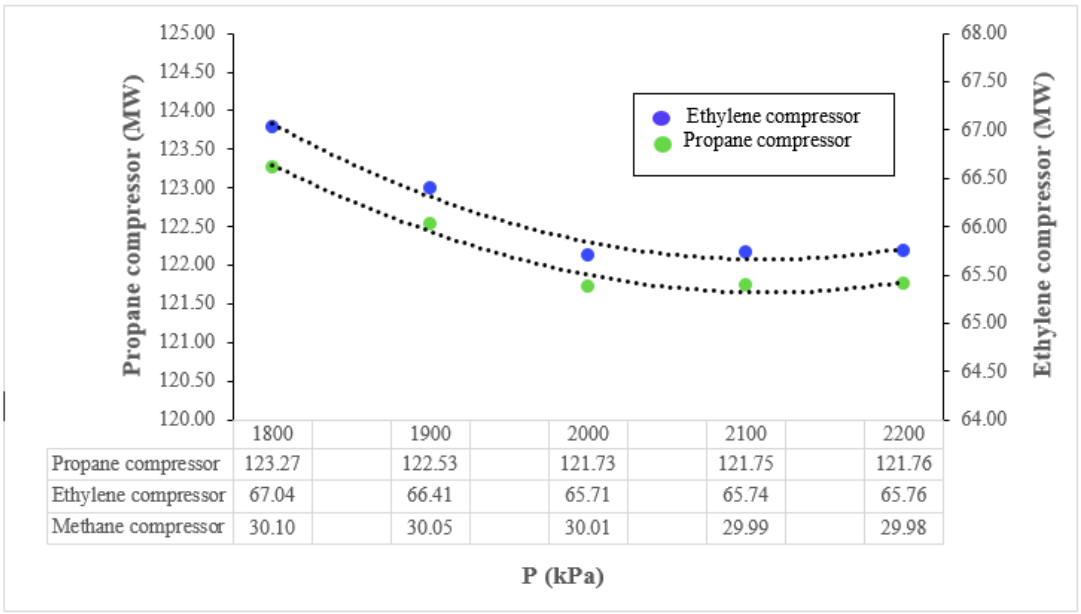

	1800	1900	2000	2100	2200
Propane compressor	123.27	122.53	121.73	121.75	121.76
Ethylene compressor	67.04	66.41	65.71	65.74	65.76
Methane compressor	30.10	30.05	30.01	29.99	29.98

Figure 6.3: Effect of deethaniser (De-C2) column pressures on the refrigerant's compressor power.

6.4.2 Effect of De-C2 column pressures on heat exchangers duty and UA

Figure 6.4 shows the effect of De-C2 column pressures on heat exchangers duty. As can be seen in Figure 6.4, at 2000 kPa column pressure, the duty of propane and ethylene heat exchangers are reduced by 1.2% and 1.7% respectively compared to 1800 kPa column pressure. Whereas, the duty of methane heat exchangers remained unchanged. In addition, the overall heat exchangers UA calculated by HYSYS for various De-C2 column pressures is reported in Table 6.1. As can be seen from Table 6.1, the overall heat exchangers UA obtained for propane, ethylene and methane refrigerants at 2000 kPa column pressure are reduced by 1.65%, 1.05% and 0.1% respectively in comparison to 1800 kPa column pressure. Having a lower UA value not only reduces the equipment size but also the capital cost.

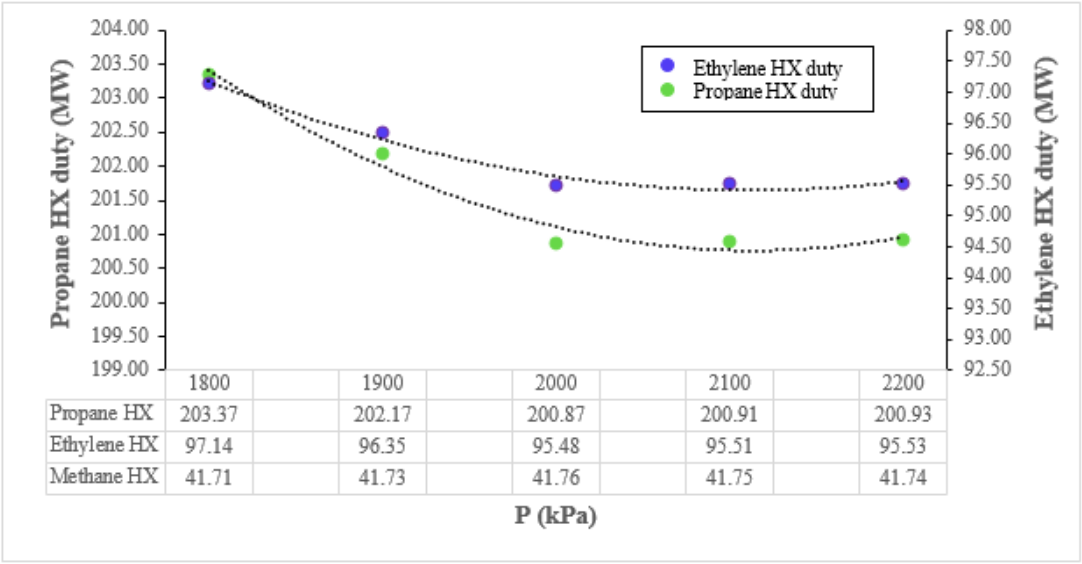

Figure 6.4: Effect of deethaniser (De-C2) column pressures on the refrigerants heat exchangers duty.

Table 6.1: Effect of deethaniser (De-C2) column pressures on overall heat exchanger UA.

De-C2 column pressure (kPa)	1800	1900	2000	2100	2200
Propane UA (kW/°C)	14, 986.2	14, 911.7	**14,829.5**	14, 832.9	14, 834.5
Ethylene UA (kW/°C)	7,460.40	7,402.55	**7, 336.44**	7,341.99	7, 346.46
Methane UA (kW/°C)	3, 954.86	3, 951.83	**3, 950.15**	3, 948.56	3, 946.89

6.4.3 Effect of De-C2 column pressures on the refrigerants flow rate

Figure 6.5 shows the effect of De-C2 column pressures on refrigerants flow rate. As depicted in Figure 6.5, at De-C2 column pressure of 2000 kPa the refrigerants flow rate of propane and ethylene are reduced by 1.2% and 1.75% respectively compared to 1800 kPa column pressure. Whereas, the methane refrigerant flow rate almost keeps constant with the increase of De-C2 column pressures. From the results, it indicates that although the cooling temperature range for all these exchangers remained the same, changing the De-C2 column pressure affects the overall compressors power, heat exchangers duty and UA and refrigerants flow rate. Hence, varying the De-C2 column pressure optimises the process efficiency of an LNG plant.

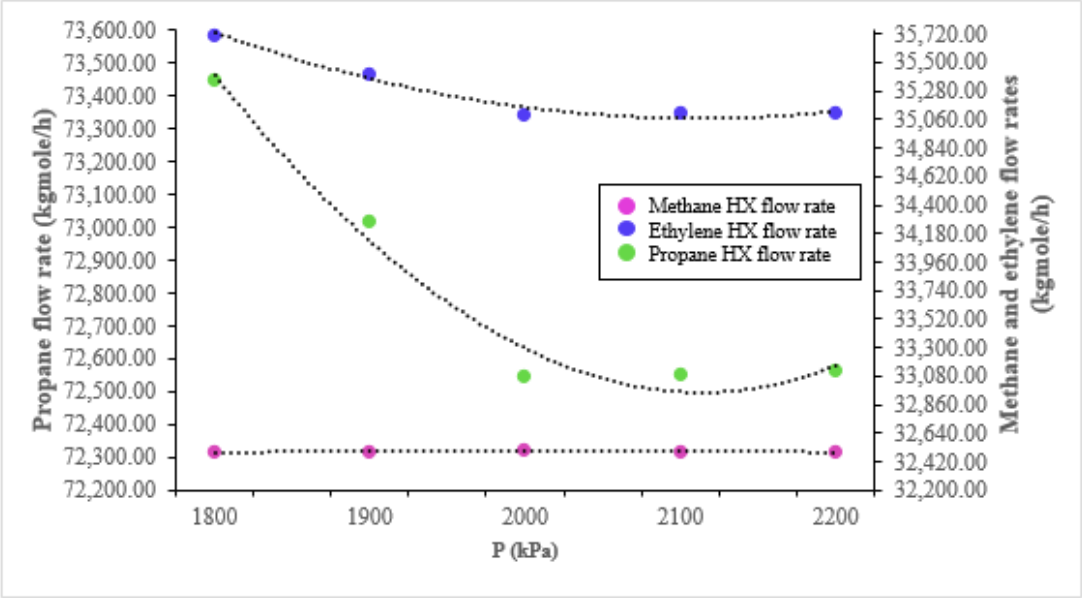

Figure 6.5: Effect of deethaniser (De-C2) column pressures on refrigerants flow rate.

6.4.4 Effect of De-C2 column pressure on LNG production and its higher heating value (HHV)

The effect of De-C2 column pressures on LNG production and its HHV is illustrated in Figure 6.6. As can be seen from Figure 6.6, the LNG production and HHV is high at low De-C2 column pressure and gradually decreased with increase in the De-C2 column pressure. At 2000 kPa De-C2 column pressure, the LNG production and HHV increased by 0.3% and 0.1% respectively compared to 2200 kPa column pressure. The increased in HHV is due to the presence of many heavier components such as ethane and propane at the overhead product stream of the De-C2 column (*stream 23*) compared to 2100 kPa and 2200 kPa De-C2 column pressures as shown in Table 6.2. This finding is agreement with Mokhatab, Mark [30] statement.

Besides, as can be seen in Table 6.2, the ethane purity is also the highest at 2000 kPa De-C2 column pressure compared to other column pressures. This indicates that 2000 kPa De-C2 column pressure is the optimal pressure that gives high ethane recovery. Moreover, the prescribed LNG HHV specification and 5 MTPA LNG capacity for this process are also met at 2000 kPa De-C2 column pressure.

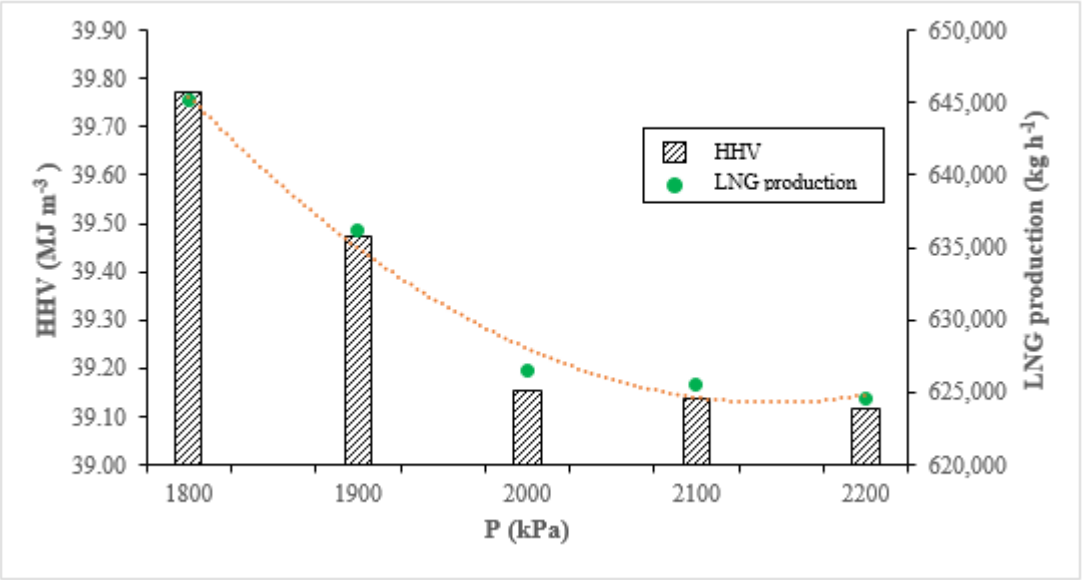

Figure 6.6: Effect of deethaniser (De-C2) column pressure on higher heating value (HHV) and LNG production.

Table 6.2: Results of deethaniser column overhead product stream (*stream 23*).

De-C2 (kPa)	1800		1900		2000		2100		2200	
	C_2H_6	C_3H_8	C_2H_6	C_3H_8	C_2H_6	C_3H_8	C_2H_6	C_3H_8	C_2H_6	C_3H_8
Mole fraction	0.7579	0.2355	0.8215	0.1715	**0.9003**	0.0922	0.8958	0.0965	0.8912	0.1010
Flow rate (kgmole h^{-1})	**2,014.5**	**625.8**	2,014.5	420.6	2,007.9	205.6	1,968.4	212.2	1,927.2	218.5

Given these results, it shows that the LNG capacity, its final product quality and ethane purity all hinged on the De-C2 column pressure. This indicates that the De-C2 column pressure also plays a significant role in enhancing the overall process performance.

6.4.5 Energy and exergy analyses results of various De-C2 column pressures

The overall refrigeration cycle efficiency is evaluated by analysing the COP. As can be seen in Figure 6.7, the COP increases with increasing in the De-C2 column pressure and then it decreases at 2100-2200 kPa. The COP is highest at De-C2 column pressure of 2000 kPa which is 0.27% higher compared to 1800 kPa column pressure. Higher COP indicates that the process is energy efficient. As liquefaction of natural gas consumes a significant amount of energy i.e. 1188 kJ of energy for liquefaction of 1 kg [88], this small increase in the COP is indeed a significant saving. Based on this observation, the De-C2 column pressure plays an important role in optimising the efficiency of the integrated process.

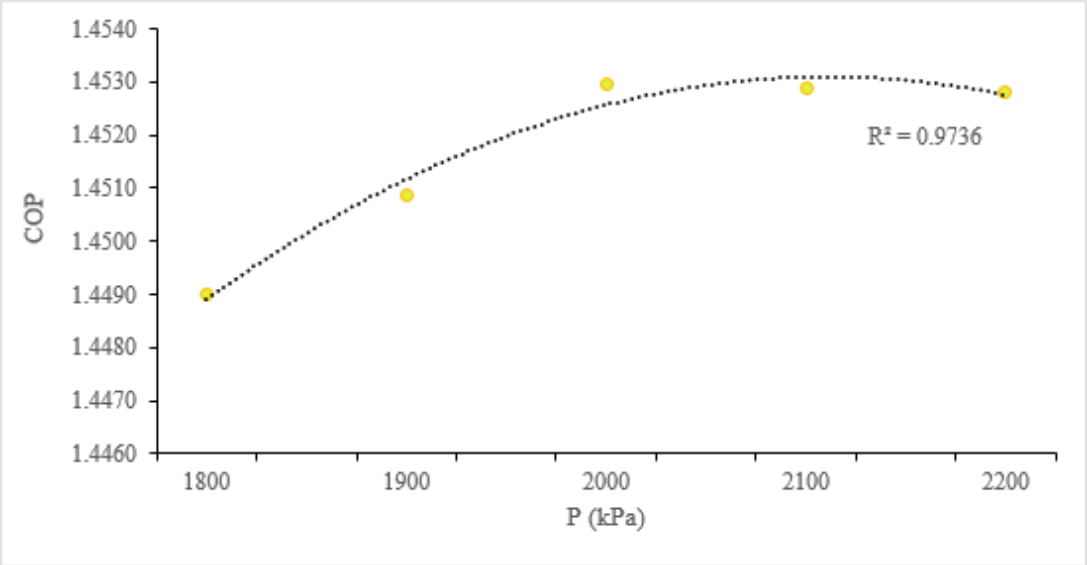

Figure 6.7: Effect of deethaniser (De-C2) column pressures on COP.

6.4.5.1 Exergy loss results for all unit operation

The exergy loss is calculated for the following unit operation compressors, heat exchangers (HX), De-C2 pump (P-100), valves, mixers, and air coolers (AC) using expressions presented in Table 2.5 [30]. Figure 6.8 shows the exergy loss of compressors and heat exchangers for various De-C2 column pressures. As can be seen in Figure 6.8, at 1800 kPa column pressure, the exergy loss of compressors and heat exchangers are first high and then decline at 2000 kPa and again show a minor increase at 2100-2200 kPa. The lowest exergy loss of compressors and heat exchangers were observed at column pressure of 2000 kPa which are lower by 1.95% and 1.4% respectively in comparison to 1800 kPa column pressure.

Meanwhile, at column pressure of 1800 kPa, the exergy loss of the heat exchangers is high because of an increase in the heat exchanger duty requirement as indicated in Figure 6.4. Whereas, increased in the exergy loss of compressors is contributed due to the increase in the refrigerants flow rate as shown in Figure 6.5. A further rise in the exergy loss observed at 2100-2200 kPa for compressors and heat exchangers is due to an increase in the enthalpy and entropy difference of the NG stream across E-1402 exchanger as shown in Table 6.3. The lowest exergy loss of compressors and heat exchangers was observed at 2000 kPa column pressure which is lower by 1.97% and 1.4% respectively in comparison to 1800 kPa column pressure. This is due to low enthalpy and entropy change of the NG stream was observed in E-1402 exchanger at this pressure as shown in the same table**.** The effect of different operating pressures of De-C2 column on E-1401 exchanger remained the same because it is located upstream of De-C2 column, hence no changes are detected.

The efficiency of the integrated process can be improved by reducing the exergy loss exhibited by the heat exchangers and compressors. The exergy loss of the heat exchangers can be reduced by minimising the temperature approach (T_{app}) between the hot and cold streams which will match the cooling curves better [132]. Another option is by using a plate fin heat exchanger (PFHE) instead of using an ordinary shell and tube heat exchanger. It has various advantages namely high heat transfer coefficient and area density, small temperature difference ($1^{o}C$ or below) can be tolerated within this unit and it can be also designed to handle multiple streams. This permits the heat exchanger network to be accommodated in a single unit [102].

Whereas for the compressor, the exergy loss can be minimised by using a higher polytropic efficiency compressor which will reduce the outlet temperature of the compressor, hence reducing the overall power consumption. Besides, this option will also reduce the cooling load of the AC which results in lower exergy loss. Although these options could optimise the process efficiency, the cost associated with installing new equipment needs to be evaluated to determine its feasibility.

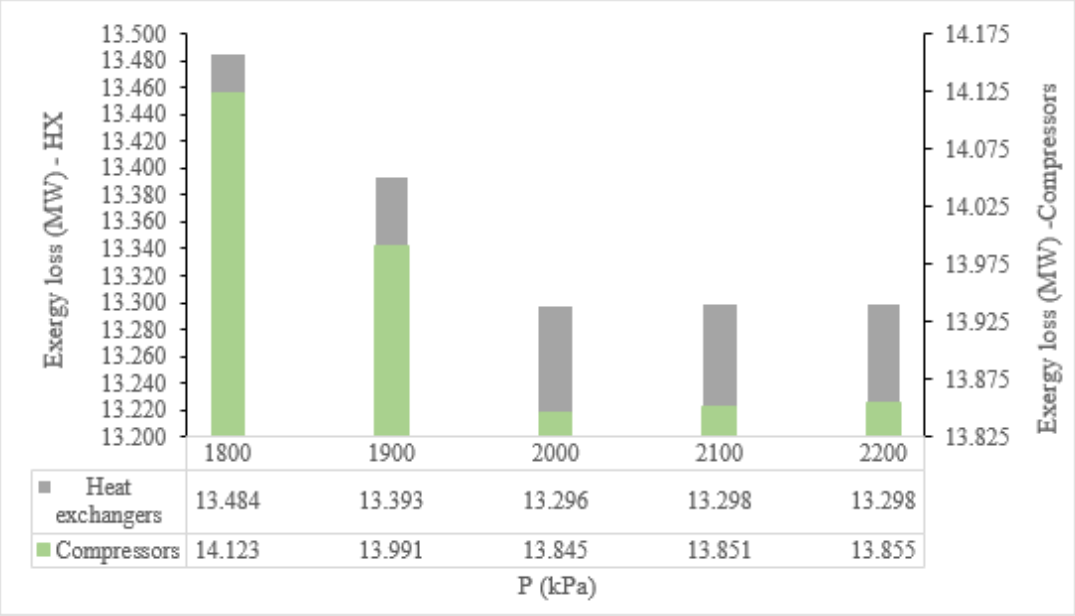

Figure 6.8: Exergy loss of compressors and heat exchangers (HX) at various De-C2 column pressures.

Table 6.3: Enthalpy and entropy difference of natural gas, ethylene and methane streams across heat exchangers.

	E-1401	E-1402	E-1401	E-1402	E-1401	E-1402	E-1401	E-1402	E-1401	E-1402
De-C2 P (kPa)	1800		1900		2000		2100		2200	
ΔH										
NG	-115.81	-62.08	-115.81	-58.71	-115.81	-54.73	-115.81	**-55.09**	-115.81	**-55.38**
CH_4	-41.09	-376.75	-41.09	-376.75	-41.09	-376.75	-41.09	-376.75	-41.09	-376.75
C_2H_4	471.36	438.07	471.36	438.07	471.36	438.07	471.36	438.07	471.36	438.07
$T_{o*}\Delta S$										
NG	-154.24	-102.03	-154.24	-96.61	-154.24	-90.20	-154.24	**-90.79**	-154.24	**-91.29**
CH_4	-54.00	-603.44	-54.00	-603.44	-54.00	-603.44	-54.00	-603.44	-54.00	-603.44
C_2H_4	711.33	757.28	711.33	757.28	711.33	757.28	711.33	757.28	711.33	757.28

Unit ΔH and TΔS are in kJ kg^{-1}

Figure 6.9 illustrates the exergy loss of the De-C2 pump (P-100) and valves for various De-C2 column pressures. As can be seen in Figure 6.9, the exergy loss of the De-C2 pump (P-100) and valves reduced with increased in the De-C2 column pressure. At 2200 kPa column pressure, the exergy loss of the De-C2 pump (P-100) and valves are reduced by 43.4% and 1.8% respectively compared to 1800 kPa column pressure.

Meanwhile, the inlet and outlet pressure of the De-C2 pump (P-100) and valves is shown in Table 6.4. The exergy loss of the De-C2 pump and valves are influenced by the pressure difference across these unit operations. As shown in Table 6.4, at 1800 kPa column pressure, the exergy loss of both unit operations is high because of the large pressure difference (1600 kPa). Whereas, at 2200 kPa column pressure, the exergy loss is low due to small pressure difference (1200 kPa). Hence, varying the De-C2 column pressure affects the process parameters which will influence the process efficiency.

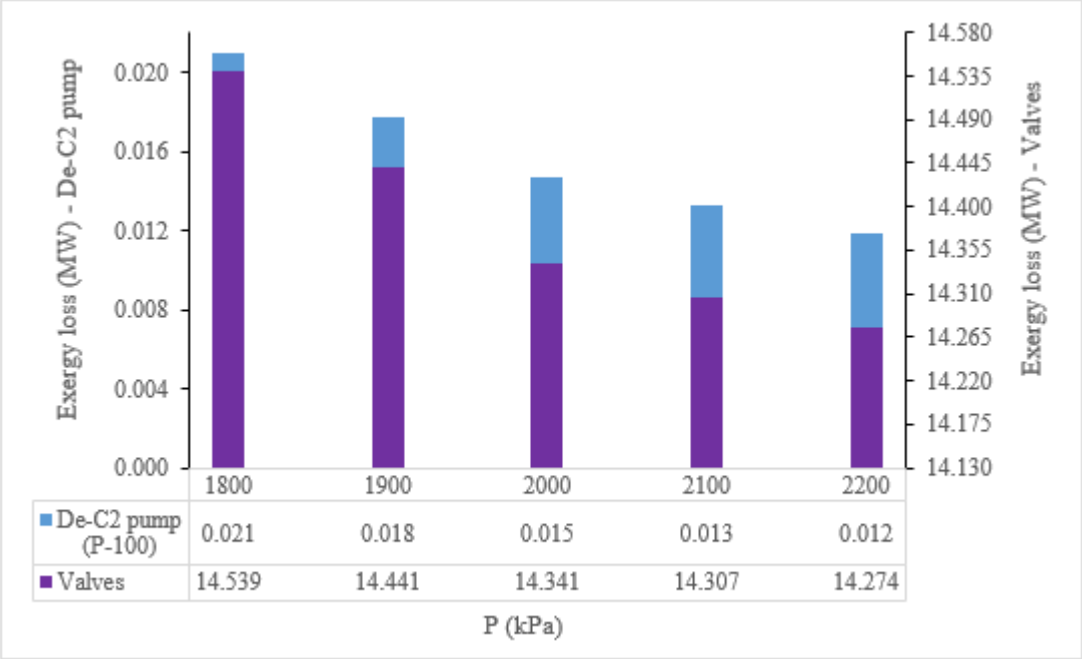

Figure 6.9: Exergy loss of De-C2 pump (P-100) and valves at various De-C2 column pressures.

Table 6.4: Pressure difference across VLV-103 and De-C2 pump (P-100) for various De-C2 column pressures.

De-C2 P(kPa)	1800		1900		2000		2100		2200	
	Inlet	Outlet	Inlet	Outlet	Inlet	Outlet	Inlet	Outlet	Inlet	Outlet
VLV-103	3400	1800	3400	1900	3400	2000	3400	2100	3400	2200
De-C2 pump (P-100)	1780	3380	1880	3380	1980	3380	2080	3380	2180	3380

Figure 6.10 shows the exergy loss of mixers and air coolers (AC) at various De-C2 column pressures. As can be seen in Figure 6.10, at 1800 kPa column pressure the exergy loss of mixers and air coolers (AC) is first high and then decline at 2000 kPa followed by a minor rise at 2100-2200 kPa. At 2000 kPa column pressure the exergy loss of mixers and AC is declined by 10.7% and 1.4% respectively in comparison to 1800 kPa column pressure. At 1800 kPa column pressure the exergy loss of mixer is high because of an increase in the natural gas flow rate at M-100 as shown in Table 6.5 (Figure 6.1 see the location of M-100). This also resulted in an increase in LNG capacity (Figure 6.6).

Meanwhile, the rise in the exergy loss of the AC is due to the increase in the refrigerant flow rate (Figure 6.5) which increases the cooling duty of AC. The exergy loss of the AC can be reduced by using extended surface tubes (i.e. high transverse fins) that will increase the heat transfer rate per-unit-length of the tube [102]. Also, by using a higher polytropic efficiency compressor as previously mentioned in section 6.4.5.1.

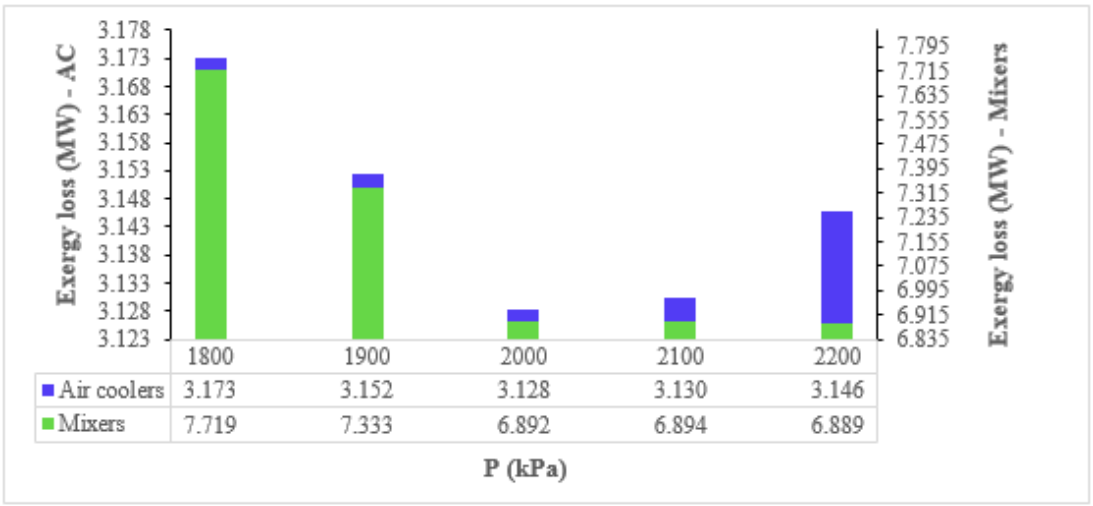

Figure 6.10: Exergy loss of mixers and air coolers (AC) at various De-C2 column pressure.

Table 6.5: Natural gas flowrate at M-100.

De-C2 P (kPa)	1800	1900	2000	2100	2200
M-100 (kg/h)	691, 911.3	682,835.8	673,139.9	672,242.6	671,284.6

As observed in Figure 6.8 to Figure 6.10 manipulating the De-C2 column has impacted the exergy loss of each unit. Based on the above results, three main primary contributors of the exergy loss were identified namely compressors, heat exchangers and valves that affect the process efficiency of the LNG plant. By using the exergy analysis, the process efficiency of the integrated process can be optimised as it involved a detailed analysis of the thermodynamic properties which provides a better understanding of the changes that occur within the process. By using this information, appropriate adjustment can be made to the operating parameter and the equipment to optimise the process efficiency.

6.5 Conclusions

The integrated LNG/NGL cascade process is optimised by manipulating the De-C2 column pressure. The efficiency of the process is evaluated through energy and exergy calculations. Results indicate that overall about 3.25% energy savings and a 0.27% increase in the COP are obtained at 2000 kPa De-C2 column pressure compared to 1800 kPa column pressure. Additionally, the exergy loss exhibited by the unit operation at 2000 kPa De-C2 column pressure has reduced by 3.5% compared to the column pressure of 1800 kPa. This demonstrates that the occurrence of thermodynamic inefficiency at 2000 kPa is minimal. Meanwhile, the prescribed LNG HHV (39.12 – 41.92 MJ/m^3) and LNG capacity of 5 MTPA are met at this column pressure. In addition, varying the De-C2 column pressure also affects the process parameters significantly as discussed in section 6.4. In a nut shell, the De-C2 column pressure is an important process parameter that affects the process performance, LNG HHV and efficiency. Moreover, it provides the flexibility to the LNG plants to meet different LNG product specifications when the market demands changes.

Chapter 7 Conclusions and recommendations for future studies

7.1 Conclusions

The aim of this thesis is to optimise the cascade LNG process both from operation and design perspectives and focused on a single large integrated LNG/NGL plant. In this thesis, the cascade LNG process of 5 MTPA production plant was modelled and simulated using Aspen HYSYS 7.2. The cascade process was optimised in three steps. Firstly, the three-stage propane pre-cooling cycle was optimised by manipulating the evaporators pressures. Six case studies were studied by varying the cooling load of propane evaporator at the intermediate stages. Based on the case studies results, the optimal operating conditions of the propane evaporator was selected that gives maximum energy reduction and highest process efficiency. The second step of optimisation was by using the optimal operating conditions of the propane pre-cooling cycle, the cascade process was further optimised by evaluating two different integrated LNG/NGL configurations. These integrated designs were evaluated based on several criteria such as to meet the desired LNG capacity and its HHV specification, consume less energy and possess the highest process efficiency. Based on the optimal design of integrated LNG/NGL configuration, the last step was that the cascade process was finally optimised by manipulating the deethaniser (De-C2) column pressure. Five operating pressures of De-C2 column were studied that gave less energy consumption and improved energy efficiency. All the energy and efficiency calculations and evaluations were done by using the first and second law of thermodynamics.

Based on the results obtained, the optimal operating conditions of propane pre-cooling cycle for the intermediate stages are as follows; 5^{o}C, 0^{o}C, -40^{o}C which is Case 6. About 13.5% power reduction is achieved using this operating condition compared to the baseline case. Besides, Case 6 also gives the highest COP (1.65), lowest SP (0.205 MWh/tonne of LNG) and highest exergy efficiency (40.22%). This shows an increment of 15.51% and 18.75% for COP and exergy efficiency respectively and 13.5% reduction in SP. This shows a significant increase in the overall performance of the refrigeration cycle. In addition, the total exergy loss exhibited by all the unit operation dropped by 21.8% i.e. from 98.86 MW to 77.32 MW.

The optimisation of propane pre-cooling cycle shows that changing the operating conditions of the propane evaporator stage can be considered as an option to minimise the energy consumption of the process which does not involve any additional cost. Besides, the evaporator pressure is also considered an important degree of freedom. This is because it changes the cut point temperature between refrigeration levels [102] which then changes the cooling load. Additionally, this enhancement not only reduces the propane compression power but also reduces the size of the heat exchanger as well as the refrigeration flow rate.

Meanwhile, configuration 2 (C2) gives the optimal integrated LNG/NGL design. The results indicate that by operating De-C2 column as a total condenser, the compressor power is reduced by 4.82% compared to configuration 1 (C1). Further, the rise of 2.39% is observed in the LNG capacity which is close towards meeting the desired LNG capacity (5 MTPA). In addition, about 1,050.88 Btu/Scf of the LNG HHV is obtained which is in the range of the requirement that is (1,050 to 1,125 Btu/Scf). From the process efficiency context, the COP of performance of C2 showed an increased by 1.3% than C1. Whereas, the specific power (SP) for C2 is 7.1% lower than C1 which is also much lower compared to the one reported in the literature [128] which is in the range of 0.28 to 0.5. The total exergy loss calculated is also reduced by 7.32% compared to C1. Also, C2 attained the highest exergy efficiency i.e. 10.83% more than C1. This indicates that C2 has minimal irreversibilities and the process is energy efficient.

The above study shows that modification in the integrated liquefaction process design can minimise the energy consumption of the process as well as improve the efficiency and other process parameters. C2 was then used to further optimise the cascade process by manipulating the De-C2 column pressure. Results indicate that overall about 3.25% energy savings and a 0.27% increase in the COP are obtained at 2000 kPa De-C2 column pressure compared to 1800 kPa column pressure. Additionally, the exergy loss exhibited by the unit operations at 2000 kPa De-C2 column pressure is 3.5% lower compared to the column pressure of 1800 kPa. This demonstrates that the occurrence of thermodynamic inefficiency at 2000 kPa column pressure is minimal. Meanwhile, the prescribed LNG HHV and the targeted 5 MTPA LNG capacity are met at this column pressure.

To summarise, by optimising the propane pre-cooling evaporator pressure, changing the design configuration of the integrated LNG/NGL process and through manipulation of De-C2 column pressure, the total amount of power, SP, exergy loss and refrigerant flow rate reduction achieved are 21.6%, 20.6%, 32.6% and 18.8% respectively. Whereas, the percentage increase in the total amount of COP and exergy efficiency obtained is 17.1% and 29.6% accordingly. This shows a significant improvement in the process efficiency of the integrated cascade liquefaction process for 5 MTPA production plant which not only reduced the operating cost but also the capital cost. Comparing these findings with the conventional arrangement of optimised cascade process for the same capacity; about 2.8% and 22.2% reduction in the total compressor power and specific power (SP) are obtained respectively which indeed is a significant saving [104]. Therefore, this optimisation approached can be applied especially during the feasibility study of LNG plants.

7.2 Recommendations for future studies

Based on the conclusions in the previous section, several areas of improvement have been identified for future works which are as follows:

1. The optimisation of the cascade process should also include economic aspects to identify the feasibility of the proposed optimisation approach. For example, the exergy concept is combined with the engineering economy principles which is called thermoeconomics. This approach permits the actual cost sources at the equipment level to be recognized such as the capital, operating, maintenance costs and cost linked with the exergy loss [94].
2. The propane pre-cooling cycle can also be optimised by considering another type of refrigerant such as propylene instead of propane. The boiling point temperature at atmospheric pressure of propylene is -47.7^{o}C compared to propane which is -42^{o}C [102]. There is a possibility to reduce the cooling load of the ethylene refrigeration cycle as the propylene can cool the process gas down to -45^{o}C.
3. The effect of varying the pressure drop across the heat exchangers and distillation columns and changing the compressor polytropic efficiency are other parameters that need to be studied to investigate their effect on the process performance and efficiency.
4. Modelling the cascade process in another process simulation software such as SIMSCI Pro-II and comparing the results with Aspen HYSYS is another option to optimise the process efficiency.
5. Since the actual plant data that available is only limited to some unit operations, it is recommended to have actual plant data of an existing LNG plant that utilise this cascade process. The actual plant data can be used to develop a rating model. This rating model can be used to optimise the process ensuring the optimisation approaches do not violate the actual plant design. Besides, the information about the operating, capital, and maintenance costs can also be estimated.

Appendix A – Process simulation data

Chapter 4

Case 1: Heat balance of propane and process streams (NG, ethylene and methane) for propane pre-cooling cycle.

Propane enthalpy	Hin (MJ/kg)	Hout (MJ/kg)	Delta H (MJ/kg) [out-in]	Propane mass f.r (kg/h)	Propane duty (MW)
HP	-2.78	-2.40	0.38	370880.97	39.42
MP	-2.78	-2.41	0.38	57205.65	5.98
LP	-2.78	-2.44	0.34	1752235.15	167.84
					213.24
NG enthalpy	Delta H (MJ/kg) [out-in]	NG mass f.r (kg/h)	NG Duty (MW)	Total Q NG (MW)	
HP	-0.07	767835.43	-14.88	-53.88	
MP	-0.02	767835.43	-3.25		
LP	-0.17	767835.43	-35.75		
Ethylene enthalpy		C2H4 mass f.r (kg/h)	Ethylene Duty (MW)	Total C2H4 Q (MW)	
HP	-0.08	1074067.27	-24.54	-148.11	
MP	-0.01	1074067.27	-2.74		
LP	-0.40	1074067.27	-120.83		
Methane enthalpy		CH4 mass f.r (kg/h)	Methane Duty (MW)	Total CH4 Q (MW)	
LP	-0.08	521720.75	-11.25	-11.25	
			Total Q process side (MW)	-213.25	

Case 6: Heat balance of propane and process streams (NG, ethylene and methane) for propane pre-cooling cycle.

Propane enthalpy	Hin (MJ/kg)	Hout (MJ/kg)	Delta H (MJ/kg) [out-in]	Propane mass f.r (kg/h)	Propane duty (MW)
HP	-2.86	-2.44	0.42	1522573.60	176.20
MP	-2.86	-2.44	0.41	106809.07	12.21
LP	-2.86	-2.45	0.40	221735.54	24.92
					213.34
NG enthalpy	Delta H (MJ/kg) [out-in]	NG mass f.r (kg/h)	NG Duty (MW)	Total Q NG (MW)	
HP	-0.17	767835.43	-37.26	-53.88	
MP	-0.02	767835.43	-5.08		
LP	-0.05	767835.43	-11.53		
Ethylene enthalpy		C2H4 mass f.r (kg/h)	Ethylene Duty (MW)	Total C2H4 Q (MW)	
HP	-0.45	1075627.11	-133.43	-148.33	
MP	-0.02	1075627.11	-5.29		
LP	-0.03	1075627.11	-9.61		
Methane enthalpy		CH4 mass f.r (kg/h)	Methane Duty (MW)	Total CH4 Q (MW)	
HP	-0.04	522507.98	-5.51	-11.13	
MP	-0.01	522507.98	-1.84		
LP	-0.03	522507.98	-3.78		
			Total Q process side (MW)	-213.34	

Chapter 5

Configuration 1 (C1) - Heat balance of LNG and NGL integration using a compressor.

Propane enthalpy	Hin (MJ/kg)	Hout (MJ/kg)	Delta H (MJ/kg) [out-in]	Propane mass f.r (kg/h)	Propane duty (MW)
HP	-2.78	-2.40	0.38	361078.18	38.38
MP	-2.78	-2.41	0.38	56094.28	5.87
LP	-2.78	-2.44	0.34	1697460.99	162.59
					206.84
NG enthalpy	Delta H (MJ/kg) [out-in]	NG mass f.r (kg/h)	NG Duty (MW)	Total Q NG (MW)	
HP	-0.07	767835.43	-14.88	-53.88	
MP	-0.02	767835.43	-3.25		
LP	-0.17	767835.43	-35.75		
Ethylene		C2H4 mass f.r (kg/h)	Ethylene Duty (MW)	Total C2H4 Q (MW)	
HP	-0.08	1028469.95	-23.50	-141.82	
MP	-0.01	1028469.95	-2.62		
LP	-0.40	1028469.95	-115.70		
Methane		CH4 mass f.r (kg/h)	Methane Duty (MW)	Total CH4 Q (MW)	
LP	-0.08	520803.00	-11.13	-11.13	
			Total Q process side (MW)	-206.84	

Configuration 2 (C2) – Heat balance of LNG and NGL integration using a pump.

Propane enthalpy	Hin (MJ/kg)	Hout (MJ/kg)	Delta H (MJ/kg) [out-in]	Propane mass f.r (kg/h)	Propane duty (MW)
HP	-2.78	-2.40	0.38	351642.71	37.38
MP	-2.78	-2.41	0.38	55024.55	5.76
LP	-2.78	-2.44	0.34	1646879.91	157.74
					200.88
NG enthalpy	Delta H (MJ/kg) [out-in]	NG mass f.r (kg/h)	NG Duty (MW)	Total Q NG (MW)	
HP	-0.07	767835.43	-14.88	-53.88	
MP	-0.02	767835.43	-3.25		
LP	-0.17	767835.43	-35.75		
Ethylene		C2H4 mass f.r (kg/h)	Ethylene Duty (MW)	Total C2H4 Q (MW)	
HP	-0.08	984490.61	-22.50	-135.76	
MP	-0.01	984490.61	-2.51		
LP	-0.40	984490.61	-110.75		
Methane		CH4 mass f.r (kg/h)	Methane Duty (MW)	Total CH4 Q (MW)	
LP	-0.08	521631.30	-11.23	-11.23	
			Total Q process side (MW)	-200.86	

Heat balance for integrated LNG/NG process at De-C2 column pressure of 1800 kPa.

Ethylene enthalpy check	Hin (MJ/kg)	Hout (MJ/kg)	Delta H (MJ/kg) [out-in]	C2H4 mass f.r (kg/h)	C2H4 Q (MW)
C2H4 enthalpy					
MP	1.27	1.74	0.47	234112.16	30.65
LP	1.27	1.71	0.44	546379.27	66.49
				Total C2H4 (MW)	97.14
NG enthalpy	Delta H (MJ/kg) [out-in]	NG mass f.r (kg/h)	NG Duty (MW)	Total Q NG (MW)	
MP	-0.12	767835.43	-24.70	-36.63	
LP	-0.06	691911.32	-11.93		
Methane enthalpy					
MP	-0.04	521301.90	-5.95	-60.50	
LP	-0.38	521301.90	-54.56		
			Total Q process side (MW)	-97.14	

Heat balance for integrated LNG/NG process at De-C2 column pressure of 1900 kPa.

Ethylene enthalpy check	Hin (MJ/kg)	Hout (MJ/kg)	Delta H (MJ/kg) [out-in]	C2H4 mass f.r (kg/h)	C2H4 Q (MW)
C2H4 enthalpy					
MP	1.27	1.74	0.47	234112.16	30.65
LP	1.27	1.71	0.44	539869.77	65.69
				Total C2H4 (MW)	96.35
NG enthalpy	Delta H (MJ/kg) [out-in]	NG mass f.r (kg/h)	NG Duty (MW)	Total Q NG (MW)	
MP	-0.12	767835.43	-24.70	-35.84	
LP	-0.06	682838.02	-11.14		
Methane enthalpy	Delta H (MJ/kg) [out-in]	C1 mass f.r (kg/h)	C1 Duty (MW)	Total Q C1 (MW)	
MP	-0.04	521334.81	-5.95	-60.51	
LP	-0.38	521334.81	-54.56		
			Total Q process side (MW)	-96.35	

Heat balance for integrated LNG/NG process at De-C2 column pressure of 2000 kPa.

Ethylene enthalpy check	Hin (MJ/kg)	Hout (MJ/kg)	Delta H (MJ/kg) [out-in]	C2H4 mass f.r (kg/h)	C2H4 Q (MW)
C2H4 enthalpy					
MP	1.27	1.74	0.47	234112.16	30.65
LP	1.27	1.71	0.44	532712.59	64.82
				Total C2H4 (MW)	95.48
NG enthalpy	Delta H (MJ/kg) [out-in]	NG mass f.r (kg/h)	NG Duty (MW)	Total Q NG (MW)	
MP	-0.12	767835.43	-24.70	-34.94	
LP	-0.05	673139.96	-10.23		
Methane enthalpy	Delta H (MJ/kg) [out-in]	C1 mass f.r (kg/h)	C1 Duty (MW)	Total Q C1 (MW)	
MP	-0.04	521631.30	-5.95	-60.54	
LP	-0.38	521631.30	-54.59		
			Total Q process side (MW)	-95.48	

Heat balance for integrated LNG/NG process at De-C2 column pressure of 2100 kPa.

Ethylene enthalpy check	Hin (MJ/kg)	Hout (MJ/kg)	Delta H (MJ/kg) [out-in]	C2H4 mass f.r (kg/h)	C2H4 Q (MW)
C2H4 enthalpy					
MP	1.27	1.74	0.47	234112.16	30.65
LP	1.27	1.71	0.44	532997.56	64.86
				Total C2H4 (MW)	95.51
NG enthalpy	Delta H (MJ/kg) [out-in]	NG mass f.r (kg/h)	NG Duty (MW)	Total Q NG (MW)	
MP	-0.12	767835.43	-24.70	-34.99	
LP	-0.06	672242.64	-10.29		
Methane enthalpy	Delta H (MJ/kg) [out-in]	C1 mass f.r (kg/h)	C1 Duty (MW)	Total Q C1 (MW)	
MP	-0.04	521460.29	-5.95	-60.52	
LP	-0.38	521460.29	-54.57		
			Total Q process side (MW)	-95.51	

Heat balance for integrated LNG/NG process at De-C2 column pressure of 2200 kPa.

Ethylene enthalpy check	Hin (MJ/kg)	Hout (MJ/kg)	Delta H (MJ/kg) [out-in]	C2H4 mass f.r (kg/h)	C2H4 Q (MW)
C2H4 enthalpy					
MP	1.27	1.74	0.47	234112.16	30.65
LP	1.27	1.71	0.44	533181.37	64.88
				Total C2H4 (MW)	95.53
NG enthalpy	Delta H (MJ/kg) [out-in]	NG mass f.r (kg/h)	NG Duty (MW)	Total Q NG (MW)	
MP	-0.12	767835.43	-24.70	-35.03	
LP	-0.06	671284.62	-10.33		
Methane enthalpy					
MP	-0.04	521283.53	-5.95	-60.50	
LP	-0.38	521283.53	-54.55		
			Total Q process side (MW)	-95.53	

Appendix B – Published works

Journal of Natural Gas Science and Engineering 29 (2016) 125–133

Contents lists available at ScienceDirect

Journal of Natural Gas Science and Engineering

journal homepage: www.elsevier.com/locate/jngse

A case study: Application of energy and exergy analysis for enhancing the process efficiency of a three stage propane pre-cooling cycle of the cascade LNG process

Nazreen Begum Najibullah Khan [a, b, *], Ahmed Barifcani [a], Moses Tade [a], Vishnu Pareek [a]

[a] Department of Chemical Engineering, Curtin University of Technology, GPO Box U1987, Perth, Western Australia, 6001, Australia
[b] Faculty of Chemical Engineering and Natural Resources University Malaysia Pahang, Lebuhraya Tun Razak, 26300, Gambang, Kuantan, Pahang Darul Makmur, Malaysia

ARTICLE INFO

Article history:
Received 12 August 2015
Received in revised form
18 December 2015
Accepted 19 December 2015
Available online 25 December 2015

Keywords:
Propane pre-cooling
Exergy loss
Refrigeration
Cascade cycle
Energy enhancement

ABSTRACT

The propane pre-cooling cycle has been widely used in most LNG plants as the first cooling cycle in the natural gas liquefaction process. As LNG plants consume high amounts of energy, enhancements in the process design and plant operation will minimize the overall energy consumption of the plant. The aim of this study is to enhance the process efficiency of a three stage propane pre-cooling cycle of the Cascade LNG process for the large-scale LNG train by determining the optimal operating conditions of the propane evaporator that will minimize the overall energy consumption. Energy and exergy analysis methods are adopted to evaluate the process efficiency of the propane pre-cooling cycle. Six case studies were presented to determine the optimal operating conditions of the propane evaporator that gives maximum energy reduction. The propane pre-cooling cycle is modelled and simulated using Aspen HYSYS with detailed thermodynamic information obtained to calculate the exergy loss. The results of the energy and exergy analysis indicate that Case 6 gives the highest coefficient of performance (COP) and the maximum exergy efficiency compared to the baseline case, which are 15.51% and 18.76% respectively. The results indicate that by reducing the cooling duty at the intermediate stages of propane evaporator about 13.5% energy saving can be achieved compared to the baseline case.

© 2015 Elsevier B.V. All rights reserved.

1. Introduction

As the demand on LNG is drastically increasing and the discovery of new large gas fields is continuously taking place worldwide, the pace of change and development in LNG liquefaction technology is becoming more rapid than ever before. LNG production is estimated to hit 320 million tonnes per annum (MTPA) by 2015 and to 450 MTPA by 2020 as reported by Wood (Wood, 2012). In order to meet this escalating demand, most of the existing and new LNG plants are looking for opportunities to make a further increase in their LNG capacity and building larger LNG trains which will provide economic benefits and be process efficient. Since the 1970s, when the kick started for the LNG plant and until the present day, three main LNG processes have been applied in the LNG plants viz. Single mixed refrigerant (SMR), Propane precooled mixed refrigerant (C3MR) and cascade liquefaction process (Lim et al., 2013). In the last 10–15 years, the innovations of LNG technologies have drastically progressed whereby new LNG processes have been introduced such as Mixed fluid cascade (MFC), Air Products (AP-X™), Dual mixed refrigerant (DMR) and Parallel mixed refrigerant (PMR) (Castillo et al., 2010). Most of the existing LNG plants have three main cooling cycles, namely the pre-cooling, liquefying and sub-cooling cycle. Earlier LNG plants that employed the SMR process did not have the pre-cooling cycle, instead the natural gas was cooled directly to −160 °C using a single mixed refrigerant. The pre-cooling cycle is the first cycle in an LNG process which removes the heat from natural gas to a temperature range between −30 °C to −55 °C depending on the pre-cooling

Abbreviations: AC, air cooler; COP, coefficient of performance; EOS, equation of state; HP, high pressure; HX, heat exchanger; LNG, liquefied natural gas; LP, low pressure; MP, medium pressure; MTPA, million tonnes per annum; PR, Peng Robinson; UA, product of overall heat transfer coefficient and heat exchanger area; SP, specific power.

* Corresponding author. Department of Chemical Engineering, Curtin University, Bentley Campus, Perth, Western Australia, 6102, Australia
E-mail address: n.najibullahkhan@postgrad.curtin.edu.au (N.B. Najibullah Khan).

http://dx.doi.org/10.1016/j.jngse.2015.12.034
1875-5100/© 2015 Elsevier B.V. All rights reserved.

Nomenclature

E_x	exergy [MW]
$Ex_{HX,\ loss}$	exergy loss of heat exchanger [MW]
$Ex_{COMP,\ loss}$	exergy loss of compressor [MW]
$Ex_{v,\ loss}$	exergy loss of valve [MW]
$Ex_{MIX,\ loss}$	exergy loss of mixer [MW]
$Ex_{AC,\ loss}$	exergy loss of air cooler [MW]
e	specific exergy (MJ/kg)
H	enthalpy (MJ/kg)
n	mass flow rate [kg/s]
P	pressure [bar]
Q	refrigeration duty [MW]
S	entropy [MJ/kg K]
T_0	ambient temperature [K]
W	compressor power [MW]

Subscripts

f	fluid
i	inlet
o	outlet

Greek symbol

n_{ex}	exergy efficiency

List of symbols

C_2H_6	ethane
C_3H_8	propane
CH_4	methane
N_2	nitrogen

technology applied. As a result of technological advancement, the pre-cooling cycle can now be designed using either pure refrigerant or mixed refrigerant. Castillo et al. (Castillo et al., 2013) reported that 95% of the current LNG plants employ the pre-cooling cycle; 85% of which are dominated by propane refrigerant compared to mixed refrigerant.

Thermodynamic analysis has been widely used in the LNG plants to determine the sources and locations of the main process irreversibilities that occur within the process or are due to an individual unit operation. Energy analysis or the first law of thermodynamic method only indicates the energy conservation of the overall process which is measured using two parameters i.e. COP and specific power (SP). However, to locate the irreversibility that occurs within the unit operation of the process, the exergy analysis method is applied. These methods are widely applied by other scholars to evaluate the energy conversion process efficiency. Vatani et al. (Vatani et al., 2014), Kanoglu (Kanoglu, 2002), Cipolato, et al. (Cipolato et al., 2012), Al-Otaibi et al. (Al-Otaibi et al., 2004) and Mehrpooya et al. (Mehrpooya et al., 2006) applied the energy and exergy analysis methods for analysing the process efficiency of various LNG processes. In a nutshell, these methods are also widely used in some power plants as mentioned in the following references (Cihan et al., 2006; Aljundi, 2009; Kaushik et al., 2011).

Converting natural gas to liquid utilizes an extensive amount of energy. According to Alfadala et al. (Hasan et al., 2009), a typical base load LNG plant consumes about 5.5–6 kWh of energy per kgmole of LNG produced. An energy-efficient refrigeration system will enhance the plant operation and provide economic benefits (Lee et al., 2002). Several authors have discussed the area of enhancing the efficiency of the pre-cooling cycle. Paradowski et al. (Paradowski et al., 2004) discussed two operating parameters of the pre-cooling cycle in the C3MR process that can enhance the process efficiency plus debottleneck the existing LNG plant capacity to 5.5 MTPA. The pre-cooling temperature of the low pressure (LP) stage and the propane compressor speed were the operating parameters that were adjusted to meet the new capacity requirement.

Castillo et al. (Castillo and Dorao, 2013) studied suitable choices of refrigerants that are applicable for pre-cooling cycle by analysing the effects of various refrigerants (i.e. N_2, CH_4, C_2H_6, C_3H_8) on the compressor power using the Linde-Hampson process. It was found that compared to other refrigerants, propane has a higher specific refrigerant effect which makes it the preferred refrigerant to be used in the pre-cooling cycle. Ransbarger (Ransbarger, 2007) studied the comparison between three stage and four stage propane cycles for the cascade LNG process which resulted in a power reduction of 1%; nonetheless the economic evaluations did not justify the increased cost associated with the additional stage. Evolution in the design of the propane pre-cooling cycle has emerged in recent decades. In this context, various studies have been presented that were related to the enhancement of the efficiency of the propane cycle with respect to significant changes made in the process configuration. Mortazavi et al. (Mortazavi et al., 2012) suggested the replacement of the conventional expansion valves in the C3MR process with expanders to improve the liquefaction efficiency. In another study, Mortazavi, et al. (Mortazavi et al., 2010) investigated the usage of waste heat from gas turbines by installing absorption chillers in the propane cycle of the C3MR process. Kalinowski et al. (Kalinowski et al., 2009) proposed the replacement of the propane evaporator with an absorption refrigeration system utilizing waste heat from the electrical power generating gas turbines.

Although many studies have been conducted focussing on the efficiency enhancement of the LNG plants through modification of the process configuration (Kanoglu, 2002; Mortazavi et al., 2012, 2010; Kalinowski et al., 2009; Remeljej and Hoadley, 2006), there is only very scant information available which focuses on the operation perspective. In this study, we to analyse the impact of changing the operating conditions of the propane evaporator towards the energy consumption of the process. Six case studies are proposed with different operating conditions applied to the propane evaporator. The development of these case studies is discussed in Section 2.2 of the manuscript. The sensitivity of COP, specific power (SP), exergy loss and exergy efficiency are analysed for all case studies presented.

1.1. Description of propane pre-cooling cycle process

Treated feed gas enters the three stage propane cycles at 29 °C and 75 bar and is cooled to −40 °C. The propane evaporator (i.e. kettle type) also cools methane and condenses ethylene. Cooling of the process stream is achieved by the evaporation of propane in the pool on the shell side with the process streams flowing inside the immersed tubes. The propane compressor (i.e. centrifugal type) with side streams recovers the evaporated propane and compresses the vapour to 18 bar. Propane is finally condensed at 49 °C using the air cooler. The condensed propane is then recycled back to the propane evaporator. Fig. 1 shows the simplified process scheme of propane pre-cooling cycle.

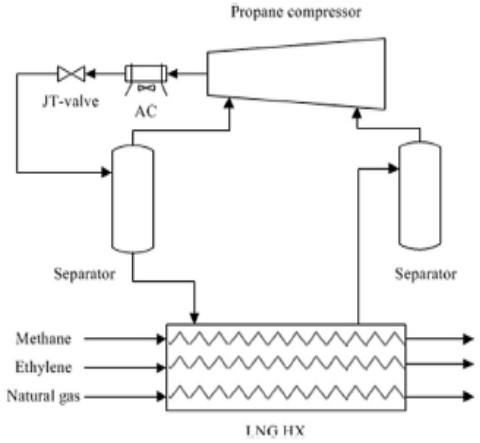

Fig. 1. Simplified process scheme of propane pre-cooling cycle. Only one stage is shown for simplicity.

2. Simulation method and modelling assumptions

Aspen HYSYS which is a steady state process modelling software was employed to model the three stage propane pre-cooling refrigeration cycles. Peng Robinson equation of state (PR-EOS) fluid package was used for modelling the property of the substances. This process simulator is well known for modelling the LNG processes and has been widely used by others (Hatcher et al., 2012; Khan et al., 2013; Aspelund et al., 2010; Cao et al., 2006). The feed gas composition and modelling assumptions are summarized in Tables 1 and 2 respectively.

The following are the constraints applied in modelling the propane pre-cooling cycle:

1. Temperature approach (T_{app}) in the LNG heat exchanger should be above 2 °C to prevent temperature cross.
2. The inlet temperature of propane compressor should be above its dew point temperature to safeguard the operation of the compressor.

2.1. Process simulation description

In this study, six case studies as shown in Table 3 have been studied with different operating conditions applied at each evaporator stage to analyse the performance of the propane pre-cooling cycle. The operating conditions of the propane evaporator is changed through an expansion valve that is located upstream of each evaporator (i.e. CV-1: HP stage; CV-2: MP stage and CV-3: LP stage) as depicted in Fig. 2. The expansion valve pressure is the key manipulated variable that is adjusted to obtain the desired cooling duty for each stage propane evaporator and also to maintain the temperature approach above 2 °C. Discharge pressure of LP and MP stage propane compressors is connected to the MP and HP propane evaporator stage respectively to obtain the resultant compressor power as shown in Figs. 2 and 3. Propane pre-cooling cycle configuration for the baseline case and case 6 are also shown in Figs. 2 and 3 respectively and changes made on the operating parameters are marked with dotted lines on these figures.

Table 1
Feed gas composition after sweetening.

Component[a]	Mole fraction
Nitrogen	0.0028
Methane	0.8974
Ethane	0.0496
Propane	0.0343
i-Butane	0.0079
n-Butane	0.0073
i-Pentane	0.0005
n-Pentane	0.0002
n-Hexane	0.0000
Total	1.0000

[a] Feed gas composition obtained from LNG plant located in Southeast Asia region.

Table 2
Modelling assumptions.

Natural gas temperature	29 °C
Natural gas pressure	75 bar
Natural gas flow rate	41,700 kgmole/h
Compressor polytropic efficiency	80%
Pressure drop in LNG heat exchanger	0.2 bar
Pressure drop in air cool heat exchanger	0.3 bar
Minimum temperature approach in heat exchanger	>2 °C
Ambient temperature	27 °C
Air cooler exit temperature	49 °C

Table 3
Propane evaporator operating conditions for all case studies.

Case studies	Propane evaporator operating conditions
Case 1[a]	−25 °C, −30 °C, −40 °C
Case 2	−15 °C, −20 °C, −40 °C
Case 3	−10 °C, −15 °C, −40 °C
Case 3	−5 °C, −10 °C, −40 °C
Case 5	0 °C, −5 °C, −40 °C
Case 6	5 °C, 0 °C, −40 °C

[a] (−25 °C, −30 °C, −40 °C means process exit temperature at HP, MP and LP stage respectively).

2.2. Case studies development of propane pre-cooling cycle

These six case studies were derived by analysing various operating conditions of current LNG plants located in Southeast Asia region, Australia and also based on the information available from the literature (Kanoglu, 2002; Paradowski et al., 2004; Castillo and Dorao, 2013; Ransbarger, 2007; Mortazavi et al., 2012, 2010; Kalinowski et al., 2009; Remeljej and Hoadley, 2006; Helgestad, 2009). Fig. 4 illustrates the development of the propane pre-cooling cycle case studies.

Case studies presented are defined as follows:

Case 1: Baseline case (i.e. higher cooling duty at the intermediate stages (i.e. HP and MP stage)).

Case 6: (i.e. lower cooling duty at intermediate stages).

3. Energy analysis

Energy consumption and process efficiency of the overall process are determined through energy analysis. This method has two quantitative parameters; COP and SP. COP is a standard criterion applied in evaluating the efficiency of a cryogenic system. It is defined as the ratio of total heat removed by refrigerant to the amount of power required by the system (Eq. (1)) while SP is defined as total power consumption per unit mass of LNG (Eq. (2)).

$$COP = Q/W \quad (1)$$

$$SP(MWh/\text{tonne LNG}) = \sum W_{req} \Big/ \dot{m}_{LNG} \quad (2)$$

where the nomenclature for the above equations are as follows: Q is

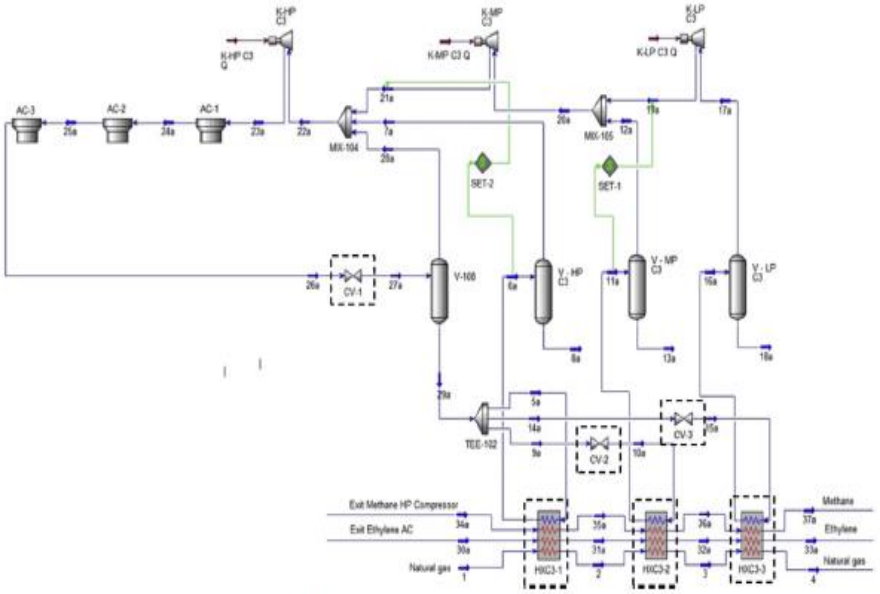

Fig. 2. Propane pre-cooling cycle Case 1 configuration.

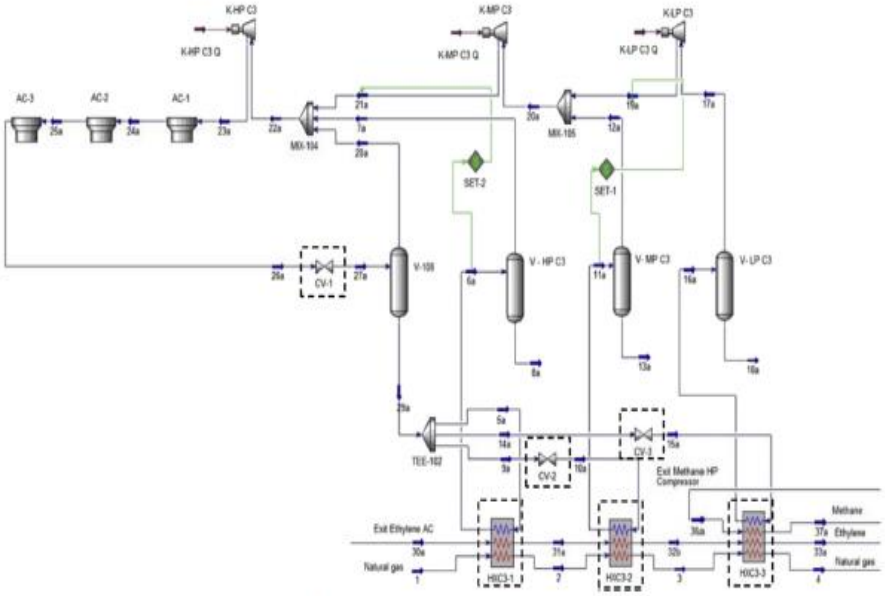

Fig. 3. Propane pre-cooling cycle Case 6 configuration.

refrigeration duty (MW); W is compressor power (MW), ΣW_{req} is the total compressor power required (MW) and $\dot{m}_{LNG}$ is the amount of LNG produced in tonne/h.

3.1. Exergy analysis

In this study, exergy analysis is applied to locate the irreversibility that occurs within the unit operations of the propane pre-cooling cycle. This method identifies the individual unit operation that exhibits a higher amount of lost work which gives the process engineer valuable information for improving the process from the equipment and process design point of view. Exergy which is derived from the second law of thermodynamics is defined as the amount of reversible work achieved by a system when the system components are brought into thermodynamic equilibrium state with its environment in a reversible process (Szargut, 1980). The exergy change of a system is a function of two main parameters which are the enthalpy and entropy. Change in exergy (ΔEx) between the initial and the final state of a system is expressed as:

$$\Delta E_X = (H_o - H_i) - T_o(S_o - S_i) \quad (3)$$

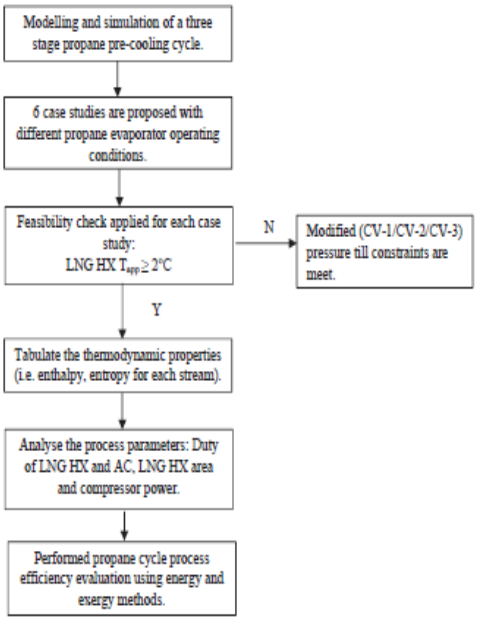

Fig. 4. Development of propane pre-cooling cycle case studies.

where T_o is the ambient temperature, H_o and S_o represent the enthalpy and entropy of the outlet stream and H_i and S_i represent the enthalpy and entropy of the inlet stream respectively. The difference of this property will define whether the processing system requires or produces work as the systems moves from initial state to final state. If the exergy difference (ΔE_x) is greater than 0, this indicates that the processing system produces work, whereas if the exergy difference is less than 0, this indicates the processing system requires work from the outer system for the state change (Xu et al., 2013).

The exergy efficiency of the process is defined as the ratio of the difference between the total compressor power required and the total exergy loss to the total amount of power required by the system (Eq. (4)). The exergy efficiency is expressed as:

$$\eta_{ex}(\%) = \left(\frac{\sum W_{req} - \sum W_{loss}}{\sum W_{req}}\right) \times 100 \quad [6] \qquad (4)$$

where ΣW_{loss} is the total exergy loss work from each unit operation.

The expressions to determine the exergy loss for all the unit operations in this study are summarized in Table 4.

In the above equations, $\dot{m}$ is the mass flow rate of propane at the inlet stream (kg/s), W is the compressor power (MW), S is the entropy (MJ/kg K), $\dot{m}_a$ is the mass flow rate of air (kg/s) and e is the specific exergy (MJ/kg) for the respective stream.

Thermodynamic analysis comprising of the first and second law is used in this study to overcome the limitations of the deterministic optimization method i.e. a numerical approach which excludes the uncertainty changes involved in the design process, hence it is not considered as the best option for many actual engineering problems (Mokhatab, 2013). Additionally, the optimization result obtained using this method causes ambiguity because it is not embedded with any process knowledge (i.e. enthalpy and entropy) (Khan et al., 2013). Knowing these important process parameters for each process stream provides a better understanding of the changes occurring within the process. Hence, necessary adjustment can be done on the operating parameter to improve the process performance.

Table 4
Exergy loss calculation of various unit operations in propane cycle.

LNG heat	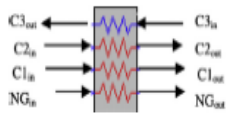	$Ex_{HX,loss} = \dot{m} \sum ex_i - ex_o$
Compressor	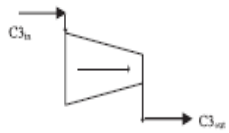	$Ex_{COMP,loss} = \dot{m}(ex_i - ex_o) - W$
Valves	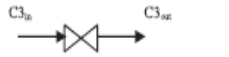	$Ex_{V,loss} = \dot{m} T_o(S_o - S_i), h_i = h_o$
Mixer		$Ex_{MIX,loss} = \dot{m}_1 e_1 + \dot{m}_2 e_2 = \dot{m}_3 e_3$
Air cooler	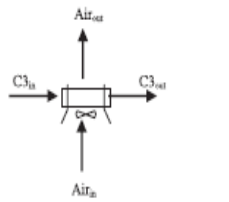	$Ex_{AC,loss} = (\dot{m}_f e_f + \dot{m}_a e_a)_i - (\dot{m}_f e_f + \dot{m}_a e_a)_o$

4. Results and discussion

Operating conditions of the baseline (Case 1) and Case 6 are summarized in Table 5. The effect of different operating conditions at each evaporator stage on the heat exchangers, compressors and air coolers are discussed in the Section 4.1.

4.1. Results of different operating conditions of propane evaporator on the process parameters

A simple and practical way of minimizing the energy consumption of a process is by adjusting the operating conditions of it. Based on the case studies presented, different propane evaporator operating conditions affect the overall energy consumption of the process. As depicted in Fig. 5, Case 6 consumes the lowest compression power and air cooler duty which are 129.36 MW and 342.60 MW respectively compared to the baseline case. This can be translated into an energy saving of 13.5% and 5.57% for the compressor power and air cooler duty respectively. Meanwhile, as can be seen in Fig. 6, the total propane flow rate of Case 6 is also reduced by 8.6% compared to the baseline case. Though, the overall duty of the propane evaporator remains constant, having a greater cooling duty at the intermediate stages of propane evaporator results in the increased of power consumption, air cooler duty and propane flow rate which reduces the process efficiency.

Distribution of the propane evaporator duty at each stage and its total area required for all case studies are reported in Fig. 7 and Table 6. As can be seen in Fig. 7, the cooling duty is transferred from the HP stage to the LP stage of propane evaporator (i.e. Case 1 to Case 6). Duty of the propane evaporator is determined using (Eq. (5)). Rearranging (Eq. (5)) gives (Eq. (6)) which is used to determine the propane evaporator area. The overall heat transfer coefficient (U) for propane refrigeration cycles was taken as an average value of 425 W/(m^2 K) (Campbell, 2004). Based on this U value, the propane evaporator area for each case was determined. As shown in Table 6, Case 6 gives the lowest propane evaporator area for the same cooling duty which is 46.89% lower compared to the baseline case (Case 1). This indicates that increasing the cooling duty at the intermediate stages of the propane evaporator results in the increased of the total propane evaporator area.

$$Q = UA\Delta T_{LMTD} \tag{5}$$

$$\text{Whereby } A = Q/(U \cdot \Delta T_{LMTD}) \tag{6}$$

Q = Duty of propane evaporator (MW)
U = Overall heat transfer coefficient (MW/m^2 K)
ΔT_{LMTD} = log min temperature difference (K)
A = propane evaporator area (m^2)

Table 5
Operating conditions of each stream in propane refrigeration cycle.

	(Case 1)				Case 6			
Stream no	x	T (°C)	P (bar)	S (kJ/kg K)	x	T (°C)	P (bar)	S (kJ/kg K)
1	1	29	75	7.98	1	29	75	7.98
2	0.99	−25	74.80	7.34	1	5	74.80	7.74
3	0.98	−30	74.60	7.25	1	0	74.60	7.69
4	0.92	−40	74.40	7.02	0.92	−40	74.40	7.02
5a	0	−27.49	1.85	1.56	0	2.12	5.05	1.84
6a	1	−23	1.85	3.26	1	7	5.05	3.23
7a	1	−23	1.85	3.26	1	7	5.05	3.23
8a	0	−23	1.85	1.60	0	7	5.05	1.88
9a	0	−27.49	1.85	1.56	0	2.12	5.05	1.84
10a	0.02	−32.34	1.53	1.56	0.03	−2.96	4.32	1.84
11a	1	−27	1.53	3.27	1	2	4.32	3.23
12a	1	−27	1.53	3.27	1	2	4.32	3.23
13a	0	−27	1.53	1.57	0	2	4.32	1.84
14a	0	−27.49	1.85	1.56	0	2.12	5.05	1.84
15a	0.07	−42.19	1.01	1.57	0.24	−42.19	1.01	1.88
16a	1	−33	1.01	3.32	1	−25	1.01	3.37
17a	1	−33	1.01	3.32	1	−25	1.01	3.37
18a	0	−33	1.01	1.57	0	−25	1.01	1.59
19a	1	−16.34	1.53	3.34	1	35.95	4.32	3.43
20a	1	−19.77	1.53	3.32	1	34.91	4.32	3.43
21a	1	−11.98	1.85	3.33	1	41.83	5.05	3.43
22a	1	−24.25	1.85	3.25	1	24.18	5.05	3.33
23a	1	79.88	18	3.35	1	85.16	18	3.38
24a	1	70	17.70	3.29	1	70	17.70	3.29
25a	1	60	17.40	3.23	1	60	17.40	3.23
26a	0	49	17.10	2.28	0	49	17.10	2.28
27a	0.50	−27.48	1.85	2.40	0.35	2.12	5.05	2.32
28a	1	−27.48	1.85	3.23	1	2.12	5.05	3.20
29a	0	−27.48	1.85	1.56	0	2.12	5.05	1.84
30a	1	49	24.10	5.38	1	49	24.10	5.38
31a	0	−25	23.90	3.67	1	5	23.90	5.11
32a	0	−30	23.70	3.60	1	0	23.70	5.08
33a	0	−40	23.50	3.46	0	−40	23.50	3.46
34a[a]	1	−10.01	36.50	9.17	–	–	–	–
35a[b]	1	−25	36.30	9.02	–	–	–	–
36a	1	−30	36.10	8.97	1.00	−9.97	36.50	9.17
37a	1	−40	35.90	8.86	1	−40	36.30	8.86

[a,b] There is no stream data for case 6 due to the exit temperature of methane stream is −9.97 °C and the cooling range for case 6 is (5 °C, 0 °C, −40 °C). Therefore methane stream enters HXC3-3. Refer to Fig. 4 for the configuration.

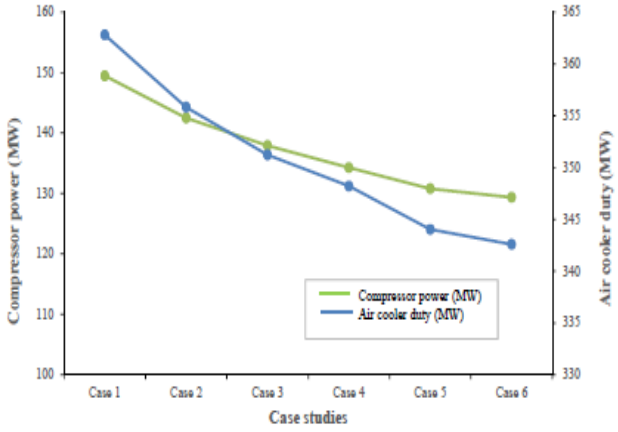

Fig. 5. Effect of different operating conditions of propane evaporator on compressor power and air cooler duty.

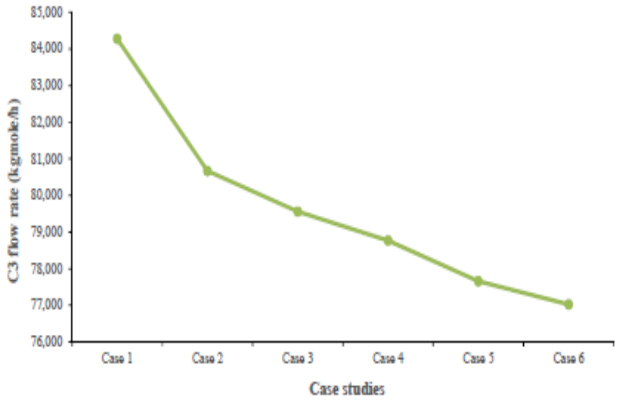

Fig. 6. Effect of different operating conditions of propane evaporator on propane flow rate.

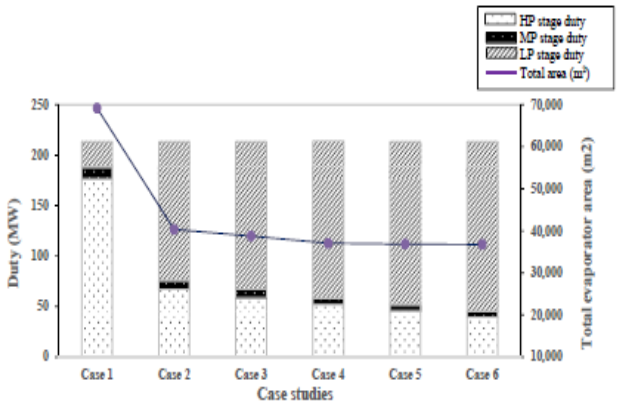

Fig. 7. Effect of different operating conditions of propane evaporator on its duty and total area.

4.2. Sensitivity analysis of propane pre-cooling cycle

In this study, the sensitivity of COP, SP, exergy loss and exergy efficiency of the propane pre-cooling cycle were analysed with respect to different operating conditions of the propane evaporator. Effect of different evaporator operating conditions on COP and SP are presented in Fig. 8. The exergy loss and exergy efficiency results are shown in Table 7 and Fig. 9.

As can be seen in Fig. 8, the COP of Case 6 increases by 15.51% while the SP reduces by 13.5% in comparison to the baseline case

Table 6
Propane evaporator duty for each stage and its total area for all case studies.

	Case 1	Case 2	Case 3	Case 4	Case 5	Case 6
Duty (MW)						
HP	176.20	67.34	58.65	52.19	45.64	39.42
MP	12.21	8.72	8.36	6.33	6.13	5.98
LP	24.92	137.28	146.27	155.46	161.47	167.84
Total area (m^2)	69,183.61	40,320.54	38,753.54	37,047.88	36,826.10	36,746.38

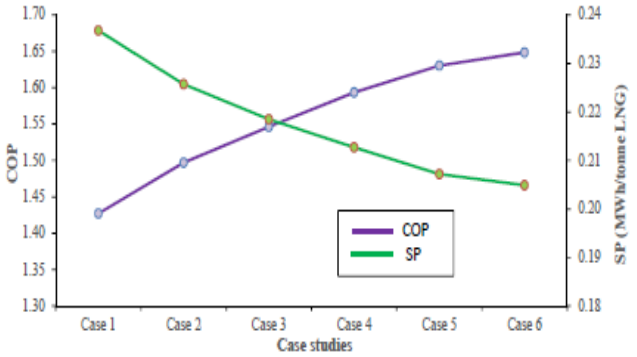

Fig. 8. Effect of different operating conditions of propane evaporator on COP and SP.

Table 7
Exergy loss of each unit operation in propane cycle and exergy efficiency (%).

Exergy loss (MW)	Case 1	Case 2	Case 3	Case 4	Case 5	Case 6
Heat exchangers	16.63	20.34	20.01	20.02	19.78	20.00
Compressors	30.89	28.55	27.45	26.56	25.73	25.35
Valves	38.52	28.62	25.66	22.90	20.69	19.37
Air coolers	12.74	12.20	13.08	11.61	11.77	11.49
Mixer	0.08	0.76	0.85	0.96	1.04	1.11
η_{ex}(%)	33.87	36.52	36.89	38.90	39.58	40.22

(case 1). Based on the above observation, the required shaft power can be minimized by reducing the cooling duty at the intermediate stages of the propane evaporator. Variation of the cooling duty in the propane evaporator is achieved by manipulation of the expansion valve which is located prior to each stage.

Exergy loss for each unit operation in the propane pre-cooling cycle was determined using the equations as presented in Table 4. As shown in Table 7, the valves, compressors and heat exchangers were identified as the primary contributors to the exergy loss in the propane cycle. For the baseline case (Case 1), the valves allocated the highest exergy loss, 38.52%, followed by the compressors, 30.89% and the heat exchangers, 16.63%. Valves provided the highest exergy loss in the baseline case due to increase in entropy generation when larger pressure drop is applied across the system. Compressors are the second contributor in exergy loss due to the increase in power demand when increase in cooling duty occurred at the intermediate stages. However, for all other case studies the exergy loss across the other components reduced marginally when a lower cooling duty was applied at the intermediate stages. The exergy efficiency of Case 1 is the lowest (33.87%) which indicates that larger irreversibilities occur within the process. Case 6 shows the highest exergy efficiency (40.22%) which indicates high potential improvement of the process. Based on Fig. 9, the total exergy loss decreases by 21.78% for Case 6 compared to the baseline case which improved the overall process efficiency. From the results it can be deduced that change in the operating conditions of the propane evaporator results in a lower entropy generation which

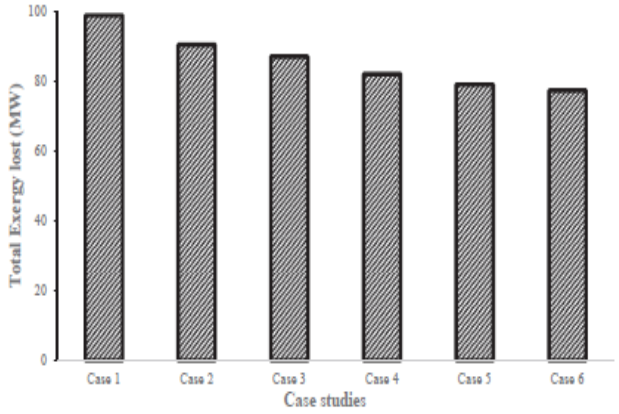

Fig. 9. Total exergy loss for each case studies.

reduces the exergy loss and increases the exergy efficiency. Exergy loss is influenced by larger temperature or pressure difference applied across the refrigerant stream and not by the number of equipment used in the propane cycle (Yoon et al., 2014).

Based on the exergy analysis, it can be concluded that both the valves and the compressors are the main contributors of exergy loss. These unit operations can be improved by replacing the existing JT valves with two phase expanders (Mortazavi et al., 2012) or by using a higher efficiency compressor (He and Ju, 2014). Nevertheless, the reduction in the energy consumption by installing these new components should be economically assessed to determine its feasibility.

5. Conclusion

In this study, enhancement in the process efficiency of a three stage propane pre-cooling cycle was studied using energy and exergy analysis. The results shows that Case 6 achieves the highest COP (1.65), lowest SP (0.205 MWh/tonne of LNG) and highest exergy efficiency (40.22%) due to low cooling duty distribution at the intermediate stages. Energy and exergy analysis can be a useful guide in enhancing the process efficiency of the existing LNG plant and also as a reference for future greenfield LNG projects. Changing the operating conditions of propane evaporator stage can be considered as an option to minimize energy consumption of the process which does not involve any additional cost. Additionally, this enhancement not only reduces the propane compression power but also reduces the size of the heat exchanger as well as the refrigeration rate. Reducing energy consumption leads to smaller equipment sizes which generally reduce the capital and operating costs of the LNG plants.

6. Recommendations

In this study, no consideration is made from economic point of view. As this process is considered as licenced processed, cost related to the proprietary equipment such as compressor and heat exchanger are treated confidential. Thus, the detailed breakdowns on the equipment size, price, licencing fees are not available. Therefore, future work is to be considered which simultaneously provide the trade-off between the capital and operating cost of the plant with exergy analysis.

Acknowledgement

The authors wish to acknowledge the Ministry of Education (MOE) of Malaysia and University Malaysia Pahang for funding the presented study. The authors also wish to acknowledge the support provided by staff from Curtin University, Australia.

References

Al-Otaibi, D.A., Dincer, I., Kalyon, M., 2004. Thermoeconomic optimization of vapor-compression refrigeration systems. Int. Commun. Heat Mass Transf. 31, 95–107.
Aljundi, I.H., 2009. Energy and exergy analysis of a steam power plant in Jordan. Appl. Therm. Eng. 29, 324–328.
Aspelund, A., Gundersen, T., Myklebust, J., Nowak, M.P., Tomasgard, A., 2010. An optimization-simulation model for a simple LNG process. Comput. Chem. Eng. 34, 1606–1617.
Campbell, J.M., 2004. Gas Conditioning and Processing : Volume 2, The Equipment Modules/by John M. Campbell, eighth ed. John M. Campbell and Company, Norman, Oklahoma.
Cao, W.-s., Lu, X.-s., Lin, W.-s., Gu, A.-z., 2006. Parameter comparison of two small-scale natural gas liquefaction processes in skid-mounted packages. Appl. Therm. Eng. 26, 898–904.
Castillo, L., Dorao, C.A., 2013. On the conceptual design of pre-cooling stage of LNG plants using propane or an ethane/propane mixture. Energy Convers. Manag. 65, 140–146.
Castillo, L., Nadales, R., González, C., Dorao, C., Viloria, A., 2010. Technology selection for liquefied natural gas (LNG) on base-load plants. In: Jornadas de Investigación de la Facultad de Ingeniería (JIFI). Universidad Central de Venezuela.
Castillo, L., Majzoub Dahouk, M., Di Scipio, S., Dorao, C.A., 2013. Conceptual analysis of the precooling stage for LNG processes. Energy Convers. Manag. 66, 41–47.
Cihan, A., Hacihafizoğlu, O., Kahveci, K., 2006. Energy–exergy analysis and modernization suggestions for a combined-cycle power plant. Int. J. Energy Res. 30, 115–126.
Cipolato, L., Lirani, M.C.A., Costa, T.V., Fábrega, E.M., d'Angelo, J.V.H., 2012. Exergetic Optimization of a Refrigeration Cycle for Natural Gas Liquefaction, vol. 31, pp. 440–444.
Hasan, M.M.F., Karimi, I.A., Alfadala, H.E., 2009. Optimizing compressor operation in an LNG plant. In: Alfadala, H., Reklaitis, G.V.R., El-Halwagi, M.M. (Eds.), Proceedings of the 1st Annual Gas Processing Symposium. Elsevier, Amsterdam.
Hatcher, P., Khalilpour, R., Abbas, A., 2012. Optimisation of LNG mixed-refrigerant processes considering operation and design objectives. Comput. Chem. Eng. 41, 123–133.
He, T., Ju, Y., 2014. Design and optimization of a novel mixed refrigerant cycle integrated with NGL recovery process for small-scale LNG plant. Ind. Eng. Chem. Res. 53, 5545–5553.
Helgestad, D.-E., 2009. Modelling and optimization of the C3MR process for liquefaction of natural gas. Process Syst. Eng. 44.
Kalinowski, P., Hwang, Y., Radermacher, R., Al Hashimi, S., Rodgers, P., 2009. Application of waste heat powered absorption refrigeration system to the LNG recovery process. Int. J. Refrig. 32, 687–694.
Kanoglu, M., 2002. Exergy analysis of multistage cascade refrigeration cycle used for natural gas liquefaction. Int. J. Energy Res. 26, 763–774.
Kaushik, S.C., Reddy, V.S., Tyagi, S.K., 2011. Energy and exergy analyses of thermal power plants: a review. Renew. Sustain. Energy Rev. 15, 1857–1872.
Khan, M.S., Lee, S., Rangaiah, G.P., Lee, M., 2013. Knowledge based decision making method for the selection of mixed refrigerant systems for energy efficient LNG processes. Appl. Energy 111, 1018–1031.
Lee, G., Smith, R., Zhu, X., 2002. Optimal synthesis of mixed-refrigerant systems for low-temperature processes. Ind. Eng. Chem. Res. 41, 5016–5028.
Lim, W., Choi, K., Moon, I., 2013. Current status and perspectives of liquefied natural Gas (LNG) plant design. Ind. Eng. Chem. Res. 52, 3065–3088.
Mehrpooya, M., Jarrahian, A., Pishvaie, M.R., 2006. Simulation and exergy-method analysis of an industrial refrigeration cycle used in NGL recovery units. Int. J. Energy Res. 30, 1336–1351.
Mokhatab, S., 2013. Handbook of Liquefied Natural Gas. Elsevier Science, Burlington.
Mortazavi, A., Somers, C., Alabdulkarem, A., Hwang, Y., Radermacher, R., 2010. Enhancement of APCI cycle efficiency with absorption chillers. Energy 35, 3877–3882.
Mortazavi, A., Somers, C., Hwang, Y., Radermacher, R., Rodgers, P., Al-Hashimi, S., 2012. Performance enhancement of propane pre-cooled mixed refrigerant LNG plant. Appl. Energy 93, 125–131.
Paradowski, H., Bamba, M., Bladanet, C., 2004. Propane precooling cycles for increased LNG train capacity. In: 14th International Conference and Exhibitions on Liquefied Natutal Gas Doha, Qatar 21-24 March, pp. 1–18.
Ransbarger, W., 2007. A fresh look at LNG process efficiency. LNG Ind. 1–6.
Remeljej, C., Hoadley, A., 2006. An exergy analysis of small-scale liquefied natural gas (LNG) liquefaction processes. Energy 31, 2005–2019.
Szargut, J., 1980. International progress in second law. Anal. Energy 5, 709–718.
Vatani, A., Mehrpooya, M., Palizdar, A., 2014. Energy and exergy analyses of five conventional liquefied natural gas processes. Int. J. Energy Res. 1843–1863.
Wood, D.A., 2012. A review and outlook for the global LNG trade. J. Nat. Gas Sci. Eng. 9, 16–27.
Xu, X., Liu, J., Jiang, C., Cao, L., 2013. The correlation between mixed refrigerant composition and ambient conditions in the PRICO LNG process. Appl. Energy 102, 1127–1136.
Yoon, J.-I., Choi, K.-H., Lee, H.-S., Kim, H.-J., Son, C.-H., 2014. Assessment of the performance of a natural gas liquefaction cycle using natural refrigerants. Heat Mass Transf. 51, 95–105.

The APPEA Journal 2016, 56, 606
https://doi.org/10.1071/AJ15112

Extended abstract

Exergy analysis of an ethylene refrigeration cycle integrated with a NGL recovery process for a large LNG train

Nazreen Begum Najibullah Khan[A,B], Ahmed Barifcani[A,C], Moses Tade[A] and Vishnu Pareek[A]

[A]Curtin University.
[B]University Malaysia Pahang.
[C]Department of Petroleum Engineering.

Abstract. The natural gas liquefaction process consists of a sequence of refrigeration cycles that consumes a considerable amount of energy. The separation of natural gas (NG) from the natural gas liquids (NGL) is considered to be one of the significant parts in the liquefaction of natural gas, as this will influence the LNG product quality. The integration of NGL section with the liquefaction process is one of the fundamental ways to improve the efficiency of the process and provide economic benefit from operating and capital cost perspectives.

In this extended abstract, two different configurations of NGL section integrated with the ethylene refrigeration cycle for the Cascade LNG plant—processing 5 million tonnes per annum (MTPA)—are proposed. The objectives of the proposed concepts are to meet the LNG higher heating value (HHV) specification and to achieve minimum power consumption for the refrigeration cycle. Exergy analysis is used as a thermodynamic tool to evaluate the efficiency of the process.

The process was simulated using Aspen HYSYS and the results of the proposed configurations are presented and analysed. The proposed configurations can be used to produce LNG and NGL with minimum energy consumption.

Introduction

The history of liquefied natural gas (LNG) plants started more than five decades ago, whereby the first LNG plant that was built in Kenai, Alaska, used a cascade LNG process. In the earlier design of LNG plants, the natural gas liquids (NGL) units were built upstream of the liquefaction unit and there was no integration between these two units (Elliot *et al.* 2005). As the demand of building larger and process efficient LNG plants is increasing drastically (Spilsbury *et al.* 2005), many of the LNG process licensers such as Air Products (APCI), ConocoPhilips (COP) and Shell have developed various integrated processes. For example, Conoco Philips, has applied this integrated concept to three of the LNG plants that resulted in about 7% increase in the LNG production for the same required power (Elliot *et al.* 2005). Fluor Technologies reported that a 10% energy saving is obtained by the integration of LNG and NGL processes (Brostow and Roberts, 2013).

In a standalone LNG plant, the required refrigerant such as propane is obtained from external cycles and separate heat exchangers, while in the integrated processes, the required refrigerant is obtained from joint refrigeration cycles and shared devices (Mehrpooya *et al.* 2014). In addition, there are other advantages of these integrated processes such as reduction in the capital and operating cost of the plant, elimination of combined emissions of carbon dioxide (CO_2) and nitrogen oxides (NO_x), improvement of the overall thermodynamic process efficiency, and it can assist in meeting the higher heating value (HHV) specification (Elliot *et al.* 2005; Spilsbury *et al.* 2005). In another study, NGL facilities have been introduced at LNG receiving terminals to meet stringent HHV specifications set by the local stakeholders (Cho *et al.* 2005). Hence, having integrated LNG and NGL facilities will provide flexibility in meeting the HHV requirement, and improve the process efficiency of the plant as well as provide economic benefits.

In this study, two different configurations of integrated LNG and NGL processes for a cascade LNG process are proposed. The desired LNG capacity for this study is five million tonnes per annum (MTPA). The aim of this study is to evaluate which configuration meets the required HHV specification and gives minimum power consumption. The process efficiency of these configurations is evaluated using the exergy method, which will be further explained in the methodology section of this extended abstract.

Journal compilation © APPEA 2016

Process description of the integrated LNG and NGL configurations

The separation of heavies' hydrocarbon or NGL are performed in the ethylene refrigeration cycle. This cycle is considered the key section of the cascade LNG process whereby ethylene (C_2H_4) is used to liquefy the natural gas and condenses the methane refrigerant. The separation of natural gas from the NGL is performed using a demethaniser column that operated at 34 bar. The bottom product from the demethaniser column (i.e. NGL) is fed to the deethaniser column at 20 bar. The top product from the deethaniser column is mixed with the top product from the demethaniser column and is further cooled to –95°C using ethylene refrigerant. The separation of methane from NGL components using ethylene refrigeration cycle will determine the final HHV specification of the LNG product.

Configuration 1: The deethaniser column overhead is operated as a partial condenser, the top vapour product is compressed to 33.8 bar and mixed with the top product stream of demethaniser column, and the liquid ethane is recovered as product. Figure 1 represents the simple embodiment of LNG and NGL integration using a compressor.

Configuration 2: The deethaniser column overhead is operated as a total condenser, liquid ethane is split into two streams. The first portion of liquid ethane is pumped to 33.8 bar and mixed with the top product stream of demethaniser column. The second portion of liquid ethane is recovered as product. Figure 2 represents the simple embodiment of LNG and NGL integration using a pump.

Methodology

In this study, a commercial process simulation software—ASPEN HYSYS—is used to simulate the LNG and NGL processes, and the Peng Robinson equation of state (EOS) was used to determine the physiochemical properties of the natural gas substances. The required HHV for this process is 1,050–1,125 Btu/scf. The operating conditions of the process remained unchanged so that the effect of the changes made in the process configurations towards the power consumption and in meeting the HHV requirement can be analysed. The following are the modelling assumptions applied in this study: adiabatic efficiency of the pump is 85%, and compressors polytropic efficiency is 80%. All compressors are assumed to be centrifugal type.

Exergy, which is derived from the second law of thermodynamics, is defined as the maximum theoretical work achievable by a system when the system is brought into equilibrium state with the environment (Moran 2011). Exergy analysis is a useful method applied in evaluating the performance

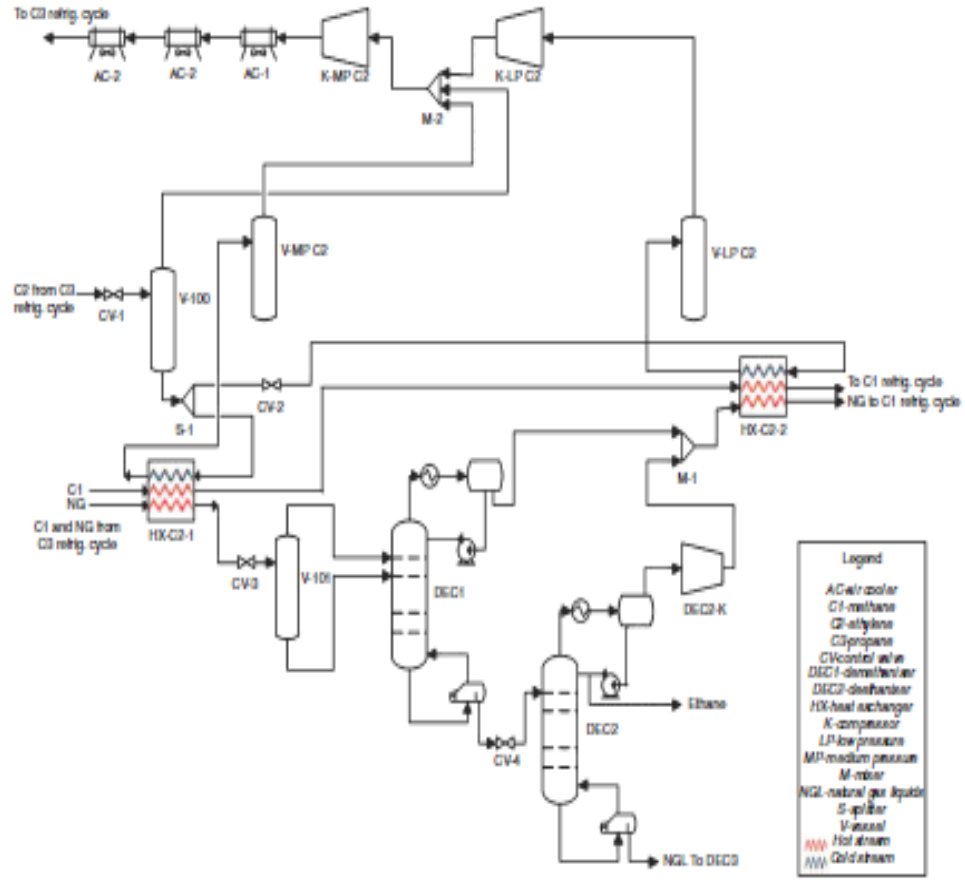

Figure 1. Configuration 1.

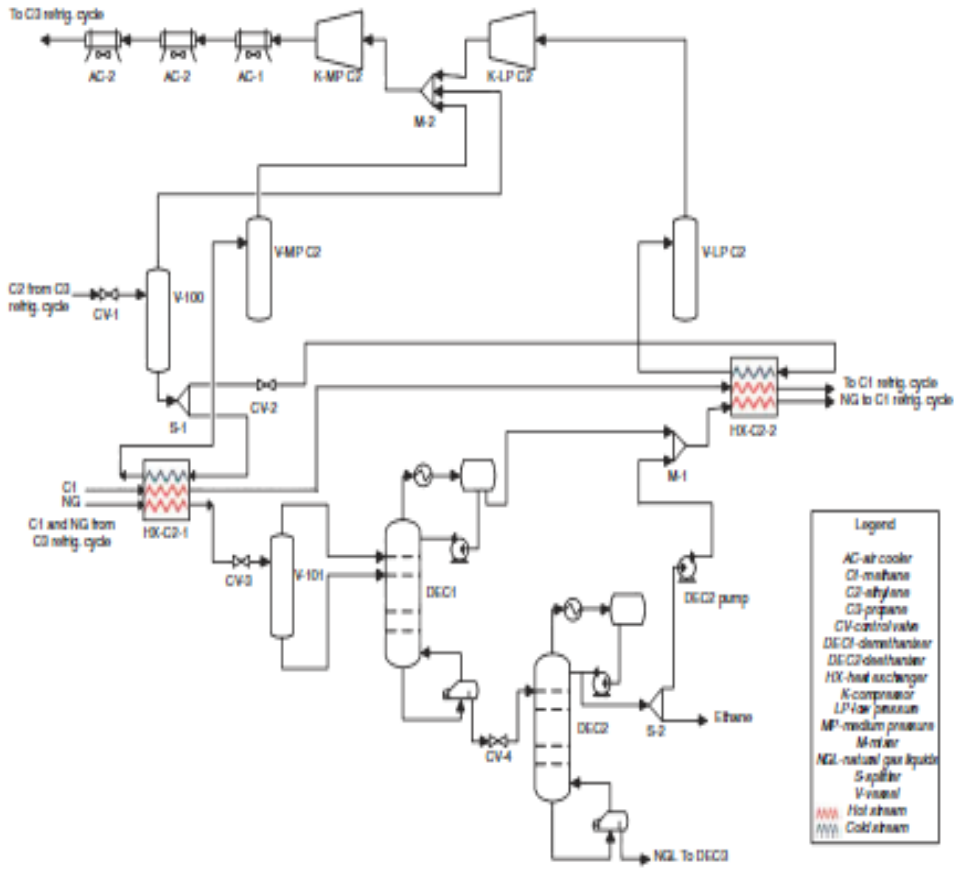

Figure 2. Configuration 2.

of the energy systems and chemical processes, optimisation and also for improving the process design (Kanoglu 2002).

The exergy analysis is performed by obtaining the exergy loss from the following equipment; namely heat exchangers, compressors, valves, air coolers and mixers. Exergy loss for each piece of equipment is calculated using Equation 1.

$$\Delta Ex = (H - T_o S)_{state2} - (H - T_o S)_{state1} \qquad (1)$$

In Equation 1, ΔEx is the change of exergy loss from state 2 to state 1, H is the enthalpy (MJ/kg), T_o is the ambient temperature (K), and S is the entropy (MJ/kgK).

Process efficiency of both configurations is evaluated by determining the exergy efficiency. Exergy efficiency can be defined as Equation 2:

$$\eta_{ex}(\%) = \frac{(\Sigma W_{req} - \Sigma W_{loss})}{\Sigma W_{req}} \times 100 \qquad (2)$$

In equation 2, η_{ex} is the exergy efficiency (%), ΣW_{req} is the total compressor power required (MW), and ΣW_{loss} is the total exergy loss work (MW) from each unit operation.

Results and discussion

The simulations results of the proposed configurations are summarised in Table 1. These configurations are analysed based on two criteria: meeting the specified HHV value, and minimum power consumption.

The results showed that configuration 2 gives the best results in meeting the HHV requirement (1,050.88 Btu/scf) with the lowest power consumption (65.71 MW). This shows a reduction in power consumption by 4.82% compared to configuration 1.

Meanwhile, the exergy analysis results indicate that the exergy efficiency of configuration 2 increases by 10.83% compared to configuration 1. The total amount of exergy loss dissipated by the unit operations in configuration 2 also reduces by 7.32%. This shows that by performing the exergy analysis on energy processes, it acts as a guideline in the process design of an LNG plant. This information is useful for project execution as well, as it reduces the capital and operating cost of the LNG plant (Finn *et al.* 1999).

The LNG production is also impacted with different configurations of integrated LNG and NGL processes. In configuration 2, the LNG production shows an increase of 2.39% compared to configuration 1.

Table 1. Simulation results of two different configurations of integrated LNG and NGL recovery process

	Configuration 1	Configuration 2
HHV (Btu/scf)	1,040.30	1,050.88
Compressor power (MW)	69.04	65.71
Exergy loss (MW)	55.59	51.52
η_{ex} (%)	19.48	21.59
LNG production (kg/h)	611,806.08	626,482.42

This implies that change in the process configurations of ethylene refrigeration cycle and NGL recovery process has a great impact in meeting the required HHV specification, and also reduces the power consumption of the liquefaction process. Decreasing the power consumption will improve the efficiency of the overall process, and thus provide economic benefits.

Conclusion

In this study, two different configurations of integrated LNG and NGL processes for the cascade LNG process are proposed. These configurations are simulated, using Aspen HYSYS, and exergy analysis method is selected to evaluate the efficiency of the process. Meeting the HHV specification and achieving minimum power consumption are the objectives of this study. The simulation results demonstrated that configuration 2 meets the required HHV specification (1,050.88 Btu/scf) and reduces the power consumption by 4.82% compared to configuration 1. Exergy efficiency of configuration 2 also increases by 10.83% compared to configuration 1. Based on these results, it can be concluded that configuration 2 can be used to produce both LNG and NGL at minimum energy consumption. Having these integrated concepts gives flexibility to the plant to switch their operation by either producing more LNG or more NGL when the market conditions are changing.

Future work

In this study, the exergy analysis for demethaniser and deethaniser is excluded due to insufficient information (enthalpy and entropy) for each tray. A detailed dynamic simulation is proposed for these configurations to obtain this information. Additionally, there is no consideration made from economic perspective to evaluate the feasibility of these proposed configurations. Therefore, future work should consider analysing these configurations using the exergy analysis that gives economic trade-off between the operating and capital cost of the integrated LNG and NGL plant.

Acknowledgements

The authors would like to acknowledge the Ministry of Education (MOE) of Malaysia and University Malaysia Pahang for funding the presented study. The authors also would like to acknowledge the support provided by the staff from Curtin University, Australia.

References

Brostow, A. A., And Roberts, M. J. (2013). Integrated NGL recovery in the production of liquefied natural gas. USA Patent No US 20130061632A1.

Cho, J., Vega, F. D. L, Kotzot, H., and Durr, C. (2005). Innovative gas processing with various LNG sources. *LNG journal* January/February 23–27.

Elliot, D., Qualls, W., Huang, S., Chen, J., Lee, R., Yao, J. And Zhang, Y. (2005). Benefits of integrating NGL extraction and LNG liquefaction technology. AIChE Spring National Meeting, Conference Proceedings, Cincinnati, Ohio, 30 October–4 November, 1943–1958.

Finn, A. J, Johnson, G. L., and Tomlinson, T. R. (1999). Developments in natural gas liquefaction. *Hydrocarbon Processing* 78(4), 1–18.

Kanoglu, M. (2002). Exergy analysis of multistage cascade refrigeration cycle used for natural gas liquefaction. *International Journal of Energy Research* 26(8), 763–774.

Mehrpooya, M., Hosseini, M., and Vatani, A. (2014). Novel LNG-based integrated process configuration alternatives for coproduction of LNG and NGL. *Industrial & Engineering Chemistry Research* 53(45), 17705–17721.

Moran, M. J. (2011). Fundamentals of engineering thermodynamics. Hoboken, New Jersey: Wiley.

Spilsbury, C., McIlwaihlin, S., and Kennington, B. (2005). Optimising the LNG liquefaction process. *LNG journal* January/February 40–43.

The authors

Nazreen Begum Najibullah Khan completed her BSc (chemical engineering) degree from University Teknologi Mara (Malaysia) in 2007. She commenced her PhD research in natural gas processing at Curtin University, in September 2013. Nazreen received a scholarship from the Ministry Higher of Education Malaysia and University Malaysia Pahang, Malaysia, to pursue her postgraduate study.

Ahmed Barifcani received his bachelor degree, masters and PhD in chemical engineering from University of Birmingham, UK. He is Associate Professor at Curtin University. He is also Fellow member of IChemE (FIChemE) and CSi of the Institution of Chemical Engineers. Ahmed has more than 30 years of industrial experience in operation, design, engineering, construction and project management in the fields of oil refining, gas processing, LNG and petrochemicals. He has 10 years' experience at Curtin University in doing research on CO2 capture, hydrates flow assurance, gas separation processes and MEG reovery research. He is also teaching undergraduate courses in petroleum engineering and supervising chemical engineering design and research projects. Additionally, Ahmed is also supervising PhD students in chemical engineering, petroleum engineering and at the corrosion centre.

Moses Tade received his bachelor degree in chemical engineering with first class honours from the University of Ife (now Obafemi Awolowo University), Ile-Ife, Nigeria. He was awarded the prestigious Commonwealth Scholarship for his masters and PhD in chemical engineering at Queen's University, Kingston, Ontario, Canada. Moses joined Curtin University as a Lecturer and earned the Personal Chair of Process Systems Engineering in 1999. He was the Head of Chemical Engineering from 2001–07 and then the Dean of Engineering from 2008 to November 2014. Moses became the Deputy Pro Vice Chancellor, Faculty of Science and Engineering in December 2014 and was awarded a John Curtin Distinguished Professor at Curtin University in 2012 for his significant contributions to chemical engineering research in the field of process systems engineering. He has also received substantial funding from both industry and the Australian Research Council (ARC) for his projects. He has successfully supervised more than 30 PhD students, several masters' students, and research fellows. Moses has published four books on various aspects of his work as well as more than 250 research papers in refereed international journals and conference proceedings. Moses is a Fellow of IChemE and an Honorary Fellow of Engineers Australia, and was listed in the Top 100 Most Influential Engineers in 2008. He is presently the President of the Australian Council of Engineering Deans (2015 and 2016) and a member of the ARC College of Experts (from 2014–16).

Vishnu Pareek received his BE Hons (Rajasthan), MTech (IIT-Dehli) and PhD in chemical engineering from (UNSW), Australia. He is the Professor and Head of School of Chemical and Petroleum Engineering at Curtin University.

Appendix C – Author attribution statements by the co-authors

To Whom It May Concern

I, *Nazreen Begum Najibullah Khan*, contributed *to the background, modelling and simulation, thermodynamic analyses and all the results, discussion and conclusion* to the paper publication entitled *Najibullah Khan, N.B., A. Barifcani, M. Tade, and V. Pareek, A case study: Application of energy and exergy analysis for enhancing the process efficiency of a three stage propane pre-cooling cycle of the cascade LNG process. Journal of Natural Gas Science and Engineering, 2016.* ***29****: p. 125-133.*

DOI *(http://dx.doi.org/10.1016/j.jngse.2015.12.034)*

I, as a Co-Author, endorse that this level of contribution by the candidate indicated above is appropriate.

Nazreen Begum Najibullah Khan

(Signature of Co-Author 1)

Ahmed Barifcani

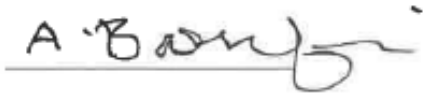

(Signature of Co-Author 2)

Moses Tade

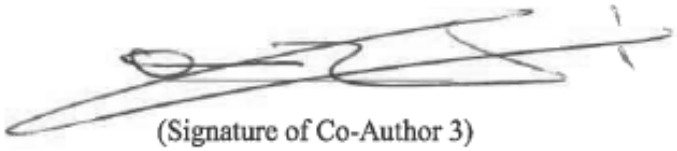

(Signature of Co-Author 3)

Vishnu Pareek

(Signature of Co-Author 4)

To Whom It May Concern

I, *Nazreen Begum Najibullah Khan*, contributed *to the background, modelling and simulation, thermodynamic analyses and all the results, discussion and conclusion* to the paper publication entitled *Najibullah Khan, N.B., A. Barifcani, M. Tade, and V. Pareek, Exergy analysis of an ethylene refrigeration cycle integrated with a NGL recovery process for a large LNG train. The APPEA Journal, 2016.* ***56****(2): p. 606-606.* ***DOI*** *(https://doi.org/10.1071/AJ15112)*

I, as a Co-Author, endorse that this level of contribution by the candidate indicated above is appropriate.

Nazreen Begum Najibullah Khan

(Signature of Co-Author 1)

Ahmed Barifcani

(Signature of Co-Author 2)

Moses Tade

(Signature of Co-Author 3)

Vishnu Pareek

(Signature of Co-Author 4)

To Whom It May Concern

I, *Nazreen Begum Najibullah Khan*, contributed *to the background, modelling and simulation, thermodynamic analyses and all the results, discussion and conclusion* to the paper publication *entitled Najibullah Khan, N.B., A. Barifcani, M. Tade, and V. Pareek, Effect of deethaniser (De-C2) column pressure on the process efficiency of an integrated LNG/NGL Plant,* to be submitted to another journal.

I, as a Co-Author, endorse that this level of contribution by the candidate indicated above is appropriate.

Nazreen Begum Najibullah Khan

(Signature of Co-Author 1)

Ahmed Barifcani

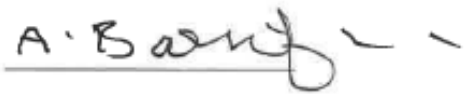

(Signature of Co-Author 2)

Moses Tade

(Signature of Co-Author 3)

Vishnu Pareek

(Signature of Co-Author 4)

To Whom It May Concern

I, *Nazreen Begum Najibullah Khan,* contributed *to the detailed literature review of LNG processes, the process flow schemes and all other work* to the paper publication *entitled Najibullah Khan, N.B., A. Barifcani, M. Tade, and V. Pareek, A review of LNG processes that are suitable for a single large-scale LNG train,* to be submitted to another journal.

I, as a Co-Author, endorse that this level of contribution by the candidate indicated above is appropriate.

Nazreen Begum Najibullah Khan

(Signature of Co-Author 1)

Ahmed Barifcani

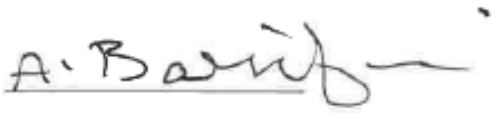

(Signature of Co-Author 2)

Moses Tade

(Signature of Co-Author 3)

Vishnu Pareek

(Signature of Co-Author 4)

References

1. ExxonMobil, *The Outlook for Energy : A view to 2040*. 2011. p. 43.
2. BP. *Statistical Review of World Energy*. 2018; 67th:[Available from: https://www.bp.com/en/global/corporate/energy-economics/statistical-review-of-world-energy.html.
3. Kumar, S., et al., *LNG: An eco-friendly cryogenic fuel for sustainable development.* Applied Energy, 2011. **88**(12): p. 4264-4273.
4. Okamura, T., M. Furukawa, and H. Ishitani, *Future forecast for life-cycle greenhouse gas emissions of LNG and city gas 13A.* Applied Energy, 2007. **84**(11): p. 1136-1149.
5. Correljé, A.F., *Markets for natural gas.* Encyclopedia of Energy, 2004. **3**: p. 799-808.
6. Dong, K., R. Sun, J. Wu, and G. Hochman, *The growth and development of natural gas supply chains: The case of China and the US.* Energy Policy, 2018. **123**: p. 64-71.
7. Oshima, K., et al., *The utilization of LH2 and LNG cold for generation of electric power by a cryogenic type stirling engine.* Cryogenics, 1978. **18**(11): p. 617-620.
8. Angelino, G., *The use of liquid natural gas as heat sink for power cycles.* Journal of Engineering for Power, 1978. **100**(1): p. 169-177.
9. Karashima, N. and T. Akutsu. *Development of LNG cryogenic power generation plant*. in *Proc., Intersoc. Energy Convers. Eng. Conf.;(United States)*. 1982. Tokyo Electric Power Company, Inc., Japan.
10. Kim, C., S. Chang, and S. Ro, *Analysis of the power cycle utilizing the cold energy of LNG.* International Journal of Energy Research, 1995. **19**(9): p. 741-749.
11. Aspelund, A. and T. Gundersen, *A liquefied energy chain for transport and utilization of natural gas for power production with CO 2 capture and storage–Part 1.* Applied Energy, 2009. **86**(6): p. 781-792.
12. Zhang, N. and N. Lior, *A novel near-zero CO 2 emission thermal cycle with LNG cryogenic exergy utilization.* Energy, 2006. **31**(10): p. 1666-1679.
13. De Carvalho Jr, A.V., *Natural gas and other alternative fuels for transportation purposes.* Energy, 1985. **10**(2): p. 187-215.
14. HS., W., *Liquid natural gas a transport fuel in heavy trucking industry, technical report, sponsored by US department of energy*. 1994-1995.
15. Litzke, W.-L. and J. Wegrzyn, *Natural gas as a future fuel for heavy-duty vehicles*. 2001, SAE Technical Paper.
16. S., H., *LNG as alternative transport fuel. Natural gas solution for heavy vehicles seminar.* 2009: Melbourne.

17. Letter, I.C.N., *The fertilizer industry as the largest domestic consumer of LNG*, in *Indonesian Commercial News Letter*. 1991: Indonesia.
18. Jaramillo, P., W. Griffin, and H. Matthews, *Comparative Life-Cycle Air Emissions of Coal, Domestic Natural Gas, LNG, and SNG for Electricity Generation.* Environmental Science & Technology, 2007. **41**(17): p. 6290-6296.
19. U.S. *Annual Energy Outlook 2016 with projections to 2040*. 2016.
20. Kirillov, N., *Liquefied Natural Gas as a Motor Fuel and a Refrigerant: Methodology of Evaluation of Ecological Suitability of Truck-Mounted Refrigerating Systems.* Chemical and Petroleum Engineering, 2002. **38**(5): p. 344-350.
21. AS, L.H.K.S. *The LNG future seen from a ship owner*. in *Magalog conference*. 2007.
22. Hekkert, M.P., F.H.J.F. Hendriks, A.P.C. Faaij, and M.L. Neelis, *Natural gas as an alternative to crude oil in automotive fuel chains well-to-wheel analysis and transition strategy development.* Energy Policy, 2005. **33**(5): p. 579-594.
23. Hondo, H., *Life cycle GHG emission analysis of power generation systems: Japanese case.* Energy, 2005. **30**(11): p. 2042-2056.
24. Kannan, R., K.C. Leong, R. Osman, and H.K. Ho, *Life cycle energy, emissions and cost inventory of power generation technologies in Singapore.* Renewable and Sustainable Energy Reviews, 2007. **11**(4): p. 702-715.
25. Chem, O., *Schaum's outline series*.
26. Lim, W., K. Choi, and I. Moon, *Current Status and Perspectives of Liquefied Natural Gas (LNG) Plant Design.* Industrial & Engineering Chemistry Research, 2013. **52**(9): p. 3065-3088.
27. Wood, D.A., *A review and outlook for the global LNG trade.* Journal of Natural Gas Science and Engineering, 2012. **9**: p. 16-27.
28. NETL, D., *Liquefied Natural Gas: Understanding the Basic Facts*. 2005.
29. Klinkenbijl, J.M., M.L.Dillon, and E.C. Heyman, *Gas Pre-Treatment and their impact on Liquefaction Processes*, in *78th Annual GPA Convention* 1999: Nashville, TN, USA.
30. Mokhatab, S., J.Y. Mark, J.V. Valappil, and D.A. Wood, *Handbook of liquefied natural gas*, ed. J.Y. Mak, J.V. Valappil, and D.A. Wood. 2013, Burlington: Elsevier Science.
31. Mortazavi, A., et al., *Performance enhancement of propane pre-cooled mixed refrigerant LNG plant.* Applied Energy, 2012. **93**: p. 125-131.
32. Hudson, H.M., J.D. Wilkinson, K.T. Cuellar, and M.C. Pierce, *Integrated liquids recovery technology improves LNG production efficiency*, in *82nd Convention of the Gas Processors Association*. 2003: Midland, Texas, USA. p. 1-9.

33. Elliot, D., et al., *Benefits of integrating NGL extraction and LNG liquefaction technology.* AIChE Journal, 2005: p. 1943-1958.
34. Cuellar, K.T., J.D. Wilkinson, H.M. Hudson, and M.C. Pierce, *CO-Producing LNG from cyrogenic NGL recovery plants* in *81st Convention of the Gas Processors Association*. 2002: Dallas, Texas, USA. p. 1-8.
35. Kanoğlu, M., *Cryogenic turbine efficiencies.* Exergy, An International Journal, 2001. **1**(3): p. 202-208.
36. (EIA), U.S.E.I.A., *The Global Liquefied Natural Gas Market: Status & Outlook*. 2003.
37. Hasan, M.M.F., I.A. Karimi, and H.E. Alfadala. *Optimizing Compressor Operation in an LNG Plant*. in *Proceedings of the 1st Annual Gas Processing Symposium*. 2009. Amsterdam: Elsevier.
38. Hatcher, P., R. Khalilpour, and A. Abbas, *Optimisation of LNG mixed-refrigerant processes considering operation and design objectives.* Computers & Chemical Engineering, 2012. **41**: p. 123-133.
39. Union, I.G., *IGU World Gas LNG report* in *27th World Gas Conference* 2018, International Gas Union: Washington DC. p. 1-106.
40. Spilsbury, C., S. McLauchlin, and B. Kennington, *Optimising the LNG liquefaction Process.* LNG journal, 2005(January/February): p. 40-43.
41. McKeever, J., M. Pillarella, and R. Bower, *An ever evolving technology.* LNG Industry Spring, 2008.
42. Pillarella, M., J.C. Bronfenbrenner, Y. Liu, and M. Roberts. *Large LNG trains: Developing the optimal process cycle*. in *Gastech 2005 Conference & Exhibition, Bilbao, Spain*. 2005.
43. Wood, D., *Profitable year so far, but cost and demand challenges confront suppliers.* World Oil, 2007. **228**(10): p. 129-132.
44. Li, Y., X. Wang, and Y. Ding, *An optimal design methodology for large-scale gas liquefaction.* Applied Energy, 2012. **99**: p. 484-490.
45. Eaton, A., et al. *Lowering LNG unit costs through large and efficient LNG liquefaction trains–What is the optimal train size*. in *AIChE Spring Meeting, New Orleans, Louisiana*. 2004.
46. Paradowski, H., M. Bamba, and C.Bladanet, *Propane Precooling Cycles for Increased LNG Train Capacity*, in *14th International Conference and Exhibitions on Liquefied Natural Gas* 2004: Doha, Qatar 21-24 March. p. 1-18.
47. Vatani, A., M. Mehrpooya, and B. Tirandazi, *A novel process configuration for co-production of NGL and LNG with low energy requirement.* Chemical Engineering and Processing: Process Intensification, 2013. **63**: p. 16-24.

48. Melaaen, I. and G. Owren, *How do the inaccuracies of enthalpy and vapour-liquid equilibrium calculations influence baseload LNG plant design?* Computers & chemical engineering, 1996. **20**(1): p. 1-11.
49. Wang, M., J. Zhang, and Q. Xu, *Optimal design and operation of a C3MR refrigeration system for natural gas liquefaction.* Computers & Chemical Engineering, 2012. **39**: p. 84-95.
50. Mehrpooya, M., A. Jarrahian, and M.R. Pishvaie, *Simulation and exergy-method analysis of an industrial refrigeration cycle used in NGL recovery units.* International Journal of Energy Research, 2006. **30**(15): p. 1336-1351.
51. Kanoglu, M., *Exergy analysis of multistage cascade refrigeration cycle used for natural gas liquefaction.* International Journal of Energy Research, 2002. **26**(8): p. 763-774.
52. Najibullah Khan, N.B., A. Barifcani, M. Tade, and V. Pareek, *Exergy analysis of an ethylene refrigeration cycle integrated with a NGL recovery process for a large LNG train.* The APPEA Journal, 2016. **56**(2): p. 606-606.
53. Najibullah Khan, N.B., A. Barifcani, M. Tade, and V. Pareek, *A case study: Application of energy and exergy analysis for enhancing the process efficiency of a three stage propane pre-cooling cycle of the cascade LNG process.* Journal of Natural Gas Science and Engineering, 2016. **29**: p. 125-133.
54. Remeljej, C. and A. Hoadley, *An exergy analysis of small-scale liquefied natural gas (LNG) liquefaction processes.* Energy, 2006. **31**(12): p. 2005-2019.
55. Vatani, A., M. Mehrpooya, and A. Palizdar, *Energy and exergy analyses of five conventional liquefied natural gas processes.* International Journal of Energy Research, 2014: p. 1843-1863.
56. Cipolato, L., et al., *Exergetic optimization of a refrigeration cycle for natural gas liquefaction.* 2012. **31**: p. 440-444.
57. Lee, G., R. Smith, and X. Zhu, *Optimal synthesis of mixed-refrigerant systems for low-temperature processes.* Industrial & engineering chemistry research, 2002. **41**(20): p. 5016-5028.
58. Nogal, F.D., J.-K. Kim, S. Perry, and R. Smith, *Optimal design of mixed refrigerant cycles.* Industrial & Engineering Chemistry Research, 2008. **47**(22): p. 8724-8740.
59. Cammarata, G., A. Fichera, and D. Guglielmino, *Optimization of a liquefaction plant using genetic algorithms.* Applied Energy, 2001. **68**(1): p. 19-29.
60. Aspelund, A., et al., *An optimization-simulation model for a simple LNG process.* Computers & Chemical Engineering, 2010. **34**(10): p. 1606-1617.
61. Shukri, T., *LNG technology selection.* Hydrocarbon engineering, 2004. **9**(2): p. 71-74.

62. Pettersen, J., *LNG plant equipment (Statoil)*, in *Seminar with Supplier Association Murmanshelf*. 2012: Murmansk, Russia.
63. Pillarella, M., Y.-N. Liu, J. Petrowski, and R. Bower. *The C3MR liquefaction cycle: versatility for a fast growing, ever changing LNG Industry*. in *15th International Conference on LNG*. 2007. Barcelona, Spain.
64. Liu, Y., C. Lucas, R. Bower, and J. Bronfenbrenner, *Reducing LNG costs by better capital utilization*, in *13th International Conference and Exhibition on Liquefied Natural Gas (LNG 13)*. 2001: Seoul, Korea. p. 14-17.
65. Chang, H.-M., M.J. Chung, S. Lee, and K.H. Choe, *An efficient multi-stage Brayton–JT cycle for liquefaction of natural gas.* Cryogenics, 2011. **51**(6): p. 278-286.
66. Brimm, A.E., S. Ghosh, and D. Hawrysz, *Operating Experience With the Split MR Machinery Configuration of the C3MR LNG Process.* SPE Projects, Facilities & Construction, 2006. **1**(02): p. 1-5.
67. Chiu, C.-H., T. Tsang, M. Chapeaux, and C. Chen, *Improve Energy Efficiency in LNG Production for Baseload LNG Plants*, in *25th World Gas Conference*. 2012: Kuala Lumpur, Malaysia.
68. Nored, M. *A historical review of turbomachinery for LNG applications*. in *LNG17*. 2013. Houston, Texas, USA
69. Roberts, M.J., Y.-N. Liu, J.C. Bronfenbrenner, and J.M. Petrowski. *Reducing LNG capital costs in today's competitive environment* in *14th International Conference and Exhibition on Liquefied Natural Gas (LNG 14)*. 2004. Doha, Qatar.
70. Thompson, G., et al. *Qatargas II: Full Supply Chain Overview*. in *LNG 14th Conference. Qatar*. 2004.
71. Bukowski, J., Y.N. Liu, S. Boccella, and L. Kowalski. *Innovations-in-natural-gas-liquefaction-technology for future LNG plants and floating LNG facilities*. in *International Gas Union Research Conference*. 2011.
72. Castaneda, G., *FLNG process and safety considerations.* LNG Journal, 2015.
73. van de Graaf, J.M. and B. Pek, *Large-capacity LNG trains–The shell parallel mixed refrigerant process.* LNG Review 2005, 2005.
74. Fisher, B. and P. Boutelant. *A new LNG process is now available*. in *GPA Europe Technical Meeting, London, England*. 2002.
75. Martin, P., J. Pigourier, and P. Boutelant. *Liquefin: An innovative process to reduce LNG costs*. in *22nd World Gas Conference, Tokyo, Japan*. 2003.
76. *LNG Solutions from the leader in Cryogenics 'Air Liquide'*. LNG Industry, 2017: p. 1-68.

77. Burin de Roziers, T. and B. Fischer. *New Trends in LNG Process Design*. in *GPA Europe Meeting, London, England (Feb. 19, 1999)*. 1999.
78. Knott, T., *Cool future for gas.* Frontiers, 2001: p. 10-16.
79. Heiersted, R., R. Jensen, R. Pettersen, and S. Lillesund. *Capacity and technology for the Snøhvit LNG plant*. in *LNG 13 Conference*. 2001.
80. Bach, W., *Developments in the mixed fluid cascade process (MFCP) for LNG baseload plants.* Reports on science and technology, 2002. **63**: p. 25-28.
81. Statoil. *Snohvit LNG Project*. 2005.
82. Martin, P.-Y., J. Pigourier, and B. Fischer. *Natural gas liquefaction processes comparison*. in *14th International Conference & Exhibition on liquefied Natural gas (LNG 14)*. 2004. Doha, Qatar.
83. Houser, C.G. and L.C. Krusen. *Phillips Optimized Cascade LNG Process*. in *Gastech 96 Conference and Exhibition*. 1996. Vienna, Austria.
84. Andress, D. and R. Watkins. *Beauty of simplicity: Phillips optimized cascade LNG liquefaction process*. in *AIP Conference Proceedings*. 2004. AIP.
85. Company, C., *ConocoPhillips Liquefied Natural Gas Brochure*, C. Company, Editor. 2016.
86. Jamieson, D., P. Johnson, and P. Redding. *Targeting and achieving lower cost liquefaction plants*. in *12th International Conference and Exhibition on Liquefied Natural Gas (LNG 12)*. 1998. Perth, Australia.
87. Company, C., *ConocoPhillips Optimized Cascade Process Brochure*, C. Company, Editor. 2009.
88. Finn, A.J., G.L. Johnson, and T.R. Tomlinson, *Developments in natural gas liquefaction.* Hydrocarbon Processing, 1999. **78**(4): p. 1-18.
89. Diocee, T.S., P. Hunter, A. Eaton, and A. Avidan. *Atlantic LNG Train 4 "The World's Largest LNG train"*. in *14th International Conference and Exhibition on Liquefied Natural Gas (LNG 14)* 2004. Doha, Qatar.
90. Avidan, A., F. Richardson, K. Anderson, and B. Woodard. *LNG Plant Scale-up Could Cut Costs Further*. in *Fundamentals of the Global LNG Industry*. 2001. London, UK: Petroleum Economist.
91. Company, P.P., *LNG showpiece after 20 years of operation.* Performance, 1990. **103**(May/June): p. 19-20.
92. Fatt, C.C. and A. Omarali, *Brunei LNG's MCHE replacement project.* LNG journal, 2005: p. 57-58.
93. Cengel, Y.A. and M.A. Boles, *Thermodynamics : an engineering approach*. 6th ed, ed. M.A. Boles. 2002, Boston, Mass.: Boston, Mass. : McGraw-Hill Higher Education.

94. Moran, M.J., *Engineering thermodynamics*, in *The CRC Handbook of Mechanical Engineering, Second Edition*. 2004, CRC Press.
95. Szargut, J., *International Progress in Second Law Analysis* Energy 1980. **5**: p. 709-718.
96. Kidnay, A.J. and W. Parrish, *Fundamentals of natural gas processing*. 2nd ed, ed. W.R. Parrish and D.G. McCartney. 2006, Boca Raton: CRC Press.
97. Chang, H.-M., *A thermodynamic review of cryogenic refrigeration cycles for liquefaction of natural gas.* Cryogenics, 2015. **72**: p. 127-147.
98. Moran, M.J. and H.N. Shapiro, *Fundamentals of engineering thermodynamics* 5th ed, ed. H.N. Shapiro. 2006, Chichester, West Sussex, England; Hoboken, NJ: John Wiley & Sons.
99. Kidnay, A.J. and W. Parrish, *Chapter 13: Liquefied Natural Gas*, in *Fundamentals of natural gas processing*, W. Parrish, Editor. 2006, Boca Raton : CRC Press: Boca Raton.
100. Khan, M.S., S. Lee, M. Getu, and M. Lee, *Knowledge inspired investigation of selected parameters on energy consumption in nitrogen single and dual expander processes of natural gas liquefaction.* Journal of Natural Gas Science and Engineering, 2015. **23**: p. 324-337.
101. Foglietta, J.H., *Consider dual independent expander refrigeration for LNG production.* Hydrocarbon Processing, 2004. **83**(1): p. 39-44.
102. Smith, R., *Chemical Process Design and Integration* 2005, Chichester, West Sussex, England: John Wiley & Sons Ltd.
103. Khan, M.S. and M. Lee, *Design optimization of single mixed refrigerant natural gas liquefaction process using the particle swarm paradigm with nonlinear constraints.* Energy, 2013. **49**: p. 146-155.
104. Yoon, J.-I., et al., *Efficiency of Cascade Refrigeration Cycle Using C3H8, N2O, and N2.* Heat Transfer Engineering, 2013. **34**(11-12): p. 959-965.
105. Balaras, C.A. and S.M. Jeter, *A methodology for selecting and screening novel refrigerants for use as alternative working fluids.* Energy Conversion and Management, 1991. **31**(4): p. 389-398.
106. Yoon, J.-I., et al., *Assessment of the performance of a natural gas liquefaction cycle using natural refrigerants.* Heat and Mass Transfer, 2014. **51**(1): p. 95-105.
107. Sarkar, J., S. Bhattacharyya, and A. Lal, *Selection of suitable natural refrigerants pairs for cascade refrigeration system.* Journal of Power and Energy, 2013. **227**(5): p. 612-622.

108. American Society of Heating, R. and E. Air-Conditioning, *ASHRAE, handbook of Fundamentals* American Society of Heating, Refrigerating and Air-Conditioning Engineers handbook. Fundamentals. 1993, Atlanta, Ga.: Atlanta, Ga. : American Society of Heating, Refrigerating, and Air-Conditioning Engineers, Inc.

109. Poling, B.E., J.M. Prausnitz, and J.P. Connell, *The properties of gases and liquids / Bruce E. Poling, John M. Prausnitz, John P. O'Connell*. 5th ed. 2001, New York: New York : McGraw-Hill.

110. Fox, M.A., *Refrigerants and Halocarbons*, in *Glossary for the Worldwide Transportation of Dangerous Goods and Hazardous Materials*. 1999, Springer. p. 215-217.

111. Liu, Y.N., T. Daugherty, and J. Brofenbrenner. *LNG liquefier cycle efficiency*. in *Twelfth International Conference and Exhibition on Liquefied Natural Gas, Perth, Australia*. 1998.

112. Rant, Z., *Exergy, a new word for technical available work.* Forsch. Ing. Wis, 1956. **22**(1): p. 36-37.

113. Sato, N., *Chemical energy and exergy: an introduction to chemical thermodynamics for engineers*. 2004: Elsevier.

114. Aspelund, A., D.O. Berstad, and T. Gundersen, *An Extended Pinch Analysis and Design procedure utilizing pressure based exergy for subambient cooling.* Applied Thermal Engineering, 2007. **27**(16): p. 2633-2649.

115. Cihan, A., O. Hacıhafızog˘lu, and K. Kahveci, *Energy–exergy analysis and modernization suggestions for a combined-cycle power plant.* International Journal of Energy Research, 2006. **30**(2): p. 115-126.

116. Wang, H., X. Shi, and D. Che, *Thermodynamic optimization of the operating parameters for a combined power cycle utilizing low-temperature waste heat and LNG cold energy.* Applied Thermal Engineering, 2013. **59**(1-2): p. 490-497.

117. Aljundi, I.H., *Energy and exergy analysis of a steam power plant in Jordan.* Applied Thermal Engineering, 2009. **29**(2–3): p. 324-328.

118. Kaushik, S.C., V.S. Reddy, and S.K. Tyagi, *Energy and exergy analyses of thermal power plants: A review.* Renewable and Sustainable Energy Reviews, 2011. **15**(4): p. 1857-1872.

119. Yin, Q., et al. *Economic analysis of mixed-refrigerant cycle and nitrogen expander cycle in small scale natural gas liquefier*. in *AIP conference proceedings*. 2008. AIP.

120. Helgestad, D.-E., *Modelling and optimization of the C3MR process for liquefaction of natural gas.* Process Systems Engineering, 2009: p. 44.

121. Castillo, L., M. Majzoub Dahouk, S. Di Scipio, and C.A. Dorao, *Conceptual analysis of the precooling stage for LNG processes.* Energy Conversion and Management, 2013. **66**: p. 41-47.
122. Castillo, L. and C.A. Dorao, *On the conceptual design of pre-cooling stage of LNG plants using propane or an ethane/propane mixture.* Energy Conversion and Management, 2013. **65**: p. 140-146.
123. Ransbarger, W., *A fresh look at LNG process efficiency.* LNG industry, 2007(SPRING).
124. Majzoub, M., *Evaluation and Selection of the Pre-cooling Stage for LNG Processes*. 2012, Norwegian University of Science and Technology.
125. Fathalla, B.M., *Enhancing Propane Refrigerant Performance at Pre-cooling stage during hot climate conditions at LNG plants - Case study from Egypt*. 2013, Universiti Teknologi Petronas.
126. Mortazavi, A., et al., *Enhancement of APCI cycle efficiency with absorption chillers.* Energy, 2010. **35**(9): p. 3877-3882.
127. Kalinowski, P., et al., *Application of waste heat powered absorption refrigeration system to the LNG recovery process.* International Journal of Refrigeration, 2009. **32**(4): p. 687-694.
128. Mehrpooya, M., M. Hossieni, and A. Vatani, *Novel LNG-Based Integrated Process Configuration Alternatives for Coproduction of LNG and NGL.* Industrial & Engineering Chemistry Research, 2014. **53**(45): p. 17705-17721.
129. Cho, J., F.d.l. Vega, H. Kotzot, and C. Durr, *Innovative Gas Processing with various LNG sources.* LNG Journal, 2005(January/February): p. 23-27.
130. Brostow, A.A. and M.J. Roberts, *Integrated NGL recovery in the production of liquefied natural gas*. 2013, Air Products and Chemicals, Inc., Allentown, PA (US) US 20130061632A1: USA. p. 1-22.
131. Khan, M.S., Y.D. Chaniago, M. Getu, and M. Lee, *Energy saving opportunities in integrated NGL/LNG schemes exploiting: Thermal-coupling common-utilities and process knowledge.* Chemical Engineering and Processing: Process Intensification, 2014. **82**: p. 54-64.
132. He, T. and Y. Ju, *Design and Optimization of a Novel Mixed Refrigerant Cycle Integrated with NGL Recovery Process for Small-Scale LNG Plant.* Industrial & Engineering Chemistry Research, 2014. **53**(13): p. 5545-5553.
133. Ransbarger, W.L., *Intermediate pressure LNG refluxed NGL recovery process (US 20080098770 Al)*. 2008, ConocoPhilips Company: USA.
134. Filstead, C., *Camel LNG Plant: World's Largest.* Hydrocarbon Processing, 1965. **44**: p. 135-138.

135. Fahmy, M.F.M., H.I. Nabih, and M. El-Nigeily, *Enhancement of the efficiency of the Open Cycle Phillips Optimized Cascade LNG process.* Energy Conversion and Management, 2016. **112**: p. 308-318.
136. Shin, J., S. Yoon, and J.-K. Kim, *Application of exergy analysis for improving energy efficiency of natural gas liquids recovery processes.* Applied Thermal Engineering, 2015. **75**: p. 967-977.
137. Lee, S., N.V.D. Long, and M. Lee, *Design and Optimization of Natural Gas Liquefaction and Recovery Processes for Offshore Floating Liquefied Natural Gas Plants.* Industrial & Engineering Chemistry Research, 2012. **51**(30): p. 10021-10030.
138. Mehrpooya, M., A. Vatani, and S.M. Ali Mousavian, *Introducing a novel integrated NGL recovery process configuration (with a self-refrigeration system (open–closed cycle)) with minimum energy requirement.* Chemical Engineering and Processing: Process Intensification, 2010. **49**(4): p. 376-388.
139. Lim, W., et al., *Efficient Configuration of a Natural Gas Liquefaction Process for Energy Recovery.* Industrial & Engineering Chemistry Research, 2014. **53**(5): p. 1973-1985.
140. Mehrpooya, M., F. Gharagheizi, and A. Vatani, *Thermoeconomic analysis of a large industrial propane refrigeration cycle used in NGL recovery plant.* International Journal of Energy Research, 2009. **33**(11): p. 960-977.
141. Al-Azzawi, N.M., *Optimal design variables for low temperature distillation columns in the ethylene plant at petrochemical complex -1 (PC1)-Basrah for revamping*, in *Chemical Engineering*. 2007, University of Technology, Baghdad: Iraq. p. 244.
142. *Engineering Data Book (SI Version)*. 2004, Gas Processors Suppliers Association: Tulsa, Oklahoma, United States of America.
143. Castillo, L., et al., *Technology selection for liquefied natural gas (LNG) on base-load plants*, in *Jornadas de Investigación de la Facultad de Ingeniería (JIFI). Universidad Central de Venezuela*. 2010.
144. Al-Otaibi, D.A., I. Dincer, and M. Kalyon, *Thermoeconomic optimization of vapor-compression refrigeration systems.* International Communications in Heat and Mass Transfer, 2004. **31**(1): p. 95-107.
145. Khan, M.S., S. Lee, G.P. Rangaiah, and M. Lee, *Knowledge based decision making method for the selection of mixed refrigerant systems for energy efficient LNG processes.* Applied Energy, 2013. **111**: p. 1018-1031.
146. Cao, W.-s., X.-s. Lu, W.-s. Lin, and A.-z. Gu, *Parameter comparison of two small-scale natural gas liquefaction processes in skid-mounted packages.* Applied Thermal Engineering, 2006. **26**(8-9): p. 898-904.

147. Xu, X., J. Liu, C. Jiang, and L. Cao, *The correlation between mixed refrigerant composition and ambient conditions in the PRICO LNG process.* Applied Energy, 2013. **102**: p. 1127-1136.
148. Campbell, J.M., *Gas conditioning and processing : volume 2, the equipment modules / by John M. Campbell*. 8th ed. The equipment modules, ed. R.A. Hubbard. Vol. 2. 2004, Norman, Oklahoma: John M. Campbell and Company.
149. Brostow, A.A. and M.J. Roberts, *Integrated NGL recovery in the production of liquefied natural gas*, I. Air Products and Chemicals, Editor. 2012, Google Patents: US.
150. Moran, M.J., *Fundamentals of engineering thermodynamics* 7th ed.. ed. Engineering thermodynamics, ed. M.J. Moran. 2011, Hoboken, New Jersey: Wiley

Every reasonable effort has been made to acknowledge the owners of copyright material. I would be pleased to hear from any copyright owner who has been omitted or incorrectly acknowledged.